Untersuchungen zur metallfreien Katalyse mit einem Pyridonat-Boran-Komplex und zu Carboborierungen von Alkinen und Allenen

Inauguraldissertation zur Erlangung des Doktorgrades der Naturwissenschaftlichen Fachbereiche im Fachgebiet Organische Chemie der Justus-Liebig-Universität Gießen

vorgelegt von

Max Hasenbeck

aus Meckenheim

Betreuer: Dr. Urs Gellrich

Gießen 2022

I suspect that no invention has ever been made without some fortuitous help.

William Knowles

Versicherung nach §17 der Promotionsordnung

Ich erkläre: Ich habe die vorgelegte Dissertation selbstständig und ohne unerlaubte fremde Hilfe und nur mit den Hilfen angefertigt, die ich in der Dissertation angegeben habe. Alle Textstellen, die wörtlich oder sinngemäß aus veröffentlichten Schriften entnommen sind, und alle Angaben, die auf mündlichen Auskünften beruhen, sind als solche kenntlich gemacht. Ich stimme einer evtl. Überprüfung meiner Dissertation durch eine Antiplagiat-Software zu. Bei den von mir durchgeführten und in der Dissertation erwähnten Untersuchungen habe ich die Grundsätze guter wissenschaftlicher Praxis, wie sie in der „Satzung der Justus-Liebig-Universität Gießen zur Sicherung guter wissenschaftlicher Praxis“ niedergelegt sind, eingehalten.

Max Hasenbeck Ort, Datum

Erstgutachter: Dr. Urs Gellrich

Zweitgutachter: Prof. Dr. Peter R. Schreiner, PhD

Inhaltsverzeichnis

1 Abstract

Gellrich showed 2018 that the intramolecular *frustrated Lewis pair* boroxypyridine **1** reversible activates H_2 under mild conditions. During the bond activation process the covalent O−B bond changes to a dative bond in the product complex of pyridone and Piers' borane ($HB(C_6F_5)_2$) **2**. This concept, in analogy to *metal-ligand cooperation*, was coined *boron-ligand cooperation*. The change in the bonding mode facilitates the dissociation of the borane after bond activation which is then available for follow-up reactivity, *e.g.* hydroborations. This work investigates the application of this concept in catalysis. The boroxypyridine **1** catalyses the allylation of nitriles by *in situ* generated allylboranes from H_2 and allenes, the semihydrogenation of terminal and internal alkynes, and the *gem*-selective homodimerization of terminal alkynes by *in situ* generated alkynylboranes. Additionally, it facilitates the efficient catalytic dehydrogenation of ammonia borane using 6-*tert*-butylthiopyridone as organocatalyst.

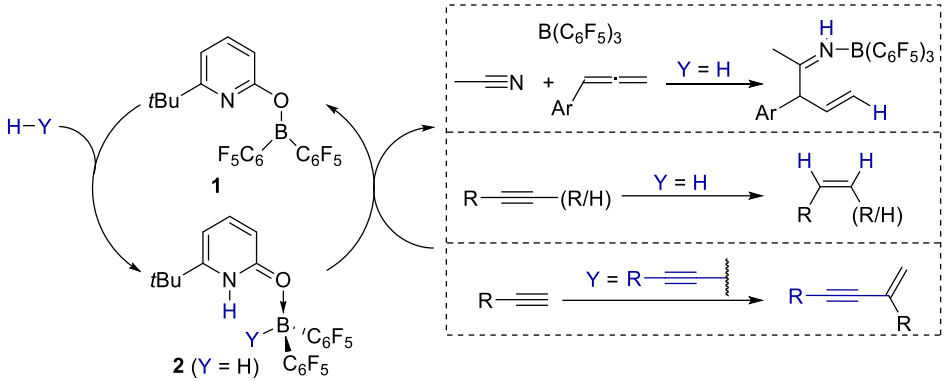

Furthermore, novel C–C coupling methods by carboborations of electron-poor alkenylboranes and $B(C_6F_5)_3$ with terminal allenes and alkynes were developed. The reaction of BCF with arylallenes yields C_6F_5-substituted indenes with simultaneous release of Piers' borane *via* a 1,1-carboboration. Alkenylboranes can be synthesized *in situ* via the hydroboration of alkynes with Piers' borane. With allenes they form boryl substituted 1,4-dienes *via* a 1,2-carboboration. With additional alkyne, they tetramerize to tetrahydropentalenes in a reaction sequence presumably initiated by three 1,2-carboborations.

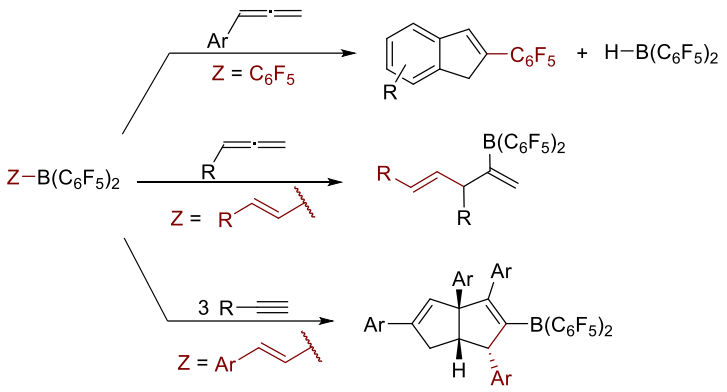

2 Zusammenfassung

2018 zeigte Gellrich, dass das intramolekulare *frustrierte Lewis-Paar* Boroxypyridin **1** H_2 reversibel unter milden Bedingungen aktivieren kann. Im Zuge der Bindungsaktivierung kommt es zu einem Wechsel der kovalenten O–B Bindung zu einer dativen Bindung im Produktkomplex aus Pyridon und Piers Boran ($HB(C_6F_5)_2$) **2**. In Analogie zur *Metall-Liganden-Kooperation* kann dieses Konzept als *Bor-Liganden-Kooperation* beschrieben werden. Der Wechsel des Bindungsmodus im Zuge der Bindungsaktivierung ermöglicht die Dissoziation des Borans, welches für Folgereaktionen, z.B. Hydroborierungen, zur Verfügung steht. Diese Arbeit beschäftigt sich mit der Anwendung dieses Konzepts in der Katalyse. Boroxypyridin **1** katalysiert die Allylierung von Nitrilen mit *in situ* erzeugten Allylboranen aus H_2 und Allenen, die Semihydrierung von terminalen und internen Alkinen mit H_2, und die *gem*-selektive Dimerisierung terminaler Alkine durch *in situ* erzeugte Alkinylborane. Es ermöglicht außerdem die effiziente Dehydrierung von Amminboran durch 6-*tert*-butylthiopyridon als Organokatalysator.

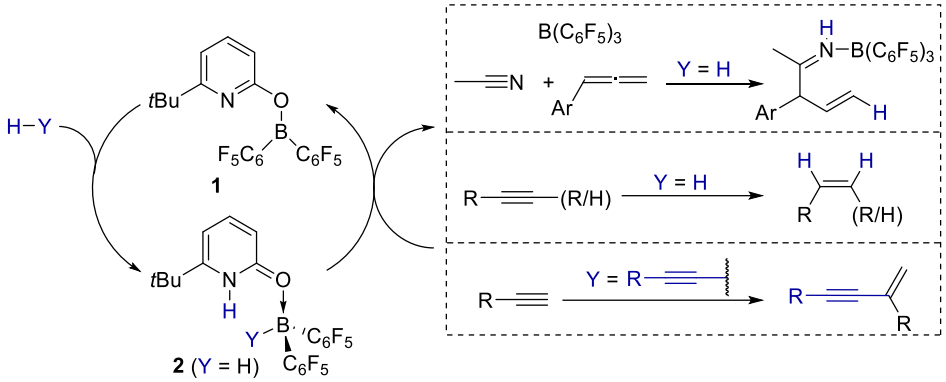

Zusätzlich wurden unkatalysierte Carboborierungen von elektronenarmen Alkenylboranen und $B(C_6F_5)_3$ (BCF) mit terminalen Allenen und Alkinen als C–C-Knüpfungsmethoden entwickelt. So führte die Reaktion von Arylallenen mit BCF über eine 1,1-Carboborierung unter Freisetzung von Piers Boran zu C_6F_5-substituierten Indenen. Alkenylborane können *in situ* durch die Hydroborierung von Alkinen mit Piers Boran synthetisiert werden. Diese reagieren mit Allenen in einer 1,2-Carboborierung zu borylsubstituierten 1,4-Dienen und tetramerisieren mit weiteren Äquivalenten Alkin in einer vermutlich durch drei 1,2-Carboborierungen initiierten Reaktionssequenz zu Tetrahydropentalenen.

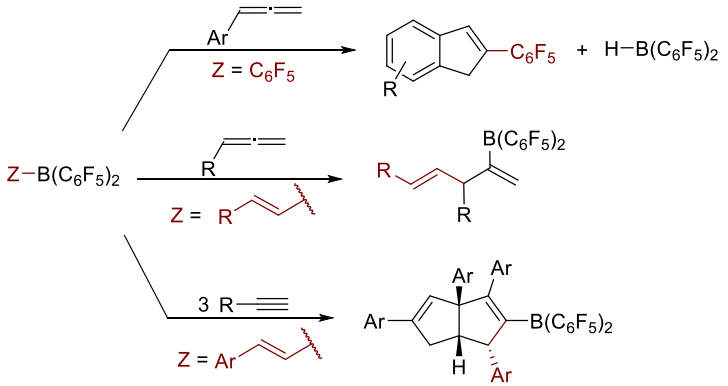

3 Einleitung

Die Entwicklung neuer übergangsmetallbasierter Katalysatoren im Laufe des 20. Jahrhunderts erweiterte die chemisch synthetischen Möglichkeiten enorm und ermöglichte die Synthese von Molekülen ungeahnter Komplexität. Der enorme Einfluss von übergangsmetallbasierten Katalysatoren zeigt sich daran, dass allein in den 2000er Jahren die Arbeiten für die Entwicklung von Katalysatoren für *enantioselektive Reduktionen und Oxidationen* (2001)[1], *Metathese* (2005)[2] und *Kreuzkupplungen* (2010)[3] mit dem Nobelpreis ausgezeichnet wurden. Neben komplexen chemischen Transformationen für die Synthese von Feinchemikalien im Labor ermöglichen Übergangsmetalle industrielle Prozesse im Multitonnenmaßstab mit Katalysatorladungen von teilweise weit unter einem Molprozent.[4,5]

Die Reaktivität von Übergangsmetallen wird durch ihre Kombination energetisch zugänglicher gefüllter und leerer d-Orbitale bestimmt, die gleichzeitig als Elektronendonor und -akzeptor fungieren können und kooperativ mit einer Vielzahl von Substraten reagieren. Häufig verwendete Übergangsmetalle in der Katalyse wie beispielsweise Rhodium, Iridium oder Palladium sind jedoch teuer und toxisch und ihr Vorkommen ist begrenzt.[6] Neben dem reinen Erkenntnisgewinn besteht somit auch im Kontext der *Grünen Chemie* langfristig ein Interesse an der Entwicklung übergangsmetallfreier Synthesemethoden und Katalysatoren.[7] Dies zeigt sich im Besonderen seit den 2000er Jahren mit dem Aufkommen der 2021 mit dem Nobelpreis ausgezeichneten (*asymmetrischen*) *Organokatalyse*[8] und dem Konzept der *frustrierten Lewis-Paare* (s.u.).

Bei Versuchen, die Reaktivität von Übergangsmetallen durch Hauptgruppenverbindungen zu imitieren, werden häufig borbasierte Verbindungen verwendet, da Bor durch sein freies p-Orbital als Elektronenakzeptor reagieren kann. Im Falle der äußerst reaktiven niedervalenten Bor-Verbindungen mit B–B-π-Bindungen und den Carbenen analogen Borylenen liegt die Elektronendonorfunktionalität analog zu den Übergangsmetallen auch direkt am Bor. Diese Stoffklassen seien hier der Vollständigkeit halber erwähnt und für einen detaillierten Überblick sei auf entsprechende Übersichtsartikel verwiesen.[9,10]

Die im Zuge dieser Promotion bearbeiteten Projekte beschäftigen sich mit der Reaktivität der häufiger vorkommenden Stoffklasse der Borane. Diese reagieren selbst nur als Elektronenakzeptoren, können jedoch mit einem zusätzlichen Elektronendonor unter gewissen Umständen den Übergangsmetallen ähnliche Reaktivität zeigen, wobei Elektronenakzeptor- und Elektronendonorfunktionalität nicht mehr am selben Atom liegen (*frustrierte Lewis-Paare*). Die kooperative Reaktivität aus Elektronenakzeptor und -donor bei Hauptgruppenverbindungen wird auch als *metallomimetisch* bezeichnet.[9] Das erste Kapitel dieser Einleitung beschäftigt sich mit dem Konzept der *Bor-Liganden-Kooperation*, einem speziellen Reaktionsmodus bestimmter *frustrierter Lewis-Paare*, und dessen Anwendung in der Katalyse.

Ohne zusätzlichen Elektronendonor wird die Reaktivität von Boranen häufig durch deren Funktion als Elektronenakzeptor bestimmt. So können sehr elektronenarme Borane beispielsweise mit C–C-π-Bindungen in Alkinen oder Allenen in sog. *Carboborierungen* reagieren, mit denen sich das zweite Kapitel dieser Einleitung beschäftigt.

3.1 Bor-Liganden-Kooperation

Die *Bor-Liganden-Kooperation* (BLK) lässt sich als Kombination der beiden Konzepte der *frustrierten Lewis-Paare* (FLP) und der *Metall-Liganden-Kooperation* (MLK) beschreiben. Im Folgenden werden diese drei Konzepte vorgestellt und repräsentative Beispiele für die Anwendung der BLK in der Katalyse aufgezeigt. Im Kontext der BLK beschreiben zwei Unterkapitel zum einen die Synthese und Anwendung von nukleophilen Allylboranen und zum anderen Methoden zur Dehydrierung von Amminboran. Für ein im Zuge dieser Promotion verfasster Mini-Übersichtsartikel über BLK siehe Kapitel 5.6.

3.1.1 Metall-Liganden-Kooperation

Klassische Übergangsmetallkomplexe aktivieren Moleküle direkt am Metallzentrum durch oxidative Addition. Schema 1a zeigt dies am Beispiel der oxidativen Addition von H_2 an Vaskas Iridiumkomplex **3**.[11] Dabei wird H_2 homolytisch zu zwei Hydridoliganden gespalten (Schema 1a). Während beide Wasserstoffe von der Oxidationsstufe 0 zu −1 reduziert werden, wird aus dem Ir(I)- ein Ir(III)-Zentrum in **4**. Die Liganden beeinflussen die sterischen und elektronischen Eigenschaften des Komplexes, sind jedoch an der Spaltung von H_2 nicht direkt beteiligt. Im Kontrast dazu beschreibt die MLK eine Situation, bei der der Ligand aktiv an der Bindungsspaltung beteiligt ist.

Ein frühes Beispiel dafür sind die Rutheniumphosphinkomplexe von Noyori und Mitarbeitern für die Hydrierung von Carbonylverbindungen. Durch Zugabe von Kaliumhydroxid und Ethylendiamin erhöhte sich die Reaktionsgeschwindigkeit bei der Reduktion von Acetophenon zu 1-Phenylethanol stark.[12,13] Die Forscher vermuteten, dass sich unter den Reaktionsbedingungen Rutheniumamid-Komplex **5** bildet, der H_2 unter aktiver Beteiligung des Amid-Stickstoffs spaltet (Schema 1b). Im Zuge der heterolytischen H_2-Spaltung in ein formales Proton und Hydrid kommt es zu einem Bindungswechsel eines X- zu einem L-Typ Liganden in Komplex **6**.[14]

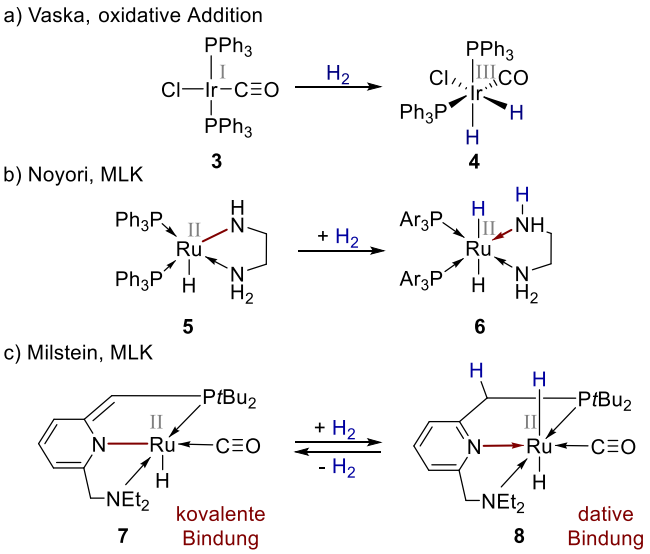

Schema 1: Beispiele für die Aktivierung von H_2 durch oxidative Addition und Metall-Liganden-Kooperation.

Die Bindung eines X-Typ Liganden zum Metall kann dabei auch als kovalente Bindung bezeichnet werden, bei deren Bildung sowohl Ligand als auch Metall ein Elektron zur Bindung beisteuern. Die Bindung eines L-Typ Liganden wird auch als koordinative Bindung bezeichnet. Formal kommen in diesem Fall beide Bindungselektronen vom Liganden. Bei einer formalen heterolytischen Dissoziation

des Komplexes sind X-Typ Liganden anionisch und L-Typ Liganden neutral. Dieser Mechanismus der Bindungsaktivierung wurde experimentell und computerchemisch ausführlich untersucht.[15,16] Neuere computerchemische Studien von Dub untersuchen, in welchem Umfang dieser Mechanismus in der Katalyse eine Rolle spielt.[17] Während bei der H_2-Aktivierung durch Komplex **5**, der direkt am Ruthenium gebundene Amid-Stickstoff an der Bindungsspaltung beteiligt ist, verläuft dies bei dem von Milstein und Mitarbeitern entwickelten Ruthenium-Pinzetten-Komplex **7** über eine Rearomatisierung des Enamid-Liganden zu einem dativen Pyridin-Liganden in **8** (Schema 1c).[18] Während das Ruthenium in der heterolytischen H_2-Spaltung den hydridischen Wasserstoff bindet, wird der ungesättigte Seitenarm des PNN-Liganden protoniert. Auch hier kommt es im Zuge der Bindungsaktivierung zu einem Wechsel eines X- zu einem L-Typ Liganden. In beiden Fällen ändert sich die Oxidationsstufe des Rutheniums nicht. Milstein und Khusnutdinova definieren in ihrem ausführlichen Übersichtsartikel drei Kriterien für die MLK[19]:

"*1. Sowohl das Metall als auch der Ligand nehmen an Bindungsbildungs- oder Bindungsspaltungsschritten teil.*

2. Sowohl das Metall als auch der Ligand werden bei der Bindungsaktivierung chemisch modifiziert.

3. Die Koordinationsweise des kooperativen Liganden unterliegt einer signifikanten Veränderung in der ersten Koordinationsschale infolge der Bindungsaktivierung."

Kriterium drei beschreibt hierbei den bereits erwähnten Wechsel eines X- zu einem L-Typ Liganden.

Die Anwendung der MLK in der Katalyse ist vielfältig. Neben Hydrierungen[5,12,20] konnten Milstein und Mitarbeiter durch Verwendung von Komplex **7** sekundäre Amide aus Alkoholen und primären Aminen synthetisieren, wobei als einziges Nebenprodukt H_2 entsteht (Schema 2).[21] Die Reaktion verläuft über die Dehydrierung des Alkohols zum Aldehyd, nukleophiler Angriff des Amins unter Bildung des Halbaminals und erneuter Dehydrierung. Dabei dient Komplex **7** zur H_2-Abspaltung vom Alkohol bzw. Halbaminal. Der nach der Dehydrierung entstandene Komplex **8** setzt elementaren Wasserstoff frei und regeneriert so Katalysator **7**. In welchem Umfang und bei welchen Systemen der Mechanismus über eine Dearomatisierung/Aromatisierungssequenz in der Katalyse eine Rolle spielt, ist noch Gegenstand einer wissenschaftlichen Debatte.[22]

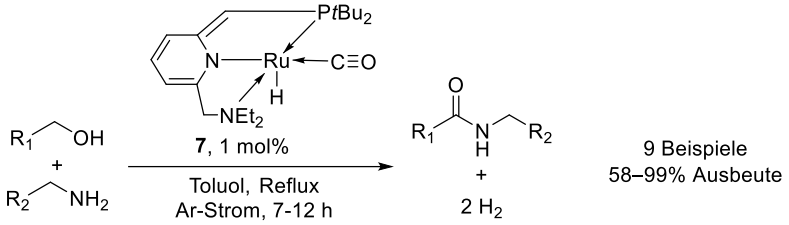

Schema 2: Synthese sekundärer Amide durch dehydrogenative Kupplung von Alkoholen und primären Aminen katalysiert durch Ruthenium-Komplex **7**.

Des Weiteren können die chirale Ruthenium-Diamid-Komplexe von Noyori wie **9** in der enantioselektiven Transferhydrierung von Ketonen eingesetzt werden (Schema 3).[16,23] Als Wasserstoffsurrogat dient dabei Isopropanol, das von Komplex **9** über MLK unter Beteiligung des Amid-Stickstoffs zu Aceton dehydriert wird und anschließend den abgespaltenen Wasserstoff auf das Substrat überträgt. Durch Abdestillation des niedrig siedenden Acetons kann das Gleichgewicht weiter auf die Produktseite verschoben werden.

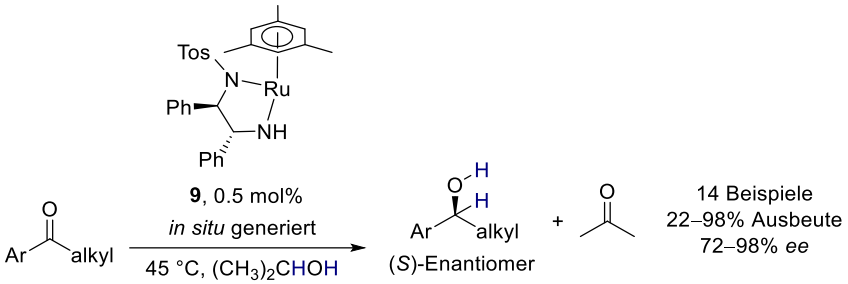

Schema 3: Enantioselektive Transferhydrierung von Ketonen mit Isopropanol katalysiert durch Komplex **9** über MLK.

Das Konzept der MLK wurde auf eine Vielzahl weiterer Übergangsmetalle, Liganden und Anwendungen übertragen. Für einen umfangreicheren Überblick sei hier auf entsprechende Übersichtsartikel verwiesen.[19,24]

3.1.2 Frustrierte Lewis-Paare

Die reversible Aktivierung von H_2 war bis zu den 2000er Jahren nur für Übergangsmetallkomplexe bekannt. Zwar berichten einzelne wissenschaftliche Arbeiten, dass Supersäuren,[25] Alkyl- oder Iodoborane[26] und starke Basen wie Kalium-*tert*-butanolat[27] unter harschen Bedingungen die Hydrierung von Kohlenwasserstoffe oder Ketonen unter hohen H_2-Drücken katalysieren können, aber die direkte und reversible Aktivierung von H_2 durch metallfreie Systeme konnte nicht beobachtet werden. Dies änderte sich durch die Entdeckung der *frustrierten Lewis-Paare*. Dabei bezeichnen FLP eine Kombination aus Lewis-Säure und -Base, die durch sterische Abstoßung keine klassischen Lewis-Addukte bilden können und somit mit anderen (kleinen) Molekülen reagieren. Bereits Brown und Mitarbeiter beobachteten 1942, dass Trimethylboran mit Pyridin ein Lewis-Addukt bildet, jedoch aufgrund sterischer Abstoßung zwischen den Methylgruppen nicht mit 2,6-Lutidin (Schema 4).[28]

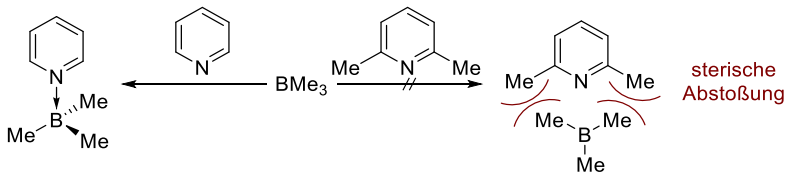

Schema 4: Beobachtung von Brown zur Reaktion von BMe_3 mit Pyridin und 2,6-Lutidin.

Die Gruppe um Stephan synthetisierte 2006 das Phosphinboran **10**, welches aufgrund von sterischer Abschirmung durch die Mesityl- und Pentafluorphenylsubstituenten in Lösung als Monomer vorliegt.[29] Durch das ungequenchte Lewis-acide und Lewis-basische Zentrum kann **10** kooperativ als Elektronendonor und -akzeptor mit H_2 zu Phosphinoborat **11** reagieren. Unter Hitze gibt dieses H_2 unter Regeneration von **10** ab (Schema 5a). Der Begriff *frustriertes Lewis-Paar* wurde ein Jahr später in einer Publikation derselben Gruppe erstmalig verwendet.[30]

Neben der sterischen Abschirmung muss die energetische Lage des Lewis-Basen zentrierten HOMO (engl. für *highest occupied molecular orbital*) und Lewis-Säuren zentrierten LUMO (engl. für *lowest unoccupied molecular orbital*) passend sein, um eine kooperative Reaktion mit H_2 oder anderen Substraten zu ermöglichen. Praktisch wird dies meistens durch eine energetische Anhebung des HOMO durch elektronenschiebende Gruppen am Lewis-basischen Zentrum und Absenkung des LUMO durch elektronenziehende Gruppen am Lewis-aciden Zentrum erreicht. Dies wurde unter anderem

systematisch von der Gruppe um Paradies untersucht.[31] Aus diesem Grund werden häufig elektronenreiche Phosphine oder Amine als Lewis-Basen und elektrophile Borane wie $B(C_6F_5)_3$ (BCF) **12** oder $B(C_6F_5)_2$ substituierte Moleküle als Lewis-Säure eingesetzt. BCF ist ähnlich Lewis-acide wie Borhalogenide (z.B. BCl_3), im Vergleich z.B. gegenüber Luft jedoch wesentlich stabiler.[32,33]

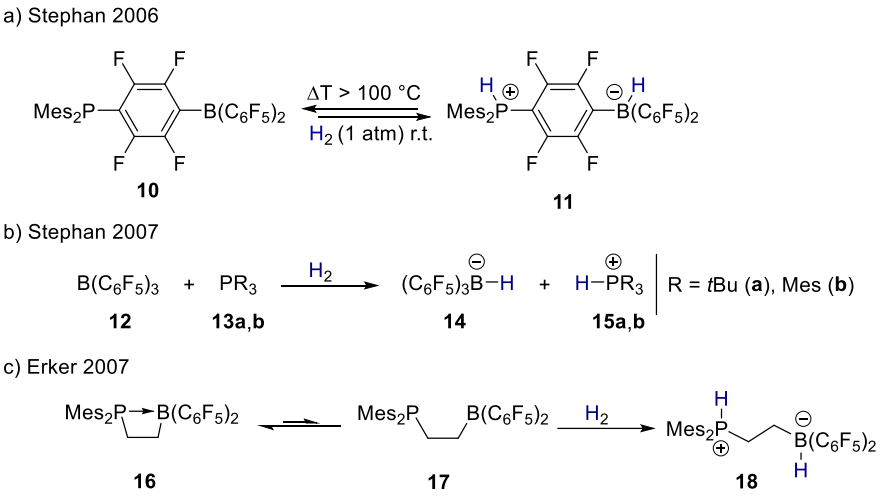

Schema 5: Beispiele von FLP für die Aktivierung von H_2.

2007 zeigte Stephans Gruppe, dass die intermolekulare Kombination aus BCF **12** und den Phosphinen **13a** und **13b** in Lösung nicht miteinander reagieren, jedoch H_2 zu Hydroborat **14** und den Phosphoniumkationen **15a** und **15b** spalten (Schema 5b).[34] Erkers Gruppe zeigte 2007, dass das zyklische Addukt **16** im Gleichgewicht mit seiner offenen Form **17** steht, die wiederum in der Lage ist H_2 zu Phosphinoborat **18** zu spalten (Schema 5c).[35]

Das Konzept der FLP lässt sich auch für die Bindungsaktivierung anderer Moleküle nutzen. Die Kombination aus BCF **12** und Phosphin **13a** aktiviert Olefine wie Ethylen in einer 1,2-Addition unter Bildung des Zwitterions **19**[30], während das geminale FLP **20** CO_2 zu Heterozyklus **21** anbindet (Schema 6).[36] Des Weiteren gelang die Aktivierung anderer kleiner Moleküle wie N_2O[37], SO_2[38] oder verschiedener Isocyanide.[39]

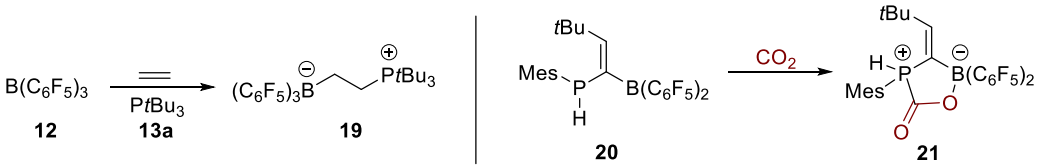

Schema 6: Beispiele für die Aktivierung von Ethylen und CO_2 durch FLP.

Neben Boranen, Aminen und Phosphinen können auch andere Elemente oder funktionelle Gruppen in FLP verwendet werden. Als Lewis-Basen konnten beispielsweise *N*-heterocyclische Carbene[40] oder Verkades Superbase[41] eingesetzt werden, während die Bandbreite von Lewis-Säuren unter anderem auf Kohlenstoff[42], Aluminium[43], Silizium[44] oder Borenium-Kationen[45] erweitert werden konnte. Des Weiteren können auch bestimmte Lewis-Addukte über einen FLP-Mechanismus H_2 aktivieren können.[46-48]

Der Mechanismus der H_2-Aktivierung wurde intensiv durch computerchemische Methoden von den Arbeitsgruppen von Pápai und Grimme erforscht.[49–53] Beide Gruppen gehen davon aus, dass sich Lewis-Säure und -Base vor der Reaktion mit H_2 zu einem sog. *Begegnungskomplex* zusammenfinden.

Dieser leicht endergon gebildete Komplex wird hauptsächlich durch dispersive Wechselwirkungen zwischen den sterisch anspruchsvollen Resten von Lewis-Säure und -Base stabilisiert (Abbildung 1). Die theoretische Vorhersage dieses Komplexes wurde durch Moleküldynamiksimulation gestützt[54] und konnte experimentell unter anderem durch NMR[55] und Neutronenstreuung[56] nachgewiesen werden.[57]

Der Modus der H_2-Spaltung unterscheidet sich in beiden Modellen. Das „*electron transfer*" (ET) Modell nach Pápai beschreibt die Spaltung von H_2 durch einen simultanen Elektronentransfer (Abbildung 1, oben). Dabei werden die σ-Elektronen der H_2-Bindung in das freie p-Orbital der Lewis-Säure doniert, während das freie Elektronenpaar der Lewis-Base in das σ*-Orbital von H_2 doniert.[49,50,53,54] Das „*electric field*" Modell (EF) von Grimme beschreibt, dass Lewis-Säure und -Base des FLP ein elektrisches Feld erzeugen, das stark genug ist, um H_2 barrierefrei zu spalten (Abbildung 1, unten). Die experimentell beobachtete Aktivierungsenergie muss aufgrund des Eintritts von H_2 in die Kavität des FLP und der damit verbundenen geometrischen Verzerrung des Begegnungskomplexes aufgebracht werden.[51,52] Zwar konnte Pápai zeigen, dass das bei sechs beispielhaft untersuchten FLP erzeugte elektrische Feld zu schwach und inhomogen ist, um H_2 zu spalten[53], jedoch bestätigte Pinter die Wichtigkeit des elektrischen Felds für die Polarisation der σ-Elektronen in H_2 für den darauf folgenden Elektronenübertrag.[58] Zusätzlich konnte gezeigt werden, dass bei bestimmten FLP die H_2-Aktivierung über Radikale abläuft (sog. *frustrated radical pairs*).[59]

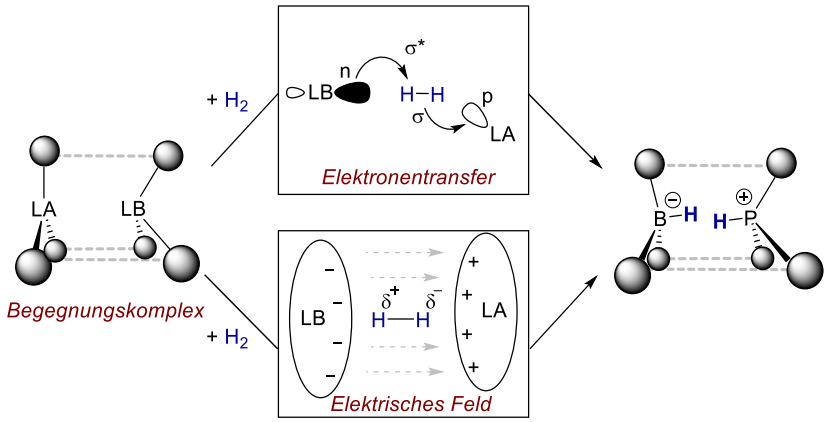

Abbildung 1: Schematische Darstellung des EF und ET Modells zur H_2-Spaltung durch FLP.

Die Aktivierung von H_2 prädestiniert die FLP als Katalysatoren für Hydrierungen.[60] 2008 gelang es den Gruppen um Stephan und Klankermeyer, sterisch gehinderte Imine und Aziridine zu den entsprechenden Aminen durch Verwendung von BCF **12** zu hydrieren (Schema 7a).[61] Dabei dient das Substrat selbst als Lewis-Base im FLP. Nach der H_2-Aktivierung wird ein Hydrid von Hydroborat **14** auf das protonierte Iminium- bzw. Aziridinium-Kation übertragen. Auch die Amin-Produkte selbst können mit BCF **12** H_2 aktivieren und als Protonenquelle dienen.[62] Aufgrund der Oxophilie der borbasierten Lewis-Säuren ist die katalytische Hydrierung von Ketonen und Aldehyden durch FLP schwierig.[35] Ashley und Stephan lösten dieses Problem parallel 2014 durch den dualen Einsatz von Ethern als Lösungsmittel und Lewis-Base (Schema 7b).[63] Über die Jahre wurden weitere Protokolle unter anderem für die Hydrierung von Heterocyclen[64], Amiden[65], Olefinen[66], Allenen[67], Phosphanoxiden[68] sowie enantioselektive Varianten entwickelt.[69] Für einen vollständigen Überblick sei hier auf entsprechende Übersichtsartikel verwiesen.[70]

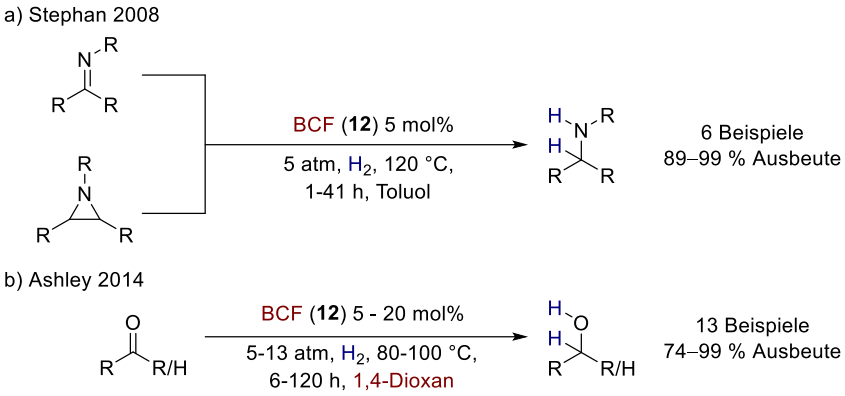

Schema 7: Katalytische Hydrierungen von Iminen, Aziridinen und Carbonylverbindungen durch FLP.

Die Hydrierung von unpolarisierten Alkinen ist für FLP problematisch, da die nach der H_2-Aktivierung entstandenen Borate nicht mit C–C-Dreifachbindungen reagieren und die protonierten Lewis-Basen nicht acide genug sind, um Alkine zu protonieren. Durch einen alternativen Reaktionsmodus über eine Hydroborierung gelang Repo und Mitarbeitern 2013 die katalytische (*Z*)-selektive Semihydrierung von internen Alkinen durch das *in situ* generierte FLP **22** (Schema 8).[71] Der Präkatalysator **23** aktiviert H_2 und spaltet über eine Protodeborylierung Pentafluorbenzol ab. Der aktive Katalysator **22** hydroboriert das Alkin zum Alkenylboran **24**. Dieses aktiviert H_2, bildet Zwitterion **25** und setzt das Produkt durch eine Protodeborylierung frei (Schema 8). Neben Hydrierungen gelang der Einsatz von FLP für die Aktivierung der zur H–H Bindung ähnlichen H–Si Bindung in Hydrosilylierungen[72] und der Hydroaminierung von terminalen Alkinen.[73]

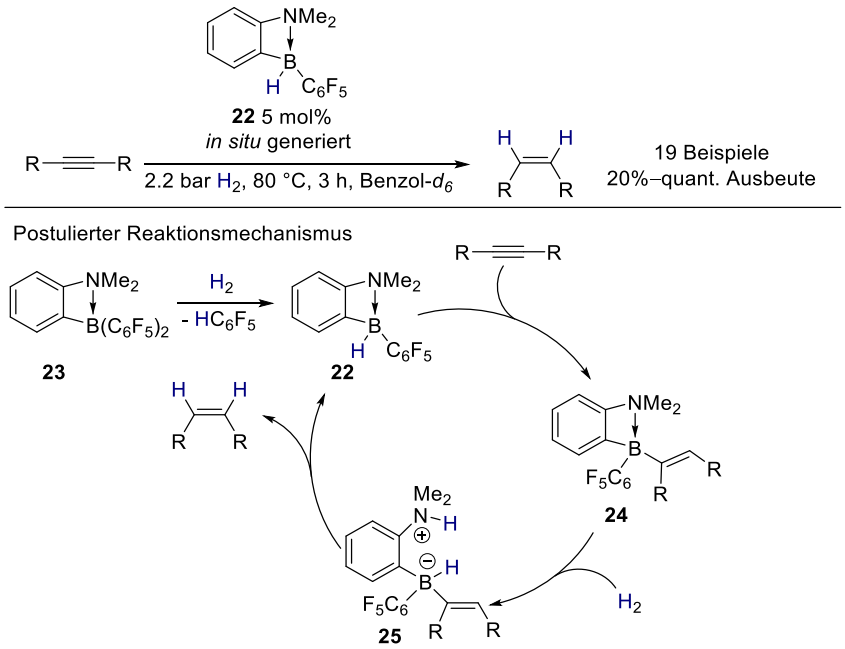

Schema 8: (*Z*)-selektive Semihydrierung von internen Alkinen durch **22** und der postulierte Reaktionsmechanismus.

3.1.3 Konzept und Beispiele der Bor-Liganden-Kooperation

Die BLK überträgt das Konzept der MLK auf metallfreie Systeme. Es beschreibt die Bindungsaktivierung bestimmter borhaltiger FLP. Im Zuge der heterolytischen Bindungsaktivierung kommt es zu einer Reorganisation von π-Elektronen. Dies führt zu einem Wechsel im Bindungsmodus zwischen Bor und einem Substituenten. In Analogie zum Wechsel eines X- zu einem L-Typ Liganden (siehe Schema 1) für Übergangsmetallkomplexe bei der MLK kann dies für Hauptgruppenverbindungen als Wechsel einer kovalenten zu einer dativen Bindung beschrieben werden (Schema 9).

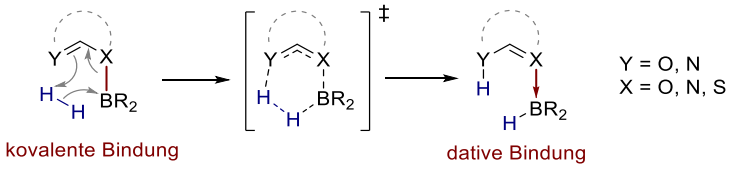

Schema 9: Allgemeines Konzept der BLK am Beispiel der H_2-Aktivierung.

FLP, MLK und BLK haben als Konzepte gemeinsam, dass die Bindungsaktivierung durch eine kooperative Reaktion des Substrats mit einem Lewis-aciden und Lewis-basischen Zentrum stattfindet.[74] Die Besonderheit der BLK (und MLK für Metalle) liegt im Wechsel des Bindungsmodus. So entsteht bei der Bindungsaktivierung von H_2 durch BLK als Produkt ein dativ gebundener Borankomplex (Schema 9), während bei klassischen FLP ein Hydroborat entsteht (vgl. Schema 5).

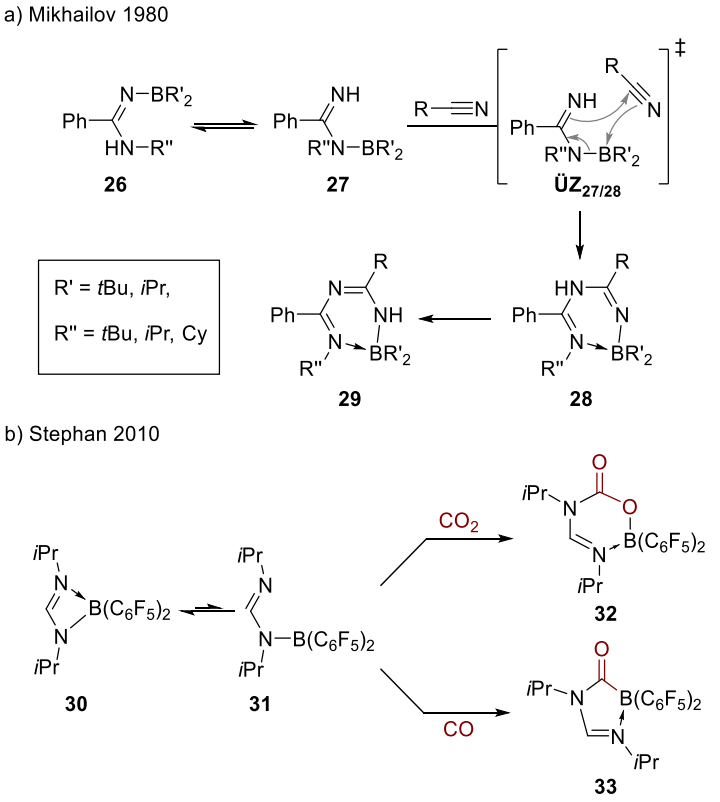

Schema 10: Beispiele von BLK durch Reaktivität von Boramidinen.

Ein frühes Beispiel für die BLK, ist die 1980 entdeckte Addition von Nitrilen an die Boramidine **26** zu den Aminoboranen **29**.[75] Die Autoren vermuteten, dass **26** im Gleichgewicht mit der tautomeren Form **27** steht. Diese reagiert mit Nitrilen via Übergangszustand **ÜZ$_{27/28}$**, wo es zur Verschiebung der π-Elektronen kommt und die vormalig kovalente N–B-Bindung zu einer dativen in Produkt **28** wird,

welches zuletzt zu **29** tautomerisiert (Schema 10a). Stephan und Mitarbeiter zeigten 30 Jahre später, dass das Boramidin **30** über seine offene Form **31** unter anderem mit CO_2 und CO zu den zyklischen Boran-Komplexen **32** und **33** reagiert.[76] Auch hier kommt es zum Wechsel einer kovalenten N–B-Bindung in **31** zu einer dativen Bindung in **32** und **33** (Schema 10b). Diese Boramidinate konnten auch für die Bindungsaktivierung von Alkinen, Isonitrilen, Aldehyden und Nitrilen eingesetzt werden, die über BLK verläuft.[77] In keinem der gezeigten Fälle gelang jedoch die Aktivierung von H_2.

Dies gelang zuerst durch das Pyrazolboran **34** von Tamm und Mitarbeitern (Schema 11).[78] Neben der irreversiblen Anbindung von H_2 in **35** und CO_2 in **36** gelang die Aktivierung von terminalen Alkinen zu **37**, Benzonitril zu **38** und Paraformaldehyd zu **39**. In allen Produkten kommt es laut Kristallstrukturanalyse zu einer Verlängerung der N–B-Bindung und Verkürzung bzw. Verlängerung der entsprechenden C–C-Bindungen im Pyrazolring, wie es nach den gezeigten Lewis-Strukturen in Schema 11 zu erwarten wäre. Dies unterstützt die Beschreibung des Bindungswechsels einer kovalenten zu einer dativen N–B-Bindung in den Pyrazol-Boran-Komplexen **35**-**39** unter gleichzeitiger Reorganisation der π-Elektronen im Pyrazolkern.

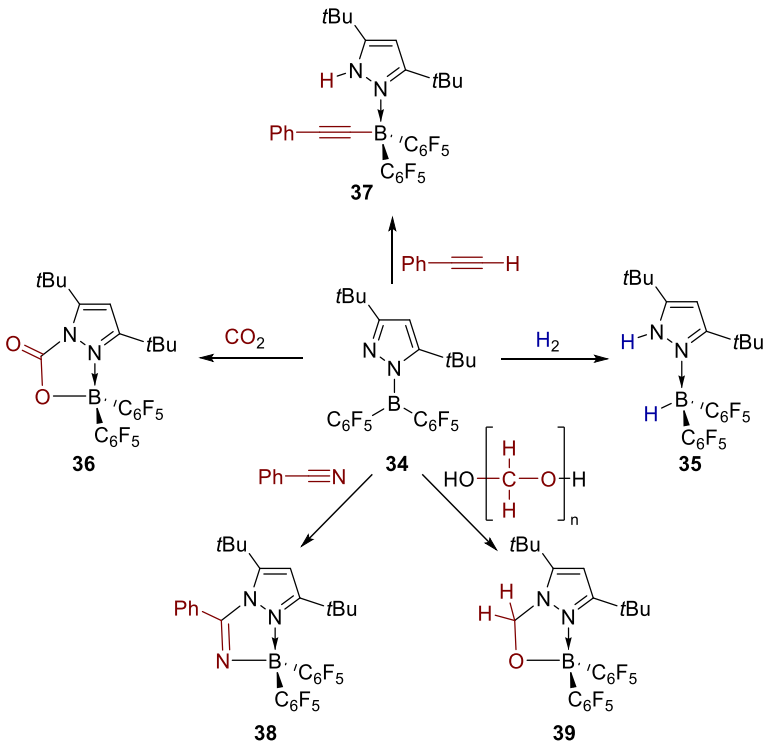

Schema 11: Bindungsaktivierung via BLK durch Pyrazolboran **34**.

Der erste konzeptionell geplante Versuch die Bindungsaktivierung über eine Rearomatisierung analog zu Milsteins Ruthenium-Pinzetten-Komplexen auf metallfreie Systeme zu übertragen, geschah durch eine computerchemische Studie von Wang und Mitarbeitern 2011.[79] Die Autoren berechneten, dass Enamidboran **40** mit einer Aktivierungsbarriere von 25.2 kcal mol^{-1} über Übergangszustand **ÜZ$_{40/41}$** unter Rearomatisierung des Pyridinrings H_2 spaltet und sich Komplex **41** bildet (Schema 12). Die Rückreaktion hingegen sollte aufgrund der Stabilität des Pyridinrings nicht möglich sein. Die Autoren vermuteten jedoch, dass die experimentelle Realisierung dieses Systems aufgrund von Nebenreaktion von **40** wie z.B. Dimerisierung nicht möglich sei.

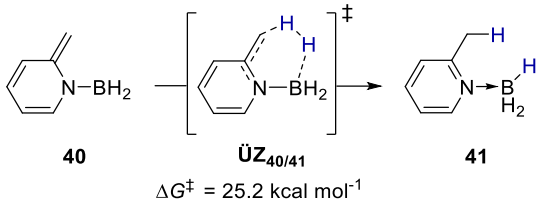

Schema 12: Übertragung des Bindungsaktivierungskonzepts der MLK auf metallfreie Systeme durch computerchemische Studien. Theorielevel: CCSD(T)/6-311++G(2d,p)//MP2/6-31G(d,p).

Von dieser Arbeit inspiriert, synthetisierten Gellrich und Milstein Aminoboran **42**, welches bei erhöhten Temperaturen H_2 abspaltet und Boran **43** mit einem dearomatisierten Pyridinring bildet (Schema 13).[80] Während im Zuge der H_2-Abspaltung der Pyridinring dearomatisiert, gewinnt der fünfgliedrige Borazyklus in **43** an Aromatizität und wird so stabilisiert. Die Autoren zeigten diesen Transfer von Aromatizität unter anderem durch die Berechnung der entsprechenden NICS-Werte (engl. *nucleus independent chemical shift*).[81]

Komplex **43** reagierte zwar nicht mit H_2, jedoch aktivierte er die N–H-Bindung von Benzylamin und die O–H von Benzoesäure kooperativ über den nukleophilen Enaminkohlenstoff als Lewis-Base und Bor als Lewis-Säure unter Rearomatisierung des Pyridinrings. Dabei bildet sich im ersteren Fall Aminoboran **44** und im letzteren Fall **45**. Im Zuge dieser Reaktionssequenzen ändert sich die dative Pyridin-N–B-Bindung in **42** zu einer kovalenten in **43** und bei der Reaktion mit Benzylamin und Benzoesäure wieder zu einer dativen Bindung in **44** und **45** (Schema 13). In dieser Publikation wird der Begriff *„boron-ligand cooperation“* erstmalig genutzt.

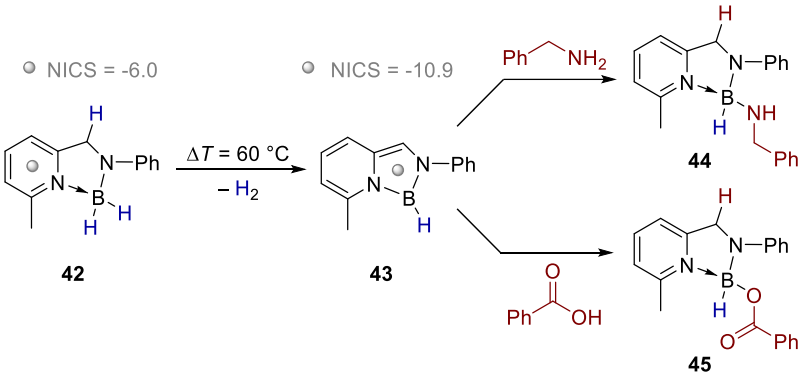

Schema 13: H_2-Abspaltung durch **42** und N–H bzw. O–H Aktivierung durch **43**. Theorielevel: M06-2X/def2-TZVPP.

Die reversible H_2-Aktivierung durch BLK gelang Gellrich im Jahr 2018 durch Zugabe von Piers Boran ($HB(C_6F_5)_2$) **46** zu 6-*tert*-butyl-2-pyridon **47**.[82] Dadurch bildet sich das Lewis-Addukt Pyridon-Boran **2**. Dieses verliert beim Erhitzen H_2 unter der Bildung von Boroxypyridin **1**, welches im Gleichgewicht mit der Pyridonat-Struktur **1'** steht (Schema 14). Reaktion mit H_2 führt zur Regeneration von **2**. Laut computerchemischen Rechnungen ist die Reaktion thermoneutral, während die H_2-Aktivierung ausgehend von **1'** eine freie Aktivierungsenthalpie von 19.6 kcal mol^{-1} benötigt, was in exzellenter Übereinstimmung mit den experimentellen Beobachtungen ist. Der Wechsel einer dativen O–B Bindung in **2** zu einer kovalenten Bindung in **1** im Zuge der H_2-Abspaltung bzw. umgekehrt im Zuge der H_2-Aktivierung konnte durch computerchemische und experimentelle Untersuchungen gestützt werden. Laut Rechnungen erhöht sich die Bindungslänge der C–O-Bindung im Zuge der H_2-Abspaltung von 1.27 Å auf 1.36 Å während sich die O–B-Bindung von 1.55 Å auf 1.36 Å verkürzt. Experimentell zeigt sich eine typische C=O Streckschwingungsbande im IR-Spektrum von **2**. Die Berechnung von NICS-

Werten zeigt, dass im Zuge der H_2-Abspaltung von **2** zu **1** die Aromatizität zunimmt. Die potentielle Anwendung von Boroxypyridin **1** und Derivaten für die Hydrierung von CO_2 wurde computerchemisch durch die Arbeitsgruppe von Chattaraj untersucht.[83] Im Zuge dieser Arbeit konnte gezeigt werden, dass Pyridon-Boran **2** stöchiometrisch Benzaldehyd über BLK reduzieren kann (siehe Kapitel 5.1).

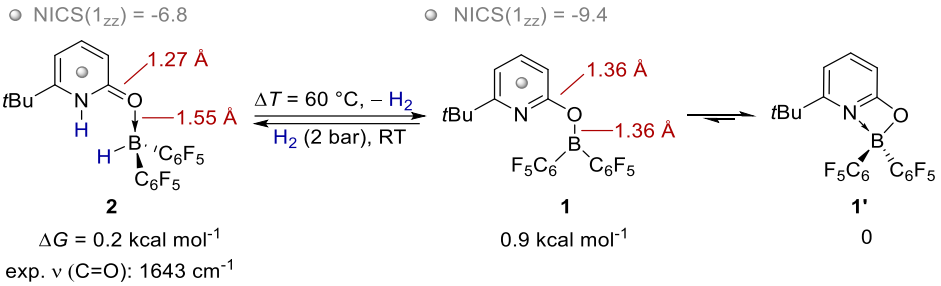

Schema 14: Reversible H_2-Aktivierung durch Boroxypyridin **1**. NICS-Werte berechnet mit PBE0/def2-TZVP mit der GIAO Methode, Bindungslängen berechnet mit PBE0-D3(BJ)/def2-TZVP und freie Enthalpien berechnet mit SMD(Benzol)-DLPNO-CCSD(T)/def2-TZVP//PBE0-D3(BJ)/def2-TZVP.

3.1.4 Anwendung der Bor-Liganden-Kooperation in der Katalyse

Der Wechsel einer kovalenten zu einer dativen Bindung im Zuge der Bindungsaktivierung mittels BLK impliziert eine interessante Folgereaktivität für die entsprechenden Systeme. Laut der IUPAC-Definition nach Haaland[84] ist eine dative Bindung schwächer als eine kovalente Bindung und der energetisch günstigste Mechanismus der Dissoziation in der Gasphase oder einem inerten Lösungsmittel ist die heterolytische Bindungsspaltung.[85] Dies ermöglicht die Dissoziation des Borans aus dem Produktkomplex nach der Bindungsaktivierung (Schema 15).

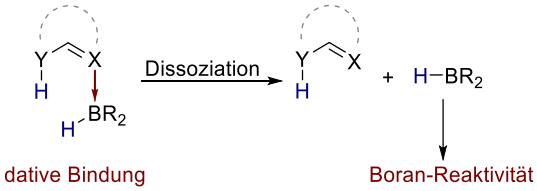

Schema 15: Schematische Darstellung der Dissozation eines dativ gebundenen Boran Komplexes.

Dies ermöglichte beispielsweise die Transferborylierung von Furylcatecholboran **48** auf verschiedene Heterozyklen, wo die Dissoziation im Zuge der BLK für die Freisetzung des Produkts und Regeneration des Katalysators verantwortlich ist.[86,87] Fontaine und Mitarbeiter entwickelten zwei Katalysatorgenerationen. Mit Thiopyridon **49** werden 25 mol% Katalysatorladung und fünf Äquivalente Furylcatecholboran benötigt. Durch Verwendung von Thiothiazolon **50** konnte die Katalysatorladung bei bis zu 71 % besseren Ausbeuten auf 5 mol% und die benötigten Äquivalente Furylcatecholboran **48** auf zwei reduziert werden (Schema 16).

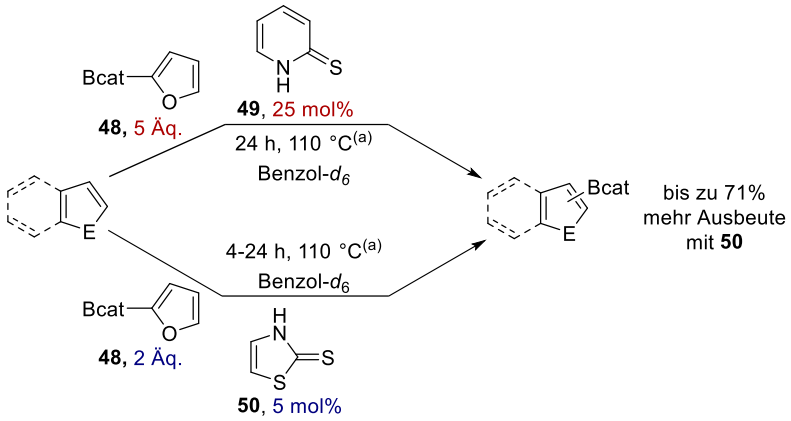

Schema 16: Transferborylierung von Furylcatecholboran auf Heterozyklen katalysiert durch **49** und **50**. (a) geschlossenes Reaktionssystem.

Der postulierte Mechanismus ist für beide Katalysatoren analog und wird in Schema 17 allgemein erläutert. Im ersten Schritt bildet das S–H-Tautomer des Katalysators **51** mit **48** das Lewis-Addukt **52**. Dieses wird anschließend unter Abspaltung von Furan konzertiert zu **53** boryliert, was mit einem Bindungswechsel der dativen N–B zu einer kovalenten Bindung einhergeht. Der Borylrest wird anschließend konzertiert auf das Substrat übertragen, wobei es wieder zum Bindungswechsel in **54** kommt. Dies ermöglicht die Dissoziation des borylierten Substrats **55** und regeneriert den Katalysator.

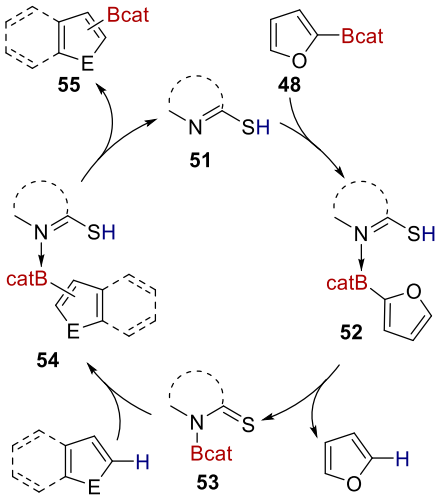

Schema 17: Mechanismus für die Transferborylierung von Furylcatecholboran **48** auf verschiedene Heterozyklen.

Durch Verwendung von Thioimidazolon **56** konnte die Substratbreite auf terminal Alkine erweitert werden.[87] Die *in situ* generierten Alkinylborane nutzten Fontaine und Mitarbeiter außerdem für die Michaeladdition an Chalkone zu Alkinonen mit katalytischen Mengen **57** (Schema 18).[87]

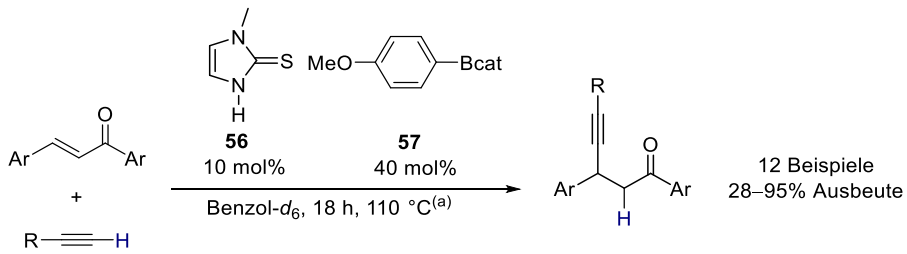

Schema 18: Bildung von Ketoalkinen aus Alkinen und Chalkonen (a) geschlossenes Reaktionsgefäß.

Im ersten Schritt wird analog, wie in Schema 17 gezeigt, der aktive Katalysator **58** durch die Borylierung von **56** über das S–H-Tautomer **60** durch Anisylcatecholboran **57** erzeugt (Schema 19). Dieser boryliert anschließend ein terminales Alkin unter Bildung von **59**. Der Bindungswechsel ermöglicht die Dissoziation von Alkinylboran **61**, das in einer Michaeladdition an Chalkone zu **62** addiert. Diese bilden ein Lewis-Addukt mit **60**. Durch eine Protodeborylierung von **63** bildet sich der Produktkomplex **64**.

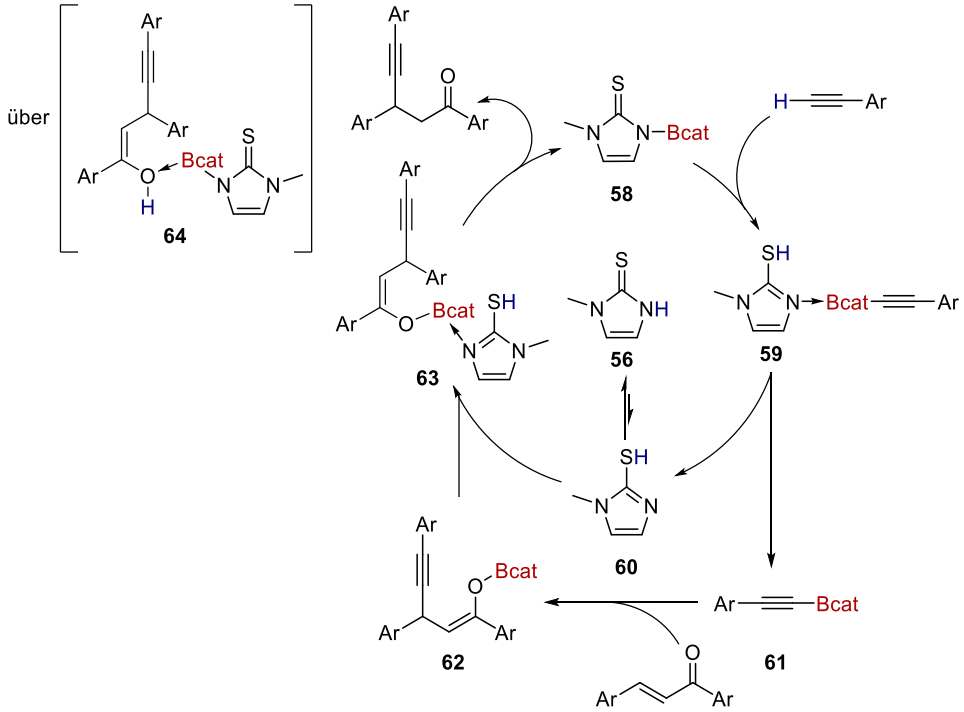

Schema 19: Mechanismus der Bildung von Alkinonen durch *in situ* Erzeugung von Alkinylboranen und Addition an Chalkone.

Der erneute Wechsel des Bindungsmodus der O–B und N–B Bindung ermöglicht die Freisetzung des Produkts durch Dissoziation und regeneriert den Katalysator **58**. Dies von den Autoren als *„boron recycling“* benannte Prinzip benötigt nur katalytische Mengen Bor und wird durch die BLK ermöglicht.

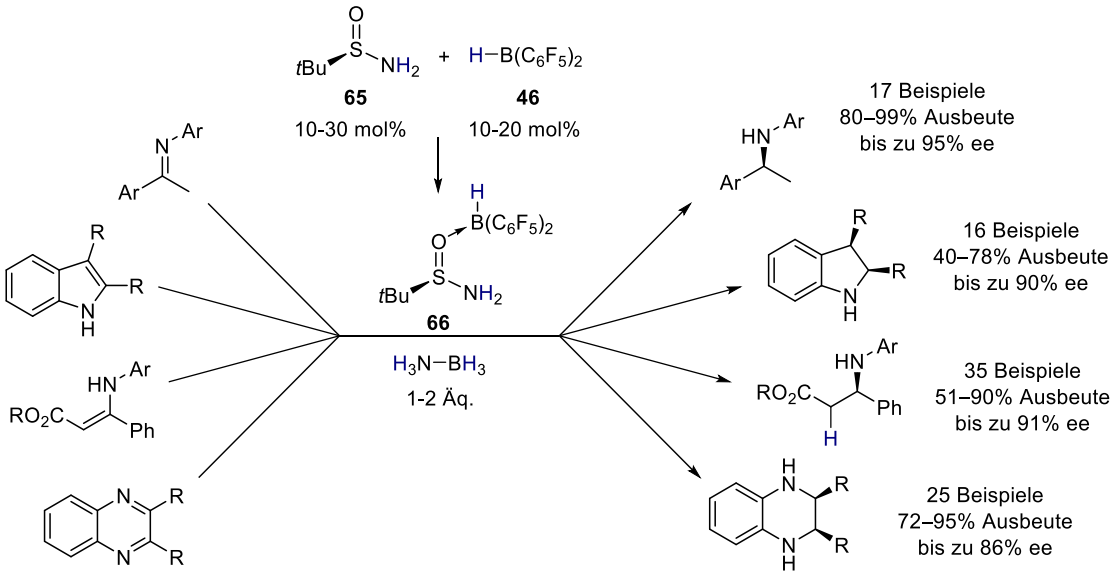

Schema 20: Substratbreite der enantioselektiven Transferhydrierung durch **66** und Amminboran.

Eine weitere Anwendung der BLK zeigte die Gruppe um Du in der substratbreiten enantioselektiven Transferhydrierung verschiedener ungesättigter Stickstoffverbindungen mit Amminboran. Als Katalysator diente dabei das chirale Sufinamid **65** in Kombination mit Piers Boran **46**. Als Substrate eigneten sich Imine[88], Indole[89], Enamine[90] und substituierte Chinoxaline (Schema 20).[91]

Die Autoren gehen aufgrund ihrer mechanistischen Untersuchungen davon aus, dass das Lewis-Addukt **66** der aktive Katalysator ist.[88] Dieser transferiert seinen hydridischen und protischen Wasserstoff konzertiert auf das Substrat, wobei sich das dehydrierte Aminoboran **67** bildet (Schema 21). Dieses wird über den sechsgliedrigen Übergangszustand **ÜZ$_{67/68}$** durch Amminboran rehydriert. In diesem Zuge ändert sich die kovalente N–B-Bindung zu einer dativen in **68**. Dies ermöglicht die Dissoziation vom Piers Boran **46** und die Rekoordination am Sauerstoff und regeneriert so den Katalysator **66**.

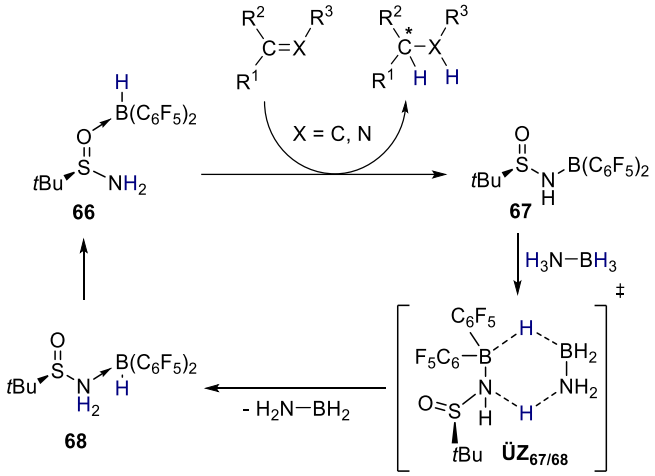

Schema 21: Postulierter Mechanismus der enantioselektiven Transferhydrierung.

Im Zuge dieser Arbeit wurden synthetische Anwendungen der BLK mit Boroxypyridin **1** als Katalysator untersucht. Durch H_2-Aktivierung von **1** gelang die *Z*-selektive Semihydrierung von internen und terminalen Alkinen über *in situ* erzeugte Alkenylborane (Schema 22, linker Katalysezyklus). Dabei aktiviert Boroxypyridin **1** H_2, wobei es zum Bindungswechsel einer kovalenten O–B zu einer dativen Bindung in **2** kommt. Dies ermöglicht die Dissoziation von Piers Boran **46**, welches das Substrat zum Alkenylboran **69** hydroboriert. Das Alkenylboran **69** bildet mit Pyridon **47** den Borankomplex **70**, welcher über eine Protodeborylierung das Produkt freisetzt und den Katalysator regeneriert (siehe Kapitel 5.4).

Ohne H_2 und in Anwesenheit terminaler Alkine katalysiert Boroxypyridin **1** deren *gem*-selektive Homodimisierung (Schema 22, rechter Katalysezyklus). Ähnlich der H_2 Spaltung aktiviert **1** die C–H-Bindung terminaler Alkine unter Bildung von Borankomplex **71**. Der Wechsel im Bindungsmodus der O–B-Bindung ermöglicht in diesem Fall die Dissoziation von Alkinylboran **72**, welches mit einem weiteren Äquivalent Alkin über eine 1,2-Carboborierung Enin **73** bildet. Durch Anlagerung an Pyridon **47** bildet sich Komplex **74**. Eine darauffolgende Protodeborylierung regeneriert den Katalysator Boroxypyridin und setzt das Produkt frei (siehe Kapitel 5.2).

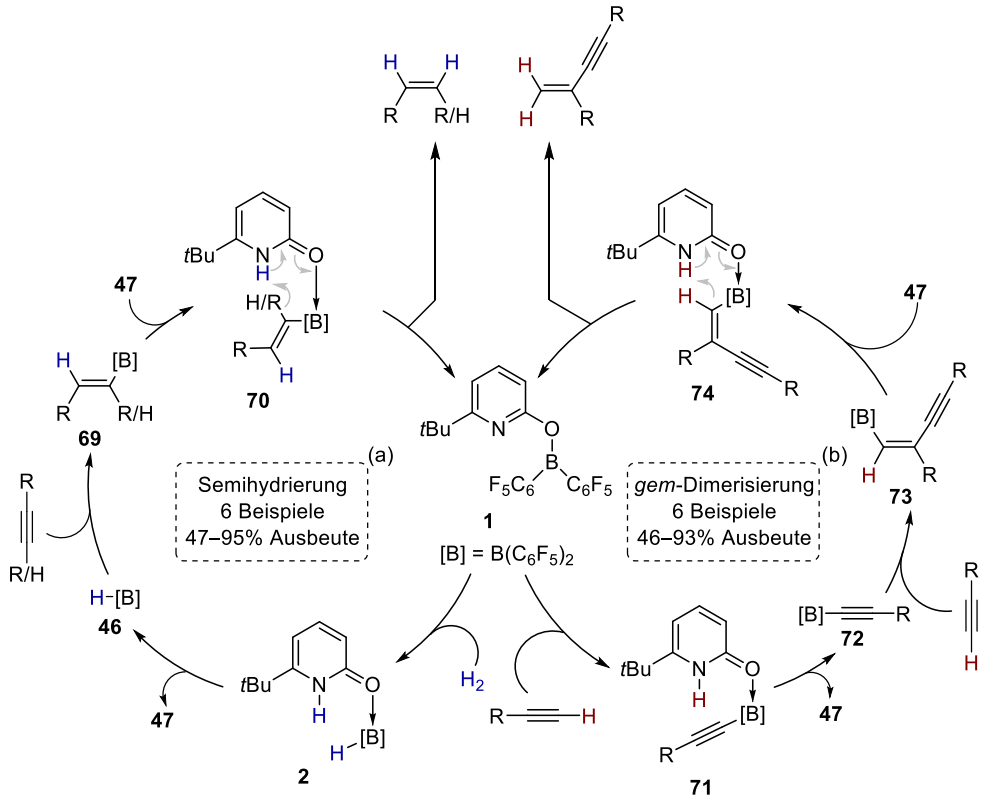

Schema 22: Mechanismus der Semihydrierung von internen und terminalen Alkinen und der *gem*-Dimerisierung von terminalen Alkinen katalysiert durch Boroxypyridin **1**.
(a) Reaktionsbedingungen: 5-10 mol% **1**, 5 bar H_2, *n*-Hexan, 80 °C, 20 h (b) 20 mol% **1**, Toluol, 100 °C, 6 h.

3.1.4.1 Allylierung von Acetonitril mit katalytischen Mengen Allylboran mittels BLK

Allylborane sind eine wichtige Klasse von Nukleophilen in der Organischen Synthese und werden häufig in der Totalsynthese von komplexen Molekülen verwendet.[92] In der Reaktion mit Elektrophilen, wie z.B. Aldehyde oder Ketone übertragen sie (bei der Verwendung chiraler Borane auch enantioselektiv) eine Allylgruppe unter der Bildung des entsprechenden Homoallylalkohols nach Aufarbeitung (Schema 23a).[93] Synthetisiert werden können Allylborane z.B. durch die Addition von Allylorganometall-Reagenzien an Bormethoxide oder durch die regioselektive Hydroborierung von Allenen oder 1,3-Dienen.[94] Die Gruppe um Brown synthetisierte beispielsweise Allylboran **76** durch die Hydroborierung von 1,1-Dimethylbuta-1,2-dien durch 9-BBN **75** (Schema 23b).[94]

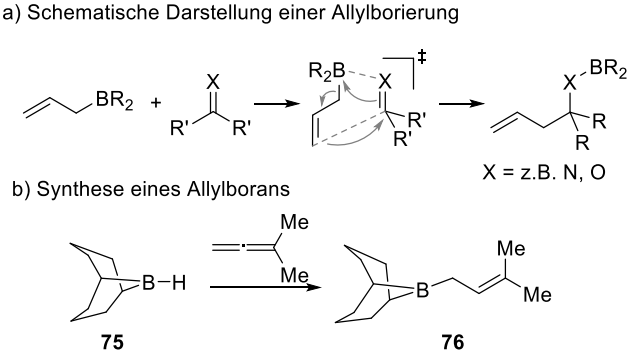

Schema 23: (a) Schematische Darstellung einer Allylierung durch ein Allylboran und (b) Synthese von Allylboran **76** durch die Hydroborierung von 1,1-Dimethylbuta-1,2-dien mit 9-BBN **75**.

Die Gruppe um Danishefsky nutzte Allylboran **76** in der Totalsynthese von Gypsetin **79**.[95] Dabei wird das chlorierte Indolderivat **77** in C2-Position von **76** allyliert, wobei nach Aufarbeitung Intermediat **78** erhalten wird, welches anschließend zum Zielmolekül Gypsetin umgewandelt wird (Schema 24). Wie schon in Schema 23 gezeigt, wurde Allylboran **76** über eine Hydroborierung synthetisiert.

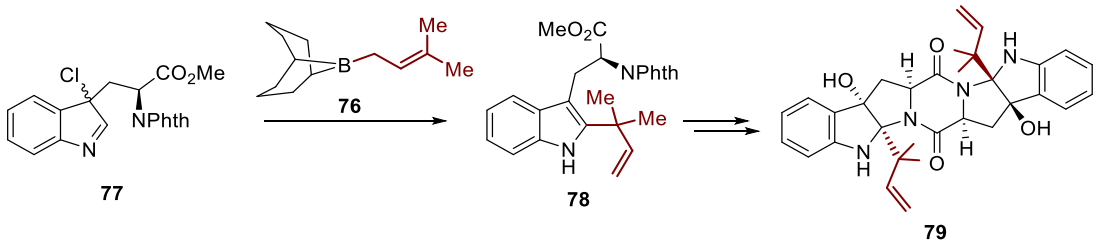

Schema 24: Allylborierung als Teil der Totalsynthese von Gypsetin **79**.

Wie in Kapitel 3.1.4 gezeigt, entsteht nach der H_2-Aktivierung durch Boroxypyridin **1** und Dissoziation aus **2** Piers Boran **46**. Dieses kann genutzt werden, um *in situ* die terminale C–C-Doppelbindung von Allenen unter Bildung eines Allylborans zu hydroborieren. In Anwesenheit von Acetonitril als Elektrophil und BCF als zusätzliche Lewis-Säure ermöglichte Boroxypyridin **1** eine Allylierung von Acetonitril zu den entsprechenden Allyliminen mit nur katalytischen Mengen eines *in situ* erzeugten Allylborans.

Der postulierte Mechanismus ist dabei ähnlich dem in Schema 22 abgebildeten. Boroxypyridin **1** aktiviert H_2 und bildet Pyridon-Boran **2**, das in Pyridon **47** und Piers Boran **46** dissoziiert (Schema 25). Durch die Hydroborierung eines Allens durch Piers Boran **46** bildet sich Allylboran **80**, das Acetonitril zum Imin-Boran-Komplex **81** allyliert. Nach Rekoordination von **81** an Pyridon **47** und barrierefreiem Protonübertrag zu Komplex **82** dissoziiert das Allylimin und wird von BCF **12** als Lewis-Addukt abgefangen, wobei gleichzeitig Katalysator **1** regeneriert wird (siehe Kapitel 5.5).

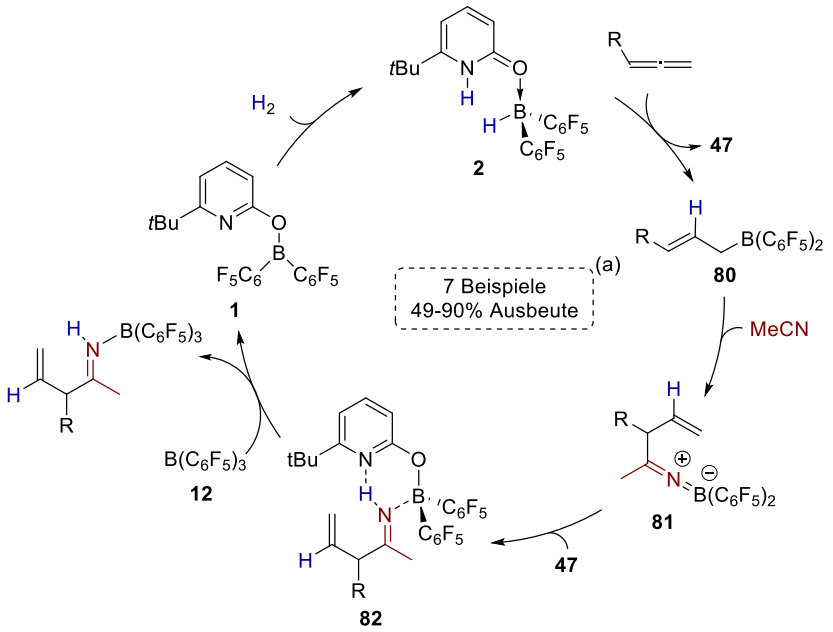

Schema 25: Mechanismus der Allylierung von Acetonitril, katalysiert durch Boroxypyridin **1**. (a) Reaktionsbedingungen: 10 mol% **1**, 1.1 bar H_2, Benzol, 80 °C, 16 h–7 Tage.

3.1.4.2 Katalytische Dehydrierung von Amminboran mittels BLK

Mit drei hydridischen sowie drei protischen Wasserstoffatomen und einem entsprechenden Wasserstoff-Gewichtsanteil von 19,6 % ist Amminboran (AB) als potentielles Wasserstoffspeichermaterial interessant.[96] Pro Molekül AB können bis zu drei Äquivalente H_2 abgespalten werden. Die thermische Freisetzung von mehr als einem Äquivalent H_2 benötigt jedoch Temperaturen von (weit) über 100 °C und ist mit signifikanter Zersetzung verbunden.[97] Katalysatoren, welche die H_2-Abspaltung aus AB bei niedrigeren Temperaturen selektiv katalysieren, basieren häufig auf Übergangsmetallkomplexen der fünften und sechsten Periode.[98] Aber auch Nickel und Eisen basierte Komplexe katalysieren die AB-Dehydrierung mit hohen Wechselzahlen.[99] Beispiele für metallfreie Systeme sind starke Brønsted-Basen[100] und -Säuren.[101] Wegner und Mitarbeiter zeigten, dass eine Bisboran basierte Lewis-Säure die Abspaltung von bis zu 2,5 Äquivalenten H_2 aus AB bei 60 °C katalysieren kann.[102]

Durch ihre Fähigkeit, H_2 (reversibel) zu spalten, wurden auch FLP als mögliche Katalysatoren für die AB Dehydrierung untersucht. Die Polarisation der Wasserstoffatome in AB in hydridische und protische Wasserstoffe prädestiniert diese zur Reaktion mit Lewis-aciden bzw. Lewis-basischen Zentren, wie sie in FLP vorhanden sind. Miller und Gruppe entdeckten, dass das prototypische FLP aus Phosphin **13a** und BCF **12** stöchiometrisch H_2 aus AB entfernen kann.[103] Die ionischen Produkte **15a** und **14** spalten jedoch selbst kein H_2 ab, was eine Katalyse verhindert (Schema 26a). Die Gruppe um Slootweg fand 2013 heraus, dass das geminale Al/P-FLP **83** stöchiometrisch unter H_2-Abspaltung an AB addiert. Eine Katalyse wird durch Verwendung von Dimethylamminboran **84** ermöglicht.[104] Dabei entsteht das Zwitterion **85**, das unter Bildung von **86** das FLP **83** als Katalysator regeneriert (Schema 26b).

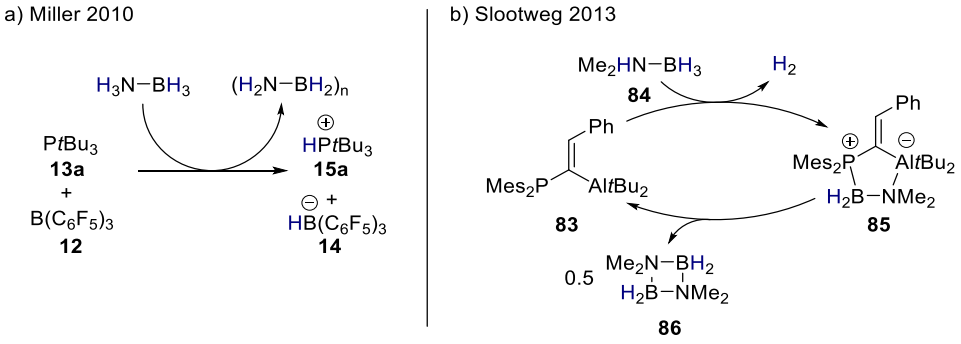

Schema 26: Katalytische und stöchiometrische Dehydrierung von Amminboranen durch FLP.

Aldridge *et al.* nutzten für die katalytische AB Dehydrierung das Xanthen basierte FLP **87**.[105] Im ersten Schritt des Katalysezyklus wird die B–H-Bindung von AB unter Bildung von **88** gespalten (Schema 27). Dieses reagiert in einer dehydrogenativen Kupplung mit einem weiteren Äquivalent AB zu **89**. Durch weitere Kupplung mit AB und anschließendem Ringschluss spaltet sich **90** ab und der Katalysator wird regeneriert. Im weiteren Verlauf der Reaktion wird **90** durch **87** weiter zu Borazin **91** dehydriert. Mit einer Wechselzahl von 4 h^{-1} ist **87** jedoch wesentlich weniger reaktiv als übergangsmetallbasierte Katalysatoren.

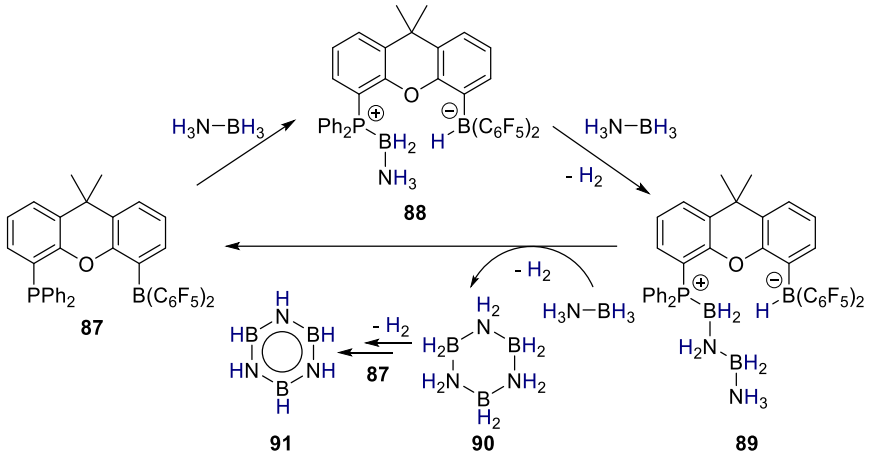

Schema 27: Mechanismus der katalytischen Dehydrierung von AB durch das Xanthen-basierte FLP **87**.

Im Zuge dieser Arbeit konnte gezeigt werden, das Thiopyridon **92** als Organokatalysator die AB-Dehydrierung über BLK mit einer Wechselzahl von 88 h^{-1} über BLK katalysiert. Schema 28 zeigt den postulierten Mechanismus dieser Dehydrierung. Im verwendeten Lösungsmittel THF liegt Thiopyridon **92** als wasserstoffbrückengebundenes Dimer $\mathbf{92_2}$ vor. Über diese Struktur tautomerisiert es zum Mercaptopyridindimer $\mathbf{93_2}$. Das Monomer **93** reagiert nach Dissoziation mit der sauren S–H-Funktionalität mit AB über $\mathbf{ÜZ_{93/94}}$ in einer dehydrogenativen Kupplung zu Addukt **94**. Die Wasserstoffbrückenbindung des Pyridinstickstoffs zum N–H prädestiniert diesen für eine intramolekulare Deprotonierung unter Reorganisation von π-Elektronen. Der mit der Deprotonierung einhergehende Wechsel der kovalenten S–B-Bindung zu einer dativen, ermöglicht die Dissoziation von **95** und regeneriert unter Dimerisierung mit **92** den Katalysator $\mathbf{92_2}$ (siehe Kapitel 5.3). Im Laufe der Reaktion reagiert **95** weiter zu Borazin **91** und Polyborazylen.

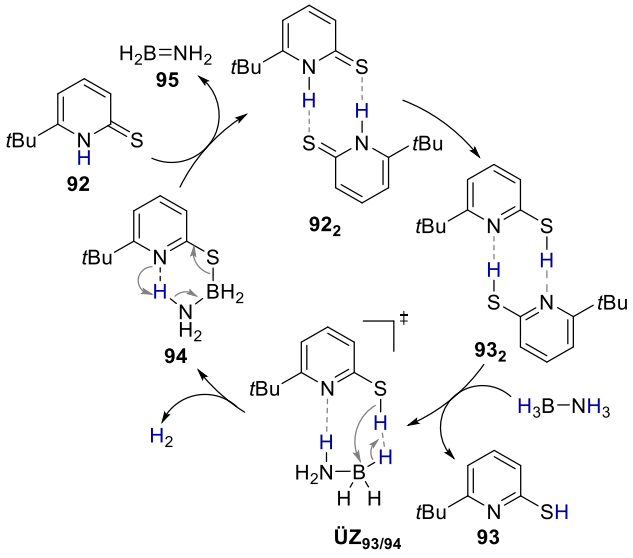

Schema 28: Mechanismus der katalytischen Dehydrierung von AB durch Thiopyridon **92**.

Für Beispiele für die katalytische AB Dehydrierung über z.B. heterogene Systeme oder Nanopartikel sei hier auf entsprechende Übersichtsartikel verwiesen.[106] Eine weitere große Herausforderung für den Einsatz von AB als Wasserstoffspeichermaterial ist die Regeneration des verbrauchten AB, meistens aus Borazin, Polyborazylen. Ein großer Fortschritt wurde dabei durch die Gruppe von Gordon erzielt, die durch Hydrazin AB aus Borazin und Polyborazylen fast quantitativ regenerieren konnten.[107]

3.2 Carboborierungen

Borane können mit C–C-Mehrfachbindungen unter Bildung einer neuen C–B- und C–C-σ-Bindung unter Bruch der C–C-π-Bindungen und einer ursprünglichen C–B-σ-Bindung reagieren. Diese Carboborierungen sind synthetisch von Interesse, da sie neben einer neuen C–C-Bindung das Substrat borylieren. Borylgruppen können z.B. durch die immens wichtige Suzuki-Miyaura-Kupplung weiter funktionalisiert werden.[108] Aufgrund der Stabilität der zu brechenden C–B-Bindung benötigen die meisten Carboborierungen übergangsmetallbasierte Katalysatoren.[109] Unter Verwendung von sehr Lewis-aciden Boranen oder speziellen Substraten können diese auch unkatalysiert ablaufen. Diese unkatalysierten Carboborierungen sind atom-ökonomisch und wurden in den letzten zehn Jahren verstärkt erforscht. Dabei sind 1,1-Carboborierungen, bei denen unter Wanderung eines Restes am Substrat die neue C–B- und C–C-Bindung am selben Kohlenstoff gebildet wird, häufiger als die entsprechenden 1,2-Carboborierungen (Schema 29). Im Folgenden werden Beispiele der 1,1- und 1,2-Carboborierungen erläutert.

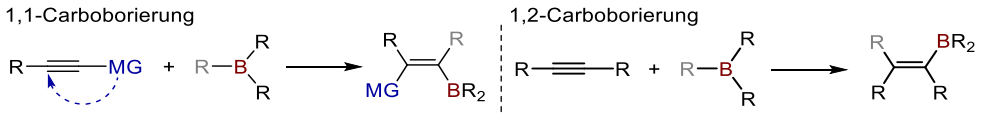

Schema 29: Schematische Darstellung von 1,1- und 1,2-Carboborierungen von Alkinen (MG engl. für *migrating group*).

3.2.1 1,1-Carboborierungen

Systematisch untersucht wurden übergangsmetallfreie Carboborierungen durch Wrackmeyer und Mitarbeiter in den 1970er Jahren.[110] In der als Wrackmeyer-Reaktion bekannten 1,1-Carboborierung reagiert Triethylboran mit dem Trimethylzinn substituierten Alkin **96** zu dem Alkenylboran **98** (Schema 30). Dabei kommt es zur Bildung des Intermediates **97**, in der die Sn–C-Bindung gebrochen wurde. Das Alkenylboran **98** bildet sich unter 1,2-Verschiebung des Zinnsubstituenten, während die neue C–C- und C–B-Bindung am selben Kohlenstoff gebildet werden. Typisch für die Wrackmeyer-Reaktion ist die Verwendung von Alkinen, die mit schwereren Elementen der vierten Hauptgruppe substituiert sind, da diese eine (partiell) positive Ladung im Reaktionsverlauf stabilisieren.[111]

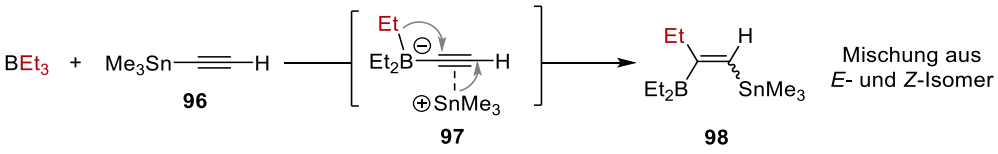

Schema 30: Wrackmeyer-Reaktion von Triethylboran mit dem Trimethylzinn substituierten Alkin **96**.

Ein Durchbruch in der Weiterentwicklung dieser Reaktionen gelang 2010 parallel den Gruppen von Erker und Berke.[112] Diese entdeckten, dass Carboborierungen unter Verwendung der Lewis-acideren $RB(C_6F_5)_2$ basierten Borane (meistens BCF **12**) auch mit unsubstituierten Alkinen ablaufen. Erker und Mitarbeiter setzten dabei symmetrische interne Alkine mit BCF **12** oder dem Methylderivat **99** um, wobei sich unter 1,2-Umlagerung eines R'-Substituenten Alkenylboran **100** bildet (Schema 31a). Diese Reaktionen benötigen neben hohen Temperaturen auch lange Reaktionszeiten.

Die Folgereaktivität der 1,1-Carboborierungsprodukte wurden ein Jahr später durch Erker untersucht. Im Zuge der Carboborierung von terminalen Alkinen mit den Boranen **12** oder **99** kommt es zur Bildung

von Alkenylboran **101** als unselektive Isomerenmischung (Schema 31b). In einer Eintopfreaktion wurde diese photochemisch zum thermodynamisch stabileren Isomer umgewandelt und die Borylgruppe anschließend in einer Suzuki-Miyaura-Reaktion mit Aryliodiden zu **102** gekuppelt.[113]

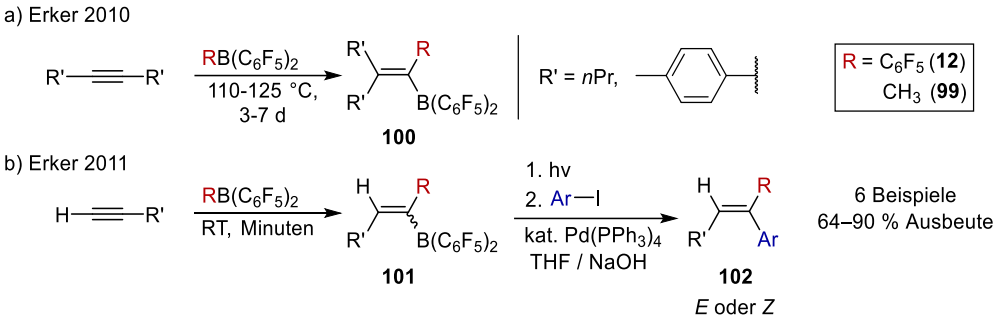

Schema 31: 1,1-Carboborierungen von internen und terminalen Alkinen durch Lewis-acide Borane.

Je nach verwendetem Substrat kann die Reaktion von Lewis-aciden Boranen mit ungesättigten Verbindungen Tandem-Reaktionen initiieren, die mehrere C–C-Bindungen in einer Reaktionssequenz knüpfen. Bei der Reaktion von Eninen mit BCF **12** können je nach Substitutionsmuster im Substrat **103**, Bizyklus **107** oder die entsprechenden Ringöffnungsprodukte **108** oder **109** isoliert werden.[114] Laut postuliertem Mechanismus wird die Reaktionssequenz durch die Koordination von BCF **12** an die Dreifachbindung der Substrate **103** in **104** initiiert. Dies aktiviert die Dreifachbindung für einen intramolekularen Angriff durch die Doppelbindung, wodurch sich Zwitterion **105** unter Ausbildung eines fünfgliedrigen Rings bildet. Durch anschließende Dreiringbildung in **106** befindet sich ein Carbokation in α-Position zur $B(C_6F_5)_3$-Gruppe. Ladungsneutralität wird durch die Wanderung eines C_6F_5-Rings in **107** in einer 1,1-Carboborierung wiederhergestellt.

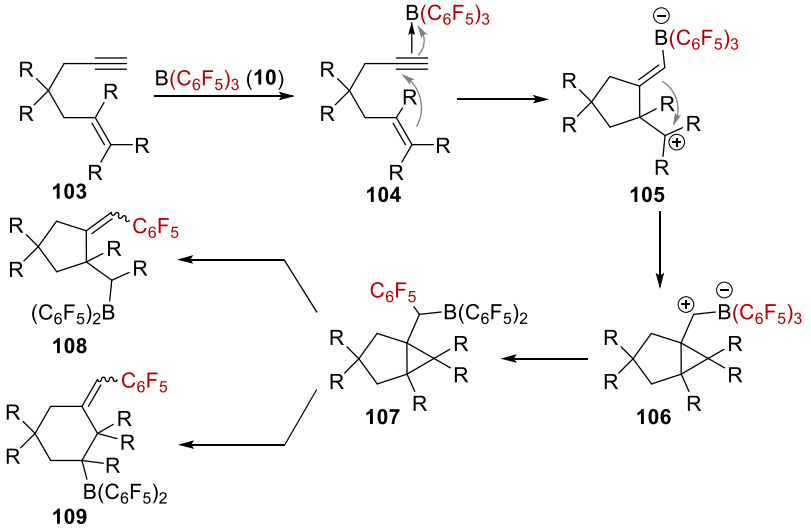

Schema 32: Tandem Reaktion von Eninen mit BCF **12**.

In ähnlichen Systemen konnte computerchemisch gezeigt werden, dass solch eine 1,2-Umlagerung eines C_6F_5-Rings barrierefrei verläuft.[115] Abhängig vom Substitutionsmuster kommt es anschließend zu einer Ringöffnung zum fünfgliedrigen Ring **108** oder sechsgliedrigen Ring **109**. In Kombination mit P*t*Bu$_3$ **13a** zeigten die Produkte **108** und **109** typische FLP-Reaktivität in der Aktivierung von H_2 und CO_2. Für einen vollständigeren Überblick über 1,1-Carboborierungen sei auf die entsprechende Literatur verwiesen.[115-117]

Im Zuge dieser Arbeit konnte gezeigt werden, dass Arylallene mit BCF **12** zu C_6F_5-substituierten Indenen **112** unter Abspaltung von Piers Boran **46** zyklisieren (Schema 33). Dabei bildet BCF **12** mit dem Allen das Zwitterion **110**. Nach einer Friedel-Crafts-artigen Zyklisierung und Rearomatisierung durch Protonenwanderung kommt es im Schlüsselschritt zu einer wie oben beschriebenen 1,2-Wanderung eines C_6F_5-Rings in **111** in einer formalen 1,1-Carboborierung. Durch eine Retrohydroborierung spaltet sich Piers Boran **46** und das Produkt Inden **112** wird gebildet (siehe Kapitel 5.7).

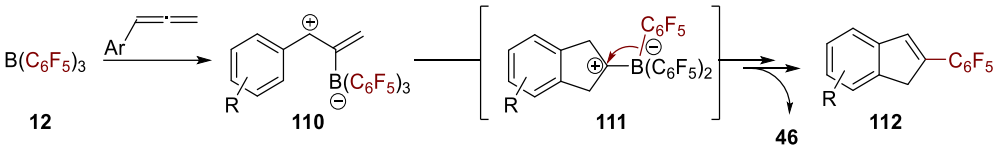

Schema 33: In dieser Arbeit untersuchte Bildung von Indenen **112** durch die Zyklisierung von Arylallenen mit BCF **12**.

3.2.2 1,2-Carboborierungen

Im Kontrast zur weit verbreiteten 1,2-Hydroborierung und verglichen mit 1,1-Carboborierungen sind unkatalysierte 1,2-Carboborierung seltener. Melen und Mitarbeiter entdeckten 2015, dass BCF **12** mit Allenylketonen **113** eine formale 1,2-Carboborierung mit der terminalen Doppelbindung des Allens eingeht.[118] Die Regioselektivität wird durch intramolekulare Bildung des sechsgliedrigen Rings in **114** mit dativer O–B-Bindung gesteuert (Schema 34a).

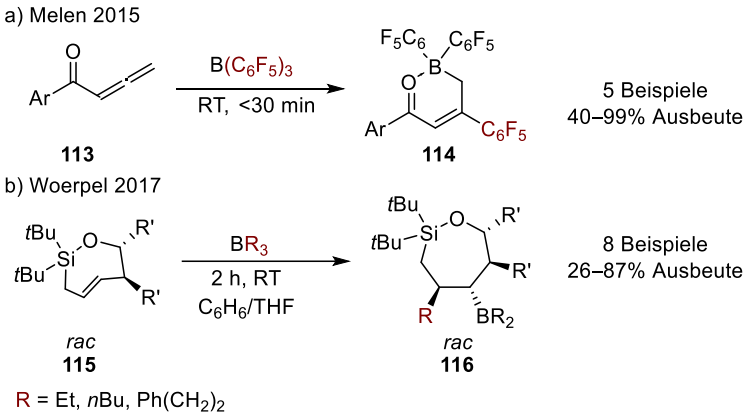

Schema 34: Beispiele für unkatalysierte 1,2-Carboborierungen.

Durch die Verwendung gespannter siebengliedriger Ringe mit einer *E*-konfigurierten Doppelbindung konnten Woerpel und Mitarbeiter statt der typischen C_6F_5-substituierten alkylsubstituierte Borane mit einer geringeren Lewis-Acidität verwenden.[119] Diese Carboborieren die Doppelbindung in **115** in einer konzertierten *syn*-Addition diastereoselektiv zu den Produkten **116** (Schema 34b).

Die durch die eingesetzten Borane übertragenen Gruppen in Carboborierungen sind häufig auf C_6F_5-Ringe (im Falle von BCF **12**) oder Alkylgruppen limitiert. Studer und Mitarbeiter zeigten 2021, dass Alkine mit Sulfonamidgruppen **117** von einer Vielzahl von Dichloroarylboranen unter selektiver Wanderung des Arylrests carboboriert werden.[120] Die luftempfindlichen Dichloroborane **118** setzten sie in einer Eintopfreaktion mit Pinakol und Triethylamin zu stabileren BPin-Derivaten **119** um (Schema 35). Die Dichlorarylborane **121** wurden *in situ* durch eine Transmetallierung der entsprechenden Silane **120** mit BCl_3 erzeugt.[121]

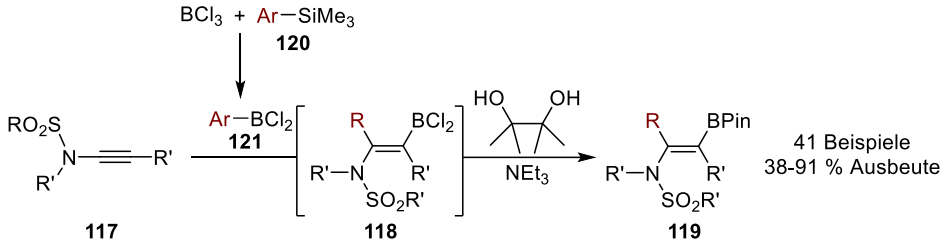

Schema 35: 1,2-Carboborierung von Alkynylsulfonamiden **117** mit Dichlorboranen **121** und Kondensation mit Pinakol.

Im Zuge dieser Arbeit konnte gezeigt werden, dass Alkenylborane **122** 1,2-Carboborierungen mit Allenen und terminalen Alkinen eingehen. Die Alkenylborane **122** werden dabei *in situ* durch die Hydroborierung von Alkinen mit Piers Boran **46** erzeugt. Durch Zugabe eines Allens bildet sich über die 1,2-Carboborierung der internen Doppelbindung des Allens das borylsubstituierte 1,4-Dien **123** (Schema 36). Durch Wechsel des Lösungsmittels von DCM zu THF/NaOH(aq.) und katalytischen Mengen $Pd(PPh_3)_4$ können diese mit Aryliodide in einer Suzuki-Miyaura-Kupplung zu den 1,4-Dienen **124** umgesetzt werden. Alle drei Reaktionspartner (Alkin, Allen und Aryliodid) können modular getauscht werden und die synthetische Vielfältigkeit dieser drei Stufen Eintopfsynthese wurde durch die Synthese 20 verschiedener Diene gezeigt (siehe Kapitel 5.9).

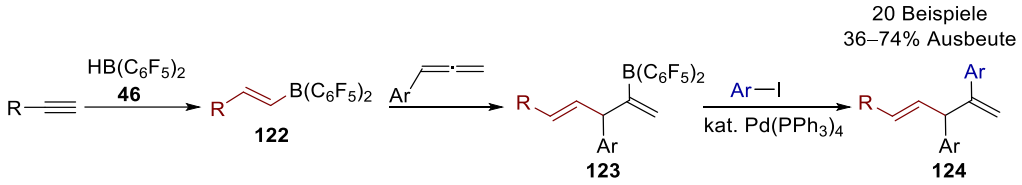

Schema 36: 1,2-Carboborierung von Allenen mit Alkenylboranen und anschließende Suzuki-Miyaura Kupplung.

Mit einem Überschuss Alkin reagieren die Alkenylborane **122** in einer Tetramerisierung zu den borylsubstituierten Tetrahydropentalenen **128** (Schema 37). Dabei deuten die mechanistischen Untersuchungen darauf hin, dass die Reaktionssequenz durch eine 1,2-Carboborierung von Alkenylboran mit einem weiteren Äquivalent Alkin zu 1,3-Dien **125** initiiert wird. Nach zwei weiteren 1,2-Carboborierungen von Alkinen bildet sich das Octatetraen **126**, was einer 8-π konratorische Elektrozyklisierung zu Cyclooctatrien **127** reagiert. Dieses bildet durch zwei konsekutive Umlagerungen Tetrahydropental **128** (siehe Kapitel 5.8). Neben computerchemischen Untersuchungen konnte die Position des ersten Äquivalents Alkin durch Deuterierungsexperimente bestimmt werden.

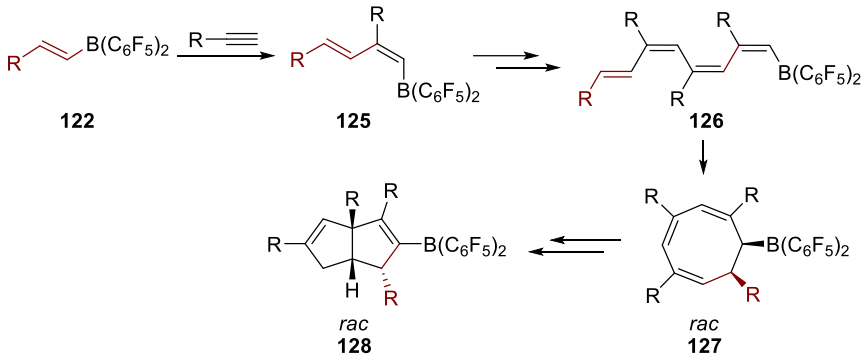

Schema 37: Piers Boran induzierte Tetramersierung von Alkinen zu Tetrahydropentalenen **128**.

4 Literaturverzeichnis

[1] a) W. S. Knowles, *Angew. Chem. Int. Ed.* **2002**, *41*, 1998–2007; *Angew. Chem.* **2002**, *114*, 2096−2107; b) R. Noyori, *Adv. Synth. Catal.* **2003**, *345*, 15–32; c) K. B. Sharpless, *Angew. Chem. Int. Ed.* **2002**, *41*, 2024–2032; *Angew. Chem.* **2002**, *114*, 2126−2135.

[2] a) Y. Chauvin, *Angew. Chem. Int. Ed.* **2006**, *45*, 3740–3747; *Angew. Chem.* **2006**, *118*, 3824−3831; b) R. H. Grubbs, *Angew. Chem. Int. Ed.* **2006**, *45*, 3760–3765; *Angew. Chem.* **2006**, *118*, 3845−3580; c) R. R. Schrock, *Angew. Chem. Int. Ed.* **2006**, *45*, 3748–3759; *Angew. Chem.* **2006**, *118*, 3832−3844.

[3] a) Richard F. Heck, „Richard F. Heck – Nobel Lecture“, abrufbar unter: <https://www.nobelprize.org/prizes/chemistry/2010/heck/lecture/>, **2010**; b) E. Negishi, *Angew. Chem. Int. Ed.* **2011**, *50*, 6738–6764; *Angew. Chem.* **2011**, *123*, 6870−6897; c) A. Suzuki, *Angew. Chem. Int. Ed.* **2011**, *50*, 6722–6737; *Angew. Chem.* **2011**, *123*, 6854−6869.

[4] a) B. Schafer, *Chem. Unserer Zeit* **2013**, *47*, 174; b) H.-U. Blaser, F. Spindler in *Comprehensive Organic Synthesis (Second Edition)* (Ed.: P. Knochel), Elsevier, Amsterdam, **2014**, pp. 274–299.

[5] M. Biosca, M. Diéguez, A. Zanotti-Gerosa in *Advances in Catalysis : Metal-catalyzed Asymmetric Hydrogenation: Evolution and Prospect* (Eds.: M. Diéguez, A. Pizzano), Academic Press, **2021**, pp. 341–383.

[6] a) H. H. Binder, *Lexikon der chemischen Elemente*. *Das Periodensystem in Fakten, Zahlen und Daten*, Hirzel, Stuttgart, **1999**; b) M. L. Zientek, P. J. Loferski, H. L. Parks, R. F. Schulte, R. R. Seal II, *Platinum-group elements*, Reston, VA, **2017**.

[7] P. T. Anastas, J. C. Warner, *Green chemistry*. *Theory and practice*, Oxford University Press, Oxford, **2000**.

[8] a) Benjamin List, „Benjamin List – Nobel Prize lecture“, abrufbar unter <https://www.nobelprize.org/prizes/chemistry/2021/list/lecture/>, **2021**; b) David W.C. MacMillan, „David W.C. MacMillan – Nobel Prize lecture“, abrufbar unter <https://www.nobelprize.org/prizes/chemistry/2021/macmillan/lecture/>, **2021**.

[9] M.-A. Légaré, C. Pranckevicius, H. Braunschweig, *Chem. Rev.* **2019**, *119*, 8231–8261.

[10] M. Soleilhavoup, G. Bertrand, *Angew. Chem. Int. Ed.* **2017**, *56*, 10282–10292; *Angew. Chem.* **2017**, *129*, 10416-10426.

[11] a) L. Vaska, J. W. DiLuzio, *J. Am. Chem. Soc.* **1961**, *83*, 2784–2785; b) L. Vaska, J. W. DiLuzio, *J. Am. Chem. Soc.* **1962**, *84*, 679–680.

[12] R. Noyori, T. Ohkuma, *Angew. Chem. Int. Ed.* **2001**, *40*, 40–73; *Angew. Chem.* **2001**, *113*, 40−75.

[13] a) C. A. Sandoval, T. Ohkuma, K. Muñiz, R. Noyori, *J. Am. Chem. Soc.* **2003**, *125*, 13490–13503; b) T. Ohkuma, H. Ooka, S. Hashiguchi, T. Ikariya, R. Noyori, *J. Am. Chem. Soc.* **1995**, *117*, 2675–2676.

[14] M. Green, *J. Organomet. Chem.* **1995**, *500*, 127–148.

[15] a) Hall, Andrew M. R., P. Dong, A. Codina, J. P. Lowe, U. Hintermair, *ACS Catal.* **2019**, *9*, 2079–2090; b) K.-J. Haack, S. Hashiguchi, A. Fujii, T. Ikariya, R. Noyori, *Angew. Chem. Int. Ed.* **1997**, *36*, 285–288; *Angew. Chem.* **1997**, *109*, 297−300; c) K. Abdur-Rashid, M. Faatz, A. J. Lough, R. H. Morris, *J. Am. Chem. Soc.* **2001**, *123*, 7473–7474.

[16] M. Yamakawa, H. Ito, R. Noyori, *J. Am. Chem. Soc.* **2000**, *122*, 1466–1478.

[17] a) P. A. Dub, J. C. Gordon, *Nat. Rev. Chem.* **2018**, *2*, 396–408; b) P. A. Dub, J. C. Gordon, *Dalton Trans.* **2016**, *45*, 6756–6781; c) N. V. Tkachenko, P. Rublev P, P. A. Dub, **2022** ChemRxiv preprint DOI: 10.26434/chemrxiv-2022-dbc0n.

[18] J. Zhang, G. Leitus, Y. Ben-David, D. Milstein, *J. Am. Chem. Soc.* **2005**, *127*, 10840–10841.

[19] J. R. Khusnutdinova, D. Milstein, *Angew. Chem. Int. Ed.* **2015**, *54*, 12236–12273; *Angew. Chem.* **2015**, *127*, 12406–12445.

[20] R. Noyori, T. Ohkuma, M. Kitamura, H. Takaya, N. Sayo, H. Kumobayashi, S. Akutagawa, *J. Am. Chem. Soc.* **1987**, *109*, 5856–5858.
[21] C. Gunanathan, Y. Ben-David, D. Milstein, *Science* **2007**, *317*, 790–792.
[22] L. N. Dawe, M. Karimzadeh-Younjali, Z. Dai, E. Khaskin, D. G. Gusev, *J. Am. Chem. Soc.* **2020**, *142*, 19510–19522.
[23] R. Noyori, S. Hashiguchi, *Acc. Chem. Res.* **1997**, *30*, 97–102.
[24] a) C. Gunanathan, D. Milstein, *Acc. Chem. Res.* **2011**, *44*, 588–602; b) C. Gunanathan, D. Milstein, *Science* **2013**, *341*, 1229712; c) D. Milstein, *Philos. Trans. R. Soc. A* **2015**, *373*, 20140189; d) T. Shimbayashi, K. Fujita, *Catalysts* **2020**, *10*, 635.
[25] a) M. Siskin, *J. Am. Chem. Soc.* **1974**, *96*, 3641; b) J. Wristers, *J. Am. Chem. Soc.* **1975**, *97*, 4312–4316.
[26] a) E. J. DeWitt, F. L. Ramp, L. E. Trapasso, *J. Am. Chem. Soc.* **1961**, *83*, 4672; b) F. L. Ramp, E. J. DeWitt, L. E. Trapasso, *J. Org. Chem.* **1962**, *27*, 4368–4372; c) M. Yalpani, R. Köster, *Chem. Ber.* **1990**, *123*, 719–724; d) M. Yalpani, T. Lunow, R. Köster, *Chem. Ber.* **1989**, *122*, 687–693; e) M. W. Haenel, J. Narangerel, U.-B. Richter, A. Rufińska, *Angew. Chem. Int. Ed.* **2006**, *45*, 1061–1066; *Angew. Chem.* **2006**, *118*, 1077–1082.
[27] a) C. Walling, L. Bollyky, *J. Am. Chem. Soc.* **1961**, *83*, 2968–2969; b) C. Walling, L. Bollyky, *J. Am. Chem. Soc.* **1964**, *86*, 3750–3752; c) A. Berkessel, T. J. S. Schubert, T. N. Müller, *J. Am. Chem. Soc.* **2002**, *124*, 8693–8698.
[28] H. C. Brown, H. I. Schlesinger, S. Z. Cardon, *J. Am. Chem. Soc.* **1942**, *64*, 325–329.
[29] G. C. Welch, R. R. S. Juan, J. D. Masuda, D. W. Stephan, *Science* **2006**, *314*, 1124–1126.
[30] J. S. J. McCahill, G. C. Welch, D. W. Stephan, *Angew. Chem. Int. Ed.* **2007**, *46*, 4968–4971; *Angew. Chem.* **2007**, *119*, 5056–5059.
[31] L. Greb, S. Tussing, B. Schirmer, P. Oña-Burgos, K. Kaupmees, M. Lõkov, I. Leito, S. Grimme, J. Paradies, *Chem. Sci.* **2013**, *4*, 2788–2796.
[32] a) A. Y. Timoshkin, G. Frenking, *Organometallics* **2008**, *27*, 371–380; b) S. Döring, G. Erker, R. Fröhlich, O. Meyer, K. Bergander, *Organometallics* **1998**, *17*, 2183–2187; c) M. A. Beckett, D. S. Brassington, S. J. Coles, M. B. Hursthouse, *Inorg. Chem. Commun.* **2000**, *3*, 530–533.
[33] Für die angewendeten Methoden zur Bestimmung der Lewis-Acidität siehe: a) M. A. Beckett, G. C. Strickland, J. R. Holland, K. Sukumar Varma, *Polymer* **1996**, *37*, 4629–4631; b) R. F. Childs, D. L. Mulholland, A. Nixon, *Can. J. Chem.* **1982**, *60*, 809–812; c) R. F. Childs, D. L. Mulholland, A. Nixon, *Can. J. Chem.* **1982**, *60*, 801–808; d) P. Laszlo, M. Teston, *J. Am. Chem. Soc.* **1990**, *112*, 8750–8754; e) U. Mayer, V. Gutmann, W. Gerger, *Monats. Chem.* **1975**, *106*, 1235–1257.
[34] G. C. Welch, D. W. Stephan, *J. Am. Chem. Soc.* **2007**, *129*, 1880–1881.
[35] P. Spies, G. Erker, G. Kehr, K. Bergander, R. Fröhlich, S. Grimme, D. W. Stephan, *Chem. Commun.* **2007**, 5072–5074.
[36] Z. Jian, G. Kehr, C. G. Daniliuc, B. Wibbeling, G. Erker, *Dalton Trans.* **2017**, *46*, 11715–11721.
[37] E. Otten, R. C. Neu, D. W. Stephan, *J. Am. Chem. Soc.* **2009**, *131*, 9918–9919.
[38] M. Sajid, A. Klose, B. Birkmann, L. Liang, B. Schirmer, T. Wiegand, H. Eckert, A. J. Lough, R. Fröhlich, C. G. Daniliuc, S. Grimme, D. W. Stephan, G. Kehr, G. Erker, *Chem. Sci.* **2013**, *4*, 213–219.
[39] O. Ekkert, G. G. Miera, T. Wiegand, H. Eckert, B. Schirmer, J. L. Petersen, C. G. Daniliuc, R. Fröhlich, S. Grimme, G. Kehr, G. Erker, *Chem. Sci.* **2013**, *4*, 2657–2664.
[40] a) J. W. Runyon, O. Steinhof, H. V. R. Dias, J. C. Calabrese, W. J. Marshall, A. J. Arduengo, *Aust. J. Chem.* **2011**, *64*, 1165–1172; b) P. A. Chase, D. W. Stephan, *Angew. Chem. Int. Ed.* **2008**, *47*, 7433–7437; *Angew. Chem.* **2008**, *120*, 7543–7547.
[41] S. Mummadi, D. K. Unruh, J. Zhao, S. Li, C. Krempner, *J. Am. Chem. Soc.* **2016**, *138*, 3286–3289.

[42] E. R. Clark, M. J. Ingleson, *Angew. Chem. Int. Ed.* **2014**, *53*, 11306–11309; *Angew. Chem.* **2014**, *126*, 11488−11491.
[43] M. Lange, J. C. Tendyck, P. Wegener, A. Hepp, E.-U. Würthwein, W. Uhl, *Chem. Eur. J.* **2018**, *24*, 12856–12868.
[44] B. Waerder, M. Pieper, L. A. Körte, T. A. Kinder, A. Mix, B. Neumann, H.-G. Stammler, N. W. Mitzel, *Angew. Chem. Int. Ed.* **2015**, *54*, 13416–13419; *Angew. Chem.* **2015**, *127*, 13614–13617.
[45] J. M. Farrell, J. A. Hatnean, D. W. Stephan, *J. Am. Chem. Soc.* **2012**, *134*, 15728–15731.
[46] a) S. J. Geier, D. W. Stephan, *J. Am. Chem. Soc.* **2009**, *131*, 3476–3477; b) S. J. Geier, T. M. Gilbert, D. W. Stephan, *J. Am. Chem. Soc.* **2008**, *130*, 12632–12633.
[47] Für eine detailliertere Diskussion über die Definition von FLP siehe: F.-G. Fontaine, D. W. Stephan, *Philos. Trans. R. Soc. A* **2017**, *375*, 20170004.
[48] Für ausgewählte Übersichtsartikel über FLP und deren Chemie siehe: a) D. W. Stephan, G. Erker, *Chem. Sci.* **2014**, *5*, 2625–2641; b) D. W. Stephan, G. Erker, *Angew. Chem. Int. Ed.* **2015**, *54*, 6400–6441; *Angew. Chem.* **2015**, *127*, 6498−6541; c) D. W. Stephan, *Acc. Chem. Res.* **2015**, *48*, 306–316; d) A. R. Jupp, D. W. Stephan, *Trends Chem.* **2019**, *1*, 35–48; e) S. A. Weicker, D. W. Stephan, *Bull. Chem. Soc. Jpn.* **2015**, *88*, 1003–1016.
[49] T. A. Rokob, A. Hamza, I. Pápai, *J. Am. Chem. Soc.* **2009**, *131*, 10701–10710.
[50] A. Hamza, A. Stirling, T. András Rokob, I. Pápai, *Int. J. Quantum Chem.* **2009**, *109*, 2416–2425.
[51] S. Grimme, H. Kruse, L. Goerigk, G. Erker, *Angew. Chem. Int. Ed.* **2010**, *49*, 1402–1405; *Angew. Chem.* **2010**, *122*, 1444−1447.
[52] B. Schirmer, S. Grimme, *Chem. Commun.* **2010**, *46*, 7942–7944.
[53] T. A. Rokob, I. Bakó, A. Stirling, A. Hamza, I. Pápai, *J. Am. Chem. Soc.* **2013**, *135*, 4425–4437.
[54] I. Bakó, A. Stirling, S. Bálint, I. Pápai, *Dalton Trans.* **2012**, *41*, 9023–9025.
[55] L. Rocchigiani, G. Ciancaleoni, C. Zuccaccia, A. Macchioni, *J. Am. Chem. Soc.* **2014**, *136*, 112–115.
[56] L. C. Brown, J. M. Hogg, M. Gilmore, L. Moura, S. Imberti, S. Gärtner, H. Q. N. Gunaratne, R. J. O'Donnell, N. Artioli, J. D. Holbrey, M. Swadźba-Kwaśny, *Chem. Commun.* **2018**, *54*, 8689–8692.
[57] A. R. Jupp, *Dalton Trans.* **2022**, *51*, 10681–10689.
[58] G. Skara, F. de Vleeschouwer, P. Geerlings, F. de Proft, B. Pinter, *Sci. Rep.* **2017**, *7*, 16024.
[59] a) F. Holtrop, A. R. Jupp, N. P. van Leest, M. Paradiz Dominguez, R. M. Williams, A. M. Brouwer, B. de Bruin, A. W. Ehlers, J. C. Slootweg, *Chem. Eur. J.* **2020**, *26*, 9005–9011; b) A. Dasgupta, E. Richards, R. L. Melen, *Angew. Chem. Int. Ed.* **2021**, *60*, 53–65; *Angew. Chem.* **2021**, *133*, 53−65; c) L. Liu, L. L. Cao, Y. Shao, G. Ménard, D. W. Stephan, *Chem* **2017**, *3*, 259–267.
[60] P. A. Chase, G. C. Welch, T. Jurca, D. W. Stephan, *Angew. Chem. Int. Ed.* **2007**, *46*, 8050–8053; *Angew. Chem.* **2007**, *42*, 8196-8199.
[61] a) D. Chen, J. Klankermayer, *Chem. Commun.* **2008**, 2130–2131; b) P. A. Chase, T. Jurca, D. W. Stephan, *Chem. Commun.* **2008**, 1701–1703.
[62] a) T. Privalov, *Eur. J. Inorg. Chem.* **2009**, *2009*, 2229–2237; b) T. A. Rokob, A. Hamza, A. Stirling, I. Pápai, *J. Am. Chem. Soc.* **2009**, *131*, 2029–2036; c) S. Tussing, L. Greb, S. Tamke, B. Schirmer, C. Muhle-Goll, B. Luy, J. Paradies, *Chem. Eur. J.* **2015**, *21*, 8056–8059; d) S. Tussing, K. Kaupmees, J. Paradies, *Chem. Eur. J.* **2016**, *22*, 7422–7426.
[63] a) D. J. Scott, M. J. Fuchter, A. E. Ashley, *J. Am. Chem. Soc.* **2014**, *136*, 15813–15816; b) T. Mahdi, D. W. Stephan, *J. Am. Chem. Soc.* **2014**, *136*, 15809–15812.
[64] T. Mahdi, Z. M. Heiden, S. Grimme, D. W. Stephan, *J. Am. Chem. Soc.* **2012**, *134*, 4088–4091.
[65] N. A. Sitte, M. Bursch, S. Grimme, J. Paradies, *J. Am. Chem. Soc.* **2019**, *141*, 159–162.
[66] L. Greb, P. Oña-Burgos, B. Schirmer, S. Grimme, D. W. Stephan, J. Paradies, *Angew. Chem. Int. Ed.* **2012**, *51*, 10164–10168; *Angew. Chem.* **2012**, *124*, 10311−10315.

[67] B. Inés, D. Palomas, S. Holle, S. Steinberg, J. A. Nicasio, M. Alcarazo, *Angew. Chem. Int. Ed.* **2012**, *51*, 12367–12369; *Angew. Chem.* **2012**, *124*, 12533−12536.

[68] A. J. Stepen, M. Bursch, S. Grimme, D. W. Stephan, J. Paradies, *Angew. Chem. Int. Ed.* **2018**, *57*, 15253–15256; *Angew. Chem.* **2018**, *130*, 15473−15476.

[69] a) Y. Liu, H. Du, *J. Am. Chem. Soc.* **2013**, *135*, 6810–6813; b) S. Wei, H. Du, *J. Am. Chem. Soc.* **2014**, *136*, 12261–12264.

[70] a) J. Paradies, *Angew. Chem. Int. Ed.* **2014**, *53*, 3552–3557; *Angew. Chem.* **2014**, *126*, 3624−3629; b) D. W. Stephan, *Chem* **2020**, *6*, 1520–1526; c) J. Lam, K. M. Szkop, E. Mosaferi, D. W. Stephan, *Chem. Soc. Rev.* **2019**, *48*, 3592–3612.

[71] K. Chernichenko, Á. Madarász, I. Pápai, M. Nieger, M. Leskelä, T. Repo, *Nat. Chem.* **2013**, *5*, 718–723.

[72] a) D. J. Parks, W. E. Piers, *J. Am. Chem. Soc.* **1996**, *118*, 9440–9441; b) D. Chen, V. Leich, F. Pan, J. Klankermayer, *Chem. Eur. J.* **2012**, *18*, 5184–5187.

[73] a) T. Mahdi, D. W. Stephan, *Angew. Chem. Int. Ed.* **2013**, *52*, 12418–12421; *Angew. Chem.* **2013**, *135*, 12644−12647; b) Y. Zhao, L. Jin, J. Guo, D. W. Stephan, *Chem. Commun.* **2022**, *58*, 3039–3042.

[74] a) L. Greb, F. Ebner, Y. Ginzburg, L. M. Sigmund, *Eur. J. Inorg. Chem.* **2020**, *2020*, 3030–3047; b) E. R. M. Habraken, A. R. Jupp, M. B. Brands, M. Nieger, A. W. Ehlers, J. C. Slootweg, *Eur. J. Inorg. Chem.* **2019**, *2019*, 2436–2442.

[75] V. A. Dorokhov, I. P. Yakovlev, B. M. Mikhailov, *Bull. Acad. Sci. USSR Div. Chem. Sci. (Engl. Transl.)* **1980**, *29*, 485–491.

[76] M. A. Dureen, D. W. Stephan, *J. Am. Chem. Soc.* **2010**, *132*, 13559–13568.

[77] A. R. Cabrera, R. S. Rojas, M. Valderrama, P. Plüss, H. Berke, C. G. Daniliuc, G. Kehr, G. Erker, *Dalton Trans.* **2015**, *44*, 19606–19614.

[78] a) E. Theuergarten, D. Schlüns, J. Grunenberg, C. G. Daniliuc, P. G. Jones, M. Tamm, *Chem. Commun.* **2010**, *46*, 8561–8563; b) E. Theuergarten, J. Schlösser, D. Schlüns, M. Freytag, C. G. Daniliuc, P. G. Jones, M. Tamm, *Dalton Trans.* **2012**, *41*, 9101–9110.

[79] G. Lu, H. Li, L. Zhao, F. Huang, P. v. R. Schleyer, Z.-X. Wang, *Chem. Eur. J.* **2011**, *17*, 2038–2043.

[80] U. Gellrich, Y. Diskin-Posner, L. J. W. Shimon, D. Milstein, *J. Am. Chem. Soc.* **2016**, *138*, 13307–13313.

[81] P. v. R. Schleyer, C. Maerker, A. Dransfeld, H. Jiao, N. J. R. van Eikema Hommes, *J. Am. Chem. Soc.* **1996**, *118*, 6317–6318.

[82] a) U. Gellrich, *Angew. Chem. Int. Ed.* **2018**, *57*, 4779–4782; *Angew. Chem.* **2018**, *130*, 4869−4872; b) D. J. Parks, R. E. von H. Spence, W. E. Piers, *Angew. Chem.* **1995**, *34*, 809-811; *Angew. Chem.* **1995**, *107*, 895-897; c) D. J. Parks, G. P. A. Yap, W. E. Piers, *Organometallics*, **1998**, *17*, 5492-5503.

[83] M. Ghara, S. Pan, P. K. Chattaraj, *Phys. Chem. Chem. Phys.* **2019**, *21*, 21267–21277.

[84] a) A. Haaland, *Angew. Chem. Int. Ed.* **1989**, *28*, 992–1007; *Angew. Chem.* **1989**, *101*, 1017−1032; b) V. I. Minkin, *Pure Appl. Chem.* **1999**, *71*, 1919–1981.

[85] Für eine detailliertere Diskussion von dativen Bindungen in Hauptgruppenverbindungen siehe: a) D. Himmel, I. Krossing, A. Schnepf, *Angew. Chem. Int. Ed.* **2014**, *53*, 370–374; *Angew. Chem.* **2014**, *126*, 378−382; b) G. Frenking, *Angew. Chem. Int. Ed.* **2014**, *53*, 6040–6046; *Angew. Chem.* **2014**, *126*, 6152−6158; c) D. Himmel, I. Krossing, A. Schnepf, *Angew. Chem. Int. Ed.* **2014**, *53*, 6047–6048; *Angew. Chem.* **2014**, *126*, 6159−6160; d) A. Nandi, S. Kozuch, *Chem. Eur. J.* **2020**, *26*, 759–772; e) R. Pietschnig, *J. Organomet. Chem.* **2007**, *692*, 3363–3369.

[86] É. Rochette, V. Desrosiers, Y. Soltani, F.-G. Fontaine, *J. Am. Chem. Soc.* **2019**, *141*, 12305–12311.

[87] V. Desrosiers, C. Z. Garcia, F.-G. Fontaine, *ACS Catal.* **2020**, *10*, 11046–11056.

[88] S. Li, G. Li, W. Meng, H. Du, *J. Am. Chem. Soc.* **2016**, *138*, 12956–12962.

[89] W. Zhao, Z. Zhang, X. Feng, J. Yang, H. Du, *Org. Lett.* **2020**, *22*, 5850–5854.
[90] W. Zhao, X. Feng, J. Yang, H. Du, *Tetrahedron Lett.* **2019**, *60*, 1193–1196.
[91] S. Li, W. Meng, H. Du, *Org. Lett.* **2017**, *19*, 2604–2606.
[92] Für ausgewählte Beispiele von Allylborierungen in Totalsynthesen siehe: a) R. C. Godfrey, N. J. Green, G. S. Nichol, A. L. Lawrence, *Nat. Chem.* **2020**, *12*, 615–619; b) C. W. Huh, W. R. Roush, *Org. Lett.* **2008**, *10*, 3371–3374; c) T. Lindel, L. Bräuchle, G. Golz, P. Böhrer, *Org. Lett.* **2007**, *9*, 283–286; d) P. Nuhant, W. R. Roush, *J. Am. Chem. Soc.* **2013**, *135*, 5340–5343.
[93] a) D. M. Sedgwick, M. N. Grayson, S. Fustero, P. Barrio, *Synthesis* **2018**, *50*, 1935–1957; b) W. R. Roush in *Comprehensive Organic Synthesis* (Eds.: B. M. Trost, I. Fleming), Pergamon, Oxford, **1991**, pp. 1–53; c) H. C. Brown, P. K. Jadhav, *J. Am. Chem. Soc.* **1983**, *105*, 2092–2093; d) U. S. Racherla, H. C. Brown, *J. Org. Chem.* **1991**, *56*, 401–404.
[94] G. W. Kramer, H. C. Brown, *J. Organomet. Chem.* **1977**, *132*, 9–27.
[95] J. M. Schkeryantz, J. C. G. Woo, P. Siliphaivanh, K. M. Depew, S. J. Danishefsky, *J. Am. Chem. Soc.* **1999**, *121*, 11964–11975.
[96] M. Dresselhaus, G. Crabtree, Buchanan Michelle, *Basic Energy Sciences, Office of Science, U.S. Department of Energy: Washington, DC* **2003**.
[97] a) U. B. Demirci, *Inorg. Chem. Front.* **2021**, *8*, 1900–1930; b) S. Frueh, R. Kellett, C. Mallery, T. Molter, W. S. Willis, C. King'ondu, S. L. Suib, *Inorg. Chem.* **2011**, *50*, 783–792.
[98] a) X. Zhang, L. Kam, R. Trerise, T. J. Williams, *Acc. Chem. Res.* **2017**, *50*, 86–95; b) C. A. Jaska, K. Temple, A. J. Lough, I. Manners, *J. Am. Chem. Soc.* **2003**, *125*, 9424–9434; c) M. C. Denney, V. Pons, T. J. Hebden, D. M. Heinekey, K. I. Goldberg, *J. Am. Chem. Soc.* **2006**, *128*, 12048–12049.
[99] a) A. Glüer, M. Förster, V. R. Celinski, Schmedt auf der Günne, Jörn, M. C. Holthausen, S. Schneider, *ACS Catal.* **2015**, *5*, 7214–7217; b) R. J. Keaton, J. M. Blacquiere, R. T. Baker, *J. Am. Chem. Soc.* **2007**, *129*, 1844–1845.
[100] D. W. Himmelberger, C. W. Yoon, M. E. Bluhm, P. J. Carroll, L. G. Sneddon, *J. Am. Chem. Soc.* **2009**, *131*, 14101–14110.
[101] F. H. Stephens, R. T. Baker, M. H. Matus, D. J. Grant, D. A. Dixon, *Angew. Chem. Int. Ed.* **2007**, *46*, 746–749; *Angew. Chem.* **2007**, *119*, 760–763.
[102] Z. Lu, L. Schweighauser, H. Hausmann, H. A. Wegner, *Angew. Chem. Int. Ed.* **2015**, *54*, 15556–15559; *Angew. Chem.* **2015**, *127*, 15777–15780.
[103] A. J. M. Miller, J. E. Bercaw, *Chem. Commun.* **2010**, *46*, 1709–1711.
[104] C. Appelt, J. C. Slootweg, K. Lammertsma, W. Uhl, *Angew. Chem. Int. Ed.* **2013**, *52*, 4256–4259; *Angew. Chem.* **2013**, *125*, 4350–4353.
[105] Z. Mo, A. Rit, J. Campos, E. L. Kolychev, S. Aldridge, *J. Am. Chem. Soc.* **2016**, *138*, 3306–3309.
[106] a) C. D. Mboyi, D. Poinsot, J. Roger, K. Fajerwerg, M. L. Kahn, J.-C. Hierso, *Small* **2021**, *17*, 2102759; b) A. Rossin, M. Peruzzini, *Chem. Rev.* **2016**, *116*, 8848–8872; c) N. C. Smythe, J. C. Gordon, *Eur. J. Inorg. Chem.* **2010**, *2010*, 509–521; d) A. Staubitz, A. P. M. Robertson, I. Manners, *Chem. Rev.* **2010**, *110*, 4079–4124; e) C. Yüksel Alpaydın, S. K. Gülbay, C. Ozgur Colpan, *Int. J. Hydrog. Energy* **2020**, *45*, 3414–3434.
[107] A. D. Sutton, A. K. Burrell, D. A. Dixon, E. B. Garner, J. C. Gordon, T. Nakagawa, K. C. Ott, J. P. Robinson, M. Vasiliu, *Science* **2011**, *331*, 1426–1429.
[108] a) M. M. Heravi, E. Hashemi, *Tetrahedron* **2012**, *68*, 9145–9178; b) I. Maluenda, O. Navarro, *Molecules*, **2015**, *20*, 7528-7557; c) A. Taheri Kal Koshvandi, M. M. Heravi, T. Momeni, *Appl. Organomet. Chem.* **2018**, *32*, e4210.

[109] a) S. K. Dorn, M. K. Brown, *ACS Catal.* **2022**, *12*, 2058–2063; b) Z. Liu, Y. Gao, T. Zeng, K. M. Engle, *Isr. J. Chem.* **2020**, *60*, 219–229; c) Y. Shimizu, M. Kanai, *Tetrahedron Lett.* **2014**, *55*, 3727–3737; d) M. Suginome, *Chem. Rec.* **2010**, *10*, 348–358.

[110] G. Menz, B. Wrackmeyer, *Z. Naturforsch. B* **1977**, *32*, 1400–1407.

[111] a) B. Wrackmeyer, E. Khan, *Eur. J. Inorg. Chem.* **2016**, *2016*, 300–312; b) B. Wrackmeyer, *Coord. Chem. Rev.* **1995**, *145*, 125–156.

[112] a) C. Chen, G. Kehr, R. Fröhlich, G. Erker, *J. Am. Chem. Soc.* **2010**, *132*, 13594–13595; b) C. Jiang, O. Blacque, H. Berke, *Organometallics* **2010**, *29*, 125–133.

[113] C. Chen, T. Voss, R. Fröhlich, G. Kehr, G. Erker, *Org. Lett.* **2011**, *13*, 62–65.

[114] M. M. Hansmann, R. L. Melen, M. Rudolph, F. Rominger, H. Wadepohl, D. W. Stephan, A. S. K. Hashmi, *J. Am. Chem. Soc.* **2015**, *137*, 15469–15477.

[115] C. Chen, F. Eweiner, B. Wibbeling, R. Fröhlich, S. Senda, Y. Ohki, K. Tatsumi, S. Grimme, G. Kehr, G. Erker, *Chem. Asian J.* **2010**, *5*, 2199–2208.

[116] a) C. Chen, C. G. Daniliuc, C. Mück-Lichtenfeld, G. Kehr, G. Erker, *Chem. Commun.* **2020**, *56*, 8806–8809; b) M. M. Hansmann, R. L. Melen, F. Rominger, A. S. K. Hashmi, D. W. Stephan, *J. Am. Chem. Soc.* **2014**, *136*, 777–782; c) R. L. Melen, M. M. Hansmann, A. J. Lough, A. S. K. Hashmi, D. W. Stephan, *Chem. Eur. J.* **2013**, *19*, 11928–11938.

[117] Für Übersichtsartikel über 1,1-Carboborierungen siehe: a) G. Kehr, G. Erker, *Chem. Commun.* **2012**, *48*, 1839–1850; b) G. Kehr, G. Erker, *Chem. Sci.* **2016**, *7*, 56–65.

[118] R. L. Melen, L. C. Wilkins, B. M. Kariuki, H. Wadepohl, L. H. Gade, A. S. K. Hashmi, D. W. Stephan, M. M. Hansmann, *Organometallics* **2015**, *34*, 4127–4137.

[119] J. R. Sanzone, C. T. Hu, K. A. Woerpel, *J. Am. Chem. Soc.* **2017**, *139*, 8404–8407.

[120] C. You, M. Sakai, C. G. Daniliuc, K. Bergander, S. Yamaguchi, A. Studer, *Angew. Chem. Int. Ed.* **2021**, *60*, 21697–21701; *Angew. Chem.* **2021**, *133*, 21865–21869.

[121] Für weitere Beispiele von 1,2-Carboborierungen siehe: a) I. A. Cade, M. J. Ingleson, *Chem. Eur. J.* **2014**, *20*, 12874–12880; b) M. Devillard, R. Brousses, K. Miqueu, G. Bouhadir, D. Bourissou, *Angew. Chem. Int. Ed.* **2015**, *54*, 5722–5726; *Angew. Chem.* **2015**, *127*, 5814–5818; c) Y. Shoji, N. Tanaka, S. Muranaka, N. Shigeno, H. Sugiyama, K. Takenouchi, F. Hajjaj, T. Fukushima, *Nat. Commun.* **2016**, *7*, 12704.

5 Veröffentlichte Projekte

5.1 Aldehyde Reduction by a Pyridone Borane Complex through Boron-Ligand-Cooperation: Concerted or Not?

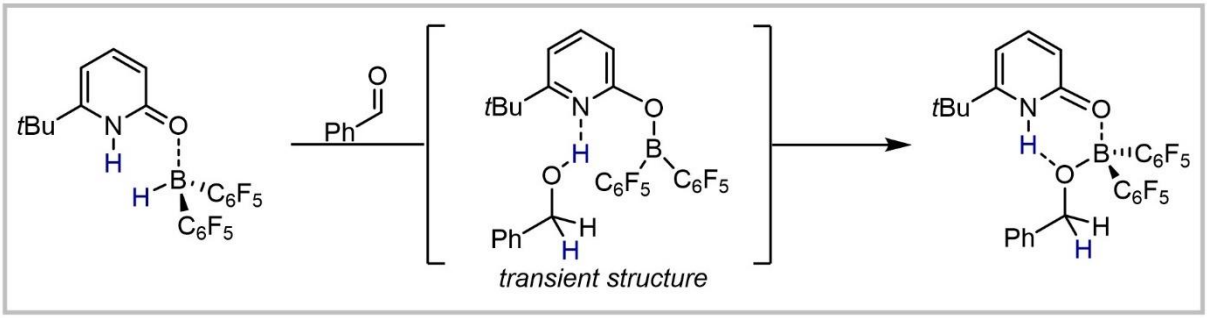

Aldehyde reduction by a pyridone borane complex was studied experimentally and computationally. The results indicate that a concerted hydrogen transfer mechanism is operative, resulting in the formation of a transient alcohol complex that undergoes a barrierless addition. The concerted hydrogen transfer is associated with a pyridone borane to boroxypyridine transformation.

Tizian Müller, Max Hasenbeck, Dr. Jonathan Becker, Dr. Urs Gellrich

Eur. J. Org. Chem. **2019**, *2019*, 451-457

DOI: 10.1002/ejoc.201800847

Akzeptiertes Manuskript online: 06.07.2018

Final veröffentlichte Version online: 23.08.2018

ChemPubSoc Europe

DOI: 10.1002/ejoc.201800847

EurJOC European Journal of Organic Chemistry

Full Paper

Boron-Ligand Cooperation

SPECIAL ISSUE

Aldehyde Reduction by a Pyridone Borane Complex through Boron-Ligand-Cooperation: Concerted or Not?

Tizian Müller,[a] Max Hasenbeck,[a] Jonathan Becker,[b] and Urs Gellrich*[a]

Abstract: The reduction of benzaldehyde by a pyridone borane complex was investigated by NMR, X-ray analysis as well as DFT and DLPNO-CCSD(T) computations. The reaction leads to the formation of a pyridone boronic ester complex stabilized by an NH···O hydrogen bond. The computations show that the hydrogenation takes place in a concerted fashion, yielding a transient benzyl alcohol boroxypyridine complex that undergoes a barrierless O–H addition. The concerted hydrogen transfer is associated with a transformation of a pyridone borane to a boroxypyridine, and thus with the interconversion of a neutral donor ligand to a covalently bound substituent.

Introduction

Since the seminal reports from Stephan and Ashley on the metal-free hydrogenation of aldehydes and ketones catalyzed by $B(C_6F_5)_3$ in an ethereal solvent, the mechanism of this transformation has gained considerable attention.[1,2] Stephan and Ashly proposed a mechanism consisting of an initial hydrogen splitting by a Frustrated Lewis Pair (FLP) formed by an ether solvent molecule and $B(C_6F_5)_3$ (Scheme 1). A hydrogen bond between the protonated ether and the carbonyl compound activates the latter towards hydride transfer (Scheme 1).

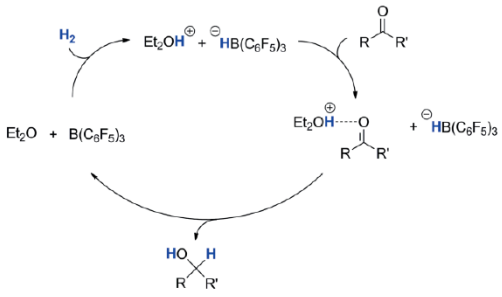

Scheme 1. Proposed mechanism for the hydrogenation of aldehydes and ketones catalyzed by $B(C_6F_5)_3$ in an ethereal solvent.

Based on DFT computations, Das et al. proposed a stepwise mechanism in which the protonation of the ketone by the protonated ether precedes hydride transfer, which is, however, somewhat conflicting with the experimentally determined pK_A values of a protonated ether and a protonated ketone.[3] A recent computational study reported by Heshmat et al. suggests, based on GGA DFT computations, a mechanism for the H_2 splitting in which the carbonyl carbon atom of a ketone coordinated to $B(C_6F_5)_3$ acts as a Lewis acid in conjunction with an ether molecule of the solvent as a Lewis base.[4]

Concerted hydrogenations via a pericyclic six-membered transition state were the generally accepted mechanistic picture for ketone reductions catalyzed by Noyori-type bisphosphine–bisamino–ruthenium complexes (Scheme 2).[5] Inspired by these systems, Li et al. computationally designed a bifunctional metal-free system, that should, according to the computations, allow concerted hydrogen transfers to carbonyl compounds (Scheme 2).[6] It should be mentioned that recent DFT studies

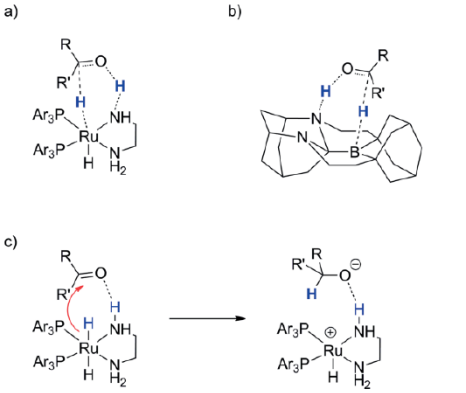

Scheme 2. a) Generally accepted concerted mechanism for the ketone reduction by Noyori-type ruthenium complexes. b) Metal-free system computationally designed by Li et al. to enable concerted ketone hydrogenation. c) Revised stepwise mechanism.

[a] Institut für Organische Chemie, Justus-Liebig-Universität Gießen, Heinrich-Buff-Ring 17, 35392 Gießen
E-mail: urs.gellrich@org.chemie.uni-giessen.de
[b] Institut für Anorganische und Analytische Chemie, Justus-Liebig-Universität Gießen, Heinrich-Buff-Ring 17, 35392 Gießen

Supporting information and ORCID(s) from the author(s) for this article are available on the WWW under https://doi.org/10.1002/ejoc.201800847.

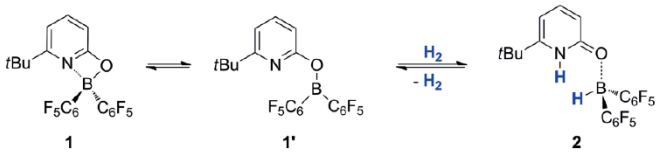

Scheme 3. Reversible hydrogen activation by **1**.

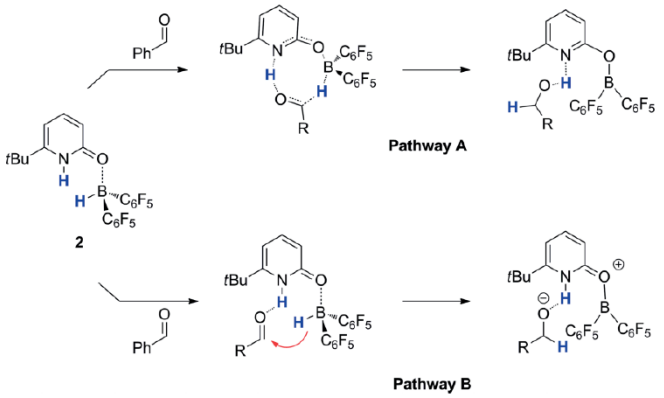

Scheme 4. Concerted aldehyde reduction involving a pyridone to oxypyridin transition (upper panel) or a stepwise mechanism involving the formation of an ion pair (lower panel).

by Dub et al. rebut a concerted mechanism for hydrogenation of ketones by Noyori-type bisphosphine bisamino ruthenium complexes.[7] Instead, based on these investigations, a stepwise mechanism commencing with a hydride transfer yielding a hydrogen bond stabilized ion pair was proposed (Scheme 2).

We recently reported reversible hydrogen activation by the boroxypyridine **1** (Scheme 3).[8] Upon hydrogen activation and formation of the pyridone borane complex **2**, the oxypyridine substituent undergoes a transformation to a pyridone ligand. In analogy to the concept of metal-ligand cooperation, this interconversion of a covalently bound substituent to a neutral donor ligand during the bond activation process was described as boron-ligand cooperation.

In the aforementioned context, we became interested to elucidate whether hydrogenation of a carbonyl compound by **2** was possible and, moreover, consisted of a concerted mechanism that involves a pyridone to oxypyridine transition, or rather proceeded via activation of the carbonyl by an NH···O hydrogen bond (Scheme 4).

For the aldehyde reduction by **2**, a concerted pathway seems plausible since the pyridone to oxypyridine transition would result in a higher degree of electron donation from oxygen to boron, rendering the boron hydride more nucleophilic.

Results and Discussion

We commenced our attempts for the reaction of **2** with 1.2 equivalents of benzaldehyde. Since our previous studies revealed that the hydrogen liberation from **2** takes place already at room temp., the reaction was performed under moderate H_2-pressure (2 bar).[8] After 18 h, complete conversion of **2** and the formation of a new borane complex was observed. Reduction of the aldehyde is evident from the detection of a signal at 4.8 ppm by ^{1}H NMR that shows an HSQC cross peak to a ^{13}C NMR signal at δ = 66.4 ppm and can, therefore, be assigned to the CH_2-group of a phenylboronic acid. Based on HH-COSY experiments, a signal at δ = 14.3 ppm can be assigned to an NH···O hydrogen bond. This is further indicative for the formation of the pyridone boronic ester complex **3** (Scheme 5). Formation of a tetra-coordinated borane is elucidated from the ^{11}B NMR shift at 6.3 ppm. A similar structure was observed upon benzaldehyde reduction with an intramolecular phosphine-borane FLP.[9]

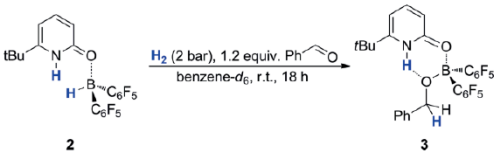

Scheme 5. Formation of **3** upon reduction of benzaldehyde by **2**.

This assignment is further supported by an excellent agreement of the experimentally found NMR shifts and those computed at PBE0-D3(BJ)/def2-TZVP (Table 1).[10]

Table 1. Comparison of selected experimentally observed and computed NMR spectroscopic data of **3**.

	exp.	PBE0-D3(BJ)/def2-TZVP[a]
^{1}H (N*H*) [ppm]	13.74	15.23
^{1}H (PhC*H*$_2$OB) [ppm]	4.56	4.76
^{11}B [ppm]	6.2	6.3
^{13}C (PhCH$_2$OB) [ppm]	66.4	68.7

[a] Computed NMR shifts are referenced to TMS (^{1}H) and $Me_3N{\cdot}BH_3$ (^{11}B).

Slow evaporation of a hexane solution of **3** yielded single crystals suitable for X-ray diffraction. The XRD structure reveals that **3** is stabilized by an N–H···O hydrogen bond (Figure 1).

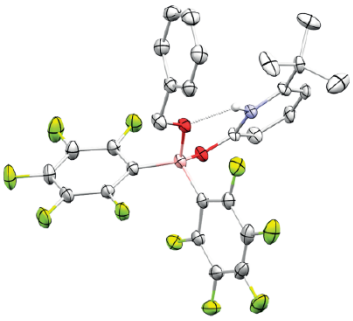

Figure 1. ORTEP representation of **3** (50 % probability ellipsoids, all hydrogens but the ones on N1 are omitted for clarity).

The structural features of the N–H···O hydrogen bond derived from X-ray analysis are in good agreement with those computed at PBE0-D3/def2-SV(P) (Table 2).

Table 2. Comparison of selected experimentally observed and computed structural features of **3**.

	XRD	PBE0-D3/def2-SV(P)[a]
d N–H···O [Å]	2.656(9)	2.594
φ N–H···O [°]	138(3)	140.9

The computations reveal a second minimum structure of **3** (Figure 2) that is more stable by 2.0 kcal/mol and differs from the XRD structure with regard to the alignment of the phenyl ring. This computed minimum structure is characterized by a close contact between the phenyl ring and one of the pentafluorophenyl rings at boron. Such an interaction is not unexpected given the large quadrupole moments with opposite signs of benzene and perfluorophenyl.[11] Indeed, phenyl–perfluorophenyl interactions have been used as a design element for supermolecular arrays.[12].

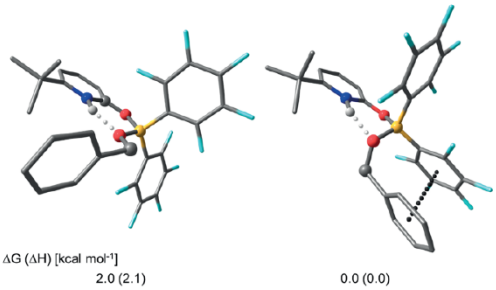

Figure 2. Conformers of **3** and their relative Gibbs free energy computed at DLPNO-CCSD(T)/def2-TZVP//PBE0-D3/def2-SV(P). The dotted black line indicates the pentafluorophenyl-phenyl interaction. Bulk solvation was considered implicitly with the SMD model for benzene.[13]

A closer inspection of the crystal structure reveals that this difference between XRD structure and the computed structure can be explained by intermolecular pentafluorophenyl-phenyl interactions in the solid state that are absent in the computed structure. Assuming that low reaction temperatures will allow the detection of possible intermediates, the aldehyde reduction by **2** was monitored at −20 °C by means of ^{1}H NMR spectroscopy (Figure 4). This experiment showed that the reaction is fast, the formation of **3** can be directly detected after addition of the aldehyde. It should further be noted that upon addition of the benzaldehyde, the previously reported bispyridone complex **4** and the uncoordinated boronic ester **5** are detectable.[13] Formation of **4** and **5** from **3** in the presence of **1**, formed upon hydrogen liberation from **2**, is predicted to be exergonic and exothermic (Scheme 6).

Over the course of 1 h at −20 °C, the signal intensity of the peaks assigned to **4** and **5** decreases, indicating that formation of **4** is reversible. While the sharp signals observed in the ^{1}H NMR of the bispyridone complex **4** indicate a symmetric structure, previous computations support a global minimum structure with an NH···O hydrogen bond. We were able to obtain

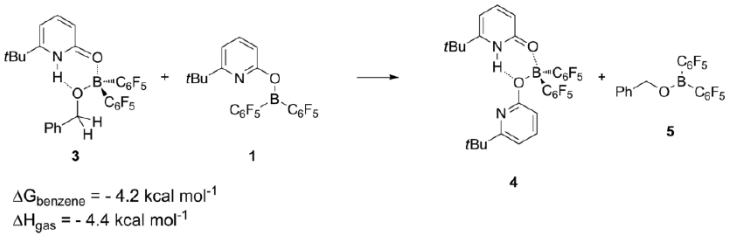

Scheme 6. Gibbs free energy and enthalpy of the formation of **4** computed at DLPNO-CCSD(T)/def2-TZVP//PBE0-D3/def2-SV(P). Bulk solvation was considered implicitly with the SMD model for benzene.

single crystals suitable for X-ray analysis after independent synthesis of **4**. The XRD structure is indeed in close agreement to the previously computed structure (Figure 3).

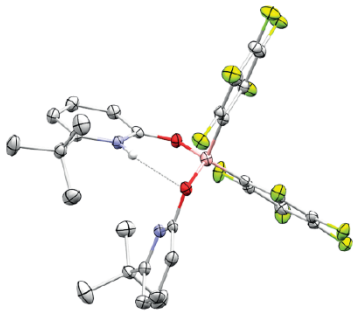

Figure 3. ORTEP representation of **4** (50 % probability ellipsoids, all hydrogens but the ones on N1 are omitted for clarity).

The low-temperature NMR experiment further revealed that a small amount of **2** is still detectable, but the corresponding shifts experienced broadening (Figure 4 and Figure S8 in the SI). The low field shift of the NH signal, which is now found at δ = 11.14 ppm, indicates the formation of the hydrogen-bonded complex of **2** and benzaldehyde **2·PhCHO** (Scheme 7). The results obtained so far, e.g., the formation of **3** (and not of a boroxypyridine-benzyl alcohol complex) as well as the formation of a hydrogen-bonded intermediate both indicate that a hydride transfer mechanism (Pathway B in Scheme 4) is operative.

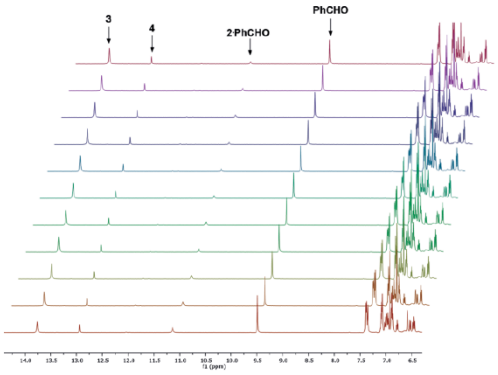

Figure 4. NMR spectra recorded every 300 s after addition of 1.2 equiv. benzaldehyde to **2** at –20 °C.

Furthermore, the low-temperature experiment clearly shows that the benzaldehyde reduction is faster than the hydrogen liberation from **2** since no H_2 pressure was applied in this experiment.

The mechanism of aldehyde reduction mediated by **2** was further investigated by accurate DLPNO-CCSD(T)/def2-TZVP//PBE0-D3/def2-SV(P) computations (Figure 5).[14] In agreement with the experimental findings, computations predict the formation of **3** to be exothermic and exergonic by –40.2 kcal/mol and –23.5 kcal/mol, respectively. However, the formation of **2·PhCHO** is predicted to be exothermic, but endergonic, which is in conflict with the experimental observations. Previous studies revealed that taking infinitely separated reactants as reference states leads to an overestimation of the entropy loss for bimolecular reactions.[15] Thus, enthalpies might be more insightful than the Gibbs free energies for the mechanism under consideration. In agreement with this assumption, the computed activation enthalpy of the benzaldehyde reduction via **TS$_{2/3}$** (11.8 kcal/mol) agrees favorably with the finding that the reaction proceeds smoothly at –20 °C. Furthermore, the computed activation enthalpy of the benzaldehyde reduction is considerably lower than the barrier for H_2 liberation from **2**, which agrees with the finding that the benzaldehyde reduction occurs without the need for H_2 pressure. Based on the mechanism discussed by Heshmat et al., a transition state in which the aldehyde, coordinated to the borane, acts as Lewis acid was also considered (**TS′$_{2/3}$**). However, this mechanistic scenario can be ruled out based on the computed high barrier. In light of the question whether a concerted mechanism via a pericyclic six-membered transition state is operative, the fact that no alcohol boroxypyridone complex could be localized is relevant and suggests a stepwise mechanism. However, a visual inspection of the imaginary frequency of **TS$_{2/3}$** indicates that the hydride transfer is associated with a proton transfer. Considering solvation implicitly with the SMD model for benzene within the structure optimizations did not alter these results.

Therefore, the intrinsic reaction coordinate (IRC) of the benzaldehyde reduction was analyzed (Figure 6). The reaction commences with the formation of a hydrogen bond between aldehyde and pyridone (Structure **A** in Figure 6). The shortening of the O···H distance by 0.3 Å in the transition structure (**TS$_{2/3}$**) reveals a concerted proton and hydride transfer. Indeed, the OH bond length of 1.00 Å in structure **B** shows that this structure can be regarded as a transient alcohol boroxypyridine complex. However, this transient structure undergoes a barrierless O–H

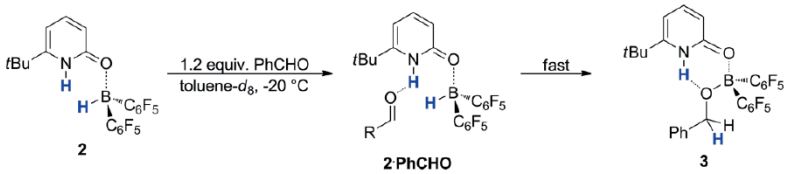

Scheme 7. Formation of **2·PhCHO** observed by a low-temperature experiment.

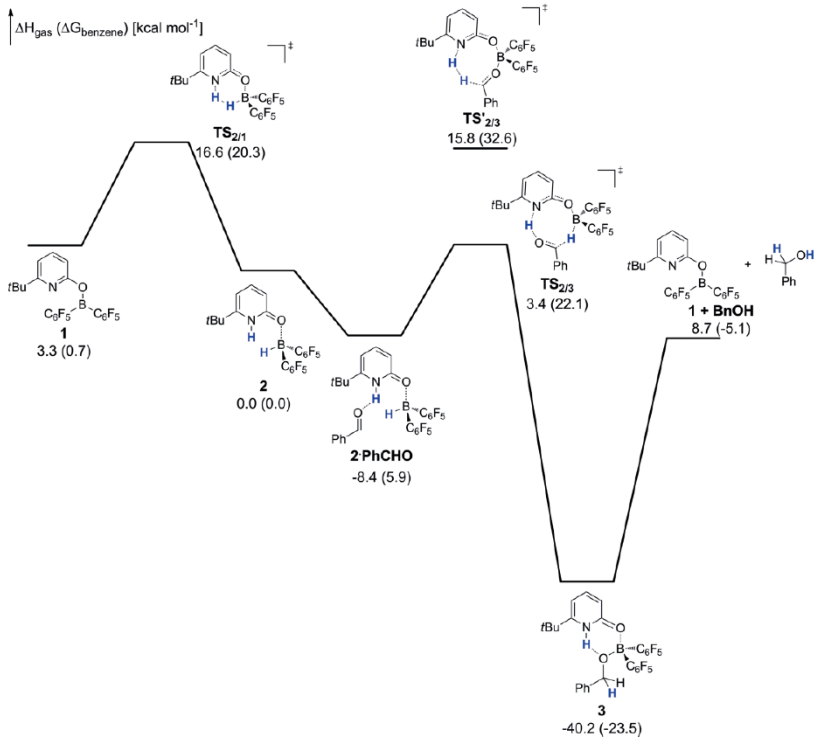

Figure 5. Gibbs free energy and enthalpy profile for the aldehyde reduction by **2** computed at DLPNO-CCSD(T)/def2-TZVP//PBE0-D3/def2-SV(P). Bulk solvation was considered implicitly with the SMD model for benzene.[13]

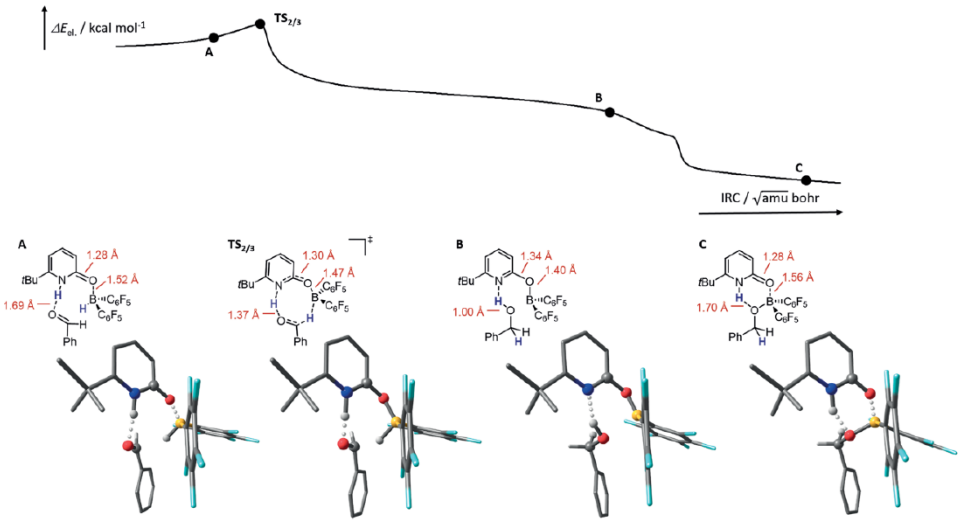

Figure 6. Intrinsic reaction coordinate associated with $TS_{2/3}$ and selected structures along the IRC.

addition, as can be deduced from the bond lengths computed for structure **C** (Figure 6). The elongation of the pyridone CO bond length and the shortening of the BO bond length furthermore indicate a boroxypyridine to pyridone transformation is associated with the concerted hydrogen transfer (Structures **A** and **B** in Figure 6). In turn, the computed bond lengths in structure **C** clearly indicate that the OH addition regenerates the pyridone borane complex. Since previous studies revealed that an increased aromaticity is indicative for a pyridone to hydroxypyridine conversion, we studied the $NICS_{1zz}$ values of the structures discussed in Figure 6.[17] Indeed, by going from **A** via **$TS_{2/3}$** to **B**, the $NICS_{1zz}$ values show an increased aromaticity of the heterocycle, indicating in agreement with the computed bond lengths a pyridone to oxypyridine transition (Figure 7). The $NICS_{1zz}$ value computed for **C** shows that the OH addition results in a decreased aromaticity, diagnostic for the reformation of a pyridone donor ligand.

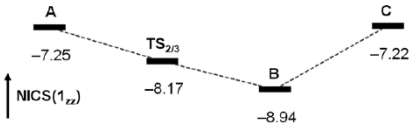

Figure 7. $NICS_{1zz}$ values for the structures discussed in Figure 4.

Conclusions

The aldehyde reduction mediated by a pyridone borane complex was studied experimentally and computationally. While conventionally, stepwise or concerted mechanisms are discussed for the carbonyl reduction by metal-free systems, we show that there is a third possibility: concerted hydrogenation yielding a transient alcohol complex that undergoes barrierless OH addition to the bifunctional system. In case of the pyridone borane complex studied herein, the concerted hydrogenation is associated with a pyridone borane to boroxypyridine transition. In turn, the barrierless OH addition regenerates the pyridone borane form.

Experimental Section

General Specifications: All manipulations with air and moisture sensitive compounds were carried out under a nitrogen atmosphere using standard Schlenk and glovebox techniques. 6-*tert*-Butyl-2-pyridone and $HB(C_6F_5)_2$ were synthesized from 3,3′-dimethyl-2-butanone and $B(C_6F_5)_3$, respectively, according to literature procedures.[18,19] Deuterated solvents were degassed with argon and kept in the glovebox over 4 Å molecular sieves. NMR spectra were recorded on Bruker Avance III HD 400 MHz and Bruker Avance III HD 600 MHz spectrometers. ^1H and ^{13}C NMR chemical shifts are referenced to residual solvent resonance peaks.

3: A solution of 6-*tert*-butyl-2-pyridone (4.5 mg, 0.03 mmol) in [D_6]benzene (0.3 mL) was added to $HB(C_6F_5)_2$ (10.8 mg, 0.03 mmol, 1 equiv.) and the suspension transferred to an NMR tube equipped with a closed J Young valve. Upon shaking of the tube, the suspension dissolved within 15 min. Benzaldehyde (3.6 µL, 3.8 mg, 0.036 mmol, 1.2 equiv.) was added. After three freeze-pump-thaw cycles, the tube was backfilled with H_2 (2 bar). The sample was stored for 18 h at r.t. and analysed by NMR spectroscopy. Crystals suitable for X-ray analysis were obtained from a saturated cyclohexane solution of **3**. ^1H NMR (600 MHz, [D_6]benzene): δ = 13.74 (s, 1 H, NH), 7.40 (br. d, J = 7.5 Hz, 2 H, PhH), 7.19–7.12 (m, 2 H, PhH), 7.10–7.05 (m, 1 H, PhH), 6.57 (dd, J = 8.8, 7.5 Hz, 1 H, *p*-pyridoneH), 6.32 (d, J = 8.7 Hz, 1 H, *m*-pyridoneH), 5.65 (dd, J = 7.5, 1.0 Hz, 1 H, *m*-pyridoneH), 4.61 (br. s, 2 H, OCH_2Ph), 0.57 (s, 9 H, CCH_3) ppm. ^{13}C NMR (151 MHz, [D_6]benzene): δ = 162.6, 157.5, 144.9 (*p*-pyridone), 133.5, 128.3 (Ph), 128.0 (Ph), 127.8 (Ph), 115.0 (*m*-pyridone), 109.3 (*m*-pyridone), 66.4 (OCH_2Ph), 34.6 (CCH_3), 27.7 ppm (CCH_3)*. (*Assignment only partially possible based on an HSQC experiment due to partial overlap with the solvent residue signals.) ^{11}B NMR (193 MHz, [D_6]benzene): δ = 6.19 ppm. ^{19}F NMR (377 MHz, [D_6]-benzene): δ = −134.20 (br), −157.12 (br), −163.88 ppm.

X-ray Analysis of 3: The X-ray crystallographic data for **3** were collected using a BRUKER/NONIUS KappaCCD detector with a BRUKER/NONIUS FR591 rotating anode radiation source and an OXFORD CRYOSYSTEMS 600 low-temperature system at 120 K using φ- and ω-scans. Mo-K_α radiation with wavelength 0.71073 Å and a graphite monochromator were used. Semi-empirical absorption corrections from equivalents were applied using SADABS.[20] The unit cell was determined using 969 reflections and the structure was solved by direct methods using SHELXT in the triclinic space group $P\bar{1}$.[21] The structure was refined against F^2 on all data by full-matrix least-squares using SHELXL2016/6.[22] All non-hydrogen atoms were refined anisotropically and C–H hydrogen atoms were positioned at geometrically calculated positions and refined using a riding model. The N–H hydrogen atom was located in the Fourier difference map and set to ideal distance. The isotropic displacement parameters of all hydrogen atoms were fixed to 1.2*x* or 1.5*x* (CH_3 hydrogens) the U_{eq} value of the atoms they are linked to. One part of the structure was found to be disordered and the disorder ratio was refined and converged to 0.59(2). The disorder was refined with the help of similar ADP restraints and similarity restraints on 1,2- and 1,3-distances. Advanced rigid bond restraints were used for the refinement of the whole structure. The crystallographic data were deposited at the Cambridge Crystallographic Data Centre as CCDC 1844627.[23]

Reaction Monitoring by ^1H NMR: A solution of 6-*tert*-butyl-2-pyridone (4.5 mg, 0.03 mmol) in [D_8]toluene (0.3 mL) was added to $HB(C_6F_5)_2$ (10.8 mg, 0.03 mmol, 1 equiv.) and the suspension transferred to an NMR tube equipped with a closed J Young valve. Upon shaking of the tube, the suspension dissolved within 15 min. A ^1H NMR was recorded at room temp. to ensure the formation of **2**. The sample was cooled to −20 °C and an additional ^1H NMR spectrum recorded at this temperature. Benzaldehyde (3.6 µL, 3.8 mg, 0.036 mmol, 1.2 equiv.) was added at room temp. and the sample immediately placed again into the precooled NMR spectroscopy. ^1H NMR spectra were recorded at −20 °C every 300 s over 1 h.

Synthesis of 4: 4 was synthesized as described previously.[8] Crystals suitable for X-ray analysis were obtained from laying a benzene solution of **4** with cyclohexane.

X-ray Analysis of 4: Diffraction data for **4** were collected at low temperatures (100 K) using φ- and ω-scans on a BRUKER D8 Venture system equipped with dual IµS microfocus sources, a PHOTON100 detector and an OXFORD CRYOSYSTEMS 700 low-temperature system. Cu-K_α radiation with wavelength 1.54178 Å and a collimating Quazar multilayer mirror were used. Semi-empirical absorption correction from equivalents was applied using SADABS.[20] The unit cell was determined using 9612 reflections and the structure was solved by direct methods using SHELXT in the monoclinic space group

Cc.[21] The structure was refined against F^2 on all data by full-matrix least-squares using SHELXL. All non-hydrogen atoms were refined anisotropically and C–H hydrogen atoms were positioned at geometrically calculated positions and refined using a riding model. The N–H hydrogen atoms were located in the Fourier difference map and set to ideal distances. The isotropic displacement parameters of all hydrogen atoms were fixed to 1.2*x* or 1.5*x* (CH_3 hydrogens) the U_{eq} value of the atoms they are linked to. The asymmetric unit contains two molecules of **4** and one cyclohexane molecule. The absolute structure could be determined using the anomalous dispersion effect with a Flack *x* parameter of 0.036(53) and a Parsons parameter of 0.021(14). The crystallographic data were deposited at the Cambridge Crystallographic Data Centre as CCDC 1845181.[23]

Computational Details: All structures were fully optimized with the hybrid version of the Perdew–Burke–Ernzerhof functional containing 25 % exact HF-exchange (PBE0) and a double zeta def2-SV(P) basis set.[10a,b,d] Dispersion interactions were taken into account with Grimme's D3 correction.[10c] Thermodynamic properties were obtained at the same level of theory from a frequency computation. Single-Point energies were computed at the DLPNO-CCSD(T) level,[14a] with the triple zeta def2-TZVP basis set.[10d] Solvent effects were taken into account implicitly using the SMD model for benzene.[16] The computed free energies were corrected with regard to the standard state by adding $RT{\cdot}\ln(c_0s/c_0g)$ (i.e., about 1.84 kcal/mol) to energies of all structures. NMR computations were done at the PBE0/def2-TZVP level with the GIAO method.[24]

Acknowledgments

This work was supported by the Fonds der Chemischen Industrie (Liebig Fellowship to U. G.). We thank Dr. H. Hausmann for assistance with NMR experiments. Continuous and generous support by Profes. Dres. P. R. Schreiner, R. Göttlich, and H. A. Wegner is acknowledged.

Keywords: Boron ligand cooperation · Coupled cluster computations · Frustrated Lewis pairs · Aldehydes · Reduction · Hydrogenation

[1] T. Mahdi, D. W. Stephan, *J. Am. Chem. Soc.* **2014**, *136*, 15809–15812.
[2] D. J. Scott, M. J. Fuchter, A. E. Ashley, *J. Am. Chem. Soc.* **2014**, *136*, 15813.
[3] a) S. Das, S. K. Pati, *Chem. Eur. J.* **2017**, *23*, 1078; b) E. Arnett, C. Y. Wu, *J. Am. Chem. Soc.* **1960**, *82*, 4999; c) H. J. Campbell, J. T. Edward, *Can. J. Chem.* **1960**, *38*, 2109.
[4] M. Heshmat, T. Privalov, *Chem. Eur. J.* **2017**, *23*, 9098.
[5] C. A. Sandoval, T. Ohkuma, K. Muniz, R. Noyori, *J. Am. Chem. Soc.* **2003**, *125*, 13490.
[6] H. Li, L. Zhao, G. Lu, F. Huang, Z.-X. Wang, *Dalton Trans.* **2010**, *39*, 5519.
[7] P. A. Dub, N. J. Henson, R. L. Martin, J. C. Gordon, *J. Am. Chem. Soc.* **2014**, *136*, 3505.
[8] U. Gellrich, *Angew. Chem. Int. Ed.* **2018**, *57*, 4779; *Angew. Chem.* **2018**, *130*, 4869.
[9] P. Spies, G. Erker, G. Kehr, K. Bergander, R. Fröhlich, S. Grimme, D. W. Stephan, *Chem. Commun.* **2007**, 5072.
[10] a) J. P. Perdew, K. Burke, M. Ernzerhof, *Phys. Rev. Lett.* **1996**, *77*, 3865; b) C. Adamo, V. Barone, *J. Chem. Phys.* **1999**, *110*, 6158; c) S. Grimme, S. Ehrlich, L. Goerigk, *J. Comput. Chem.* **2011**, *32*, 1456; d) F. Weigend, R. Ahlrichs, *Phys. Chem. Chem. Phys.* **2005**, *7*, 3297; e) Gaussian 16, Revision A.03, M. J. Frisch, G. W. Trucks, H. B. Schlegel, G. E. Scuseria, M. A. Robb, J. R. Cheeseman, G. Scalmani, V. Barone, B. Mennucci, G. A. Petersson, H. Nakatsuji, M. Caricato, X. Li, H. P. Hratchian, A. F. Izmaylov, J. Bloino, G. Zheng, J. L. Sonnenberg, M. Hada, M. Ehara, K. Toyota, R. Fukuda, J. Hasegawa, M. Ishida, T. Nakajima, Y. Honda, O. Kitao, H. Nakai, T. Vreven, J. A. Montgomery Jr., J. E. Peralta, F. Ogliaro, M. Bearpark, J. J. Heyd, E. Brothers, K. N. Kudin, V. N. Staroverov, R. Kobayashi, J. Normand, K. Raghavachari, A. Rendell, J. C. Burant, S. S. Iyengar, J. Tomasi, M. Cossi, N. Rega, J. M. Millam, M. Klene, J. E. Knox, J. B. Cross, V. Bakken, C. Adamo, J. Jaramillo, R. Gomperts, R. E. Stratmann, O. Yazyev, A. J. Austin, R. Cammi, C. Pomelli, J. W. Ochterski, R. L. Martin, K. Morokuma, V. G. Zakrzewski, G. A. Voth, P. Salvador, J. J. Dannenberg, S. Dapprich, A. D. Daniels, Ö. Farkas, J. B. Foresman, J. V. Ortiz, J. Cioslowski, D. J. Fox, *Gaussian 09, Revision*, Gaussian, Inc., Wallingford CT, **2016**.
[11] J. H. Williams, *Acc. Chem. Res.* **1993**, *26*, 593.
[12] a) G. W. Coates, A. R. Dunn, L. M. Henling, D. A. Dougherty, R. H. Grubbs, *Angew. Chem. Int. Ed. Engl.* **1997**, *30*, 248; *Angew. Chem.* **1997**, *109*, 290; b) F. Cozzi, F. Ponzini, R. Annunziata, M. Cinquini, J. S. Siegel, *Angew. Chem. Int. Ed. Engl.* **1995**, *34*, 1019; *Angew. Chem.* **1995**, *107*, 1092; c) R. Xu, W. B. Schweizer, H. Frauenrath, *Chem. Eur. J.* **2009**, *15*, 9105.
[13] For details, see the Supporting Information.
[14] a) C. Riplinger, B. Sandhoefer, A. Hansen, F. Neese, *J. Chem. Phys.* **2013**, *139*, 134101; b) F. Neese, *WIREs Comput. Mol. Sci.* **2012**, *2*, 73.
[15] a) B. Mondal, F. Neese, S. Ye, *Inorg. Chem.* **2015**, *54*, 7192; b) H. Fang, H. Jing, H. Ge, P. J. Brothers, X. Fu, S. Ye, *J. Am. Chem. Soc.* **2015**, *137*, 7122; c) G. Koleva, B. Galabov, J. Kong, H. F. Schaefer III, P. v. R. Schleyer, *J. Am. Chem. Soc.* **2011**, *133*, 19094.
[16] A. V. Marenich, C. J. Cramer, D. G. Truhlar, *J. Phys. Chem. B* **2009**, *113*, 6378.
[17] J. I. Wu, J. E. Jackson, P. v. R. Schleyer, *J. Am. Chem. Soc.* **2014**, *136*, 13526.
[18] L. Hintermann, T. T. Dang, A. Labonne, T. Kribber, L. Xiao, P. Naumov, *Chem. Eur. J.* **2009**, *15*, 7167.
[19] D. J. Parks, W. E. Piers, G. P. A. Yap, *Organometallics* **1998**, *17*, 5501.
[20] L. Krause, R. Herbst-Irmer, G. M. Sheldrick, D. Stalke, *J. Appl. Crystallogr.* **2015**, *48*, 3.
[21] G. M. Sheldrick, *Acta Crystallogr., Sect. A* **2015**, *71*, 3.
[22] G. M. Sheldrick, *Acta Crystallogr., Sect. C* **2015**, *71*, 3.
[23] CCDC 1844627 (for **3**) and 1845181 (for **4**) contain the supplementary crystallographic data for this paper. These data can be obtained free of charge from The Cambridge Crystallographic Data Centre.
[24] R. Ditchfield, *Mol. Phys.* **1974**, *27*, 789.

Received: June 1, 2018

5.2 Metal-free *gem* selective dimerization of terminal alkynes catalyzed by a pyridonate borane complex

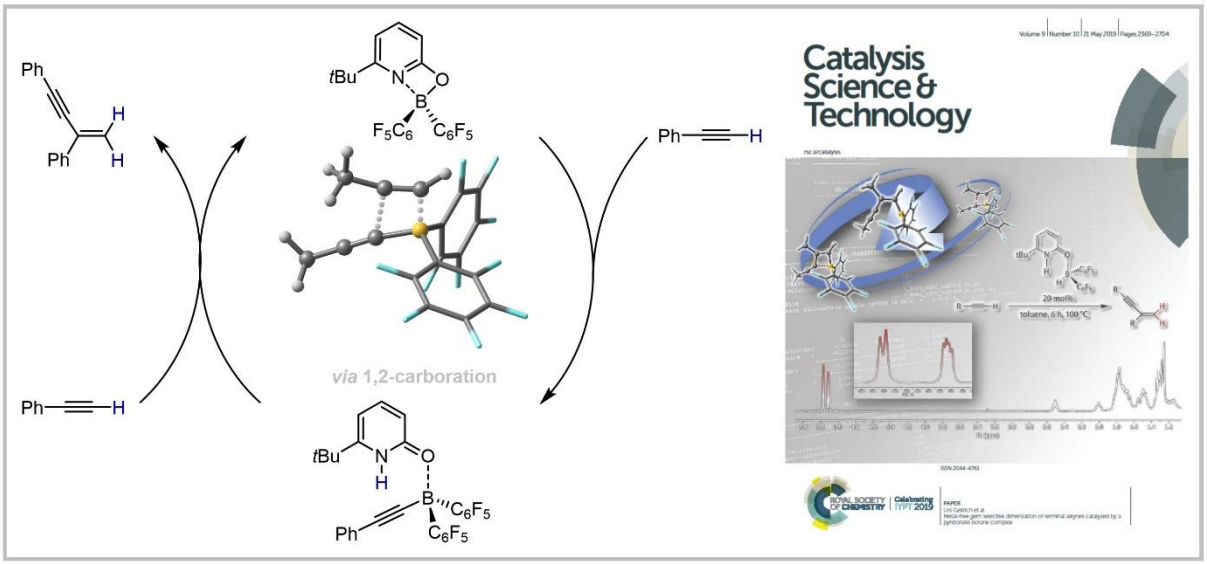

The metal-free dimerization of alkynes catalyzed by a pyridonate borane complex via a 1,2-carboration is reported.

Max Hasenbeck, Tizian Müller, Dr. Urs Gellrich,

Catal. Sci. Technol. **2019**, *9, 2438-2444*

DOI: 10.1039/C9CY00253G

Finale veröffentlichte Version online: 16.04.2019

Catalysis Science & Technology

PAPER

View Article Online
View Journal | View Issue

Cite this: *Catal. Sci. Technol.*, 2019, **9**, 2438

Metal-free *gem* selective dimerization of terminal alkynes catalyzed by a pyridonate borane complex†

Max Hasenbeck, Tizian Müller and Urs Gellrich *

Received 2nd February 2019,
Accepted 15th April 2019

DOI: 10.1039/c9cy00253g

rsc.li/catalysis

A metal free *gem* selective dimerization of terminal alkynes catalyzed by a pyridonate borane complex is described. Each individual step of the catalytic cycle was verified experimentally and a protocol for the catalytic reaction was developed. The mechanism of the reaction was further investigated by DFT and DLPNO-CCSD(T) computations. The catalytic transformation commences with C–H cleavage by a boroxypyridine that displays frustrated Lewis pair reactivity. The pyridone borane complex that forms upon C–H cleavage dissociates into a pyridone and an alkynylborane. An unprecedented 1,2-carboboration and a protodeborylation effected by the pyridone yield the 1,3-enyne and complete the catalytic cycle. The change in the coordination mode of the boroxypyridine upon C–H cleavage, described by the term boron-ligand cooperation, enables the dissociation of the formed pyridone borane complex and the 1,2-carboboration and is thus vital for the catalytic reaction.

Introduction

The dimerization of terminal alkynes *via* a formal hydroalkynylation of the carbon–carbon triple bond is an attractive route towards 1,3-enynes due to its intrinsic atom economy.[1] A variety of synthetic protocols using metal complexes as catalysts have been reported.[2] Notable recent examples include iron complex catalyzed highly regioselective reactions.[3] The activation of the terminal C_{sp}–H-bond of the alkyne by the metal complex is a prerequisite for its catalytic activity. Several inter- and intramolecular frustrated Lewis pairs (FLP) are also capable of splitting the C_{sp}–H-bond of terminal alkynes in a heterolytic fashion.[4,5]

A classic example is the reaction of the sterically encumbered tris-*tert*-butyl-phosphine and the highly Lewis acidic tris-perfluorophenylborane with phenylacetylene that yields salt **1**.[4a] We recently reported reversible H_2 activation by the boroxypyridine **2′** that is in equilibrium with the pyridonate borane complex **2** and can be regarded as a single component FLP.[6] Significantly, upon H_2 activation the boroxypyridine undergoes a change in coordination mode. The pyridone borane complex **3**, in which the pyridone is only coordinatively bound to the borane, is formed. In analogy to the term metal–ligand cooperation, this significant change in the coordination mode of a substituent that is involved in the bond activation process was described as boron-ligand cooperation.[7] We envisioned that the reaction of **2** with a terminal alkyne would, unlike the reaction of a classic FLP, not yield a borate anion, but rather a pyridone alkynylborane complex that could show further reactivity upon dissociation.

Results and discussion

Upon addition of two equivalents of phenylacetylene to **2**, complete conversion to the CH activation product **4** was observed within 15 minutes (Scheme 2). The cleavage of the C_{sp}–H bond is accompanied by the transformation of the boroxypyridine to a pyridone alkynylborane complex, evident from the experimental IR spectrum and from the computed structural changes (*vide infra*). When **4** was heated to 90 °C

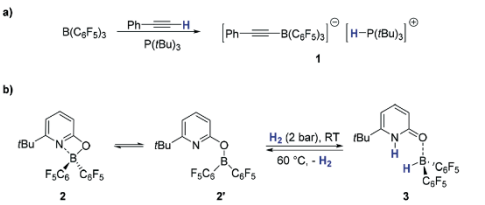

Scheme 1 a) Reaction of a classic FLP with phenylacetylene and b) reversible hydrogen activation by **2**.

Institute of Organic Chemistry, Justus-Liebig University, Heinrich-Buff-Ring 17, 35392 Giessen, Germany. E-mail: urs.gellrich@org.chemie.uni-giessen.de

† Electronic supplementary information (ESI) available: Experimental details, 1D- and 2D-NMR spectra and details of the quantum chemical calculations are given. See DOI: 10.1039/c9cy00253g

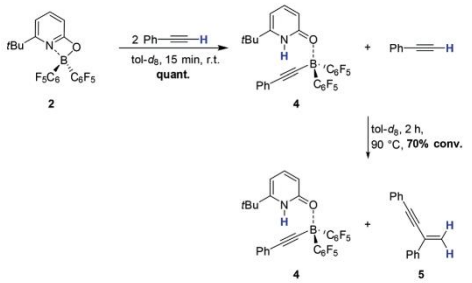

Scheme 2 Methylidyne C–H cleavage and the *gem* selective dimerization of phenylacetylene promoted by the pyridonate borane complex **2**.

in the presence of the remaining one equivalent phenylacetylene, formation of the dimerization product 1,3-diphenyl-but-3-en-1-yne **5** was observed by ^{1}H NMR (Fig. 1 and ESI†). No regioisomers of the *gem* dimer **5** could be detected.

Notably, ^{1}H and ^{11}B NMR show no significant change in the spectral features of **4**, indicating that **4** is not a reactant, but rather the resting state of a catalytic reaction (Fig. 1).

The anticipated catalytic reaction is initiated by a heterolytic CH cleavage by pyridonate borane **2** (Scheme 3). It seems further plausible to assume that the carbon–carbon bond is formed, after dissociation of **4**, by the carboboration of phenylacetylene. A final protodeborylation generates **5** and completes the cycle.[4e,8] Since dissociation of a FLP upon CH cleavage of a terminal alkyne as well as the 1,2-carboboration of an alkyne by an alkynylborane are both unprecedented, we decided to investigate the elementary steps of the presumed catalytic cycle individually.

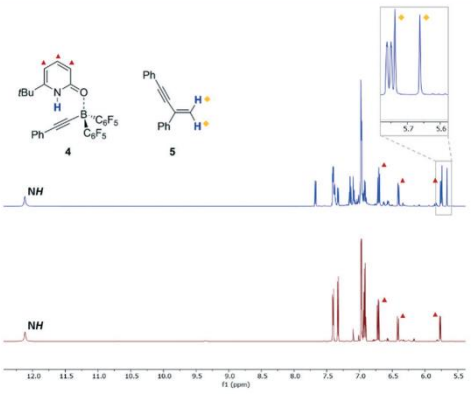

Fig. 1 ^{1}H NMR (600 MHz, toluene-d_8) of **4** in the presence of phenylacetylene (red, lower panel) and the spectrum obtained after heating the solution to 90 °C for 2 h (blue, upper panel).

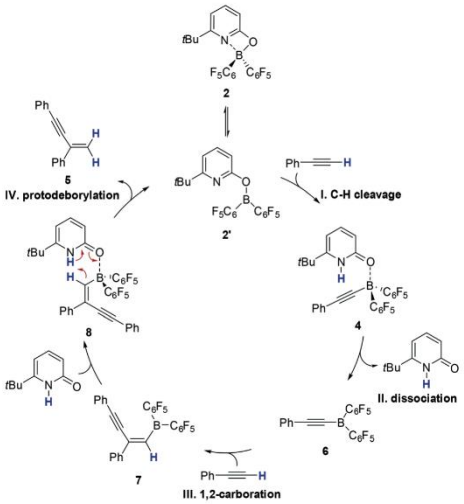

Scheme 3 Hypothetical catalytic cycle for the observed *gem* selective dimerization of phenylacetylene.

Stepwise investigation of the catalytic cycle

I. C–H cleavage. The reaction of **2** with phenylacetylene or 1-octyne is complete within 15–30 minutes (Scheme 4). The pyridone alkynylborane complexes **4** and **9** were fully characterized by NMR and IR spectroscopy.

Characteristic for the formation of **4** and **9** are the NMR signals for the NH group at 12.09 ppm and 12.50 ppm as well as ^{11}B NMR signals at −5.9 ppm and −6.3 ppm, indicating a tetravalent borane.[9] The pyridone C=O stretching vibration of **4** and **9** is found at 1642 cm^{-1}, indicating the formation of an pyridone ligand in course of the C–H cleavage. The heterolytic C–H cleavage was also investigated by accurate TightPNO-DLPNO-CCSD(T) computations (Fig. 2).[10] Since no pronounced difference regarding the reactivity of phenylacetylene or 1-octyne was found experimentally, propyne was used as model alkyne throughout this study. As anticipated, the active form is the boroxypyridine **2′** that is connected with the pyridonate borane complex **2** by the transition state $\mathbf{TS_{2/2'}}$. The boroxypyridine **2′** can be regarded as an intramolecular frustrated Lewis pair. The barrier for the exergonic C–H cleavage is computed to be 20.9 kcal mol^{-1}. The computations further reveal that the C–H cleavage is

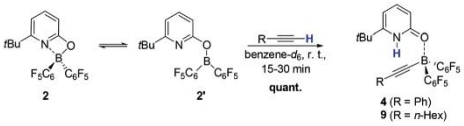

Scheme 4 Heterolytic cleavage of the methylidyne C–H bond of phenylacetylene and 1-octyne by **2**.

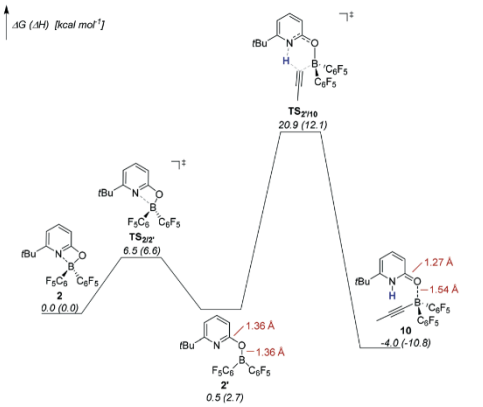

Fig. 2 Gibbs free energy and enthalpy for the heterolytic C–H cleavage computed at TightPNO-DLPNO-CCSD(T)/def2-TZVP//PBE0-D3(BJ)/def2-TZVP.[10,11] The SMD model for toluene was used to implicitly account for solvent effects.[12]

associated with shortening of the C=O bond and an elongation of the B–O bond. These structural changes indicate, in agreement with IR spectral features, the transition of the boroxypyridine to a datively bound pyridone.

II. Dissociation. If the observed C–C bond formation en route to **5** occurs *via* a 1,2-carboboration, dissociation of the pyridone alkynylborane complex would be required. This dissociation cannot be observed directly. However, when the strong Lewis acid $B(C_6F_5)_3$ is added at r.t. to a solution of **4**, exchange of the alkynylborane with $B(C_6F_5)_3$ is observed within 2 h (Scheme 5a). The exchange is evident from a shift of the NH signal in the ^{1}H NMR from 12.09 ppm to 9.54 ppm. Furthermore, a new set of signals appears in the region that is typical for the CH signals of the pyridone. The ^{11}B NMR signal shift from −6.3 ppm to −1.2 ppm. The spectroscopic data are identical to a sample of **11** obtained from 6-*tert*-butylpyridone and $B(C_6F_5)_3$. A second ^{11}B NMR signal at

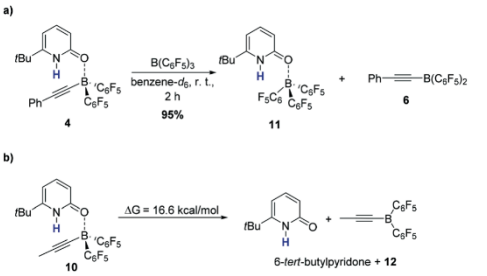

Scheme 5 a) Exchange of alkynylborane in **4** with $B(C_6F_5)_3$. b) Gibbs free energy for the dissociation of **10** computed at TightPNO-DLPNO-CCSD(T)/def2-TZVP//PBE0-D3(BJ)/def2-TZVP. The SMD model for toluene was used to implicitly account for solvent effects.

48.3 ppm indicates the presence of a trivalent borane, alkynylborane **6**.[8] Since the observed exchange cannot occur *via* an associative mechanism, the reaction indicates that dissociation of **4** can occur already at r.t. The ΔG_{Diss} of 16.6 kcal mol^{-1}, computed for the dissociation of **10** in 6-*tert*-butylpyridone and the trivalent propynylborane **12** agrees favourably with this observation (Scheme 5b). A relaxed potential energy scan did not reveal any dissociation barrier.

III. 1,2-Carboboration. The most notable step in the proposed catalytic cycle is the 1,2-carboboration. 1,1-Carboborations of metal- and silylacetylenes, referred as Wrackmeyer reaction, are well established.[13] Furthermore, carboborations of alkynes by borenium cations and 1,1-carboborations of alkynes by $B(C_6F_5)_3$ have been reported.[14–16] Recently, the 1,2-carboboration of alkynes by borafluorenes, a 1,2-halogenoboration of alkynes, a FLP-mediated 1,2-hydrocarbation of alkynes, a 1,2-carboboration of alkenes *via* a radical pathway and a *trans*-alkenylboration of propargylic alcohols were shown.[17–21] However, while a Ni-catalyzed variant exist, we are unaware of any example of an uncatalyzed 1,2-carboboration of a non-functionalized alkyne by an alkynylborane.[22] In order to study this reaction in detail, alkynylborane **6** was synthesized according to a known procedure from $ClB(C_6F_5)_2$ and the respective tin organyl. Pure **6** was isolated by crystallization from benzene/*n*-hexane.[23] The 1,2-carboboration reaction was then studied by reacting **6** with phenylacetylene. However, monitoring the reaction of **6** with 3-phenyl-1-propyne by NMR spectroscopy proved to be more insightful: in that case, HH COSY and NOSY contacts between the benzylic methylene group and the terminal C_{sp}–H allowed following the shift of this signal from 1.96 ppm to 6.80 ppm upon addition of 3-phenyl-1-propyne to a solution of **6** in benzene-d_6 at r.t. (Scheme 6).

To further support the interpretation of the NMR experiment, the shielding of **13** was computed. For that purpose, six conformers were computed at DLPNO-CCSD(T)/def2-TZVP//PBE0-D3(BJ)/def2-SVP. The relative free energies of these conformers were then used to calculate their Boltzmann-weighted contribution to the shielding that was computed with PBE0 and the triple-zeta basis set pcS-2, specifically designed for this purpose (Table 1).[24] The computed NMR shifts agree well with those observed experimentally, thus supporting the assumption that the 1,2-carboboration product **13** is formed.

Computations reveal that association of the alkynylborane with the free alkyne precedes carboboration (Fig. 3). This association is predicted to be exothermic but endergonic. The

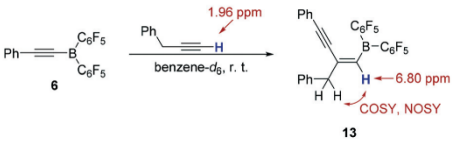

Scheme 6 1,2-Carboboration reaction with 3-phenyl-1-propyne.

Table 1 Comparison of the experimental and the computed NMR data of **13**

	Exp.[a]	PBE0/pcS-2[a,b,c]
^{1}H (PhCH_2)	3.59	3.37
^{1}H (C_{sp^2}–H)	6.80	6.58
^{11}B	59.8	57.1
^{13}C (PhCH_2)	48.9	43.0
^{13}C (C_{sp^2}–H)	138.7	143.0

[a] ^{1}H and ^{13}C NMR shifts in ppm, experimental shifts referenced to solvent residual signals of benzene-d_6 and computed shifts to benzene computed with the same protocol. [b] ^{11}B shift referenced to $Me_3N{\cdot}BH_3$ computed with the same protocol. [c] Based on a DLPNO-CCSD(T)/def2-TZVP//PBE0-D3(BJ)/def2-SVP conformer analysis.

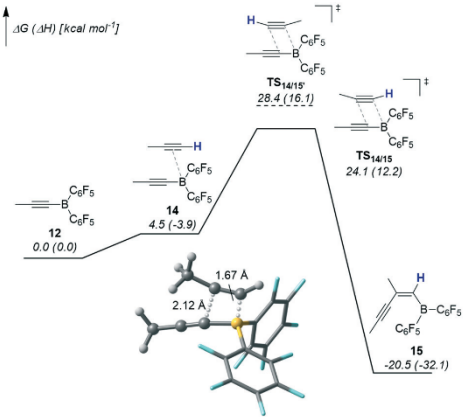

Fig. 3 Gibbs free energy and enthalpy for the 1,2-carboboration computed at TightPNO-DLPNO-CCSD(T)/def2-TZVP//PBE0-D3(BJ)/def2-TZVP. The SMD model for toluene was used to implicitly account for solvent effects. The inset shows the transition structure of the 1,2-carboboration.

carboboration takes place in a concerted fashion, but the bond formation is asynchronous with formation of the B–C bond being further advanced in the transition structure (Fig. 3, inset), which therefore bears a partial negative charge on boron and a partial positive charge on the non-terminal carbon of the former triple bond. In contrast to the stoichiometric 1,1-carboboration of alkynes by $B(C_6F_5)_3$ no zwitterionic intermediate is formed.[13a] A protodeborylation of **15** leads to the observed *gem* product. The addition of the alkynyl group to the terminal carbon (**TS$_{14/15'}$**), that would lead to a *trans*-hydroalkynylation, is disfavored by 4.3 kcal mol^{-1}. This is in agreement with the experimentally observed exclusive *gem* selectivity.

IV. Protodeborylation. In order to complete the hypothetical catalytic cycle, 6-*tert*-butylpyridone was added to a solution of **13** in benzene-d_6, resulting in formation of *gem* hydroalkynylation product **16** and bispyridone complex **17**

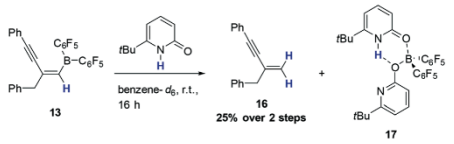

Scheme 7 Protodeborylation of **13** by 6-*tert*-butylpyridone and formation of **17**.

(Scheme 7 and Fig. 4). Complex **17** had been previously synthesized and completely characterized, including SC-XRD analysis.[25] The product of protodeborylation **16** was characterized by NMR and its identity supported further by ESI-MS analysis of the reaction mixture.

The reaction is accompanied by the formation of unidentified impurities (Fig. 4). However, by use of an internal standard the yield of **16** over the carboboration and protodeborylation steps was determined to be 25%. Note that since half of the pyridone is bound in complex **17**, the theoretical yield of **16** is 50%. A computational analysis of the transition structure of the protodeborylation revealed a shortening of the B–O bond compared to the enynylborane complex **18** (Fig. 5). Simultaneously, the C_{ipso}–O bond is elongated. This structural changes hint to the transition of the pyridone ligand back to a boroxypyridine substituent in course of the exergonic protodeborylation that completes the catalytic cycle.

Catalytic reactions

With the information on the single steps of the cycle, we attempted the catalytic *gem* selective dimerization of terminal alkynes (Scheme 8). Since our previous results showed that the pyridone borane complex **3** liberates hydrogen upon moderate heating (Scheme 1), this complex was used as catalyst, facilitating the experimental setup. With a catalyst loading of 20 mol%, phenylacetylene, *p*-tolylacetylene and *p*-*t*Bu-

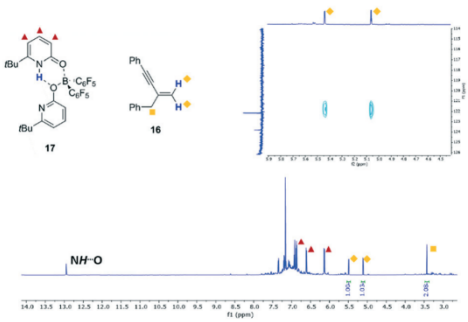

Fig. 4 ^{1}H NMR spectrum obtained upon addition of 6-*tert*-butylpyridone to **13** (600 MHz, benzene-d_6). The inset shows the corresponding HSQC spectrum.

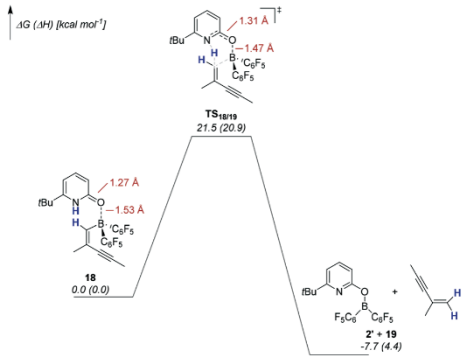

Fig. 5 Gibbs free energy and enthalpy for the protodeborylation computed at TightPNO-DLPNO-CCSD(T)/def2-TZVP//PBE0-D3(BJ)/def2-TZVP. The SMD model for toluene was used to implicitly account for solvent effects.

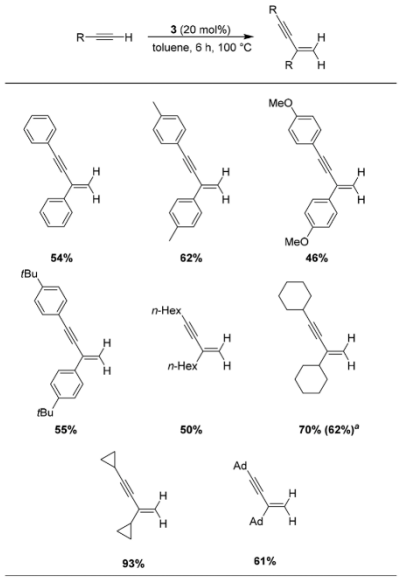

Scheme 8 *Gem* selective dimerization of terminal alkynes catalyzed by **3**. Yields determined by ^{1}H NMR with trimethoxybenzene as internal standard. Abbreviations: *t*Bu = *tert*-butyl, Ad = adamantyl. a) In parenthesis: yield of isolated product.

phenylacetylene were dimerized with fair yields from 54% to 62%. Weakly coordinating groups such as ethers are tolerated, albeit the reaction with *p*-anisolacetylene gives a slightly lower yield of 46%. The protocol can be applied to aliphatic alkynes such as 1-octyne, which displays a reactivity similar to that of phenylacetylene. Cyclohexylacetylene is dimerized with a good yield of 70%. The *gem* dimerization product of cyclopropylacetylene was obtained in excellent 93% yield. The higher reactivity of cyclopropylacetylene is attributed to the ability of the cyclopropyl group to stabilize a positive partial charge on the α-carbon in the transition structure of the carboboration.[26] Sterically demanding substituents are tolerated, as demonstrated by the successful dimerization of adamantylacetylene. The results show that the reaction is indeed catalytic with respect to pyridone borane **3**. This is, to the best of our knowledge, the first dimerization of terminal alkyne catalyzed by a metal free system. Note that the presence of 6-*tert*-butylpyridone is vital for the catalytic reaction: the isolated alkynylborane **6** does not show any catalytic activity under identical reaction conditions.

Potential energy surface of the catalytic reaction

Finally, the computed individual steps of the catalytic transformation were joined to one potential energy surface (PES, Fig. 6). For the sake of brevity, the equilibrium between **2** and **2′** (Fig. 2) is omitted. The barrier of the C–H activation is 20.9 kcal mol^{-1} as already discussed (Fig. 2). However, the possibility of free 6-*tert*-butylpyridone coordinating to **2′** reduces the enthalpic penalty associated with dissociation. Note that the coordination of free 6-*tert*-buty-pyridone to **2′**, yielding the bispyridone complex **17**, was observed experimentally in course of this study (Scheme 7). It is the 6-*tert*-butylpyridone contained within the bispyridone complex **17** that re-coordinates after the 1,2-carboboration to enynylborane **15** and effects the protodeborylation. If the PES is analyzed in terms of the "Energetic Span" concept, introduced by Kozuch and Shaik, the kinetic barrier between the pyridone alkynylborane complex **10** and the transition state of the carboboration must be regarded as the "Energetic Span", that is, the barrier, of the catalytic reaction.[27] This barrier of 25.0 kcal mol^{-1} is slightly higher than that for the protodeborylation, which is 21.5 kcal mol^{-1}. The pyridone alkynylborane complex represents the resting state of the catalytic cycle. This is in agreement with the initial NMR experiment that revealed **4** as an observable species during the catalytic reaction (Fig. 1).

Conclusions

In summary, we have documented a metal-free *gem* selective dimerization of terminal alkynes that is catalyzed by a pyridonate borane complex. Each elementary step of the catalytic reaction was examined individually and the results hint to a mechanistic scenario that consist of a 1,2-carboboration as C–C bond forming event. A change in the coordination mode of the pyridonate substituent upon C–H cleavage enables the dissociation of the pyridone borane complex and precedes the 1,2-carboboration. The novel reactivity of the pyridone borane complex reported herein might stimulate the development of novel metal-free C–C bond forming reactions.

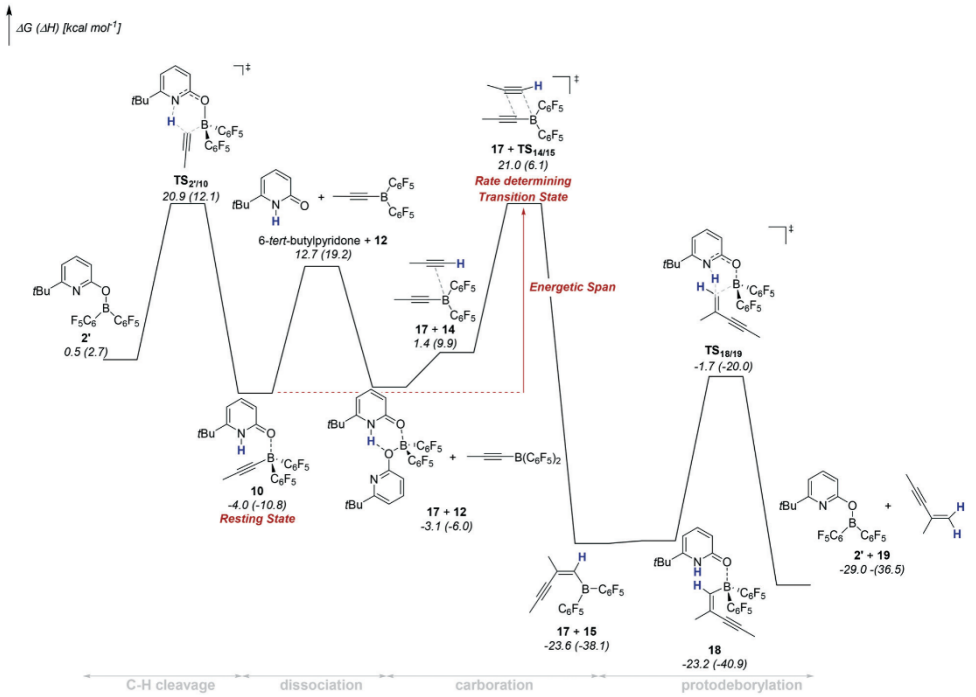

Fig. 6 PES of the *gem* selective dimerization of propyne catalyzed by **2'** computed at TightPNO-DLPNO-CCSD(T)/def2-TZVP//PBE0-D3(BJ)/def2-TZVP. All free energies and enthalpies are given with respect to two equivalents **2** and two equivalents propyne. The SMD model for toluene was used to implicitly account for solvent effects.

Conflicts of interest

There are no conflicts to declare.

Acknowledgements

This work was supported by the FCI (Liebig Fellowship to U. G.) and the DFG (Emmy-Noether program). The authors thanks Dr. H. Hausmann and Dr. D. Gerbig for assistance with NMR and IR experiments, respectively. Continuous and generous support by Profes. Dres. P. R. Schreiner, R. Göttlich, and H. A. Wegner is acknowledged.

Notes and references

1 (*a*) B. M. Trost, *Science*, 1991, **254**, 1471; (*b*) B. M. Trost, *Angew. Chem., Int. Ed. Engl.*, 1995, **34**, 259.

2 (*a*) C. S. Yi and N. Liu, *Organometallics*, 1996, **15**, 3968; (*b*) C. S. Yi and N. Liu, *Organometallics*, 1998, **17**, 3158; (*c*) K. Ogata and A. Toyota, *J. Organomet. Chem.*, 2007, **692**, 4139; (*d*) C. Conifer, C. Gunanathan, T. Rinesch, M. Hölscher and W. Leitner, *Eur. J. Inorg. Chem.*, 2015, 333; (*e*) B. Powała and C. Pietraszuk, *Catal. Lett.*, 2014, **144**, 413; (*f*) A. Kawata, V. Kuninobu and K. Takai, *Chem. Lett.*, 2009, **38**, 836; (*g*) M. Bassetti, C. Pasquini, A. Raneri and D. Rosato, *J. Org. Chem.*, 2007, **72**, 4558; (*h*) A. Hijazi, K. Parkhomenko, J.-P. Djukic, A. Chemmi and M. Pfeffer, *Adv. Synth. Catal.*, 2008, **350**, 1493; (*i*) For a recent review see: B. M. Trost and J. T. Masters, *Chem. Soc. Rev.*, 2016, **45**, 2212.

3 (*a*) O. Rivada-Wheelaghan, S. Chakraborty, L. J. W. Shimon, Y. Ben-David and D. Milstein, *Angew. Chem., Int. Ed.*, 2016, **55**, 6942; (*b*) Q. Liang, K. M. Osten and D. Song, *Angew. Chem., Int. Ed.*, 2017, **56**, 6317; (*c*) N. Gorgas, B. Stoger, L. F. Veiros and K. Kirchner, *ACS Catal.*, 2018, **8**, 7973.

4 (*a*) M. A. Dureen and D. W. Stephan, *J. Am. Chem. Soc.*, 2009, **131**, 8396; (*b*) C. F. Jiang, O. Blacque and H. Berke, *Organometallics*, 2010, **29**, 125; (*c*) M. A. Dureen, C. C. Brown and D. W. Stephan, *Organometallics*, 2010, **29**, 6594; (*d*) M. A. Dureen, C. C. Brown and D. W. Stephan, *Organometallics*, 2010, **29**, 6422; (*e*) K. Chernichenko, Á. MadarÁsz, I. PÁpai, M. Nieger, M. Leskelä and T. Repo, *Nat. Chem.*, 2013, **5**, 718; (*f*) V. Iashin, K. Chernichenko, I. Pápai and T. Repo, *Angew. Chem., Int. Ed.*, 2016, **55**, 14146; (*g*) P. Vasko, I. A. Zulkifly, M. Fuentes, Z. Mo, J. Hicks, P. C. J. Kamer and S. Aldridge, *Chem. – Eur. J.*, 2018, **24**, 10531; (*h*) X. Jie, C. G. Daniliuc, R. Knitsch, M. Ryan Hansen, H.

Eckert, S. Ehlert, S. Grimme, G. Kehr and G. Erker, *Angew. Chem., Int. Ed.*, 2019, **58**, 882.

5 For examples of FLP catalyzed C_{sp^2}–H activations see: (*a*) M.-A. Légaré, M.-A. Courtemanche, É. Rochette and F.-G. Fontaine, *Science*, 2015, **349**, 513; (*b*) K. Chernichenko, M. Lindqvist, B. Kótai, M. Nieger, K. Sorochkina, I. Pápai and T. Repo, *J. Am. Chem. Soc.*, 2016, **138**, 4860; (*c*) J. Légaré Lavergne, A. Jayaraman, L. C. Misal Castro, E. Rochette and F.-G. Fontaine, *J. Am. Chem. Soc.*, 2017, **139**, 14714; For an example of FLP mediated C_{sp^3}–H activation see: É. Rochette, M.-A. Courtemanche and F.-G. Fontaine, *Chem. – Eur. J.*, 2017, **23**, 3567.

6 U. Gellrich, *Angew. Chem., Int. Ed.*, 2018, **57**, 4779.

7 J. R. Khusnutdinova and D. Milstein, *Angew. Chem., Int. Ed.*, 2015, **54**, 12236.

8 T. Mahdi and D. W. Stephan, *Angew. Chem., Int. Ed.*, 2013, **52**, 12418.

9 S. Hermanek, *Chem. Rev.*, 1992, **92**, 325.

10 (*a*) C. Riplinger, B. Sandhoefer, A. Hansen and F. Neese, *J. Chem. Phys.*, 2013, **139**, 134101; (*b*) F. Neese, *WIREs Comput. Mol. Sci.*, 2012, **2**, 73.

11 (*a*) J. P. Perdew, K. Burke and M. Ernzerhof, *Phys. Rev. Lett.*, 1996, **77**, 3865; (*b*) C. Adamo and V. Barone, *J. Chem. Phys.*, 1999, **110**, 6158; (*c*) S. Grimme, J. Antony, S. Ehrlich and H. Krieg, *J. Chem. Phys.*, 2010, **132**, 154104; (*d*) S. Grimme, S. Ehrlich and L. Goerigk, *J. Comput. Chem.*, 2011, **32**, 1456; (*e*) F. Weigend and R. Ahlrichs, *Phys. Chem. Chem. Phys.*, 2005, **7**, 3297; (*f*) M. J. Frisch, *et al.*, *Gaussian 16, Revision A.03*, Gaussian, Inc., Wallingford CT, 2016.

12 A. V. Marenich, C. J. Cramer and D. G. Truhlar, *J. Phys. Chem. B*, 2009, **113**, 6378.

13 (*a*) B. Wrackmeyer, *Coord. Chem. Rev.*, 1995, **145**, 125; (*b*) G. Menz and B. Wrackmeyer, *Z. Naturforsch., B: J. Chem. Sci.*, 1977, **32**, 1400; (*c*) C. Bihlmayer and B. Wrackmeyer, *Z. Naturforsch., B: J. Chem. Sci.*, 1981, **36**, 1265; (*d*) B. Wrackmeyer, C. Bihlmayer and M. Schilling, *Chem. Ber.*, 1983, **116**, 3182; (*e*) A. Sebald and B. Wrackmeyer, *J. Chem. Soc., Chem. Commun.*, 1983, 309; (*f*) A. Sebald and B. Wrackmeyer, *J. Organomet. Chem.*, 1997, **544**, 105; (*g*) B. Wrackmeyer, A. Pedall and J. Weidinger, *J. Organomet. Chem.*, 2002, **649**, 225; (*h*) R. Köster, G. Seidel and B. Wrackmeyer, *Chem. Ber.*, 1989, **122**, 1825.

14 M. Devillard, R. Brousses, K. Miqueu, G. Bouhadir and D. A. Bourissou, *Angew. Chem., Int. Ed.*, 2015, **54**, 5722.

15 I. A. Cade and M. J. Ingleson, *Chem. – Eur. J.*, 2014, **20**, 12874.

16 (*a*) C. Chen, F. Eweiner, B. Wibbeling, R. Fröhlich, S. Senda, Y. Ohki, K. Tatsumi, S. Grimme, G. Kehr and G. Erker, *Chem. – Asian J.*, 2010, **5**, 2199; (*b*) F. Ge, G. Kehr, C. G. Daniliuc and G. Erker, *J. Am. Chem. Soc.*, 2014, **136**, 68; (*c*) M. M. Hansmann, R. L. Melen, M. Rudolph, F. Rominger, H. Wadepohl, D. W. Stephan and A. S. K. Hashmi, *J. Am. Chem. Soc.*, 2015, **137**, 15469; (*d*) G. Kehr and G. Erker, *Chem. Commun.*, 2012, **48**, 1839.

17 (*a*) Y. Shoji, N. Tanaka, S. Muranaka, N. Shigeno, H. Sugiyama, K. Takenouchi, F. Hajjaj and T. Fukushima, *Nat. Commun.*, 2016, **7**, 12704; (*b*) Y. Shoji, N. Shigeno, K. Takenouchi, M. Sugimoto and T. Fukushima, *Chem. – Eur. J.*, 2018, **24**, 13223.

18 A. Ueno, J. Li, C. G. Daniliuc, G. Kehr and G. Erker, *Chem. – Eur. J.*, 2018, **24**, 10044.

19 V. Fasano, L. D. Curless, J. E. Radcliffe and M. J. Ingleson, *Angew. Chem., Int. Ed.*, 2017, **56**, 9202.

20 Y. Cheng, C. Mück-Lichtenfeld and A. Studer, *J. Am. Chem. Soc.*, 2018, **140**, 6221.

21 M. Nogami, K. Hirano, M. Kanai, C. Wang, T. Saito, K. Miyamoto, A. Muranaka and M. Uchiyama, *J. Am. Chem. Soc.*, 2017, **139**, 12358.

22 M. Suginome, M. Shirakura and A. Yamamoto, *J. Am. Chem. Soc.*, 2006, **128**, 14438.

23 K. Köhler, W. E. Piers, X. Sin, Y. Feng, A. M. Bravakis, A. P. Jarvis, S. Collins, W. Clegg, G. P. A. Yap and T. B. Marder, *Organometallics*, 1998, **17**, 3557.

24 F. Jensen, *J. Chem. Theory Comput.*, 2008, **4**, 719.

25 T. Müller, M. Hasenbeck, J. Becker and U. Gellrich, *Eur. J. Org. Chem.*, 2019, **2019**, 451.

26 C. F. Wilcox, L. M. Loew and R. Hoffmann, *J. Am. Chem. Soc.*, 1973, **95**, 8192.

27 (*a*) S. Kozuch and S. Shaik, *J. Am. Chem. Soc.*, 2006, **128**, 3355; (*b*) S. Kozuch and S. Shaik, *Acc. Chem. Res.*, 2011, **44**, 101; (*c*) S. Kozuch and J. M. L. Martin, *ChemPhysChem*, 2011, **12**, 1413.

5.3 Efficient Organocatalytic Dehydrogenation of Ammonia Borane

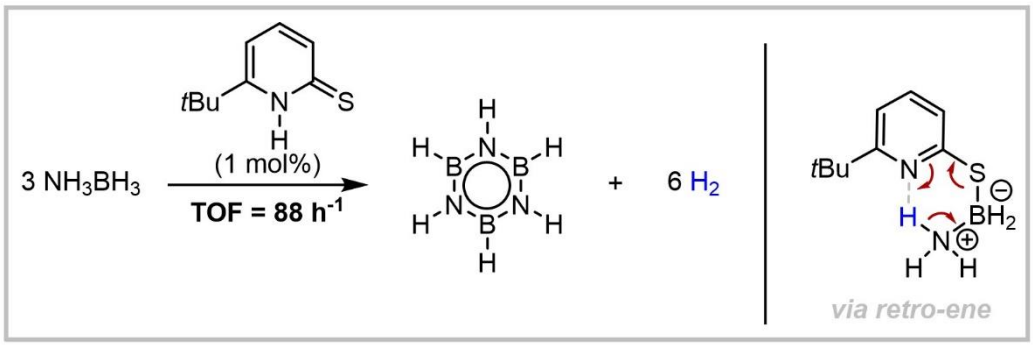

Efficient dehydrogenation of ammonia borane by the organic catalyst 6-*tert*-butyl-2-thiopyridone is described. Mechanistic investigations show that the reaction commences with dehydrogenative S−B coupling. An inorganic retro-ene reaction closes the catalytic cycle and regenerates the catalyst.

Max Hasenbeck, Dr. Jonathan Becker, Dr. Urs Gellrich

Angew. Chem. Int. Ed. **2020**, *59*, 1590-1594

DOI (englische Version):	10.1002/anie.201910636
DOI (deutsche Version):	10.1002/ange.201910636
Akzeptiertes Manuskript online:	01.10.2019
Final veröffentlichte Version online:	10.12.2019

Organocatalysis

International Edition: DOI: 10.1002/anie.201910636
German Edition: DOI: 10.1002/ange.201910636

Efficient Organocatalytic Dehydrogenation of Ammonia Borane

*Max Hasenbeck, Jonathan Becker, and Urs Gellrich**

Abstract: *Dehydrogenation of ammonia borane by sterically encumbered pyridones as organocatalysts is reported. With 6-tert-butyl-2-thiopyridone as the catalyst, a turnover frequency (TOF) of 88 h^{-1} was achieved. Experimental mechanistic investigations, substantiated by DLPNO-CCSD(T) computations, indicate a mechanistic scenario that commences with the protonation of a B–H bond by the mercaptopyridine form of the catalyst. The reactive intermediate formed by this initial protonation was observed by NMR spectroscopy and the molecular structure of a surrogate determined by SCXRD. An intramolecular proton transfer in this intermediate from the NH_3 group to the pyridine ring with concomitant breaking of the S–B bond regenerates the thiopyridone and closes the catalytic cycle. This step can be described as an inorganic retro-ene reaction.*

The controlled release of dihydrogen from ammonia borane (AB) with its H_2 content of 19.7 wt% is of interest considering its potential use as a hydrogen-storage material.[1] Several transition metals catalyze the dehydrogenation of AB efficiently.[2] Among the most effective catalysts are nickel carbene complexes and noble transition-metal complexes with pincer-type phosphine ligands, but iron pincer complexes have also proved to be effective.[3–5] Since Wegner and co-workers showed that this reaction can also be catalyzed by a bidentate Lewis acid, the dehydrogenation of AB by main group systems has attracted considerable attention.[6,7] Slootweg, Uhl, and co-workers reported a phosphine/aluminium-based frustrated Lewis Pair (FLP) that effects the stochiometric dehydrogenation of AB and the catalytic dehydrogenation of dimethylamine-borane (DMAB).[8] Aldridge et al. showed that a xanthene-based FLP catalyzes hydrogen release from AB and provided evidence for a chain-growth mechanism.[9] However, the reported turnover frequencies (TOF) of 4 h^{-1} are moderate compared to transition-metal catalysts. Earlier this year, the field was advanced by the report that a geometrically constrained phosphine-borane FLP displays improved activity for the dehydrogenation of DMAB, but the catalyst showed only moderate activity regarding dehydrogenation of AB.[10] For practical applications, an efficient and easily accessible organic catalyst is desirable. Dixon and co-workers showed that strong Brønsted acids initiate the dehydrogenation of AB, presumably by protonation of the hydridic B–H group.[11] We thus envisioned that an organic molecule possessing an acidic group and a basic site could serve as an organocatalyst for the dehydrogenation of AB by protonation of the BH_3 group and deprotonation of the NH_3 group (Scheme 1).

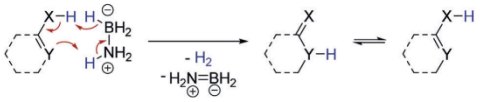

Scheme 1. The working hypothesis of this research project: Dehydrogenation of AB by an organocatalyst through simultaneous protonation and deprotonation.

This organocatalyst would have to be able to revert to its initial form in order to form a catalytic cycle. 2-Hydroxypyridine satisfies the criteria of an acidic OH group and a basic pyridine ring. Furthermore, the tautomers 2-pyridone and 2-hydroxypyridine are almost isoenergetic. We therefore considered 2-pyridone as a suitable candidate for the catalytic dehydrogenation of AB. Aside from simple 2-pyridone **1**, the sterically more encumbered 6-*tert*-butyl-2-pyridone (**2**) was tested as a catalyst. Furthermore, the more acidic thiopyridones **3** and **4** were used.[12] We attempted the dehydrogenation of AB by reacting 1 mol% of the respective organocatalyst with AB at reflux in THF (Scheme 2). The results of the catalytic reactions are summarized in Table 1.

The parent pyridone **1** shows only moderate catalytic activity. However, 1 mol% of the sterically more encumbered

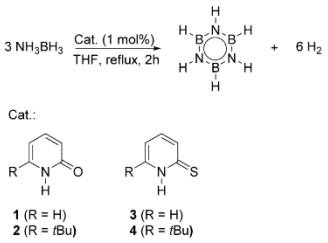

Scheme 2. Dehydrogenation of AB by various pyridine derivatives.

[*] M. Sc. M. Hasenbeck, Dr. U. Gellrich
Institut für Organische Chemie, Justus-Liebig-Universität Gießen
Heinrich-Buff-Ring 17, 35392 Gießen (Germany)
E-mail: urs.gellrich@org.chemie.uni-giessen.de
Dr. J. Becker
Institut für Anorganische und Analytische Chemie
Justus-Liebig-Universität Gießen
Heinrich-Buff-Ring 17, 35392 Gießen (Germany)
Supporting information and the ORCID identification number(s) for the author(s) of this article can be found under: https://doi.org/10.1002/anie.201910636.

Table 1: Results of the catalytic dehydrogenations of AB by pyridone derivatives (conditions shown in Scheme 2).

Catalyst	equiv H_2[a]	TOF [h^{-1}][b]	conv. AB [%][c]
1	0.06	3.2	13
2	0.62	30.8	28
3	0.10	4.8	17
4	1.76	88.0	99

[a] Based on the volumetric determination of H_2. [b] Calculated as $[H_2]\cdot[cat.]^{-1}\,h^{-1}$. [c] Determined by ^{11}B NMR using a linear fit of the AB signal/integration ratio.

6-*tert*-butyl-2-pyridone (**2**) catalyzes hydrogen release from AB with a notably higher efficiency: 0.6 equivalents of hydrogen were liberated within 2 h, which corresponds to a TOF of 31 h^{-1}. Borazine is the main product of this reaction, as demonstrated by ^{11}B NMR. Thiopyridone **3** is less active than **2** but displays a slightly higher activity than parent pyridone **1**. This result indicates that the combination of steric demand and increased acidity should lead to an active catalyst. Indeed, 1 mol% 6-*tert*-butyl-2-thiopyridone (**4**) catalyzes the liberation of 1.8 equiv H_2 from AB within 2 h, which corresponds to a TOF of 88 h^{-1}. This is, to the best of our knowledge, hitherto the highest TOF for H_2 release from AB reported for a metal-free system. Analysis of the reaction mixture shows that AB is completely converted into borazine and polyborazylene.

At 120 °C in toluene, dehydrogenation of DMAB was efficiently catalyzed by **4** (1 mol%) within 4 h (Scheme 3). This experiment demonstrates the chemical robustness of **4**.

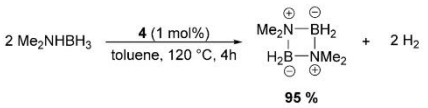

Scheme 3. Dehydrogenation of DMAB catalyzed by **4**.

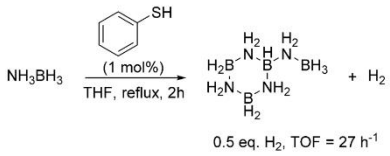

Scheme 4. Attempted dehydrogenation of AB by thiophenol. The formal charges on nitrogen and boron are omitted for clarity.

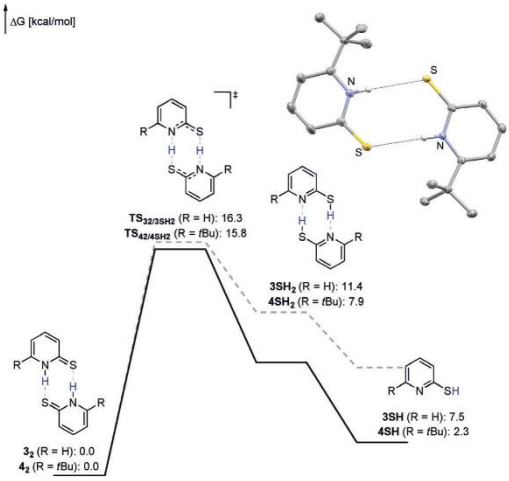

Figure 1. Gibbs free energies for the formation of **4SH** and **3SH** computed at the TightPNO-DLPNO-CCSD(T)/def2-QZVPP//PBE0-D3-(BJ)/def2-TZVP level. Solvent effects were implicitly considered using the SMD model for THF. The inset shows the molecular structure of $\mathbf{4}_2$ derived from SCXRD (ellipsoids shown at 50% probability, all hydrogen atoms attached to carbons omitted for clarity). Selected bond lengths and angles: N(H)···S: 3.46 Å, C–S: 1.70 Å, N–H···S: 173.2 °.[16]

With these unexpected results in hand, we aimed for a mechanistic understanding regarding the mode of action by which **4** catalyzes hydrogen release from AB. To verify that **4** does not act as a Brønsted acid and initiates the dehydrogenation of AB through a chain-growth mechanism, a catalytic reaction using 1 mol% thiophenol (which is more acidic than thiopyridone), was performed. This reaction led to the formation of B-(cyclotriborazanyl)-amine-borane as the main product (Scheme 4). The observed TOF of 27 h^{-1} is significantly lower than that achieved with **4** as a catalyst. This corroborates the importance of catalyst bifunctionality, that is, the presence of the basic pyridine ring for the catalytic activity of **4**. It is tempting to attribute the higher activity of the *tert*-butyl derivatives **2** and **4** to the destabilization of their respective dimers. The synthesis of **4** has been described previously, but its SCXRD structure has not been reported yet.[13] Single crystals suitable for X-ray analysis were obtained in the course of this study.[14] The SCXRD structure is that of the thiopyridone dimer $\mathbf{4}_2$ (Figure 1). The N–H···S distance of 3.46 Å is elongated by 0.17 Å compared to the C_{2h} symmetric dimer of **3**.[15]

The formation of monomeric **4SH** that is assumed to be the active catalyst was further investigated computationally at the SMD(THF)-TightPNO-DLPNO-CCSD(T)/def2-QZVPP//PBE0-D3(BJ)/def2-TZVP level (Figure 2).[17,18] Tautomerization of $\mathbf{4}_2$ requires an activation energy of 15.8 kcal mol^{-1}. The formation of **4SH** from $\mathbf{4}_2$ is slightly endergonic. In comparison, the formation of **3SH** from $\mathbf{3}_2$ is thermodynamically disfavored by 5.2 kcal mol^{-1}. This result indicates that a ground-state effect, that is the destabilization of $\mathbf{4}_2$, contributes to the activity of **4**.

We then focused our attention on the detection of potential reactive intermediates. Upon monitoring a stoichiometric reaction of **4** with AB at 60 °C by NMR, the formation of the mercaptopyridine-borane complex **5** was observed within 5 h. The NH_3 group of **5** gives rise to a coalescent signal at 5.48 ppm in the ^1H NMR spectrum. The BH_2 group shows a signal at 2.62 ppm that integrates to two. A triplet at

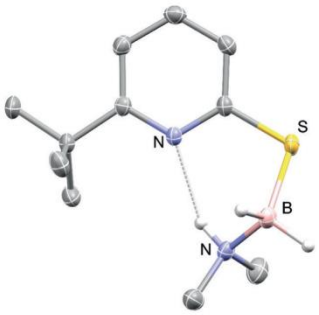

Figure 2. Molecular structure of $\mathbf{5}_{Me2}$ derived from SCXRD (ellipsoids shown at 50% probability, all hydrogen atoms attached to carbons omitted for clarity). Selected bond lengths and angles: N(H)···N: 2.8777(16) Å, B–S: 1.9107(18) Å, C-S-B: 102.61(7)°.

−13.3 ppm is observed by ^{11}B NMR, which is a typical shift for a tetracoordinated borane.[19] A NOE contact detected by NOSY NMR confirms spatial proximity between the NH_3 group and the *tert*-butyl group of the thiopyridone. Attempts to isolate **5** from solution were not successful. However, upon reaction of **4** with DMAB, a stable surrogate of **5** was obtained. The molecular structure of this surrogate $\mathbf{5}_{Me2}$, derived from SCXRD, supports the structural assignment of **5** (Figure 2). The structure shows a short N(H)···N hydrogen bond that indicates the possibility of an intramolecular proton transfer to the pyridine ring.

It is reasonable to assume that **5** is the product of a dehydrogenative coupling between the mercaptopyridine form of **4** and AB. That implies that the dehydrogenation of AB commences with this dehydrogenative coupling, which liberates the first equivalent H_2 and yielding **5**.

When NH_3BD_3 was used as the substrate in the catalytic reaction, a kinetic isotope effect (KIE) of 1.20 ± 0.15 was observed. This result is consistent with the computed transition state for the dehydrogenative coupling: While the S–H bond is ruptured, the B–H bond is only slightly distorted (Figure 3).[20] Indeed, the computed KIE for the dehydrogenative coupling of 1.01 agrees favorable with experimentally observed KIE.[21] A second AB molecule is required to stabilize the partial negative charge on the thiolate in the transition state.

Upon prolonged heating of a solution of **5**, the formation of borazine and regeneration of **4** was observed (Scheme 5). The reactivity of **5** was further investigated computationally (Figure 4). Proton transfer from the NH_3 group to the pyridine ring and the concomitant breaking of the S–B bond requires a free activation energy of 11.0 kcal mol^{-1}.[22] This result indicates that **5** is not inert at 60 °C. However, the liberation of NH_2BH_2 and the regeneration of **4** are endergonic. Therefore, **5** can be observed in a stoichiometric reaction since it is thermodynamically stable with respect to the formation of NH_2BH_2 and **4**. The fact that **5** does react to borazine and **4** at elongated reaction times further indicates that the formation of borazine renders the stoichiometric reaction exergonic (Scheme 5).[23] We note that, regarding the

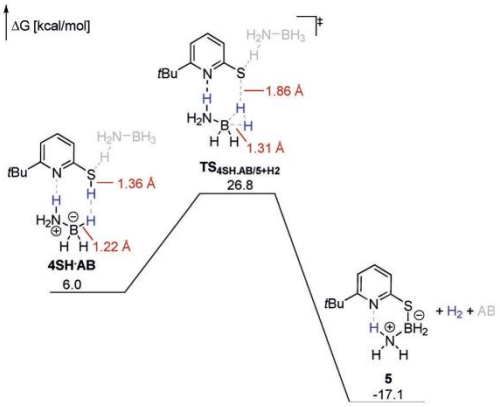

Figure 3. Gibbs free energies of the dehydrogenative coupling between **4** and AB computed at the TightPNO-DLPNO-CCSD(T)/def2-QZVPP//PBE0-D3(BJ)/def2-TZVP level. All Gibbs free energies are given with respect to $\mathbf{4}_2$ and AB_2. Solvent effects were implicitly considered using the SMD model for THF. Formal charges on nitrogen and boron in the transition state are omitted for clarity.

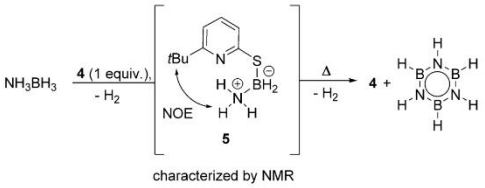

Scheme 5. Intermediate **5** observed in the stoichiometric reaction of **4** with AB by NMR. Reaction conditions: [D$_8$]THF, 60 °C.

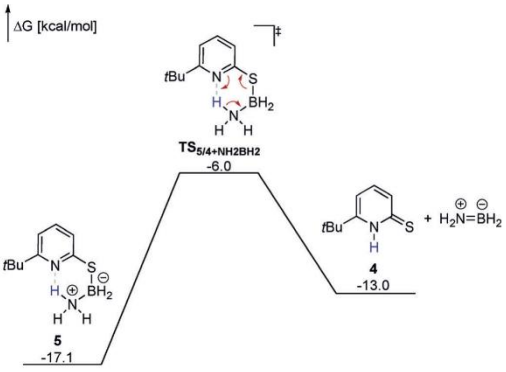

Figure 4. Gibbs free energies of the liberation of NH_2BH_2 from **5** computed at the TightPNO-DLPNO-CCSD(T)/def2-QZVPP//PBE0-D3-(BJ)/def2-TZVP level. Solvent effects were implicitly considered using the SMD model for THF. All Gibbs free energies are given with respect to $\mathbf{4}_2$ and AB_2. Formal charges on nitrogen and boron in the transitionstate are omitted for clarity.

reorganization of π-electron density, liberation of NH_2BH_2 from **5** can be described as an inorganic retro-ene reaction.

Further evidence that the retro-ene reaction is part of the catalytic cycle came from a stoichiometric experiment with **4** and ND_3BH_3. Upon reaction at elevated temperatures, the formation of borazine and incorporation of deuterium in **4** is observed (Scheme 6). A pronounced KIE of 2.4 ± 0.3 is

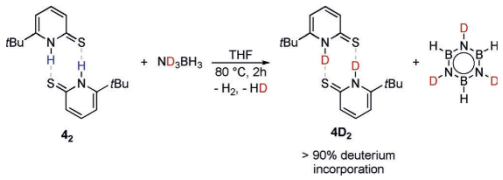

Scheme 6. Deuterium incorporation into **4** upon reaction with ND_3BH_3.

observed when ND_3BH_3 is used as the substrate in the catalytic reaction. Given the low barrier for the retro-ene reaction, this KIE is presumably due to the deuterium incorporation in **4**. Indeed, the computed KIE for the dehydrogenative coupling (see Figure 3) starting from deuterated **4SD** and ND_3BH_3 is 3.2, which is in reasonable agreement with the experimentally observed KIE.

Based on the experimental and computational investigations, we propose a mechanism for the dehydrogenation of AB by **4** that commences with tautomerization of **4** to the mercaptopyridine form **4SH,** presumably via its dimer (Scheme 7). A dehydrogenative coupling of AB with monomeric **4SH** yields borane **5**. The liberation of NH_2BH_2 regenerates monomeric **4**, which dimerizes and completes the catalytic cycle. However, contributions from an acid-induced chain-growth mechanism in the dehydrogenation of AB catalyzed by **4** cannot be excluded.

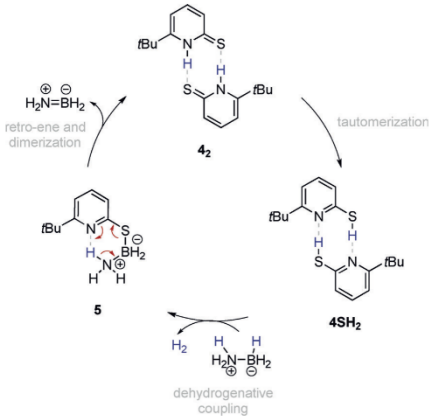

Scheme 7. Proposed mechanism for the dehydrogenation of AB catalyzed by **4**.

In summary, we have documented that hydrogen release from AB is efficiently catalyzed by 6-*tert*-butyl-2-thiopyridone. Mechanistic investigations highlight the importance of bifunctionality of thiopyridone for the catalytic activity, while the *tert*-butyl group facilitates the monomerization of **4**. The results reported herein are likely to stimulate the development of efficient organocatalysts for hydrogen-storage applications.[24]

Acknowledgements

This work was financially supported by the FCI and the DFG. The authors thank Dr. H. Hausmann and T. Müller for assistance with NMR experiments, Dr. S. Heiles for a Nano-ESI-MS analysis and Dr. D. Gerbig for fruitful scientific discussions. Continuous and generous support by Profes. Dres. P. R. Schreiner, R. Göttlich, and H. A. Wegner is acknowledged.

Conflict of interest

The authors declare no conflict of interest.

Keywords: ammonia borane · coupled-cluster computations · hydrogen storage · inorganic retro-ene reactions · organocatalysis

How to cite: *Angew. Chem. Int. Ed.* **2020**, *59*, 1590–1594
Angew. Chem. **2020**, *132*, 1606–1610

[1] a) A. Staubitz, A. P. M. Robertson, M. E. Sloan, I. Manners, *Chem. Rev.* **2010**, *110*, 4023–4078; b) A. Staubitz, A. P. M. Robertson, I. Manners, *Chem. Rev.* **2010**, *110*, 4079–4124; c) F. H. Stephens, V. Pons, R. T. Baker, *Dalton Trans.* **2007**, 2613–2626.

[2] a) C. A. Jaska, K. Temple, A. J. Lough, I. Manners, *Chem. Commun.* **2001**, 962; b) C. A. Jaska, K. Temple, A. J. Lough, I. Manners, *J. Am. Chem. Soc.* **2003**, *125*, 9424–9434; c) A. Rossin, M. Peruzzini, *Chem. Rev.* **2016**, *116*, 8848–8872.

[3] a) R. J. Keaton, J. M. Blacquiere, R. T. Baker, *J. Am. Chem. Soc.* **2007**, *129*, 1844–1845; b) X. Yang, M. B. Hall, *J. Am. Chem. Soc.* **2008**, *130*, 1798–1799; c) P. M. Zimmerman, A. Paul, Z. Zhang, C. B. Musgrave, *Angew. Chem. Int. Ed.* **2009**, *48*, 2201–2205; *Angew. Chem.* **2009**, *121*, 2235–2239; d) P. M. Zimmerman, A. Paul, C. B. Musgrave, *Inorg. Chem.* **2009**, *48*, 5418–5433.

[4] a) M. C. Denney, V. Pons, T. J. Hebden, D. M. Heinekey, K. I. Goldberg, *J. Am. Chem. Soc.* **2006**, *128*, 12048; b) A. Paul, C. B. Musgrave, *Angew. Chem. Int. Ed.* **2007**, *46*, 8153–8156; *Angew. Chem.* **2007**, *119*, 8301–8304; c) N. Blaquiere, S. Diallo-Garcia, S. I. Gorelsky, D. A. Black, K. Fagnou, *J. Am. Chem. Soc.* **2008**, *130*, 14034–14035; d) M. Käß, A. Friedrich, M. Drees, S. Schneider, *Angew. Chem. Int. Ed.* **2009**, *48*, 905–907; *Angew. Chem.* **2009**, *121*, 922–924; e) A. Friedrich, M. Drees, S. Schneider, *Chem. Eur. J.* **2009**, *15*, 10339–10342; f) A. Staubitz, M. E. Sloan, A. Robertson, A. Friedrich, S. Schneider, P. J. Gates, J. Schmedt auf der Günne, I. Manners, *J. Am. Chem. Soc.* **2010**, *132*, 13332–13345; g) A. N. Marziale, A. Friedrich, I. Klopsch, M. Drees, V. R. Celinski, J. Schmedt auf der Günne, S. Schneider, *J. Am. Chem. Soc.* **2013**, *135*, 13342–13355.

[5] A. Glüer, M. Förster, V. R. Celinski, J. Schmedt auf der Günne, M. C. Holthausen, S. Schneider, *ACS Catal.* **2015**, *5*, 7214–7217.

[6] a) Z. Lu, L. Schweighauser, H. Hausmann, H. A. Wegner, *Angew. Chem. Int. Ed.* **2015**, *54*, 15556 – 15559; *Angew. Chem.* **2015**, *127*, 15777 – 15780; b) L. Schweighauser, H. A. Wegner, *Chem. Eur. J.* **2016**, *22*, 14094 – 14103.
[7] For a recent review on AB dehydrogenation with p-block compounds see: D. H. A. Boom, A. R. Jupp, J. C. Slootweg, *Chem. Eur. J.* **2019**, *25*, 9133 – 9152.
[8] C. Appelt, J. C. Slootweg, K. Lammertsma, W. Uhl, *Angew. Chem. Int. Ed.* **2013**, *52*, 4256 – 4259; *Angew. Chem.* **2013**, *125*, 4350 – 4353.
[9] Z. Mo, A. Rit, J. Campos, E. L. Kolychev, S. Aldridge, *J. Am. Chem. Soc.* **2016**, *138*, 3306 – 3309.
[10] M. Boudjelel, E. D. Sosa Carrizo, S. Mallet-Ladeira, S. Massou, K. Miqueu, G. Bouhadir, D. Bourissou, *ACS Catal.* **2018**, *8*, 4459 – 4464.
[11] F. H. Stephens, R. T. Baker, M. H. Matus, D. J. Grant, D. A. Dixon, *Angew. Chem. Int. Ed.* **2007**, *46*, 746 – 749; *Angew. Chem.* **2007**, *119*, 760 – 763.
[12] The pK_a value of **3** in DMSO is 13.3 compared to 24.0 for **1**: F. G. Bordwell, *Acc. Chem. Res.* **1988**, *21*, 456 – 463.
[13] V. Miranda-Soto, J. Pérez-Torrente, L. A. Oro, F. J. Lahoz, M. L. Martín, M. Parra-Hake, D. B. Grotjahn, *Organometallics* **2006**, *25*, 4374 – 4390.
[14] CCDC 1944361 and 1944362 contain the supplementary crystallographic data for this paper. These data are provided free of charge from The Cambridge Crystallographic Data Centre.
[15] U. Ohms, H. Guth, A. Kutoglu, C. Scheringer, *Acta Crystallogr. Sect. B* **1982**, *38*, 831 – 834.
[16] The structure derived from SCXRD is not perfectly C2 symmetric, because the three-fold rotation axis of the trigonal space group requires one molecule to be out of plane compared to the other molecule in the asymmetric unit. Therefore, averaged values are given.
[17] a) C. Riplinger, B. Sandhoefer, A. Hansen, F. Neese, *J. Chem. Phys.* **2013**, *139*, 134101; b) F. Neese, *WIREs Comput. Mol. Sci.* **2012**, *2*, 73 – 78; c) J. P. Perdew, K. Burke, M. Ernzerhof, *Phys. Rev. Lett.* **1996**, *77*, 3865 – 3868; d) C. Adamo, V. Barone, *J. Chem. Phys.* **1999**, *110*, 6158 – 6170; e) S. Grimme, J. Antony, S. Ehrlich, H. Krieg, *J. Chem. Phys.* **2010**, *132*, 154104; f) S. Grimme, S. Ehrlich, L. Goerigk, *J. Comput. Chem.* **2011**, *32*, 1456 – 1465; g) F. Weigend, R. Ahlrichs, *Phys. Chem. Chem. Phys.* **2005**, *7*, 3297 – 3305; h) Gaussian 16, Revision A.03, M. J. Frisch et al. Gaussian, Inc., Wallingford CT, **2016**.
[18] V. Marenich, C. J. Cramer, D. G. Truhlar, *J. Phys. Chem. B* **2009**, *113*, 6378 – 6396.
[19] S. Hermanek, *Chem. Rev.* **1992**, *92*, 325.
[20] A similar transition state was observed by molecular dynamics simulations for the acid-induced dehydrogenation of AB: S. Bhunya, A. Banerjee, R. Tripathi, N. N. Nair, A. Paul, *Chem. Eur. J.* **2013**, *19*, 17673 – 17678.
[21] Note that the two B–D bonds that are not involved in the dehydrogenative coupling are shortened in the transition state, apparently compensating for the distortion of the third B–D bond.
[22] According to the computations, the barrier for the liberation of NMe_2BH_2 from $\mathbf{5_{Me2}}$ is 20.5 kcal mol^{-1}, which agrees with the observed increased stability of $\mathbf{5_{Me2}}$.
[23] Note that the trimerization of NH_2BH_2 to yield cyclotriborazane is computed to be exergonic and may thus provide further driving force. The detailed mechanism of the trimerization is reported in the Supporting Information.
[24] We note that parallel to this work, the use of thiopyridone as an organocatalyst for transfer borylations was reported: É. Rochette, V. Desrosiers, Y. Soltani, F.-G. Fontaine, *J. Am. Chem. Soc.* **2019**, *141*, 12305 – 12311.

Manuscript received: August 20, 2019
Revised manuscript received: September 18, 2019
Accepted manuscript online: October 1, 2019
Version of record online: December 10, 2019

5.4 Semihydrogenation of Alkynes Catalyzed by a Pyridone Borane Complex: Frustrated Lewis Pair Reactivity and Boron–Ligand Cooperation in Concert

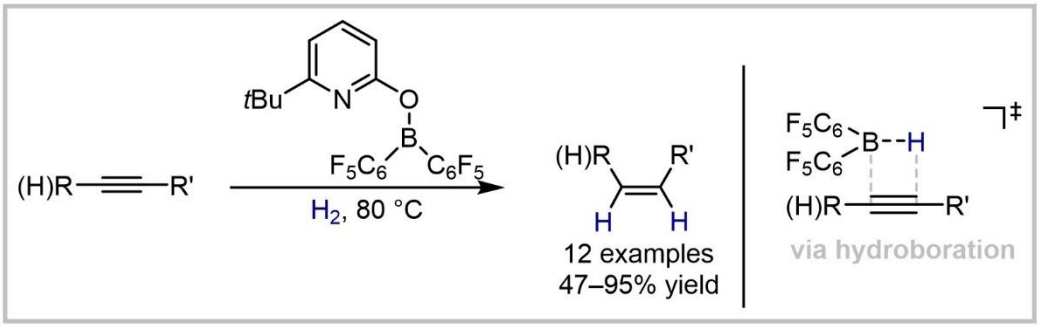

The semihydrogenation of alkynes catalyzed by a pyridonate borane complex is reported. While the catalyst can be described as an intramolecular frustrated Lewis pair, it is the change in the coordination mode of the pyridonate substituent upon H_2 bond activation that enables dissociation of the formed pyridone borane complex and hydroboration as the first C–H bond-forming step. This mode of action is referred to as boron-ligand cooperation.

Felix Wech, Max Hasenbeck, Dr. Urs Gellrich

Chem. Eur. J. **2020**, *26*, 13445-13450

DOI (englische Version): 10.1002/chem.202001276

Akzeptiertes Manuskript online: 03.04.2020

Final veröffentlichte Version online: 18.09.2020

Homogeneous Catalysis

Semihydrogenation of Alkynes Catalyzed by a Pyridone Borane Complex: Frustrated Lewis Pair Reactivity and Boron–Ligand Cooperation in Concert

Felix Wech, Max Hasenbeck, and Urs Gellrich*[a]

Abstract: The metal-free *cis* selective hydrogenation of alkynes catalyzed by a boroxypyridine is reported. A variety of internal alkynes are hydrogenated at 80 °C under 5 bar H_2 with good yields and stereoselectivity. Furthermore, the catalyst described herein enables the first metal-free semihydrogenation of terminal alkynes. Mechanistic investigations, substantiated by DFT computations, reveal that the mode of action by which the boroxypyridine activates H_2 is reminiscent of the reactivity of an intramolecular frustrated Lewis pair. However, it is the change in the coordination mode of the boroxypyridine upon H_2 activation that allows the dissociation of the formed pyridone borane complex and subsequent hydroboration of an alkyne. This change in the coordination mode upon bond activation is described by the term boron-ligand cooperation.

Introduction

The seminal finding that specific combinations of sterically encumbered Lewis bases and Lewis acids, named „frustrated Lewis pairs" (FLPs), can activate hydrogen, stimulated the development of catalytic metal-free hydrogenations.[1] Early examples included the hydrogenation of (di)imines, nitriles, aziridines, silyl enol ethers, and enamines, but the scope of FLP catalyzed hydrogenations was extended to heterocycles, alkenes, allenes, and aromatic hydrocarbons.[2,3] The heterolytic hydrogen cleavage by the FLP yields a tetravalent borohydride species. Therefore, hydrogenations by FLPs consist of a hydride and a subsequent proton transfer step (or *vice versa*) and require activated alkenes.[3] A notable exception is the semihydrogenation of alkynes catalyzed by an intramolecular FLP that was reported by Repo et al.[4] In that case, mechanistic investigations showed that the protolysis of the FLP under the reaction conditions yields an amine-hydroborane that initiates the catalytic cycle by hydroboration of the alkyne.[5] A protodeborylation of the alkenylborane yields then, in a highly stereoselective reaction, the *cis*-alkene.[6] We recently reported reversible H_2 activation by the boroxypyridine **3**.[7] A distinguishing feature of this system is that the H_2 activation is associated with a transition of the covalently bound oxypyridine substituent to a neutral pyridone donor ligand (Scheme 1). This mode of action was, in analogy to the concept of metal-ligand cooperation, termed boron-ligand cooperation. The change in the coordination mode of the pyridone substituent might enable the dissociation of the pyridone borane complex **4** in the ligand 6-*tert*-butylpyridone **5** and Piers borane **6**. Piers borane has been shown to display the typical reactivity of a trivalent borane, for example, it effects the hydroboration of alkenes and alkynes. Such dissociation is not possible for classic FLPs that, as aforementioned, therefore rather display borohydride reactivity upon H_2 activation (Scheme 1).

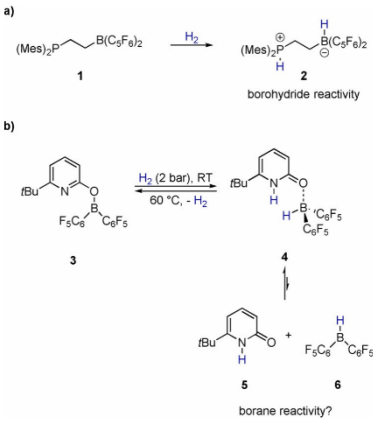

Scheme 1. A classic intramolecular FLP that displays borohydride reactivity and reversible H_2 activation by the boroxypyridine **3** that might display borane reactivity upon H_2 activation and dissociation.

[a] F. Wech, M. Hasenbeck, Dr. U. Gellrich
Institut für Organische Chemie
Justus-Liebig-Universität Gießen
Heinrich-Buff-Ring 17, 35392 Gießen (Germany)
E-mail: urs.gellrich@org.chemie.uni-giessen.de
Supporting information and the ORCID identification number(s) for the author(s) of this article can be found under:
https://doi.org/10.1002/chem.202001276.

Results and Discussion

We envisioned the hydroboration of an alkene to be a valid test reaction to elucidate whether **3** displays borane reactivity upon hydrogen activation, since hydroboration requires the presence of a trivalent borane. Indeed, when **3** was reacted with one equivalent of styrene under moderate H_2-pressure at RT, the formation of the alkyl borane **7** was observed (Scheme 2). The alkylborane **7** is also formed when styrene is reacted with the pyridone borane **4**, which supports the assumption that **4** is an intermediate in the formation of **7** starting from **3**.

The alkylborane **7** does not undergo a protodeborylation. However, we envisioned that an analogous alkenylborane, originating from a reaction sequence consisting of H_2 activation and hydroboration of an alkyne might succumb to protonolysis. This reaction would regenerate the boroxypyridine **3** and close a catalytic cycle for the hydrogenation of alkynes that consists of H_2 activation by **3**, hydroboration of an alkyne and protonolysis of the alkenylborane (Scheme 3).

Indeed, 2-hexyne was stereoselectively converted to *cis*-2-hexene in 87% yield in the presence of catalytic amounts of **4** at 80 °C under 5 bar H_2 pressure (Scheme 4). The catalyst **4** was generated in situ by coordination of **5** to Piers borane **6**. An initial screening of reaction conditions showed that a slight excess of Piers borane **6** (1.3 equivalents with respect to **5**) is beneficial to obtain reproducible good yields. Under the same conditions, *cis*-2-octene is obtained in very good yields from the hydrogenation of 2-octyne. Likewise, *cis*-3-hexene is formed upon hydrogenation of 3-hexyne in excellent yield after only 8 h reaction time. The hydrogenation of 4-methyl-2-pentyne leads to the corresponding *cis* alkene in a very good yield after 16 h reaction time. Upon hydrogenation of the respective alkyne, 1-phenyl-1-propene is obtained in an excellent yield of 93%. Ethers are suitable substrates, as proven by the successful hydrogenation of 1-(*para*-methoxyphenyl)-propyne.

While 3-hexyne is obtained after 8 h exclusively as *cis* isomer, a prolonged reaction time of 16 h led to a 1:1 mixture

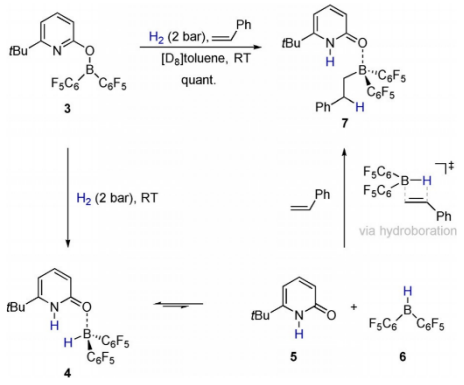

Scheme 2. Hydroboration of styrene upon H_2 activation by **3**.

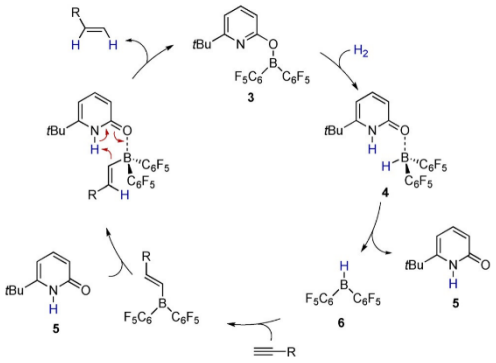

Scheme 3. Envisioned mechanism of the hydrogenation of alkynes catalyzed by **3**: H_2 activation yields the pyridone borane complex **4** that undergoes a dissociation. Piers borane **6** hydroborates an alkyne, formation of the pyridone alkenylborane complex and its protolysis are closing the catalytic cycle.

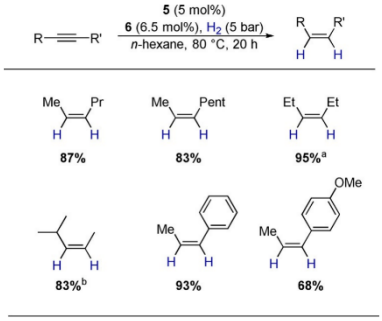

Scheme 4. Substrate scope of the semihydrogenation of internal alkynes. Yields were determined by ^{1}H NMR with trimethoxybenzene as internal standard and are given as the average of two runs a) 8 h reaction time; b) 16 h reaction time.

of the *cis* and the *trans* isomer (Scheme 5). After 20 h, the *trans* isomer is the major product. Liu et al. reported that Piers borane can isomerize *cis*-alkenes via reversible hydroboration.[5] We, therefore, assume that the catalytic reaction yields first *cis*-3-hexene that is then subsequently isomerized by the Piers borane **6** that is present in the reaction mixture. Thus, both stereoisomers are accessible with the catalytic protocol described herein.

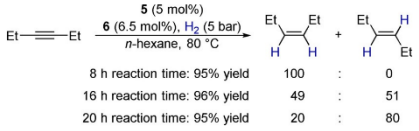

Scheme 5. Stereoselectivity of the hydrogenation of 3-hexyne in dependence of the reaction time.

The known metal-free protocols for the hydrogenation of alkynes are limited to internal alkynes. We were pleased to find that the catalyst described herein is capable to hydrogenate 1-octyne in good yield with a catalyst loading of 10 mol% (Scheme 6). The catalytic protocol can also be used for the hydrogenation of other aliphatic alkynes such as cyclohexyl- and adamantly acetylene. While aromatic rings are tolerated, the hydrogenation of phenylacetylene and *para*-(trifluoromethyl)-phenylacetylene yielded the corresponding alkenes in lower yields. Again, ethers are suitable substrates, as demonstrated by the hydrogenation of 6-methoxy-1-hexylacetylene.

With these results in hand, we aimed for a mechanistic understanding of the catalytic reaction. To verify that the pyridone **5** is indeed vital for the reaction, we attempted the hydrogenation of 2-hexyne only with Piers borane **6** as catalyst (Scheme 7). Less than 1% product was formed under reaction conditions that are identical to those reported in Scheme 4, clearly indicating that the presence of the pyridone **5** is essential for the reaction outcome.

We then focused on the identification of the resting state of the catalytic reaction. For this purpose, the catalytic hydrogenation of 3-hexyne was monitored by NMR (Scheme 8). Under 4 bar H_2-pressure, rapid formation of *cis*-3-hexene was observed at 70 °C in [D_6]benzene, which implies that the observations made by this experiment are meaningful regarding the catalytic transformation.

The bispyridone complex **8** that was previously described and characterized in detail was observed by ^{1}H NMR as the resting state of the catalytic reaction (Figure 1).[8] Furthermore, ^{1}H and ^{11}B NMR proved formation of boroxypyridine **3** with progressing reaction and hydrogen consumption. This finding strongly supports the assumption that **3** is part of the catalytic cycle.[9]

To elucidate whether the envisioned protonolysis of the alkenylborane can be assumed to be part of the catalytic reaction, **5** was added to the borane **9**, derived from the reaction of Piers borane **6** and 3-hexyne. The reaction progress at RT was monitored by NMR spectroscopy (Scheme 9). Within 30 minutes, the formation of the expected pyridone alkenylborane complex **10** was observed. Furthermore, signals that were assigned to *cis*-3-hexene, the product of the protonolysis, were detected. The presence of *cis*-3-hexene implies that boroxypyridine **3**, originating from the protonolysis must be present. Indeed, the formation of the bispyridone complex **8** that contains one equivalent of **3** was observed.

EXSY NMR spectroscopy shows an exchange of the pyridone **5** between **10** and **8** at RT, which further supports that **8** is not an unreactive, irreversibly formed species but rather a resting state. The mechanism of the catalytic reaction was further investigated computationally at revDSD-PBEP86-D4/def2-QZVPP//PBEh-3c (Figure 2).[10,11] The SMD model for *n*-hexane was used to implicitly account for solvent effects.[12] The hydro-

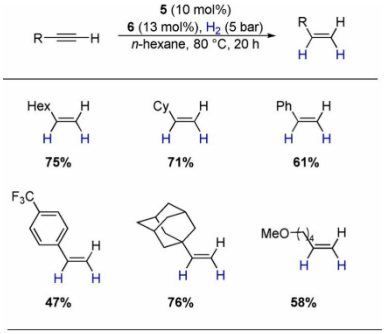

Scheme 6. Substrate scope of the semihydrogenation of terminal alkynes. Yields were determined by ^{1}H NMR with trimethoxybenzene as internal standard and are given as the average of two runs.

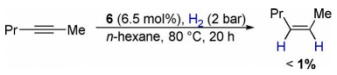

Scheme 7. Attempted hydrogenation with Piers borane **6** as the catalyst.

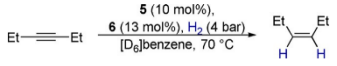

Scheme 8. NMR monitoring of the catalytic hydrogenation of 3-hexyne.

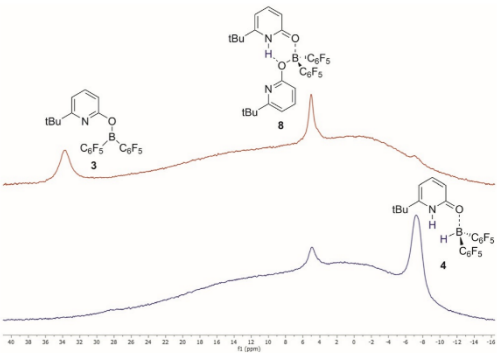

Figure 1. ^{11}B NMR spectra (193 MHz, [D_6]benzene) obtained by monitoring of the catalytic reaction (Scheme 8) before heating (blue) and after 15 h at 60 °C (red).

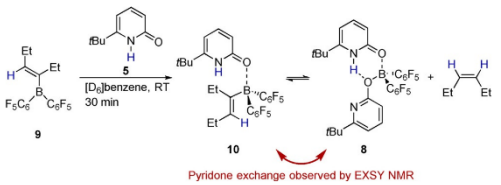

Scheme 9. Stoichiometric reaction of the alkenylborane **9** with the *tert*-butylpyridone **5**.

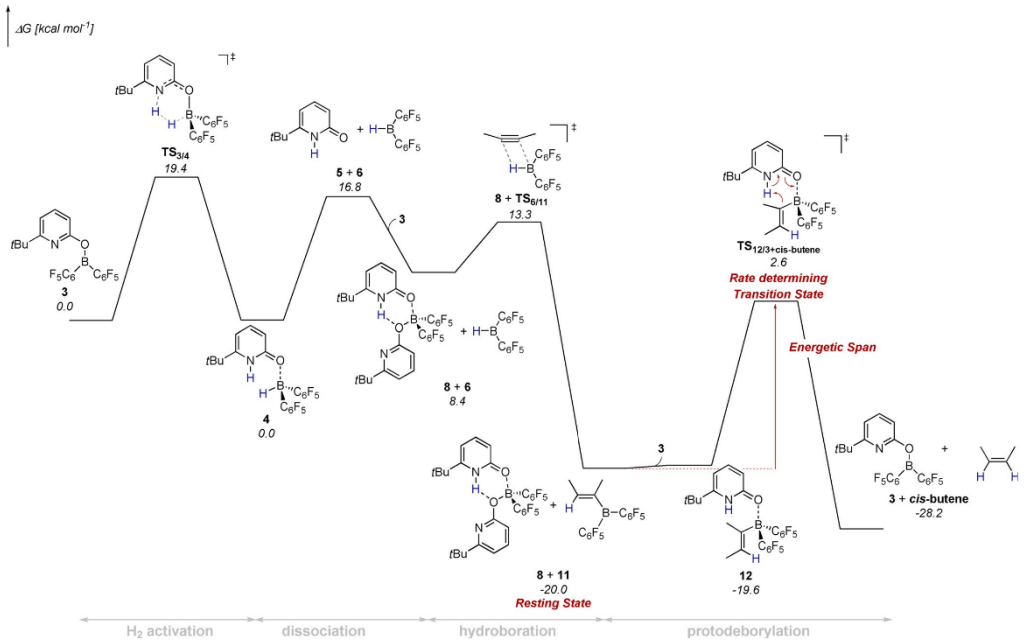

Figure 2. Gibbs free energy profile for the hydrogen activation by **3** computed at revDSD-PBEP86-D4/def2-QZVPP//PBEh-3c. Bulk solvation was considered implicitly with the SMD model for hexane.

gen activation by **3** requires a free activation energy of 19.4 kcal mol^{-1}. This elementary step is according to our computations thermoneutral, which agrees with the previously observed facile reversibility of the hydrogen activation.[7] The free energy change that is associated with the dissociation of **4** into Piers borane **6** and the pyridone **5** is 16.8 kcal mol^{-1}. Relaxed potential energy surface scans indicate that the dissociation is barrierless. As the experimental results indicate that the bispyridone complex **8** is the resting state of the transformation, we considered the coordination of the free pyridone **5** to the boroxypyridine **3**. Indeed, the formation of **8** is according to the computations exergonic. The hydroboration of the model substrate 2-butyne requires a moderate activation energy of 4.9 kcal mol^{-1} and yields the alkenylborane **11**. The bispyridone complex **8** together with **11** is the resting state of the catalytic transformation.[13] The pyridone **5**, that is bound in complex **8**, coordinates than to **11** forming the pyridone alkenylborane complex **12**.

Note that pyridone exchange between **8** and the pyridone alkenylborane complex **10** was observed experimentally by EXSY NMR. The activation barrier for the protodeborylation is 22.2 kcal mol^{-1}, which corresponds to a half-life time of **12** of 35.8 minutes at 25 °C.[14] This agrees with the experimental observation that the protodeborylation takes place at RT (Scheme 9). The „Energetic Span", that is the kinetic barrier of the catalytic transformation, is between the resting state (**8** and **11**) and the transition state of the protodeborylation.[15] Classic FLP type catalysts are not suitable for the hydrogenation of terminal alkynes, presumably because they are deactivated by an irreversible C_{sp}–H cleavage.[3] To understand why the catalyst system described herein tolerates terminal alkynes, **3** was reacted with cyclohexylacetylene at RT. As previously reported, this reaction led to the formation of the alkynylborane complex **13** (Scheme 10).[16] Upon addition of phenylacetylene

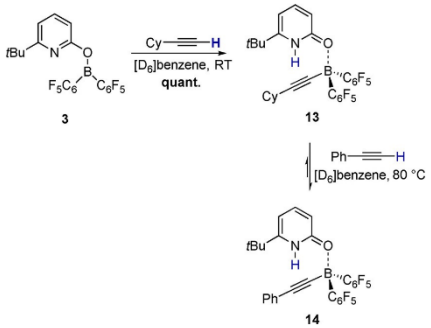

Scheme 10. C_{sp}–H cleavage of cyclohexylacetylene by **3** and exchange with phenylacetylene upon heating to 80 °C.

and heating to 80 °C, **13** was partially converted to the phenylalkynylborane complex **14**.

After 1 h at 80 °C, the ratio of **14** to **13** was 4:1. This experiment indicates that the C_{sp}–H cleavage is reversible under the reaction conditions. The assumption that the formation of the alkynylborane is reversible is further supported by DFT computations (Figure 3). According to the computations, the liberation of cyclohexylacetylene from **13** requires a free Gibbs activation energy of 24.1 kcal mol^{-1}, which corresponds to a half-life time of 79 seconds at 80 °C. The formation of the phenyl alkynyl borane complex **14** is kinetically and thermodynamically favored.

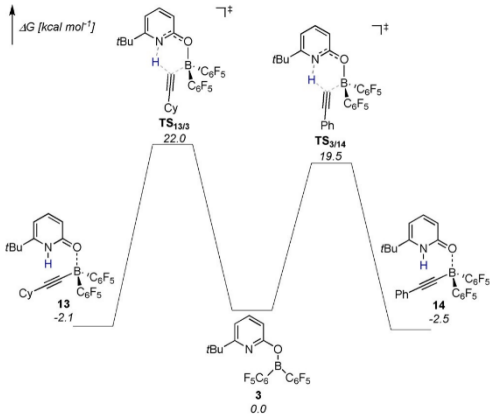

Figure 3. Gibbs free energy profile for the C_{sp}–H activation of cyclohxylacetylene and phenylacetylene by **3** computed at revDSD-PBEP86-D4/def2-QZVPP//PBEh-3c. Bulk solvation was considered implicitly with the SMD model for hexane.

The computed Gibbs free energy difference of 0.4 kcal mol^{-1} corresponds to a ratio of 2:1, which is in reasonable agreement with the experimentally observed proportion of the two alkynyl borane complexes. It is certainly the reversibility of the C_{sp}–H cleavage that allows H_2 activation in the presence of terminal alkynes and thus the first metal-free hydrogenation of terminal alkynes.

Conclusions

We have documented the efficient semihydrogenation of internal and terminal alkynes by a boroxypyridine that displays frustrated Lewis pair reactivity and is, therefore, able to activate hydrogen. However, the change in the coordination mode of the pyridonate substituent enables hydroboration as the initial step of the hydrogenation and is thus vital for the catalytic reaction. We expect this finding to pave the way for novel metal-free catalytic reactions that rely on this mode of action.

Experimental Section

General Procedure for hydrogenation of alkynes: Piers borane **6** (13.5 mg, 0.039 mmol) and 6-*tert*-butyl-2-pyridone **5** (4.5 mg, 0.030 mmol) were dissolved in *n*-hexane (5 mL) in a Fisher-Porter type 150 mL reaction vessel equipped with a stirring bar. The respective alkyne (0.60 mmol or 0.30 mmol) was added. The reaction vessel was closed and connected to an H_2 bomb with a gas hose. The hose was rinsed with H_2 several times and the reaction vessel pressurized with H_2 (5 bar). The reaction vessel was placed inside an 80 °C preheated oil bath and stirred at 1000 rpm. After 20 h, the reaction mixture was cooled to room temperature and the excess H_2 gas was released. An aliquot was taken, and the yield determined by ^{1}H NMR using 1,3,5-trimethoxybenzene as internal standard.

Acknowledgements

This work was financially supported by the FCI and the DFG. The authors thank Dr. H. Hausmann for assistance with NMR experiments. Continuous and generous support by Prof. Dr. P. R. Schreiner, Prof. Dr. R. Göttlich, and Prof. Dr. H. A. Wegner is acknowledged. Open access funding enabled and organized by Projekt DEAL.

Conflict of interest

The authors declare no conflict of interest.

Keywords: alkynes · boron–ligand cooperation · density functional calculations · frustrated Lewis pair · hydrogenation

[1] a) G. C. Welch, R. R. S. Juan, J. D. Masuda, D. W. Stephan, *Science* **2006**, *314*, 1124–1126; b) L. J. Hounjet, D. W. Stephan, *Org. Process Res. Dev.* **2014**, *18*, 385–391.

[2] a) P. A. Chase, G. C. Welch, T. Jurca, D. W. Stephan, *Angew. Chem. Int. Ed.* **2007**, *46*, 8050–8053; *Angew. Chem.* **2007**, *119*, 8196–8199; b) P. A. Chase, T. Jurca, D. W. Stephan, *Chem. Commun.* **2008**, 1701–1703; c) P. Spies, G. Erker, G. Kehr, K. Bergander, R. Fröhlich, S. Grimme, D. W. Stephan, *Chem. Commun.* **2007**, 5072–5074; d) V. Sumerin, F. Schulz, M. Atsumi, C. Wang, M. Nieger, M. Leskelä, T. Repo, P. Pyykkö, B. Rieger, *J. Am. Chem. Soc.* **2008**, *130*, 14117–14118; e) C. Jiang, O. Blacque, H. Berke, *Chem. Commun.* **2009**, 5518–5520; f) K. V. Axenov, G. Kehr, R. Fröhlich, G. Erker, *J. Am. Chem. Soc.* **2009**, *131*, 3454–3455; g) D. Chen, J. Klankermayer, *Chem. Commun.* **2008**, 2130–2131; h) D. Chen, Y. Wang, J. Klankermayer, *Angew. Chem. Int. Ed.* **2010**, *49*, 9475–9478; *Angew. Chem.* **2010**, *122*, 9665–9668; i) G. Ghattas, D. Chen, F. Pan, Klankermayer, *J. Dalton Trans.* **2012**, *41*, 9026–9028; j) G. Eros, H. Mehdi, I. Papai, T. A. Rokob, P. Kiraly, G. Tarkanyi, T. Soos, *Angew. Chem. Int. Ed.* **2010**, *49*, 6559–6563; *Angew. Chem.* **2010**, *122*, 6709–6713; k) H. D. Wang, R. Fröhlich, G. Kehr, G. Erker, *Chem. Commun.* **2008**, 5966–5968; l) D. W. Stephan, S. Greenberg, T. W. Graham, P. Chase, J. J. Hastie, S. J. Geier, J. M. Farrell, C. C. Brown, Z. M. Heiden, G. C. Welch, M. Ullrich, *Inorg. Chem.* **2011**, *50*, 12338–12348; m) Z. M. Heiden, D. W. Stephan, *Chem. Commun.* **2011**, *47*, 5729–5731.

[3] a) J. S. Reddy, B. H. Xu, T. Mahdi, R. Frohlich, G. Kehr, D. W. Stephan, G. Erker, *Organometallics* **2012**, *31*, 5638–5649; b) L. Greb, P. Oña-Burgos, B. Schirmer, S. Grimme, D. W. Stephan, J. Paradies, *Angew. Chem. Int. Ed.* **2012**, *51*, 10164–10168; *Angew. Chem.* **2012**, *124*, 10311–10315; c) L. Greb, C. G. Daniliuc, K. Bergander, J. Paradies, *Angew. Chem. Int. Ed.* **2013**, *52*, 5876–5879; *Angew. Chem.* **2013**, *125*, 5989–5992; d) B. Inés, D. Palomas, S. Holle, S. Steinberg, J. A. Nicasio, M. Alcarazo, Y. Segawa, *Angew. Chem. Int. Ed.* **2012**, *51*, 12367–12369; *Angew. Chem.* **2012**, *124*, 12533–12536; e) Y. Segawa, D. W. Stephan, *Chem. Commun.* **2012**, *48*, 11963–11965.

[4] K. Chernichenko, Á. Madarász, I. Pápai, M. Nieger, M. Leskelä, T. Repo, *Nat. Chem.* **2013**, *5*, 718–723.

[5] For further examples of metal-free semihydrogenation of alkynes that are initated by a hydroboration see: a) Y. Liu, L. Hu, H. Chen, H. Du, *Chem. Eur. J.* **2015**, *21*, 3495 – 3501; b) K. C. Szeto, W. Sahyoun, N. Merle, J. Llop Castelbou, N. Popoff, F. Lefebvre, J. Raynaud, C. Godard, C. Claver, L. Delevoye, R. M. Gauvinc, M. Taoufik, *Catal. Sci. Technol.* **2016**, *6*, 882 – 889.

[6] For examples of the semihydrogenation of alkynes by gold nanoparticle based FLPs see: a) J. L. Fiorio, N. López, L. M. Rossi, *ACS Catal.* **2017**, *7*, 2973 – 2980; b) J. L. Fiorio, R. V. Gonçalves, E. Teixeira-Neto, M. A. Ortuño, N. López, L. M. Rossi, *ACS Catal.* **2018**, *8*, 3516 – 3524.

[7] U. Gellrich, *Angew. Chem. Int. Ed.* **2018**, *57*, 4779 – 4782; *Angew. Chem.* **2018**, *130*, 4869 – 4872.

[8] T. Müller, M. Hasenbeck, J. Becker, U. Gellrich, *Eur. J. Org. Chem.* **2019**, 451 – 457.

[9] As a slight excess of borane was used (1.3 equivalents), the alkenylborane **9** was also observed. For details, see the Supporting Information.

[10] a) G. Santra, N. Sylvetsky, J. M. L. Martin, *J. Phys. Chem. A* **2019**, *123*, 5129 – 5143; b) E. Caldeweyher, C. Bannwarth, S. Grimme, *J. Chem. Phys.* **2017**, *147*, 034112; c) E. Caldeweyher, S. Ehlert, A. Hansen, H. Neugebauer, S. Spicher, C. Bannwarth, S. Grimme, *J. Chem. Phys.* **2019**, *150*, 154122; d) F. Weigend, R. Ahlrichs, *Phys. Chem. Chem. Phys.* **2005**, *7*, 3297 – 3305; e) A. Hellweg, C. Hattig, S. Hofener, W. Klopper, *Theor. Chem. Acc.* **2007**, *117*, 587 – 597; f) F. Weigend, *J. Comput. Chem.* **2008**, *29*, 167 – 175.

[11] a) S. Grimme, J. G. Brandenburg, C. Bannwarth, A. Hansen, *J. Chem. Phys.* **2015**, *143*, 054107; b) H. Kruse, S. Grimme, *J. Chem. Phys.* **2012**, *136*, 154101; c) S. Grimme, S. Ehrlich, L. Goerigk, *J. Comput. Chem.* **2011**, *32*, 1456 – 1465; d) S. Grimme, J. Antony, S. Ehrlich, H. Krieg, *J. Chem. Phys.* **2010**, *132*, 154104; e) F. Weigend, *Phys. Chem. Chem. Phys.* **2006**, *8*, 1057 – 1065.

[12] A. V. Marenich, C. J. Cramer, D. G. Truhlar, *J. Phys. Chem. B* **2009**, *113*, 6378 – 6396.

[13] The excess of Piers borane used in the catalytic experiments (0.3 equiv) will likely result in a higher concentration of the alkenylborane **11**.

[14] H. Eyring, *J. Chem. Phys.* **1935**, *3*, 107 – 115.

[15] a) S. Kozuch, S. Shaik, *J. Am. Chem. Soc.* **2006**, *128*, 3355 – 3365; b) S. Kozuch, S. Shaik, *Acc. Chem. Res.* **2011**, *44*, 101 – 110.

[16] M. Hasenbeck, T. Müller, U. Gellrich, *Catal. Sci. Technol.* **2019**, *9*, 2438 – 2444.

Manuscript received: March 14, 2020
Revised manuscript received: April 1, 2020
Accepted manuscript online: April 3, 2020
Version of record online: September 18, 2020

5.5 Formation of Nucleophilic Allylboranes from Molecular Hydrogen and Allenes Catalyzed by a Pyridonate Borane that Displays Frustrated Lewis Pair Reactivity

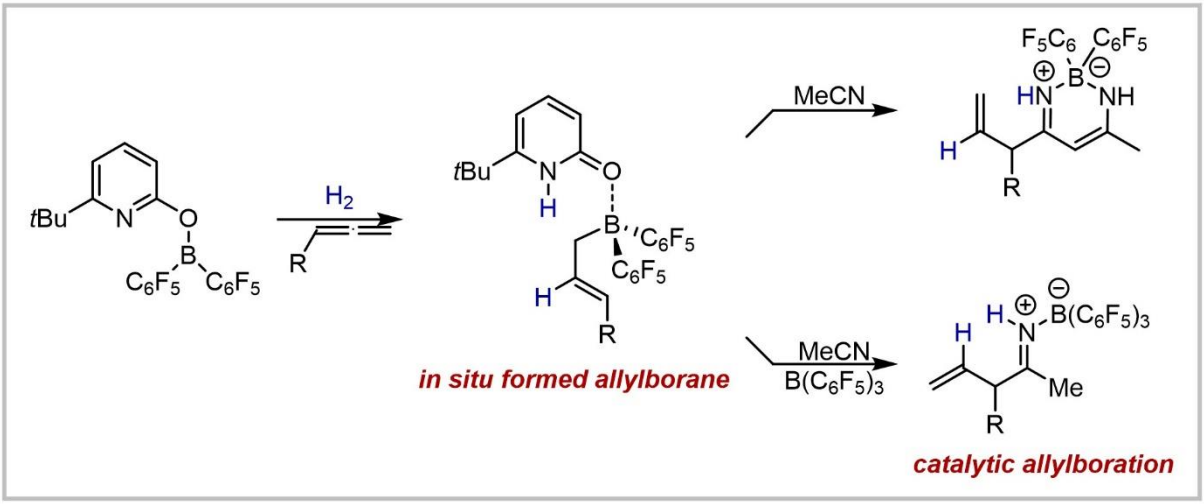

The in situ formation of nucleophilic allylboranes from H_2 and allenes is reported. The reaction is catalyzed by pyridonate borane that displays frustrated-Lewis-pair reactivity. The allylboranes that are generated in this way are reactive towards nitriles. Mechanistic investigations show that a change in the binding mode of the pyridonate substituent upon hydrogen activation is essential for the formation of the allylboranes.

Max Hasenbeck, Dr. Sebastian Ahles, Arthur Averdunk, Dr. Jonathan Becker, Dr. Urs Gellrich

Angew. Chem. Int. Ed. **2020**, *59*, 23885-23891

DOI (englische Version): 10.1002/anie.202011790

DOI (deutsche Version): 10.1002/ange.202011790

Akzeptiertes Manuskript online: 14.09.2020

Final veröffentlichte Version online: 22.10.2020

Allylboranes

How to cite: *Angew. Chem. Int. Ed.* **2020**, *59*, 23885–23891
International Edition: doi.org/10.1002/anie.202011790
German Edition: doi.org/10.1002/ange.202011790

Formation of Nucleophilic Allylboranes from Molecular Hydrogen and Allenes Catalyzed by a Pyridonate Borane that Displays Frustrated Lewis Pair Reactivity

*Max Hasenbeck, Sebastian Ahles, Arthur Averdunk, Jonathan Becker, and Urs Gellrich**

Abstract: *Here we report the in situ generation of nucleophilic allylboranes from H_2 and allenes mediated by a pyridonate borane that displays frustrated-Lewis-pair reactivity. Experimental and computational mechanistic investigations reveal that upon H_2 activation, the covalently bound pyridonate substituent becomes a datively bound pyridone ligand. Dissociation of the formed pyridone borane complex liberates Piers borane and enables a hydroboration of the allene. The allylboranes generated in this way are reactive towards nitriles. A catalytic protocol for the formation of allylboranes from H_2 and allenes and the allylation of nitriles has been devised. This catalytic reaction is a conceptually new way to use molecular H_2 in organic synthesis.*

Introduction

Allylboranes are a prevalent class of C-nucleophiles.[1–3] Classic ways for their preparation include the addition of nucleophilic allyl Grignard or allyl lithium compounds to electrophilic boron methoxides.[4] However, already in 1977 Kramer and Brown reported the formation of nucleophilic allylboranes upon hydroboration of allenes by 9-borabicyclo-[3.3.1]nonane (9-BBN, **1**) (Scheme 1).[5] The allylborane **2** prepared in this way was used in the first total synthesis of Brevianamide A, a highly challenging target for organic synthesis, reported earlier this year. This demonstrates the ongoing importance of this class of nucleophiles for organic synthesis.[6]

We recently reported reversible H_2 activation by the pyridonate borane **3** that can be described as an intramolecular frustrated Lewis pair (FLP).[7–9] A distinguishing feature of this system is that the H_2 activation is associated with a transition of the covalently bound pyridonate substituent to a datively bound pyridone ligand (Scheme 2).

Piers borane **6** has been shown to display the typical reactivity of a trivalent borane, for example, the hydroboration of unsaturated double bonds.[12] We, therefore, envisioned that Piers borane **6**, formed in situ upon H_2 activation by **3** and dissociation of **4**, is able to hydroborate an allene, yielding a nucleophilic allylborane.[1,3] The formation of a nucleophilic allylborane from H_2 and an allene would be an atom economic and conceptually new way to use molecular hydrogen for the formation of a reactive organic intermediate. Furthermore, a reaction sequence consisting of allylation of an electrophile by the allylborane formed in this

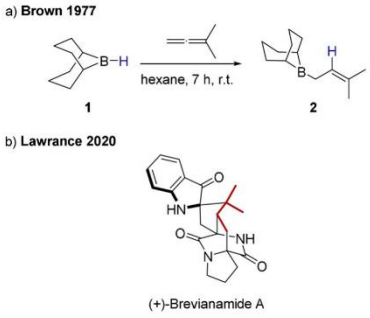

Scheme 1. a) Formation of B-3,3-dimethallyl-9-BBN **2** by hydroboration of dimethylallene reported by Brown. b) Structure of Brevianamide A with the fragment originating from an allylborane highlighted.

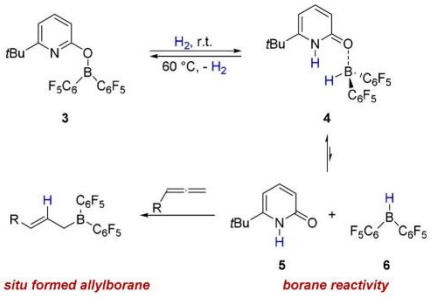

Scheme 2. Envisioned in situ formation of a nucleophilic allylborane upon hydrogen activation by **3** and hydroboration of an allene.

[*] M. Sc. M. Hasenbeck, Dr. S. Ahles, B. Sc. A. Averdunk, Dr. U. Gellrich
Institut für Organische Chemie, Justus-Liebig-Universität Gießen
Heinrich-Buff-Ring 17, 35392 Gießen (Germany)
E-mail: urs.gellrich@org.chemie.uni-giessen.de
Dr. J. Becker
Institut für Anorganische und Analytische Chemie, Justus-Liebig-Universität Gießen
Heinrich-Buff-Ring 17, 35392 Gießen (Germany)

Supporting information and the ORCID identification number(s) for the author(s) of this article can be found under: https://doi.org/10.1002/anie.202011790.

way, followed by a protodeborylation mediated by the pyridone **5**, would regenerate the pyridonate borane **3**. That would enable us to realize an allylation that requires only catalytic amounts of the pyridonate borane **3**.

Results and Discussion

To prove the working hypothesis, phenylallene was added to a solution of **3** in benzene and the reaction mixture was exposed to H_2 (1.1 bar). This led to the formation of a new borane complex that was assigned to be the pyridone allylborane complex **7** in 66% yield (Scheme 3). To substantiate the assumed reaction sequence involving a hydroboration and re-coordination of the pyridone **5** to the formed allylborane, Piers borane **6** was reacted with phenylallene (Scheme 3). At −35 °C in diethylether, phenyallene was quantitatively hydroborated and the allylborane **8** was obtained with a regioselectivity of 81:19. In the next step, the pyridone **5** was added at r.t. This yielded the pyridone allylborane complex **7** in quantitative yield.

Thus, we were able to demonstrate that it is indeed possible to form an allylborane from hydrogen and phenylallene. In the next stage of this research project, we aimed to examine if the allylboranes generated in this way could be used as nucleophiles for an allylation reaction. A prerequisite for the use of **3** for an allylation is that the pyridonate borane **3** is able to activate hydrogen in the presence of a Lewis basic electrophile. To elucidate if this condition is met and if **7** serves as a source for nucleophilic allylboranes, **3** was reacted with phenylallene and one equivalent acetonitrile under moderated H_2 pressure (1.1 bar). However, this reaction did not yield the expected allylimine, but the β-diketiminate borane complex **9** together with the bispyridone complex **10** (Scheme 4).

The β-diketiminate borane complex **9** that proved to be air stable was isolated by silica gel column chromatography in

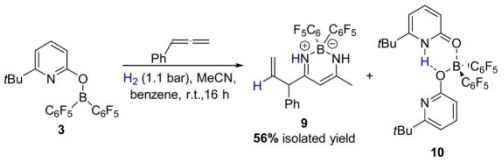

Scheme 4. Formation of the β-diketiminate borane complex **9** upon the reaction of **3** with acetonitrile and phenylallene under hydrogen pressure.

56% yield and fully characterized by NMR and ESI-MS. The structural assignment is further supported by single-crystal X-ray diffraction (SCXRD, Figure 1). The β-diketiminate borane complex **9** is reminiscent to the core structure of BODIPY dies.[15] Indeed, **9** is a fluorophore that absorbs at $\lambda_{max} = 359$ nm and emits at λ_{max}(fluorescence) = 409 nm with a molar attenuation coefficient of $\varepsilon_{359} = 6928\ cm^{-1}\ M^{-1}$ (see SI for full spectra).

The β-diketiminate borane complex **9** presumably originates from a nucleophilic attack of the enamine tautomer of an intermediately formed allylimine to acetonitrile. To verify this hypothesis and to check if an allylimine was formed as intermediate *en route* to **9**, the allylborane **8**, in situ generated by hydroboration of phenylallene, was reacted with one equivalent acetonitrile. This reaction furnished the ketiminoborane **11**, which is the allylation product of acetonitrile, in 83% yield. The formation of **11** demonstrates that allylborane **8** is indeed nucleophilic (Scheme 5).

The ^{11}B NMR shift of 21.4 ppm and the C=N stretching vibration of 1864 cm^{-1} indicate that **11** is present as monomeric ketiminoborane with linearity at nitrogen.[14] Next, pyridone **5** was added to the ketiminoborane **11**. This sequence yielded the allylimine complex **12** (Scheme 5). The NH signal of **12** is found at 10.90 ppm, indicating an N−H···N hydrogen bond. A ^{15}N-^{1}H HSQC NMR experiment shows that the proton is bound to a nitrogen with a shift of

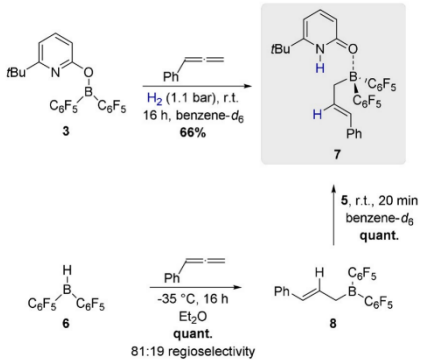

Scheme 3. Formation of the pyridone allylborane complex **7** upon hydrogen activation by **3** and the stepwise formation of **7** upon hydroboration of phenylallene by Piers borane **6** and addition of the pyridone **5**. Yields were determined by ^{1}H NMR with 1,3,5-trimethoxybenzene as internal standard.

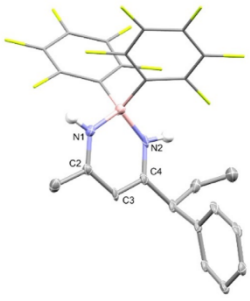

Figure 1. Molecular structure of **9** derived from SCXRD (50% probability ellipsoids, all hydrogens attached to carbons are omitted and C_6F_5 rings are shown in stick representation for clarity). Selected bond lengths and angles: N1-B: 1.528(17) Å, N1-C2 1.336(17) Å, C2-C3 1.403(19) Å, C3-C4 1.390(19) Å, N2-C4: 1.315(17) Å, N2-B: 1.539-(17) Å, C2-N1-B: 125.5(2)°, C4-N2-B: 126.7(2)°.

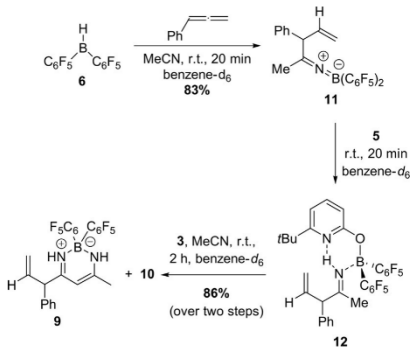

Scheme 5. Stepwise formation of the β-diketiminate borane complex **9** from Piers borane **6**. Yields were determined by ^{1}H NMR with 1,3,5-trimethoxybenzene as internal standard.

227.3 ppm. Additional ^{15}N-^{1}H HMBC NMR experiments revealed that this nitrogen couples to the methyl group and to the CHPh group of the allylimine **12** (Figure 2, for full spectra see SI).

Thus, the NMR experiment confirms the proton transfer from the pyridon **5** to the nitrogen of the ketiminoborane **11** and formation of an allylimine. The addition of one further equivalent acetonitrile and pyridonate borane **3** led to the clean formation of the β-diketiminate borane complex **9** in 86% yield (Scheme 5). This experiment strongly supports the assumption that upon the reaction of **3** with phenylallene and acetonitrile under H_2 pressure, which leads to the formation of **9**, the desired allylimine was indeed formed intermediately (Scheme 4). Therefore, the formation of **9** from phenylallene and acetonitrile proves that **3** is not only able to activate dihydrogen in the presence of acetonitrile, but also mediates the subsequent allylation, leading to an allylimine. However, the $B(C_6F_5)_2$ fragment is irreversibly bound in **9** which inhibits any further catalytic reactivity. We envisioned that the addition of a strong Lewis acid would enable us to capture the intermediately formed allylimine prior to the β-diketiminate borane complex formation (Scheme 6).

As the liberation of the allylimine from **12** would furthermore regenerate the pyridonate borane **3**, a catalytic allylation can be envisioned. Indeed, upon addition of $B(C_6F_5)_3$ the formation of the allylimine borane complex **13** from phenylallene, acetonitrile, and dihydrogen in presence of catalytic amounts of the pyridone borane complex **4** (10 mol%) was observed (Scheme 7).

The allylimine borane complex **13** proved to be air-stable and was isolated in 65% yield. However, on silica gel **13** isomerizes to the vinylimine **13′** as proven by two-dimensional TLC (see SI). Thus, the two isomers, fully characterized by NMR and ESI-MS, were obtained in a 93:7 ratio after column chromatography. The molecular structure of **13** in the solid-state was further analyzed by SCXRD (Figure 3). The allylimine borane complex **13** can be quantitatively isomerized to the vinylamine **13′** by addition of triethylamine at r.t. within minutes, indicating that **13′** is the thermodynamically more stable isomer. The molecular structure of **13′** derived from SCXRD confirms the *E*-configuration of the double bond.

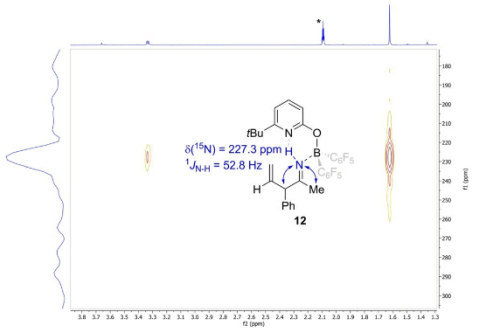

Figure 2. ^{15}N-^{1}H HMBC NMR spectrum of the allylimine complex **12** (600 MHz, [D$_8$]toluene). The blue arrows indicate the observed ^{15}N-^{1}H correlations. The signal marked with a star can be assigned to a solvent residue peak from [D$_8$]toluene.

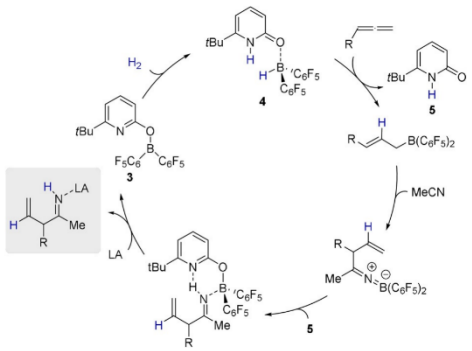

Scheme 6. Envisioned catalytic cycle for the allylation of nitriles using an additional Lewis acid that captures the allylimine (grey box) (LA = Lewis acid).

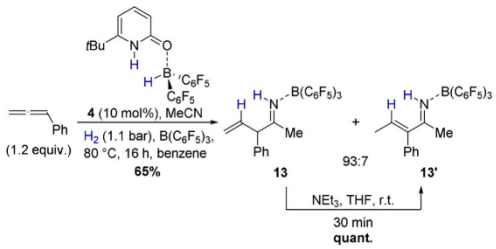

Scheme 7. Formation of the allylimine borane complex **13** catalyzed by **4**, and its isomerization to the vinylimine **13′**. One equivalent acetonitrile and $B(C_6F_5)_3$ were used.

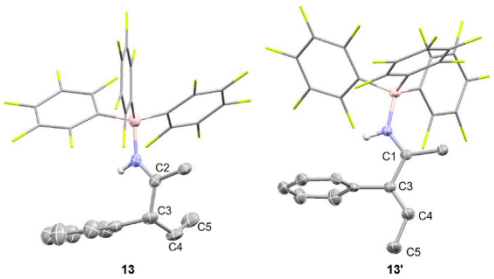

13 13'

Figure 3. Molecular structure of **13** and **13'** derived from SCXRD (50% probability ellipsoids, all hydrogens attached to carbons are omitted and C_6F_5 rings are shown in stick representation for clarity). Selected bond lengths and angles: **13**: C2-C3 1.528(8) Å, C3-C4 1.514(9) Å, C4-C5 1.310(5) Å, N1-C2-C3: 121.7(8)°, C3-C4-C5: 126.2(4)°; **13'**: C1-C3 1.4744(17) Å, C3-C4 1.3408(18) Å, C4-C5 1.497(2), N1-C1-C3: 118.07-(11)°, C3-C4-C5: 124.67(14)°.

To prove that the catalytic activity of **4** is more general, we explored next the scope and limitations of this novel allylation at the example of six different allenes (Scheme 8). Electron withdrawing groups are tolerated, but longer reaction times are required to obtain good yields. In the case of *tert*-butyl phenyl substituted allene the product **16** is only obtained in moderate yields. However, an NMR analysis of the crude reaction mixture showed that the allene is consumed after 16 h reaction time, indicating that side reactions lower the yield in this case. Aliphatic allenes are suitable substrates, but again longer reaction times are required. The formation of the adamantly substituted allylimine **19** in excellent yield further shows that sterically demanding substituents are tolerated. The products **17**, **18**, and **19** did not isomerize upon purification by silica gel chromatography. However, we

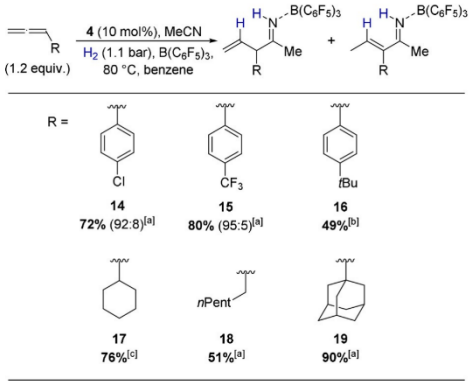

Scheme 8. Allylation of acetonitrile catalysed by **4** with different allenes. One equivalent acetonitrile and $B(C_6F_5)_3$ were used. All yields are isolated yields. The number in parenthesis indicate the ratio of allylimine to vinylimine. [a] Reaction time 5 days. [b] Reaction time 16 hours. [c] Reaction time 7 days.

demonstrated at the example of **18** that the allylimines with aliphatic substituents can be isomerized to the respective vinylimines by the addition of a base. Treatment of **18** with NEt_3 at r.t. for 30 minutes allowed us to isolate the corresponding vinylimine in 95% yield (see SI).

The mechanism of this novel catalytic transformation was further addressed by dispersion-corrected Density Functional Theory (DFT) computations at the revDSD-PBEP86-D4/def2-QZVPP//PBEh-3c level (Figure 4).[16–18] The revDSD-PBEP86-D4 functional is one of the best DFT methods for ground-state thermochemistry and kinetics as shown by benchmark computations using the GMTKN55 database.[16a,19] The SMD model for benzene was used to implicitly account for solvent effects.[20] We used 1,2-butadiene as model substrate and further assumed, that under the reaction conditions complex **20** forms upon coordination of acetonitrile to $B(C_6F_5)_3$. In agreement with previous investigations, the computations reveal that the catalytic cycle commences with hydrogen activation by the pyridonate borane **3**. The pyridone borane complex **4** that is formed in this way dissociates to liberate Piers borane **6**. As a stoichiometric amount of $B(C_6F_5)_3$ is present, we considered that the pyridone **5** coordinates to the $B(C_6F_5)_3$, which overall renders the liberation of Piers borane **6** thermodynamically more favorable. The hydroboration of the terminal allene requires passing a moderate barrier of 8.4 kcal mol^{-1} and is according to the computations exergonic by 27.6 kcal mol^{-1}.

Coordination of acetonitrile to the allylborane **22** precedes the intramolecular allylation via a cyclic six-membered transition state with a barrier of 16.2 kcal mol^{-1}. The computed structure of the ketiminoborane **24** shows a C=N=B angle of 178.7°, which agrees with the linearity at nitrogen deduced from the experimental C=N stretching vibration of **11**. Upon dissociation of pyridone $B(C_6F_5)_3$ complex **21** and recoordination of **5**, a virtually barrier-less intramolecular proton transfer yields the allylimine complex **26**. Based on our experimental findings, we propose that the allylimine complex **26** is the common intermediate for the formation of the β-diketiminate borane complex **32** and the allylimine B-$(C_6F_5)_3$ complex **28**. In the absence of $B(C_6F_5)_3$, an intramolecular proton transfer from the methyl group of the allylimine to the pyridine nitrogen that requires a Gibbs free activation energy of 21.3 kcal mol^{-1} yields the pyridone enamine borane complex **29**. Dissociation of this complex, thermodynamically favored by formation of the bispyridone complex **10**, enables the nucleophilic addition of the enamine to acetonitrile via the six-membered transition state $\mathbf{TS_{30/31}}$. While the C–C bond formation is already exergonic, the tautomerization to the diketiminate borane complex **32** provides a further decisive driving force to the reaction. In the presence of $B(C_6F_5)_3$, the kinetically favored pathway commences with the dissociation of the allylimine complex **26** that is endergonic by 14.4 kcal mol^{-1}. Coordination of the $B(C_6F_5)_3$ to the free allylimine **27** yields the allylimine $B(C_6F_5)_3$ complex **28**. The coordination of $B(C_6F_5)_3$ to the allyimine **27** imparts a barrier of 25.3 kcal mol^{-1} for the tautomerization to the pyridone enamine borane complex **29** and therefore suppresses the formation of the β-diketiminate borane complex **32**. However, according to the computations,

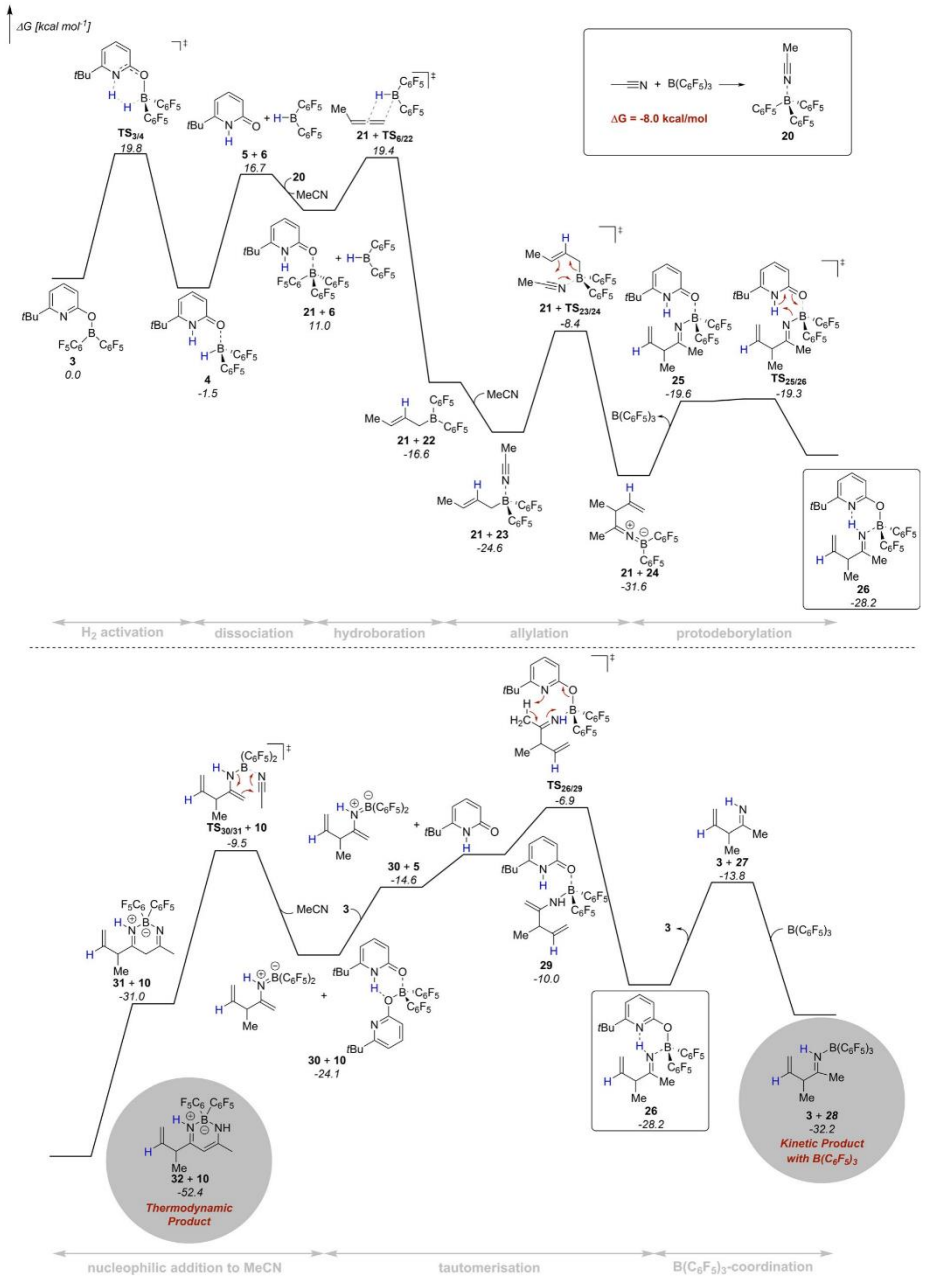

Figure 4. Potential energy surface for the formation of the β-diketiminate borane complex **32** and allylimine borane complex **28** computed at revDSD-PBEP86-D4/def2-QZVPP//PBEh-3c. The SMD model for benzene was used to implicitly account for solvent effects.

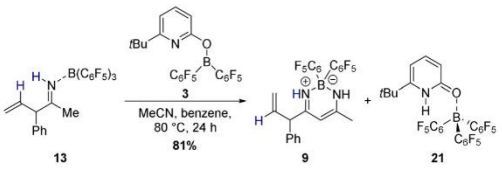

Scheme 9. Conversion of the allylimine $B(C_6F_5)_3$ complex **13** to the β-diketiminate borane complex **9**, which is the thermodynamic product of the allylation, catalyzed by **3**. Yields were determined by ^{1}H NMR with 1,3,5-trimethoxybenzene as internal standard.

the allylimine $B(C_6F_5)_3$ complex **28** must be regarded as the kinetic product while the β-diketiminate borane complex **32** is the thermodynamic product of the initial allylation. To verify this computational result experimentally, the isolated allylimine $B(C_6F_5)_3$ complex **13** was reacted with one additional equivalent MeCN and the pyridonate borane **3** at an elevated temperature of 80 °C (Scheme 9). Within 24 h, the formation of the β-diketiminate borane complex **9** in 81 % yield was observed.

This result confirms, in agreement with computations, that the β-diketiminate borane complex **9** is the thermodynamic more stable product.

Conclusion

In summary, we have documented the formation of allylboranes from molecular hydrogen and allenes mediated by a pyridonate borane. The stochiometric reaction of these in situ generated allylboranes with acetonitrile leads to a β-diketiminate borane complex. By using an additional Lewis acid, we were able to develop a method for the allylation of nitriles that requires only catalytic amounts of the pyridonate borane. Mechanistic investigations reveal that the change in the binding mode of the pyridonate substituent in course of the hydrogen activation is vital for the formation of the allylborane. The results presented herein might stimulate the development of metal-free, atom-economic catalytic allylations.

Acknowledgements

This work was supported by the FCI (Liebig Fellowship to U.G.) and the DFG (Emmy-Noether program, GE 3117/1-1). The authors thank Dr. H. Hausmann and Dr. D. Gerbig for assistance with NMR and IR experiments, respectively. Continuous support by Prof. P. R. Schreiner, R. Göttlich, and H. A. Wegner is acknowledged. Open access funding enabled and organized by Projekt DEAL.

Conflict of interest

The authors declare no conflict of interest.

Keywords: allylboranes · boron–ligand cooperation · DFT computations · frustrated Lewis pairs · hydrogen activation

[1] W. R. Roush, in *Comprehensive Organic Synthesis, Vol. 2* (Eds.: B. M. Trost, I. Fleming), Pergamon Press, New York, **1991**, pp. 1–53.
[2] a) H. C. Brown, P. K. Jadhav, *J. Am. Chem. Soc.* **1983**, *105*, 2092–2093; b) H. C. Brown, K. S. Bhat, *J. Am. Chem. Soc.* **1986**, *108*, 5919–5923; c) U. S. Racherla, H. C. Brown, *J. Org. Chem.* **1991**, *56*, 401–404; d) W. R. Roush, A. D. Palkowitz, K. Ando, *J. Am. Chem. Soc.* **1990**, *112*, 6348–6359.
[3] For selected examples of the application of allylboranes in the total synthesis of natural products see: a) J. B. Shotwell, W. R. Roush, *Org. Lett.* **2004**, *6*, 3865–3868; b) J. M. Tinsley, W. R. Roush, *J. Am. Chem. Soc.* **2005**, *127*, 10818–10819; c) P. Va, W. R. Roush, *J. Am. Chem. Soc.* **2006**, *128*, 15960–15961; d) J. M. Schkeryantz, J. C. G. Woo, P. Siliphaivanh, K. M. Depew, S. J. Danishefsky, *J. Am. Chem. Soc.* **1999**, *121*, 11964–11975; e) K. D. Carter, J. S. Panek, *Org. Lett.* **2004**, *6*, 55–57; f) T. Lindel, L. Braeuchle, G. Golz, P. Boehrer, *Org. Lett.* **2007**, *9*, 283–286; g) C. W. Huh, W. R. Roush, *Org. Lett.* **2008**, *10*, 3371–3374; h) P. Nuhant, W. R. Roush, *J. Am. Chem. Soc.* **2013**, *135*, 5340–5343.
[4] a) P. K. Jadhav, K. S. Bhat, P. T. Perumal, H. C. Brown, *J. Org. Chem.* **1986**, *51*, 432–439; b) W. R. Roush, R. L. Halterman, *J. Am. Chem. Soc.* **1986**, *108*, 294–296.
[5] G. W. Kramer, H. C. Brown, *J. Organomet. Chem.* **1977**, *132*, 9–27.
[6] R. C. Godfrey, N. J. Green, G. S. Nichol, A. L. Lawrence, *Nat. Chem.* **2020**, *12*, 615–619.
[7] U. Gellrich, *Angew. Chem. Int. Ed.* **2018**, *57*, 4779–4782; *Angew. Chem.* **2018**, *130*, 4869–4872.
[8] For early examples of Hydrogen activation by FLPs see: a) G. C. Welch, R. R. S. Juan, J. D. Masuda, D. W. Stephan, *Science* **2006**, *314*, 1124–1126; b) P. Spies, G. Erker, G. Kehr, K. Bergander, R. Fröhlich, S. Grimme, D. W. Stephan, *Chem. Commun.* **2007**, 5072–5074; c) G. C. Welch, D. W. Stephan, *J. Am. Chem. Soc.* **2007**, *129*, 1880–1881.
[9] For recent reviews on hydrogen activation by FLPs see: a) D. W. Stephan, G. Erker, *Angew. Chem. Int. Ed.* **2015**, *54*, 6400–6441; *Angew. Chem.* **2015**, *127*, 6498–6541; b) D. W. Stephan, *J. Am. Chem. Soc.* **2015**, *137*, 10018–10032.
[10] J. R. Khusnutdinova, D. Milstein, *Angew. Chem. Int. Ed.* **2015**, *54*, 12236; *Angew. Chem.* **2015**, *127*, 12406.
[11] U. Gellrich, F. Wech, M. Hasenbeck, *Chem. Eur. J.* **2020**, https://doi.org/10.1002/chem.202001276.
[12] a) D. J. Parks, R. E. von H. Spence, W. E. Piers, *Angew. Chem. Int. Ed. Engl.* **1995**, *34*, 809–811; *Angew. Chem.* **1995**, *107*, 895–897; b) E. A. Patrick, W. E. Piers, *Chem. Commun.* **2020**, *56*, 841–853.
[13] The trimerization and dimerization of allenes upon hydroboration by Piers borane was reported: a) X. Tao, G. Kehr, C. G. Daniliuc, G. Erker, *Angew. Chem. Int. Ed.* **2017**, *56*, 1376–1380; *Angew. Chem.* **2017**, *129*, 1396–1400; b) X. Tao, C. G. Daniliuc, D. Dittrich, G. Kehr, G. Erker, *Angew. Chem. Int. Ed.* **2018**, *57*, 13922–13926; *Angew. Chem.* **2018**, *130*, 14118–14122.
[14] a) V. A. Dorokhov, M. F. Lappe, *Chem. Commun.* **1968**, 250; b) J. R. Jennings, I. Pattison, C. Summerford, K. Wade, B. K. Wyatt, *Chem. Commun.* **1968**, 250–251.
[15] A. Loudet, K. Burgess, *Chem. Rev.* **2007**, *107*, 4891–4932.
[16] a) G. Santra, N. Sylvetsky, J. M. L. Martin, *J. Phys. Chem. A* **2019**, *123*, 5129–5143; b) E. Caldeweyher, C. Bannwarth, S. Grimme, *J. Chem. Phys.* **2017**, *147*, 034112; c) E. Caldeweyher, S. Ehlert, A. Hansen, H. Neugebauer, S. Spicher, C. Bannwarth, S. Grimme, *J. Chem. Phys.* **2019**, *150*, 154122; d) F. Weigend, R. Ahlrichs, *Phys. Chem. Chem. Phys.* **2005**, *7*, 3297–3305; e) A.

Hellweg, C. Hattig, S. Hofener, W. Klopper, *Theor. Chem. Acc.* **2007**, *117*, 587 – 597; f) F. Weigend, *J. Comput. Chem.* **2008**, *29*, 167 – 175.

[17] a) S. Grimme, J. G. Brandenburg, C. Bannwarth, A. Hansen, *J. Chem. Phys.* **2015**, *143*, 054107; b) H. Kruse, S. Grimme, *J. Chem. Phys.* **2012**, *136*, 154101; c) S. Grimme, S. Ehrlich, L. Goerigk, *J. Comput. Chem.* **2011**, *32*, 1456 – 1465; d) S. Grimme, J. Antony, S. Ehrlich, H. Krieg, *J. Chem. Phys.* **2010**, *132*, 154104; e) F. Weigend, *Phys. Chem. Chem. Phys.* **2006**, *8*, 1057 – 1065.

[18] All computations were performed with the ORCA program package, Version 4.2.1: a) F. Neese, *WIREs Comput. Mol. Sci.* **2012**, *2*, 73 – 78; b) F. Neese, *WIREs Comput. Mol. Sci.* **2018**, *8*, e1327.

[19] a) L. Goerigk, A. Hansen, C. Bauer, S. Ehrlich, A. Najibi, S. Grimme, *Phys. Chem. Chem. Phys.* **2017**, *19*, 32184 – 32215; b) L. Goerigk, N. Mehta, *Aust. J. Chem.* **2019**, *72*, 563 – 573.

[20] A. V. Marenich, C. J. Cramer, D. G. Truhlar, *J. Phys. Chem. B* **2009**, *113*, 6378 – 6396.

Manuscript received: August 28, 2020
Accepted manuscript online: September 14, 2020
Version of record online: October 22, 2020

5.6 Boron–Ligand Cooperation: The Concept and Applications

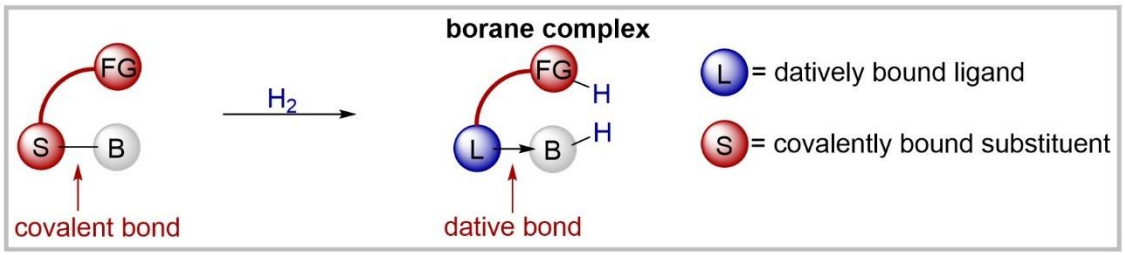

The term boron–ligand cooperation (BLC) describes a specific mode of action by which distinctive intramolecular borane-based frustrated Lewis Pairs (FLPs) activate chemical bonds. The central aspect of this concept is that the substituent at the borane that is involved in the bond activation becomes a datively bound ligand upon bond activation. The reactivity of systems that operate via BLC can complement those of classic intramolecular FLPs.

Max Hasenbeck, Dr. Urs Gellrich

Chem. Eur. J. **2021**, *27*, 5615-5626

DOI (englische Version): 10.1002/chem.202004563

Akzeptiertes Manuskript online: 09.12.2020

Final veröffentlichte Version online: 28.01.2021

Chemistry–A European Journal
Minireview
doi.org/10.1002/chem.202004563
Check for updates
Chemistry Europe
European Chemical Societies Publishing

Bond Activation

Boron–Ligand Cooperation: The Concept and Applications

Max Hasenbeck and Urs Gellrich*[a]

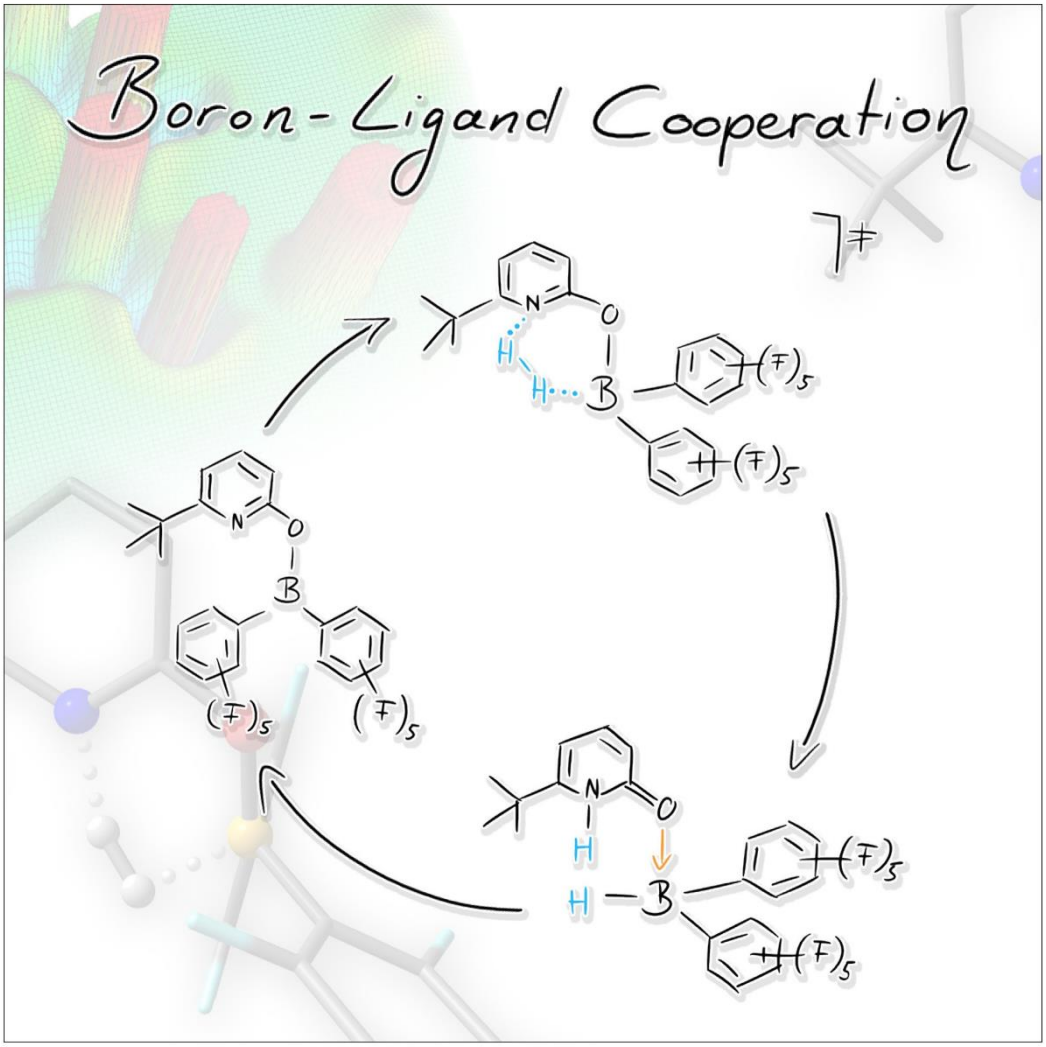

Abstract: The term boron–ligand cooperation was introduced to describe a specific mode of action by which certain metal-free systems activate chemical bonds. The main characteristic of this mode of action is that one covalently bound substituent at the boron is actively involved in the bond activation process and changes to a datively bound ligand in the course of the bond activation. Within this review, how the term boron–ligand cooperation evolved is reflected on and examples of bond activation by boron–ligand cooperation are discussed. It is furthermore shown that systems that operate via boron–ligand cooperation can complement the reactivity of classic intramolecular frustrated Lewis pairs and applications of this new concept for metal-free catalysis are summarized.

Introduction

The concept of boron–ligand cooperation was coined to describe a specific mode of bond activation by boranes that is reminiscent of the concept of metal–ligand cooperation. However, these boranes can also be described as a specific class of intramolecular frustrated Lewis pairs (FLPs). We, therefore, commence this review with a brief reflection on metal–ligand cooperation and frustrated Lewis pairs.

Metal–ligand cooperation

Metal–ligand cooperation (MLC) has emerged as a powerful tool for bond activation and catalysis in the last decades. Whereas classic transition-metal complexes activate chemical bonds by an oxidative addition at the metal center, MLC denotes a situation where one of the ligands bound to the metal center is actively involved in the bond activation process. Prime examples for bond activation by MLC are the hydrogen activation by Noyori's ruthenium catalyst **1** and by the ruthenium pincer complex **3** introduced by David Milstein and coworkers.[1,2] In the course of the hydrogen activation by the Noyori system, the amide substituent is involved in the H_2 activation. Hydrogen activation by the Milstein system is accompanied by the transfer of a proton to the benzylic position of the dearomatized pincer ligand, leading to a re-aromatization of the pyridine ring (Scheme 1).

In their comprehensive review on MLC from 2015,[3] Khusnutdinova and Milstein gave three criteria for MLC that read as:

"1) Both the metal and the ligand participate in the bond cleavage or bond formation steps;

2) Both the metal and the ligand are chemically modified during bond activation.

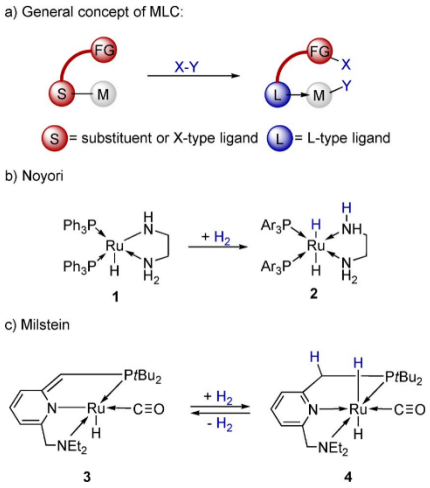

Scheme 1. The concept and examples of metal–ligand cooperation. (a) The concept of metal–ligand cooperation according to the criteria defined by Khusnutdinova and Milstein. (b) Hydrogen activation by Noyori's catalyst. (c) Reversible hydrogen activation by Milstein's pyridine-based pincer complex through an aromatization/de-aromatization sequence.

3) The coordination mode of the cooperative ligand undergoes significant changes in the first coordination sphere as a result of bond activation."

In the context of this review, it is important to emphasize the third criterion, which stipulates that the "*coordination mode of the cooperative ligand undergoes significant changes*" during bond activation. An analysis of the examples given in the review by Khusnutdinova and Milstein reveals that this change in the coordination mode can usually be described as the transition of a covalently bound substituent to a datively bound ligand. For example, the amide substituent in the Noyori system becomes a datively bound amine ligand during the bond activation. The re-aromatization that is observed upon bond activation by the Milstein pincer systems leads to the regeneration of a datively bound pyridine ligand, which was before bond activation better described as an enamide substituent. As a consequence of this change in the coordination sphere, the formal oxidation state of the ruthenium does not change. We note that inorganic chemists might prefer to describe this change in the coordination mode as the transi-

[a] *M. Hasenbeck, Dr. U. Gellrich*
Institut für Organische Chemie, Justus-Liebig-Universität Gießen
Heinrich-Buff-Ring-17, 35392 Gießen (Germany)
E-mail: urs.gellrich@org.chemie.uni-giessen.de
The ORCID identification number(s) for the author(s) of this article can be found under: https://doi.org/10.1002/chem.202004563.

tion of an X-type ligand to an L-type ligand.[4] However, we use the term "covalently bound substituent" here as equivalent to the notation X-type ligand to establish an analogy to transition-metal-free systems.

Frustrated Lewis pairs

The term frustrated Lewis pairs (FLPs) describes combinations of sterically encumbered Lewis bases and Lewis acids that are able to activate strong chemical bonds.[5,6] Classic examples for intramolecular FLPs are the covalently linked phosphine–borane pairs **5** and **7** developed by the groups of Stephan and Erker (Scheme 2).[5a,b] The hydrogen activation by these intramolecular FLPs leads to the formation of borohydrides (**6** and **8**). Numerous metal-free catalytic reactions that are based on the FLP concept have been developed in recent years.[6]

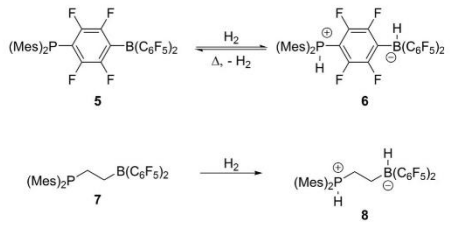

Scheme 2. Hydrogen activation by the intramolecular FLPs **5** and **7**, which leads to the formation of the borohydrides **6** and **8**.

Boron–ligand cooperation: The concept

We and others recently reported bond activation by a specific class of intramolecular FLPs in which bond activation leads to a reorganization of π-electron density within the cooperative substituent. Furthermore, bond activation is associated with a transition of the involved substituent to a datively bound ligand (Scheme 3 a). Thus, in contrast to classic FLPs, bond activation does not lead to a borate salt, but rather a borane complex. We note that the reorganization of π-electron density and the concomitant change in coordination mode of the cooperative substituent are reminiscent of hydrogen activation by Milstein's established pyridine-based pincer complexes (Scheme 3 b).[2,3] In analogy, we proposed the term boron–ligand cooperation (BLC) to describe the bond activation by these specific FLPs.

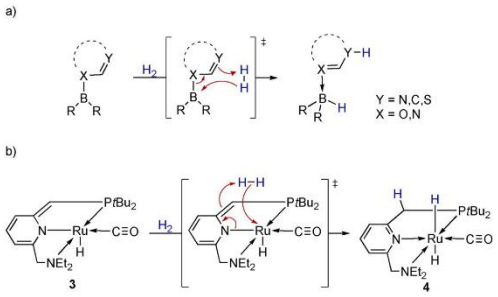

Scheme 3. Hydrogen activation by a specific class of intramolecular FLPs, which leads to a change in the bonding mode of the cooperative substituent (a) and the analogy to hydrogen activation by the pincer complex **3** (b).

Thus, the BLC concept emphasizes a change in the valence sphere of the borane as a result of the bond activation. However, the systems that operate through BLC can in their reactive state before bond activation be classified as intramolecular FLPs. The three concepts of MLC, FLPs, and BLC have in common that the bond activation involves two active sites with Lewis basic and Lewis acidic character. These similarities were noted in recent reviews by Greb and Slootweg.[7] Within the second part of this review, we will discuss examples of bond activation by BLC with a special emphasis on changes in the bonding between the substituent involved in the bond activation and the borane. In the third part, we will discuss how the novel reactivity based on BLC can complement the reactivity of FLPs and show how the BLC concept can lead to new applications for transition-metal-free catalysis.

Bond Activation by Boron–Ligand Cooperation

In the following, we will discuss examples of bond activation that fulfill the criteria for BLC formally. We will focus on the question of whether experimental and computational data further support that the transition of a covalently bound substituent to a datively bound ligand is a real chemical event.

Max Hasenbeck studied chemistry at the universities of Cologne and Düsseldorf in Germany. For his master's thesis, he worked on the computational investigation of reaction mechanisms under the supervision of Dr. Martin Breugst. After receiving his M.Sc. in 2017, he joined the group of Dr. Urs Gellrich at the Justus Liebig University Giessen for his doctoral studies working on the concept of boron–ligand cooperation and its application for catalysis.

Urs Gellrich studied chemistry at the University of Freiburg in Germany where he obtained his doctorate in 2013 for his work on supramolecular ligands under the guidance of Prof. Bernhard Breit. He then joined the group of Prof. David Milstein at the Weizmann Institute of Science as a postdoctoral researcher. In 2017, Urs started his independent career as a Liebig Fellow of the FCI at the Justus Liebig University Giessen where he is currently Emmy Noether Group Leader. His research focuses on the in silico design of novel metal-free systems for bond activation and catalysis.

Early examples of boron–ligand cooperation

In 2010, Tamm and co-workers reported the H_2 activation by the pyrazolylborane **9**, which the authors described as a bifunctional FLP (Scheme 4).[8] The authors reported the product **10** of the hydrogen activation as zwitterionic pyrazolium–borate. However, **10** can also be described as a pyrazol borane complex. The elongation of the N–B bond from 1.4281(16) Å in **9** to 1.5794(13) Å in **10**, determined by single-crystal (SC)XRD, does support this description.

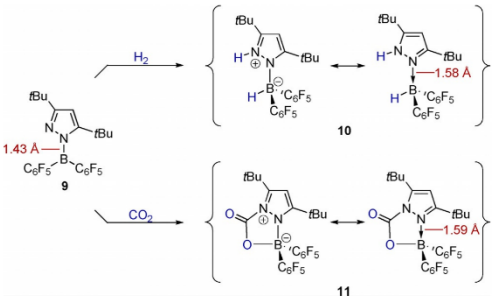

Scheme 4. Hydrogen and CO_2 activation by the pyrazolylborane **9** and the possible description of the products as zwitterionic pyrazolium–borate or as pyrazol borane complex.

A similar bond elongation is observed upon CO_2 activation by **9**, which yields **11**.[9] An alternative interpretation is that the N–B π-bonding in **9** is lost upon hydrogen activation, resulting in an elongation of this bond. However, the reported SCXRD structures further reveal that upon hydrogen activation the N1–C3 is shortened by 0.05 Å whereas the N2–C1 is elongated by 0.03 Å (Scheme 5). This change in the bond lengths, indicating a reorganization of π-electron density within the heterocycle upon hydrogen activation, is better described when **10** is depicted as a pyrazole borane complex.

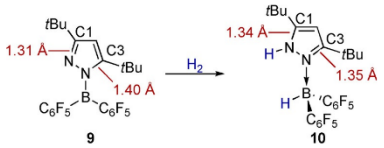

Scheme 5. Changes in the bond lengths of the heterocycle upon hydrogen activation by **9** derived from SCXRD structures.

A computational examination of boron–ligand cooperation

To mimic the reactivity of Milstein's ruthenium pyridine pincer complex by metal-free systems, Wang, Schleyer, and colleagues investigated the activation of dihydrogen by model compound **12** (Scheme 6).[10] From their computations, the authors concluded that hydrogen activation by **12** yielding **13** is kinetically feasible but that the reverse reaction is not possible. The computed nucleus independent chemical shifts (NICS(0))[11] further reveal an aromaticity gain upon hydrogen activation by **12**, which is diagnostic for the formation of a datively bound pyridine ligand.

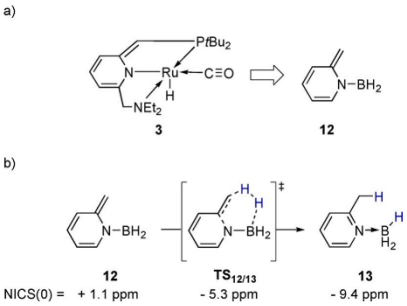

Scheme 6. The model system **12**, designed to mimic the reactivity of Milstein's ruthenium pincer complex and the re-aromatization of **12** upon hydrogen activation, which is exemplified by the computed NICS values.

Although the authors did not use the term BLC, this computational study named MLC as a design principle for bond activation by a borane.

Boron–ligand cooperation by re-aromatization of a pyridine–borane complex

Inspired by the computational work by Schleyer and Wang, Milstein and co-workers attempted to realize bond activation by a dearomatized pyridine borane experimentally.[12] Therefore, the amino-borane pyridine complex **14** was synthesized (Scheme 7). Upon moderate heating, hydrogen liberation from **14** and formation of the dearomatized aminoborane **15** was observed.

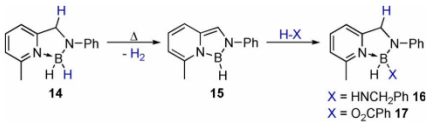

Scheme 7. Hydrogen liberation from **14** at elevated temperatures leads to de-aromatization of the pyridine ring. The reaction with benzylamine or benzoic acid results in re-aromatization of the pyridine ring.

As indicated by the ^{1}H NMR chemical shifts of **14** and **15** and the computed NICS values, the de-aromatization event is in this case better described as a shift of the aromaticity from the pyridine ring in **14** to the five-membered boracycle in **15**. The reaction of **14** with benzylamine or benzoic acid leads to N–H activation and O–H cleavage and formation of **16** and **17**, respectively. In both cases, the re-aromatization of the pyridine ring shows that the bond activation was accompanied by the change of the N–B bond from a covalent bond in **15** to a

dative bond in the pyridine amino-borane complexes **16** and **17**. To describe the reactivity of **15**, the term boron–ligand cooperation was introduced.

Boron–ligand cooperation by a pyridonate borane

In 2018, we reported reversible H_2 activation by the pyridonate borane complex **18** (Scheme 8).[13] The closed-form of the pyridonate borane **18** is in equilibrium with the open form **18′**, which can be regarded as an intramolecular FLP. Hydrogen activation by **18′** yields **19**. The hydrogen activation is reversible. Upon heating to 60 °C, **19** liberates dihydrogen and **18** is regenerated.

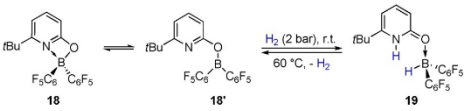

Scheme 8. Reversible hydrogen activation by **18′**, leading to the formation of the pyridone borane complex **19**.

We became interested if **19** is better described as zwitterionic borate or as a pyridone borane complex. A comparison of the computed structures of **18′** and **19** reveals an elongation of the O–B bond by 0.2 Å (Scheme 9). Furthermore, the C–O is shortened in course of the bond activation to 1.27 Å, a value that is typical for a C=O double bond. This indicates that the heterocycle in **19** is present as pyridone. In agreement with this interpretation, the C=O stretching vibration of **19** at 1643 cm^{-1} is similar to that observed for the "fixed" pyridone tautomer 1-methyl-2-pyridone.[14] The reduced aromaticity of **19** compared with **18**, deduced from the computed NICS values, is further indicative of the formation of a pyridone.[15]

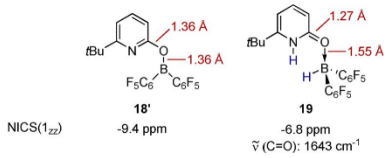

Scheme 9. Computed bond lengths and NICS values for **18′** and **19**. The description of the pyridone borane complex is further supported by the experimentally determined IR stretching vibration of **19**.

The disappearance of the covalent B–O upon dihydrogen activation of **18′** to **19** is furthermore supported by the analysis of the Laplacian of the electron density (Figure 1). For covalent bonds, the Laplacian of the electron density should show a minimum along the bond axis.[16] In the case of pyridonate borane **18′**, this is clearly visible ("blue valley", Figure 1, left side). This is not the case for pyridone borane **19** (Figure 1, right side), indicating a closed-shell interaction between O and B. An EDA-NOCV analysis further supports the change in the bonding mode of the pyridonate substituent upon hydrogen activation.[17]

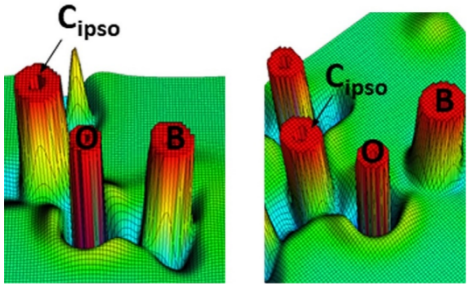

Figure 1. Analysis of the Laplacian of the electron density computed at PBE0(D3BJ)/def2-TZVP.[18] Left: pyridonate borane **18′**; right: pyridone borane complex **19**.

Boron–ligand cooperation as a concept for metal-free catalysis

The IUPAC definition of a dative bond states that "The distinctive feature of dative bonds is that their minimum-energy rupture in the gas phase or in inert solvent follows the heterolytic bond cleavage path".[19] To substantiate the presence of a dative bond in **19**, we probed the heterolytic dissociation in a pyridone and a borane (Scheme 10). As the equilibrium lies far on the side of the pyridone borane complex, there is no possibility to obtain direct spectroscopic evidence for such a dissociation. Therefore, we investigated if **19** is able to effect hydroboration, as hydroboration requires the presence of a trivalent borane.[20] Indeed, when **18′** was reacted under an H_2 atmosphere with styrene, the formation of the pyridone alkylborane **20** was observed (Scheme 10).

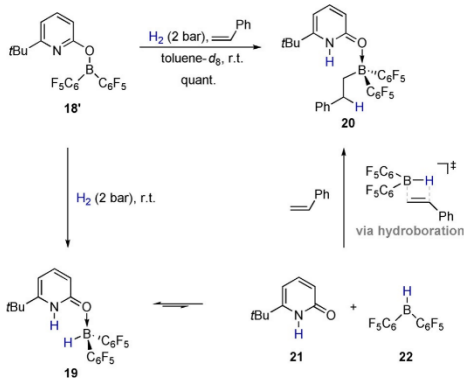

Scheme 10. Formation of the alkylborane **20**, which shows that the pyridone borane complex **19** formed upon H_2 activation by **18′** undergoes a heterolytic dissociation to pyridone **21** and Piers borane **22**.

Thus, the change of the B–O from a covalent bond to a dative bond during H_2 activation provides access to borane reactivity. Classic intramolecular FLPs rather show borohydride reactivity. In this regard, the concept of BLC complements the reactivity of classic FLPs.

Semi-hydrogenation of alkynes

Repo and co-workers showed that alkenyl borate complexes are prone to undergo intramolecular protodeborylations in the presence of protic substituents.[21] We, therefore, envisioned that a pyridone alkenylborane complex, formed analogously to **20** upon hydroboration of an alkyne, could undergo a protodeborylation yielding a *cis* alkene. This would enable the usage of **18′** as a potential hydrogenation catalyst in a sequence of H_2 activation, hydroboration, and protodeborylation. Using this strategy, several internal alkynes were hydrogenated in moderate to excellent yields under mild hydrogen pressure to the corresponding (*Z*)-alkenes (Scheme 11).[20,22]

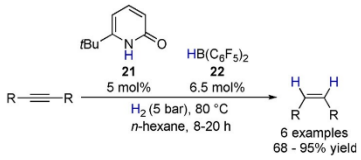

Scheme 11. *Semi*-hydrogenation of internal alkynes to the corresponding (*Z*)-alkenes.

Extended reaction times lead to the isomerization of the (*Z*)-alkenes to the corresponding (*E*)-alkenes for some substrates. We attributed this isomerization to the reversible hydroboration of alkenes by the Piers borane, which was reported earlier by the Du group.[22a] The reaction mechanism of the hydrogenation was investigated experimentally and computationally (Scheme 12). After hydrogen activation by the pyridonate borane **18′**, the resulting pyridone borane complex **19** dissociates into the pyridone **21** and Piers borane **22**. This endergonic reaction is rendered thermodynamically more favorable by the complexation of the pyridone **21** with the pyridonate borane **18′**, yielding the bispyridone complex **23**.[13,23] After hydroboration of the alkyne by Piers borane **22**, the resulting alkenylborane **24** has to re-coordinate to the pyridone **21** to undergo protonolysis. Therefore, the bispyridone complex **23** has to dissociate again into the pyridonate borane **18′** and the pyridone **21**. The latter coordinates to alkenylborane **24**, yielding the alkenylborane pyridone complex **25**. Protodeborylation liberates the (*Z*)-alkene and regenerates the catalyst **18′**.

The bispyridone complex **23** and the alkenylborane **24** were identified as the resting state of the catalytic transformation by NMR spectroscopy, whereas computations identified the protodeborylation as the turnover-determining transition state (TDTS). For 2-butyne as a model substrate, the computed kinetic barrier or *energetic span* of the catalytic cycle is 22.6 kcal

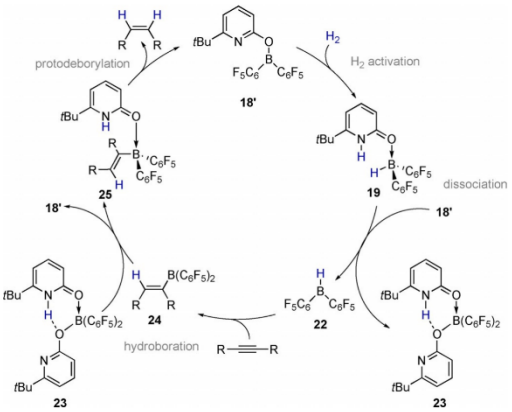

Scheme 12. Catalytic cycle of the *semi*-hydrogenation of internal alkynes to the corresponding (*Z*)-alkenes.

mol^{-1}, which is in good agreement with the experimental reaction conditions (Scheme 13).[24]

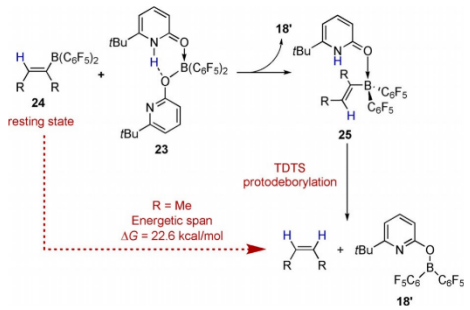

Scheme 13. Protoborylation of the alkenylborane and the computed energetic span of the catalytic cycle at revDSD-PBEP86-D4/def2-QZVPP//PBEh-3c.[25] The SMD model for *n*-hexane was used to account implicitly for solvent effects.[26]

Furthermore, several terminal alkynes could be hydrogenated in moderate to good yields although a higher catalyst loading had to be used (Scheme 14a). This is the first example of an FLP catalyst which is able to hydrogenate terminal alkynes. Other FLPs are deactivated by terminal alkynes because of an irreversible deprotonative borylation.[27] Although pyridonate borane **18′** reacts with terminal alkynes in such a deprotonative borylation, a competition experiment revealed that the C_{sp}–H cleavage is reversible, thus enabling the hydrogenation pathway (Scheme 14b).

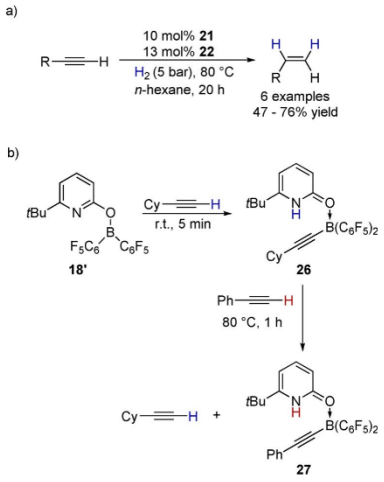

Scheme 14. (a) Scope of the *semi*-hydrogenation of terminal alkynes, (b) competition experiment of the C_{sp}–H cleavage of terminal alkynes by **18′**.

Gem-dimerization of terminal alkynes

The ability of **18′** to cleave the C_{sp}–H bond of terminal alkynes was used to develop a catalytic protocol for the first metal-free *gem*-dimerization of terminal alkynes.[28] By heating a reaction mixture of a terminal alkyne with 20 mol% of the pyridonate borane **18′**, several alkynes were dimerized to the respective enynes with exclusive *gem*-regioselectivity (Scheme 15). The active catalyst was formed *in situ* by dehydrogenation of **19**.

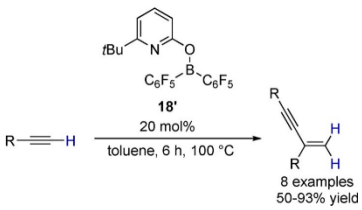

Scheme 15. *Gem*-dimerization of terminal alkynes by using pyridonate borane **18′** as the catalyst.

Mechanistic investigations reveal that for the observed reactivity, the change in the B–O bonding from a covalent to a dative bond upon C_{sp}–H activation of the terminal alkyne by the pyridonate borane **18′** is essential (Scheme 16). This change in the bond mode enables the dissociation of the pyridone alkynylborane complex **28** in the pyridone **21** and the trivalent alkynylborane **29**, which undergoes an 1,2-carboboration reaction with another equivalent of the terminal alkyne.[29] The resulting enynylborane **30** re-coordinates to the pyridone **21**, forming **31**. After protodeborylation, the *gem*-dimer is released and the catalyst **18′** is regenerated. Computations and experiments showed that the alkynylborane pyridone complex **28** is the resting state whereas the 1,2-carboboration is the TDTS of the reaction. The *energetic span* of the reaction for propyne as a model substrate was computed to be 25.0 kcal mol^{-1}.

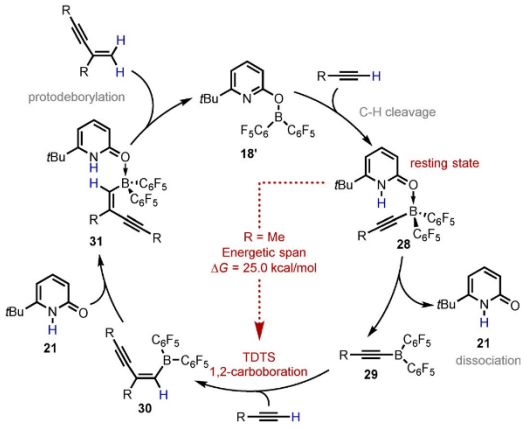

Scheme 16. Catalytic cycle of the *gem*-dimerization of terminal alkynes. The energetic span was computed at TightPNO-DLPNO-CCSD(T)/def2-TZVP//PBE0-D3(BJ)/def2-TZVP.[25,30] The SMD model for toluene was used to implicitly account for solvent effects.[26]

The 1,2-carboboration reaction was furthermore investigated by the reaction of the independently synthesized alkynylborane **32** with 3-phenylpropyne **33** (Scheme 17). The reaction yielded the enynylborane **34**, which was fully characterized by NMR spectroscopy. The addition of one equivalent of pyridone **21** yielded the enyne **35** and the bispyridone complex **23** as the protodeborylation product.

Computations showed that the 1,2-carboboration itself is concerted but highly asynchronous. The computed transition

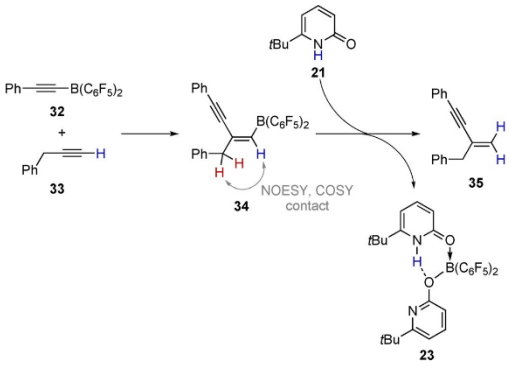

Scheme 17. 1,2-Carboboration of **33** by **32** and subsequent protodeborylation by the pyridone **21**.

state structure shows that the formation of the new C–B bond is more advanced than the formation of the new C–C bond (Figure 2).

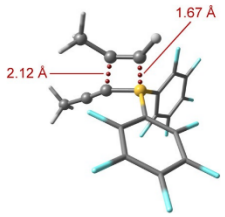

Figure 2. Computed transition state structure of the 1,2-carboboration with propyne as model substrate at PBE0(D3BJ)/def2-TZVP.[18]

Michael-addition of alkynylboranes to chalcones

Recently, Fountaine and co-workers reported the catalytic addition of *in situ* generated alkynylboranes to chalcones.[31] The active catalyst is formed by the transfer borylation of furanboronate **36** to the bifunctional mercaptoimidazole **37** (Scheme 18). The boronate moiety of **38** is transferred to a terminal alkyne (**39**), which changes the covalent N–B bond to a dative bond. This change to a dative bond enables the dissociation of the trivalent alkynylborane **40** and is thus essential for the observed reactivity. After dissociation, the free alkynylborane **40** adds to the chalcone[32] in a 1,4-addition, yielding the intermediary enolboronate **41**, which re-coordinates to imidazole **37**, yielding **42**. Protodeborylation liberates the product and regenerates the catalyst **38**. The scope was thoroughly investigated by using different alkynes and chalcone derivatives (Scheme 19). The authors demonstrated that this protocol can be transferred to different nitrogen- and sulfur-containing heterocycles as nucleophiles.

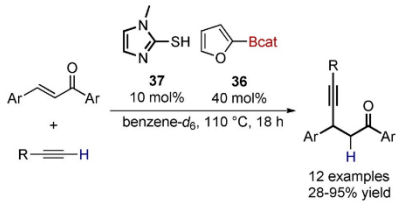

Scheme 19. Scope of the transfer borylation and the subsequent addition of alkynylboranes to chalcones.

Furthermore, potential deactivation pathways were investigated. By heating the catalyst **37** with trimethylsilylacetylene **43** and catecholboronate **36**, the formation of the boron-containing zwitterionic heterocycle **44**, which deactivates the catalyst, was observed (Scheme 20). The deactivation product is probably formed by thioboration of trimethylsilylacetylene by the *in situ* formed imidazole boronate **38**.

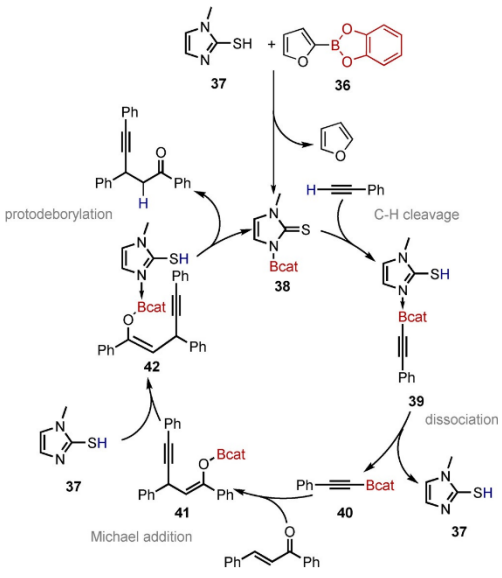

Scheme 18. Catalytic cycle of the transfer borylation, in situ formation of an alkynylborane and subsequent Michael addition to a chalcone.

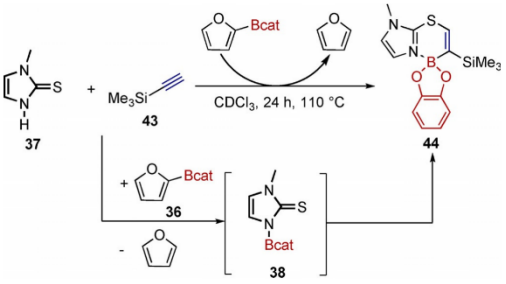

Scheme 20. Deactivation pathway of catalyst **37** by addition of trimethylsilylacetylene to imidazol boronate **38**.

Allylation of acetonitrile with in situ formed allylboranes

The allylation of electrophiles by allylboranes is an important and frequently used reaction in organic synthesis.[33,34] Brown and co-workers described the synthesis of such allylboranes by the hydroboration of allenes.[35] The approach for the synthesis of allylboranes by hydroboration of allenes in combination with BLC was used to realize a catalytic protocol for an allylation reaction requiring only catalytic amounts of an *in situ* formed allylation reagent (Scheme 21).[36] Hydrogen activation by the pyridonate borane **18′** forms the pyridone borane com-

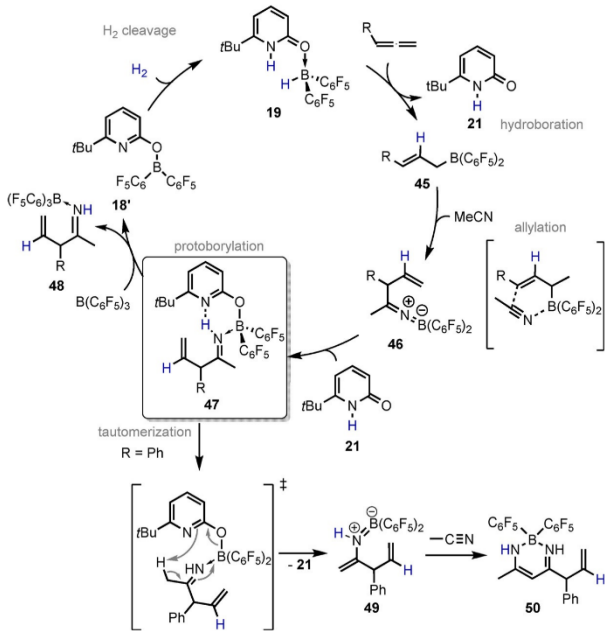

Scheme 21. Catalytic cycle of the allylation of nitriles by an in situ generated allylborane.

plex **19**, which dissociates into the pyridone **21** and Piers borane **22**. Adding an allene to the reaction mixture produces the allylborane **45**, which undergoes an allylation reaction with acetonitrile as electrophile yielding the ketiminoborane **46**. Re-coordination of the pyridone **21** to the ketiminoborane **46**, followed by a virtually barrierless proton transfer, affords complex **47** (gray rectangle in Scheme 21). This intermediate is critical for the outcome of the reaction because two different reaction paths can be observed. In the presence of $B(C_6F_5)_3$ (BCF) as an additional Lewis acid, the allylimine moiety of **47** can dissociate and form the kinetically stable complex **48** with BCF, while simultaneously catalyst **18′** is regenerated.

Without BCF, the pyridone moiety of **47** tautomerizes the allylimine to a nucleophilic enamineborane **49**, which dissociates and attacks a second equivalent of acetonitrile forming the β-diketiminate borane complex **50**. This prevents further catalytic reactivity because the $B(C_6F_5)_2$ moiety of catalyst **18′** is irreversible bound in **50**.

Both, the β-diketiminate borane **50** and the allylimine BCF complexes **48** are air- and moisture-stable and can be isolated by column chromatography in moderate to excellent yields (Scheme 22).

The formation of nucleophilic allylboranes from dihydrogen and allenes is a conceptually new way to use dihydrogen for organic synthesis.

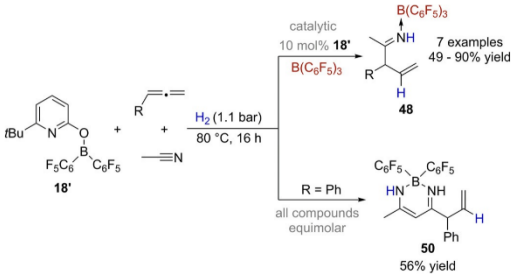

Scheme 22. Formation of the β-diketiminate borane **50** upon reaction of the pyridonate borane **18′** with an allene and acetonitrile under an H_2 atmosphere and the catalytic allylation of nitriles catalyzed by **18′** in the presence of BCF.

Transfer borylations

Fountaine and co-workers developed a catalytic protocol for the transfer borylation of 2-furylcatecholboran **36** to a wide range of heterocycles and terminal alkynes.[37,31] They developed two different types of catalysts (Scheme 23). The transfer borylation with the first catalyst—mercaptopyridine **51**—required relatively high catalyst loadings and five equivalents of the boron source catecholboronate **36** to borylate different N-, S-, and O-containing heterocycles.[37] The mercaptoimidazole **37** as the second catalyst generation was significantly more

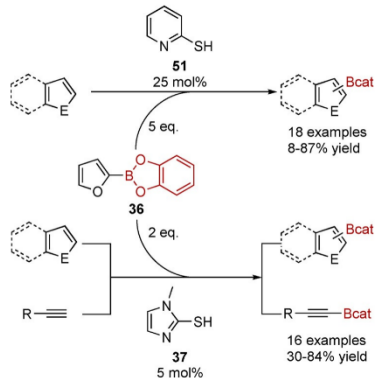

Scheme 23. Scope of the transfer borylation using **37** and **51**.

active.[31] The authors could show that they only needed 5 mol% catalyst loading to borylate the same heterocycles under milder conditions by using only two equivalents of catecholboronate **36**. Furthermore, by using **37** as the catalyst, they could expand the scope to terminal alkynes.

Both catalysts—mercaptopyridine **51** and mercaptoimidazole **37**—react through the same mechanism, which is in the following exemplified for **37** (Scheme 24). First, the nitrogen of the catalyst **37** coordinates to the catecholboronate, yielding **52**. In a protodeborylation, the boron moiety of the furan boronate **36** is transferred to the catalyst, yielding **38**. A concerted deprotonative borylation via $\mathbf{TS}_{38/37}$ transfers the boronate from the catalyst to the substrate. Here, the change from a covalent to dative N–B bond enables the dissociation of the product and regenerates the catalyst. This change of the bond mode can again be described as BLC.

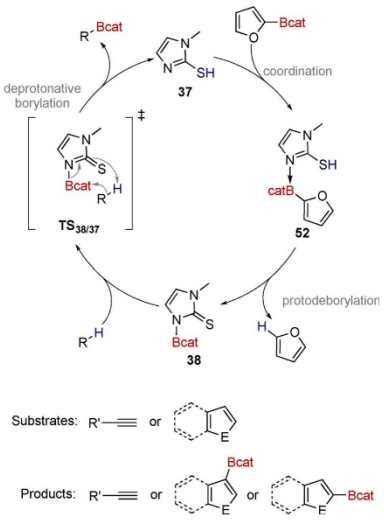

Scheme 24. Catalytic cycle of the transfer borylation.

Transfer hydrogenations with ammonia borane

Another example of BLC was presented in a series of publications on enantioselective transfer hydrogenations catalyzed by an FLP-type system by using ammonia borane as a hydrogen source. Du and co-workers showed that by using a catalytic amount of a chiral sulfinamide borane complex **53**, imines, indoles, enamines, and quinoxalines can be enantioselectively hydrogenated (Scheme 25).[38]

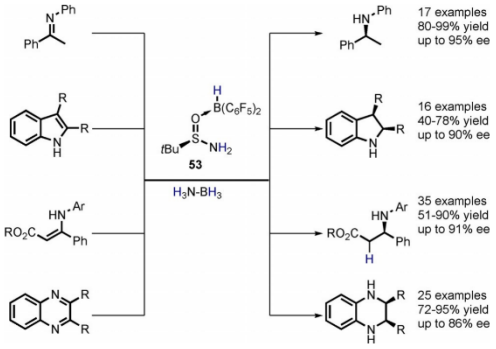

Scheme 25. Scope of the enantioselective transfer hydrogenation using **53** as the catalyst and ammonia borane as the hydrogen source.

Catalyst **53** is generated *in situ* by adding Piers borane **22** to the sulfinamide **54**. To assess the structure of the Lewis adduct formed in this way, the authors investigated the adduct formation of Piers borane **22** with all three Lewis basics sites of sulfinamide **54** computationally (Scheme 26). Based on these results, the authors concluded that the B–O coordinated form of **53** is the active catalyst.

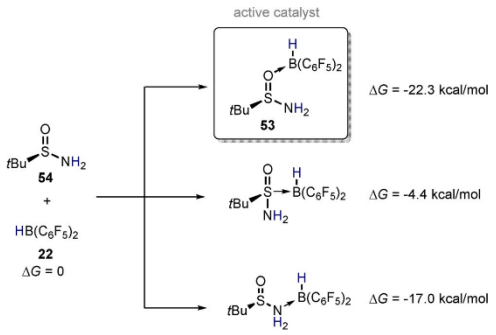

Scheme 26. Comparison of the different free complexation enthalpies of **54** and **22** computed at M06-2X/6-31G(d).[39] The PCM model for toluene was used to implicitly account for solvent effects.[40]

Mechanistic investigations revealed that the hydrogenation itself is a concerted transfer of the hydridic B–H and protic N–H of **53** to the respective substrate. However, according to DFT computations by the authors, the active species of the hydrogen transfer from the ammonia borane via $\mathbf{TS_{55/56}}$ is the sulfinamido borane **55** (Scheme 27). To regenerate the active catalyst **53**, the Piers borane moiety of **56** has to dissociate and recoordinate to the oxygen of the sulfinamide, which is only possible because of the change in bonding mode between boron and nitrogen in the course of the hydrogen transfer from the ammonia borane to **55**.

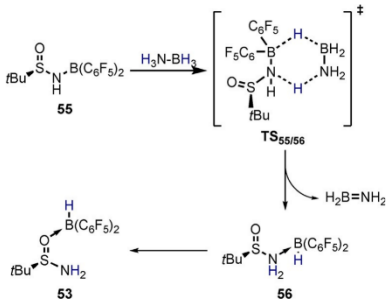

Scheme 27. Regeneration of the active catalyst **53** by hydrogen transfer from ammonia borane to sulfinamido borane **55**.

Summary and Outlook

We and others recently reported distinctive borane-based FLPs that can activate chemical bonds with a simultaneous change in the valence sphere of the borane. Specifically, the substituent at the borane that is involved in the bond activation becomes a datively bound ligand in a borane complex. To describe this mode of action, the term boron–ligand cooperation (BLC) was introduced. Within this Minireview, we provide criteria for BLC, framed in analogy to the criteria for MLC given by Khusnutdinova and Milstein. We furthermore discussed systems that fulfill these criteria. Although for some systems BLC is just a curiosity observed upon bond activation, certain systems provide access to the consequent reactivity, which can be used for novel catalytic reactions. Examples covered in this Minireview are hydroboration and 1,2-carboboration reactions or the metal-free transfer borylation for the synthesis of synthetically useful boronates. These reactivities rely on the presence of trivalent boranes formed upon dissociation of the respective borane complexes. As such a dissociation is not possible for classic intramolecular FLPs that form zwitterionic borates upon bond activation, BLC can complement the reactivity of classic FLPs. We hope that the discussion in this Minireview and the examples given stimulate the development of new metal-free catalysts.

Acknowledgments

This work was supported by the FCI (Liebig Fellowship to U.G.) and the DFG (Emmy-Noether program, GE 3117/1-1). Continuous support by Prof. Dr. P. R. Schreiner, Prof. Dr. R. Göttlich, and Prof. Dr. H. A. Wegner is acknowledged. Open access funding enabled and organized by Projekt DEAL.

Conflict of interest

The authors declare no conflict of interest.

Keywords: bond activation · boron–ligand cooperation · dissociation · frustrated Lewis pair · homogeneous catalysis

[1] a) R. Noyori, T. Ohkuma, *Angew. Chem. Int. Ed.* **2001**, *40*, 40–73; *Angew. Chem.* **2001**, *113*, 40–75; b) T. Ohkuma, H. Ooka, S. Hashiguchi, T. Ikariya, R. Noyori, *J. Am. Chem. Soc.* **1995**, *117*, 2675–2676; c) P. A. Dub, J. C. Gordon, *Nat. Rev. Chem.* **2018**, *2*, 396–408.
[2] a) J. Zhang, G. Leitus, Y. Ben-David, D. Milstein, *J. Am. Chem. Soc.* **2005**, *127*, 10840–10841; b) C. Gunanathan, D. Milstein, *Acc. Chem. Res.* **2011**, *44*, 588–602; c) D. Milstein, *Philos. T. R. Soc. A* **2015**, *373*, 20140189.
[3] J. R. Khusnutdinova, D. Milstein, *Angew. Chem. Int. Ed.* **2015**, *54*, 12236–12273; *Angew. Chem.* **2015**, *127*, 12406–12445.
[4] R. H. Crabtree, *The Organometallic Chemistry of the Transition Metals*, 4th ed., Wiley, New York, **2005**, pp. 32–35.
[5] For examples of bond activation by intramolecular boron-based FLPs, see: a) G. C. Welch, R. R. S. Juan, J. D. Masuda, D. W. Stephan, *Science* **2006**, *314*, 1124; b) P. Spies, G. Erker, G. Kehr, K. Bergander, R. Fröhlich, S. Grimme, D. W. Stephan, *Chem. Commun.* **2007**, 5072; c) Z. Jian, G. Kehr, C. G. Daniliuc, B. Wibbeling, G. Erker, *Dalton Trans.* **2017**, *46*, 11715; d) K. Chernichenko, M. Nieger, M. Leskelä, T. Repo, *Dalton Trans.* **2012**, *41*, 9029; e) K. Chernichenko, B. Kótai, I. Pápai, V. Zhivonitko, M. Nieger, M. Leskelä, T. Repo, *Angew. Chem. Int. Ed.* **2015**, *54*, 1749; *Angew. Chem.* **2015**, *127*, 1769; f) M.-A. Légaré, M.-A. Courtemanche, É. Rochette, F.-G. Fontaine, *Science* **2015**, *349*, 513; g) C. M. Mömming, E. Otten, G. Kehr, R. Fröhlich, S. Grimme, D. W. Stephan, G. Erker, *Angew. Chem. Int. Ed.* **2009**, *48*, 6643; *Angew. Chem.* **2009**, *121*, 6770; h) Z. Mo, E. L. Kolychev, A. Rit, J. Campos, H. Niu, S. Aldridge, *J. Am. Chem. Soc.* **2015**, *137*, 12227.
[6] For recent reviews about FLPs, see: a) J. Lam, K. M. Szkop, E. Mosaferi, D. W. Stephan, *Chem. Soc. Rev.* **2019**, *48*, 3592; b) D. W. Stephan, *J. Am. Chem. Soc.* **2015**, *137*, 10018; c) D. W. Stephan, *Org. Biomol. Chem.* **2012**, *10*, 5740; d) D. W. Stephan, *Science* **2016**, *354*, aaf7229; e) D. W. Stephan, G. Erker, *Chem. Sci.* **2014**, *5*, 2625; f) D. W. Stephan, G. Erker, *Angew. Chem. Int. Ed.* **2015**, *54*, 6400; *Angew. Chem.* **2015**, *127*, 6498; g) D. W. Stephan, S. Greenberg, T. W. Graham, P. Chase, J. J. Hastie, S. J. Geier, J. M. Farrell, C. C. Brown, Z. M. Heiden, G. C. Welch, M. Ullrich, *Inorg. Chem.* **2011**, *50*, 12338; h) J. Paradies, *Eur. J. Org. Chem.* **2019**, 283.
[7] a) L. Greb, F. Ebner, Y. Ginzburg, L. M. Sigmund, *Eur. J. Inorg. Chem.* **2020**, 3030; b) E. R. M. Habraken, A. R. Jupp, M. B. Brands, M. Nieger, A. W. Ehlers, J. C. Slootweg, *Eur. J. Inorg. Chem.* **2019**, 2436.
[8] E. Theuergarten, D. Schluns, J. Grunenberg, C. G. Daniliuc, P. G. Jones, M. Tamm, *Chem. Commun.* **2010**, *46*, 8561.
[9] E. Theuergarten, J. Schlösser, D. Schlüns, M. Freytag, C. G. Daniliuc, P. G. Jones, M. Tamm, *Dalton Trans.* **2012**, *41*, 9101.
[10] G. Lu, H. Li, L. Zhao, F. Huang, P. von R. Schleyer, Z.-X. Wang, *Chem. Eur. J.* **2011**, *17*, 2038.
[11] P. v. R. Schleyer, C. Maerker, A. Dransfeld, H. Jiao, N. J. R. van Eikema Hommes, *J. Am. Chem. Soc.* **1996**, *118*, 6317.
[12] U. Gellrich, Y. Diskin-Posner, L. J. W. Shimon, D. Milstein, *J. Am. Chem. Soc.* **2016**, *138*, 13307.
[13] U. Gellrich, *Angew. Chem. Int. Ed.* **2018**, *57*, 4779; *Angew. Chem.* **2018**, *130*, 4869.
[14] A. R. Katritzky, R. A. Jones, *J. Am. Chem. Soc.* **1960**, *82*, 2947.

[15] J. I. Wu, J. E. Jackson, P. von R. Schleyer, *J. Am. Chem. Soc.* **2014**, *136*, 13526.
[16] R. J. Gillespie, E. A. Robinson, *Angew. Chem. Int. Ed. Engl.* **1996**, *35*, 495; *Angew. Chem.* **1996**, *108*, 539.
[17] M. Ghara, S. Pan, P. K. Chattaraj, *Phys. Chem. Chem. Phys.* **2019**, *21*, 21267.
[18] a) J. P. Perdew, K. Burke, M. Ernzerhof, *Phys. Rev. Lett.* **1996**, *77*, 3865; b) C. Adamo, V. Barone, *J. Chem. Phys.* **1999**, *110*, 6158; c) S. Grimme, S. Ehrlich, L. Goerigk, *J. Comput. Chem.* **2011**, *32*, 1456; d) F. Weigend, R. Ahlrichs, *Phys. Chem. Chem. Phys.* **2005**, *7*, 3297.
[19] V. I. Minkin, *Pure Appl. Chem.* **1999**, *71*, 1919.
[20] F. Wech, M. Hasenbeck, U. Gellrich, *Chem. Eur. J.* **2020**, *26*, 13445.
[21] K. Chernichenko, Á. Madarász, I. Pápai, M. Nieger, M. Leskelä, T. Repo, *Nat. Chem.* **2013**, *5*, 718.
[22] For examples of alkyne hydrogenation with FLPs operating under a different mechanism, see: a) Y. Liu, L. Hu, H. Chen, H. Du, *Chem. Eur. J.* **2015**, *21*, 3495; b) K. C. Szeto, W. Sahyoun, N. Merle, J. L. Castelbou, N. Popoff, F. Lefebvre, J. Raynaud, C. Godard, C. Claver, L. Delevoye, R. M. Gauvin, M. Taoufik, *Catal. Sci. Technol.* **2016**, *6*, 882; c) J. L. Fiorio, N. López, L. M. Rossi, *ACS Catal.* **2017**, *7*, 2973; d) J. L. Fiorio, R. V. Gonçalves, E. Teixeira-Neto, M. A. Ortuño, N. López, L. M. Rossi, *ACS Catal.* **2018**, *8*, 3516-.
[23] T. Müller, M. Hasenbeck, J. Becker, U. Gellrich, *Eur. J. Org. Chem.* **2019**, 451.
[24] a) S. Kozuch, S. Shaik, *J. Am. Chem. Soc.* **2006**, *128*, 3355; b) S. Kozuch, S. Shaik, *Acc. Chem. Res.* **2011**, *44*, 101.
[25] a) G. Santra, N. Sylvetsky, J. M. L. Martin, *J. Phys. Chem. A* **2019**, *123*, 5129; b) E. Caldeweyher, C. Bannwarth, S. Grimme, *J. Chem. Phys.* **2017**, *147*, 034112; c) E. Caldeweyher, S. Ehlert, A. Hansen, H. Neugebauer, S. Spicher, C. Bannwarth, S. Grimme, *J. Chem. Phys.* **2019**, *150*, 154122; d) A. Hellweg, C. Hattig, S. Hofener, W. Klopper, *Theor. Chem. Acc.* **2007**, *117*, 587; e) F. Weigend, *J. Comput. Chem.* **2008**, *29*, 167; f) S. Grimme, J. G. Brandenburg, C. Bannwarth, A. Hansen, *J. Chem. Phys.* **2015**, *143*, 054107; g) H. Kruse, S. Grimme, *J. Chem. Phys.* **2012**, *136*, 154101; h) S. Grimme, J. Antony, S. Ehrlich, H. Krieg, *J. Chem. Phys.* **2010**, *132*, 154104; i) F. Weigend, *Phys. Chem. Chem. Phys.* **2006**, *8*, 1057.
[26] A. V. Marenich, C. J. Cramer, D. G. Truhlar, *J. Phys. Chem. B* **2009**, *113*, 6378.
[27] For examples of reactions of borane-based FLPs with terminal alkynes, see: a) M. A. Dureen, C. C. Brown, D. W. Stephan, *Organometallics* **2010**, *29*, 6594; b) M. A. Dureen, D. W. Stephan, *J. Am. Chem. Soc.* **2009**, *131*, 8396; c) C. Jiang, O. Blacque, H. Berke, *Organometallics* **2010**, *29*, 125; d) C. M. Mömming, G. Kehr, B. Wibbeling, R. Fröhlich, B. Schirmer, S. Grimme, G. Erker, *Angew. Chem. Int. Ed.* **2010**, *49*, 2414; *Angew. Chem.* **2010**, *122*, 2464; e) T. Voss, T. Mahdi, E. Otten, R. Fröhlich, G. Kehr, D. W. Stephan, G. Erker, *Organometallics* **2012**, *31*, 2367.
[28] M. Hasenbeck, T. Müller, U. Gellrich, *Catal. Sci. Technol.* **2019**, *9*, 2438.
[29] For different examples of 1,2-carboboration reactions, see: a) M. Devillard, R. Brousses, K. Miqueu, G. Bouhadir, D. Bourissou, *Angew. Chem. Int. Ed.* **2015**, *54*, 5722; *Angew. Chem.* **2015**, *127*, 5814; b) I. A. Cade, M. J. Ingleson, *Chem. Eur. J.* **2014**, *20*, 12874; c) Y. Shoji, N. Tanaka, S. Muranaka, N. Shigeno, H. Sugiyama, K. Takenouchi, F. Hajjaj, T. Fukushima, *Nat. Commun.* **2016**, *7*, 12704; d) M. F. Lappert, B. Prokai, *J. Organomet. Chem.* **1964**, *1*, 384; e) Y. Cheng, C. Mück-Lichtenfeld, A. Studer, *J. Am. Chem. Soc.* **2018**, *140*, 6221.
[30] a) C. Riplinger, B. Sandhoefer, A. Hansen, F. Neese, *J. Chem. Phys.* **2013**, *139*, 134101; b) F. Neese, *WIREs Comput. Mol. Sci.* **2012**, *2*, 73.
[31] V. Desrosiers, C. Z. Garcia, F.-G. Fontaine, *ACS Catal.* **2020**, *10*, 11046.
[32] T. R. Wu, J. M. Chong, *J. Am. Chem. Soc.* **2005**, *127*, 3244.
[33] W. R. Roush, *Comprehensive Organic Synthesis, Vol. 2* (Eds.: B. M. Trost, I. Fleming), Pergamon, New York, **1991**, pp. 1 – 53.
[34] a) H. C. Brown, P. K. Jadhav, *J. Am. Chem. Soc.* **1983**, *105*, 2092; b) H. C. Brown, K. S. Bhat, *J. Am. Chem. Soc.* **1986**, *108*, 5919; c) U. S. Racherla, H. C. Brown, *J. Org. Chem.* **1991**, *56*, 401; d) W. R. Roush, A. D. Palkowitz, K. Ando, *J. Am. Chem. Soc.* **1990**, *112*, 6348.
[35] G. W. Kramer, H. C. Brown, *J. Organomet. Chem.* **1977**, *132*, 9.
[36] M. Hasenbeck, S. Ahles, A. Averdunk, J. Becker, U. Gellrich, *Angew. Chem. Int. Ed.* **2020**, *59*, 23885; *Angew. Chem.* **2020**, *132*, 24095.
[37] É. Rochette, V. Desrosiers, Y. Soltani, F.-G. Fontaine, *J. Am. Chem. Soc.* **2019**, *141*, 12305.
[38] a) W. Zhao, Z. Zhang, X. Feng, J. Yang, H. Du, *Org. Lett.* **2020**, *22*, 5850; b) S. Li, W. Meng, H. Du, *Org. Lett.* **2017**, *19*, 2604; c) S. Li, G. Li, W. Meng, H. Du, *J. Am. Chem. Soc.* **2016**, *138*, 12956; d) W. Zhao, X. Feng, J. Yang, H. Du, *Tetrahedron Lett.* **2019**, *60*, 1193.
[39] a) Y. Zhao, D. G. Truhlar, *Acc. Chem. Res.* **2008**, *41*, 157; b) Y. Zhao, D. G. Truhlar, *Theor. Chem. Acc.* **2008**, *120*, 215; c) R. Ditchfield, W. J. Hehre, J. A. Pople, *J. Chem. Phys.* **1971**, *54*, 724; d) W. J. Hehre, R. Ditchfield, J. A. Pople, *J. Chem. Phys.* **1972**, *56*, 2257.
[40] G. Scalmani, M. J. Frisch, *J. Chem. Phys.* **2010**, *132*, 114110.

Manuscript received: October 13, 2020
Revised manuscript received: December 2, 2020
Accepted manuscript online: December 9, 2020
Version of record online: January 28, 2021

5.7 Indene formation upon borane-induced cyclization of arylallenes, 1,1-carboboration, and retro-hydroboration

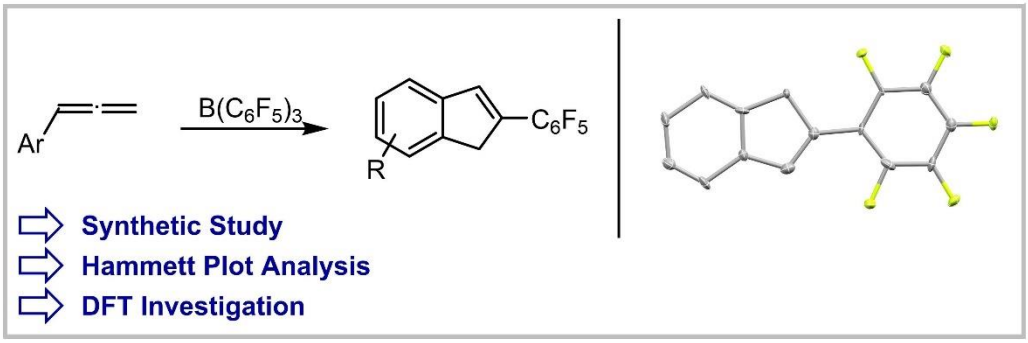

The formation of pentafluorophenyl indenes upon reaction of arylallenes with B(C6F5)3 is reported. Key steps are a 1,1-carboboration and a retrohydroboration.

Max Hasenbeck, Felix Wech, Arthur Averdunk, Dr. Jonathan Becker, Dr. Urs Gellrich

Chem. Commun. **2021**, *57*, 5518-5521

DOI (englische Version): 10.1039/D1CC01750K

Final veröffentlichte Version online: 29.04.2021

ChemComm

COMMUNICATION

View Article Online
View Journal | View Issue

Cite this: *Chem. Commun.*, 2021, **57**, 5518

Received 2nd April 2021,
Accepted 29th April 2021

DOI: 10.1039/d1cc01750k

rsc.li/chemcomm

Indene formation upon borane-induced cyclization of arylallenes, 1,1-carboboration, and retro-hydroboration†

Max Hasenbeck,[a] Felix Wech,[a] Arthur Averdunk,[a] Jonathan Becker[b] and Urs Gellrich *[a]

We herein report the reaction of arylallenes with tris(pentafluorophenyl)borane that yields pentafluorophenyl substituted indenes. The tris(pentafluorophenyl)borane induces the cyclization of the allene and transfers a pentafluorophenyl ring in the course of this reaction. A Hammett plot analysis and DFT computations indicate a 1,1-carboboration to be the C–C bond-forming step.

In 2010, Erker and co-workers reported that the reaction of the strongly Lewis acidic tris(pentafluorophenyl)borane ($B(C_6F_5)_3$) with terminal alkynes leads to a 1,1-carboboration of the alkyne.[1] The substrate scope of the 1,1-carboboration was extended to phosphinyl substituted alkynes, yielding alkenyl-bridged frustrated Lewis pairs.[2] Furthermore, the 1,1-carboboration of internal alkynes with concomitant C–C cleavage was demonstrated.[3,4] More recently, Melen *et al.* reported the 1,2-carboboration of allenyl ketones.[5]

We found now that the reaction of $B(C_6F_5)_3$ with phenylallene **1** leads to the formation of the pentafluorophenyl-substituted indene **2** (Scheme 1).[6] Our initial finding was that the addition of **1** to a solution of $B(C_6F_5)_3$ in dichloromethane-d_2 (DCM-d_2) leads to the formation of indene **2** in 48% NMR-yield within 45 minutes (Scheme 2).

Hence, the $B(C_6F_5)_3$ induces a ring closure and transfers a pentafluorophenyl ring to the allene.[7] As a side product of this reaction, we observed the allylborane **3** that is likely formed by hydroboration of the phenylallene **1**.[8] Besides, minor amounts of a vinylborane, originating from the hydroboration of the internal double bond, and a 2-boryl-hexa-1,5-dien, formed by Piers' borane induced dimerization of the allene, were detected (for details, see the ESI†). The detection of **3** gives a direct hint to the intermediate formation of Piers' borane $HB(C_6F_5)_2$ in the course of the reaction.[9] Accordingly, the reaction constitutes a formal exchange of a pentafluorophenyl group of the $B(C_6F_5)_3$ with hydrogen. The reaction was subsequently performed on a preparative scale and the indene **2** was isolated and fully characterized. The structural assignment is further supported by SCXRD (Scheme 2). We then investigated the scope of this transformation by reacting different aryl allenes with $B(C_6F_5)_3$. As the hydroboration observed in the initial experiment consumes some of the allene, these reactions were performed with two equivalents of the allene. Under these conditions, **2** was isolated in 68% yield with respect to $B(C_6F_5)_3$, the limiting reagent (Scheme 3). The same reaction with one equivalent phenylallene and norbornene as sacrificial olefine to capture Piers' borane yielded **2** in 58% yield. The benzindene **4** is obtained in 65% yield from the reaction of 1-naphthylallene with $B(C_6F_5)_3$. However, it was isolated as a mixture of isomers that differ regarding the position of the benzylic double bond. Likewise, the reaction of *p*-tolylallene and *p*-(isopropyl)phenylallene gives the indenes **5** and **6** as a mixture of regioisomers.

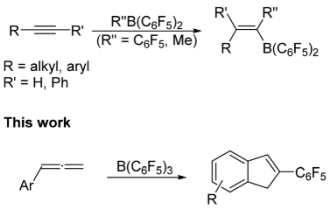

Scheme 1 The context of this work: the 1,1-carboboration of alkynes described by Erker and the borane-induced ring closure with concomitant aryl group transfer described herein.

[a] *Institut für Organische Chemie, Justus-Liebig-Universität Gießen, Heinrich-Buff-Ring 17, 35392 Gießen, Germany. E-mail: urs.gellrich@org.chemie.uni-giessen.de*
[b] *Institut für Analytische und Anorganische Chemie, Justus-Liebig-Universität Gießen, Heinrich-Buff-Ring 17, Gießen 35392, Germany*

† Electronic supplementary information (ESI) available: Experimental and computational details, spectroscopic and crystallographic data, copies of NMR spectra. CCDC 2059168. For ESI and crystallographic data in CIF or other electronic format see DOI: 10.1039/d1cc01750k

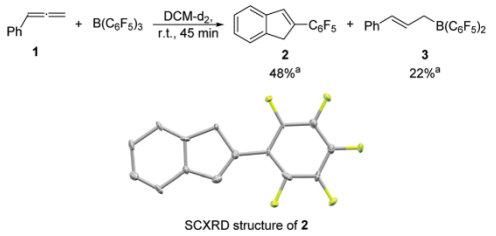

Scheme 2 Formation of the pentafluorophenyl-substituted indene **2** upon the reaction of **1** with $B(C_6F_5)_3$. [a]Yields determined by qNMR with 1,3,5-trimethoxybenzene as internal standard. The inset shows the molecular structure of **2** derived from SCXRD (50% probability ellipsoids, all hydrogen atoms are omitted for clarity).

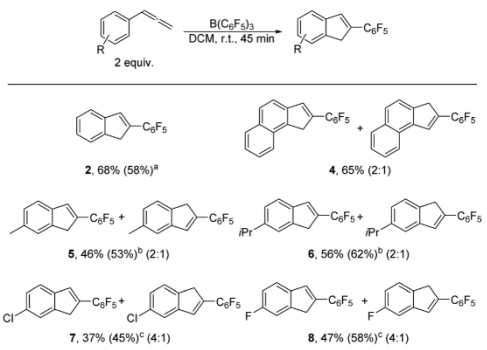

Scheme 3 Scope of the $B(C_6F_5)_3$ mediated formation of indenes from allenes. Yields of products isolated by column chromatography are given. (a) With one equivalent phenylallene and one equivalent norbornene. (b) Reaction temperature 0 °C. (c) Oil bath temperature 60 °C.

A better yield was obtained when the reactions with these substrates were run at 0 °C, presumably because of side reactions at r.t. In contrast, the reactions with *p*-(chloro)phenylallene and *p*-(fluoro)phenylallene required an elevated reaction temperature to give **7** and **8** in moderate yields. These findings indicate that electron-rich arylallenes undergo a faster cyclization whereas electron-withdrawing substituents slow down the reaction.

The effect of the substituents on the phenyl ring on the reaction rate was further assessed by a Hammett analysis (Fig. 1).[10] The negative slope of the Hammett plot and the rho value of -3.9 ± 0.7 indicate that in the rate-determining transition state of this reaction positive charge is built up in the benzylic position of the arylallene.

The increased reactivity of electron-rich allenes was used for a cyclization with a less Lewis acidic borane. The reaction of *p*-(isopropyl)phenylallene with $MeB(C_6F_5)_2$ leads to cyclization of the allene and transfer of the methyl group (Scheme 4). However, the formation of methylindene **9** required a prolonged reaction time.

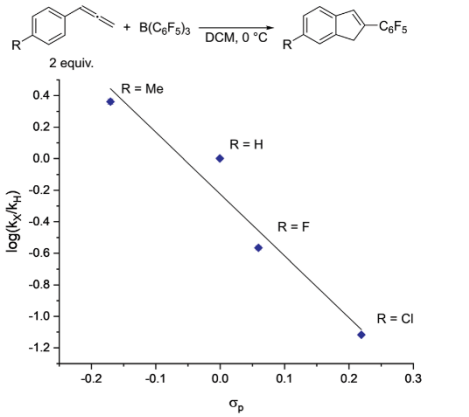

Fig. 1 Hammett plot analysis of the $B(C_6F_5)_3$- mediated formation of indenes from aryl allenes. Note that only the major isomer is shown in the scheme.

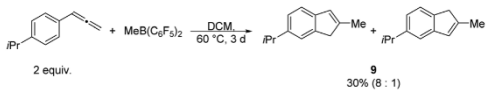

Scheme 4 Formation of the methyl indene 9 upon reaction of *p*-(isopropyl)phenylallene with $MeB(C_6F_5)_2$.

The mechanism of the $B(C_6F_5)_3$-mediated indene formation was further investigated computationally by DFT at the revDSD-PBEP86-D4/def2-QZVPP//PBEh-3c level of theory (Fig. 2).[11–13] As zwitterionic intermediates are likely involved in the reaction, the SMD solvent model for DCM was used for the structure optimizations and the single point computations.[14] We assume that the reaction commences with the addition of $B(C_6F_5)_3$ to the π-system of **1**. This step yields the zwitterion **INT-1**. The positive charge in this intermediate is stabilized by allyl and benzyl resonance. An intramolecular Friedel–Crafts alkylation *via* **TS-2** closes the five-membered ring of the indene core. We further assume that an intermolecular proton shift leads to a re-aromatization and the intermediate **INT-3** (Scheme 5). However, all attempts to optimize the structure of **INT-3** resulted in a pentafluorophenyl transfer and lead to **INT-4**. Relaxed potential energy surface scans further showed that the pentafluorophenyl transfer is a barrierless process. This finding agrees with computational studies of the 1,1-carboboration of alkynes by Erker, Grimme, and co-workers that showed that once a carbocation is formed in α-position to the $B(C_6F_5)_3$ moiety, the pentafluorophenyl transfer is barrierless.

A retro-hydroboration, *i.e.* the liberation of $HB(C_6F_5)_2$ from **Int-4**, forms product **2**. According to the computations, this step requires only a moderate activation energy of 16.7 kcal mol^{-1}. Notably, the retro-hydroboration is computed to be exergonic by 2.2 kcal mol^{-1}. According to the computations, **TS-1**, the

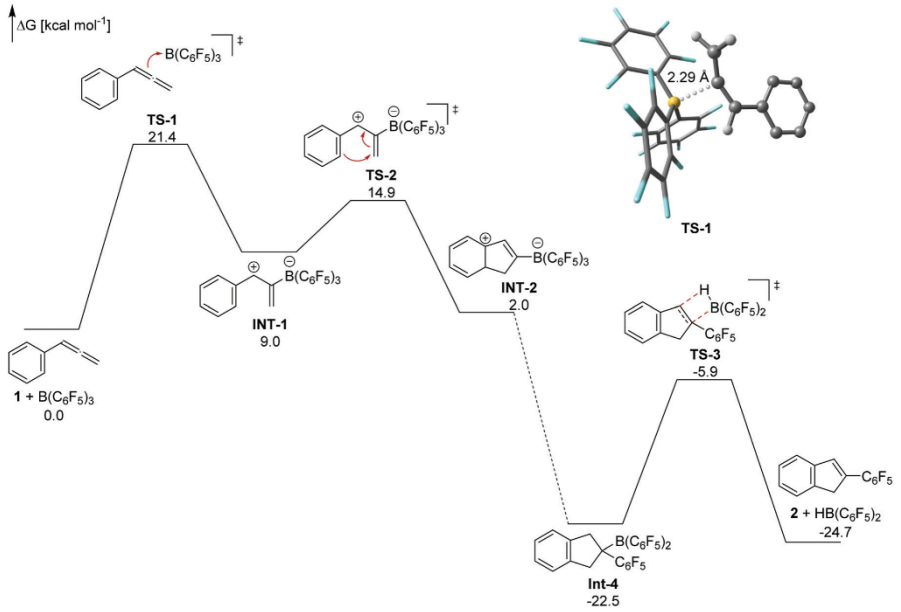

Fig. 2 Gibbs free energies of the $B(C_6F_5)_3$-mediated indene formation computed at the revDSD-PBEP86-D4/def2-QZVPP//PBEh-3c level of theory. The SMD solvent model for DCM was used for the structure optimizations and the single point computations. The inset shows the optimized structure of **TS-1**.

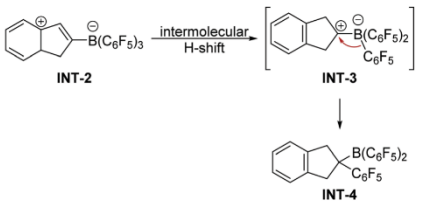

Scheme 5 Proposed mechanism for the pentafluorophenyl transfer.

addition of the phenyl allene to $B(C_6F_5)_3$, is the rate-determining transition state. In this transition state, a positive charge is built up in the benzylic position that is stabilized by electron-donating groups in the para position. Thus, the computations are in favorable agreement with the Hammett analysis. In summary, we have documented that the reaction of arylallenes with $B(C_6F_5)_3$ leads to pentafluorophenyl substituted indenes. A plausible mechanistic scenario consists of a $B(C_6F_5)_3$-induced cyclization, a pentafluorophenyl transfer, and a retro-hydroboration. This reaction is a rare example of a metal-free C_{sp^2}–C_{sp^2} bond formation.[15] The results reported herein might inspire the development of synthetic methods that rely on 1,1-carboboration and retro-hydroboration reactions.

We thank the German research foundation (DFG) for financial support (GE 3117/1-1).

Conflicts of interest

There are no conflicts to declare.

Notes and references

1 (*a*) C. Chen, F. Eweiner, B. Wibbeling, R. Fröhlich, S. Senda, Y. Ohki, K. Tatsumi, S. Grimme, G. Kehr and G. Erker, *Chem. – Asian J.*, 2010, **5**, 2199–2208; (*b*) C. Chen, T. Voss, R. Fröhlich, G. Kehr and G. Erker, *Org. Lett.*, 2011, **13**, 62–65; (*c*) B.-H. Xu, G. Kehr, R. Fröhlich, B. Wibbeling, B. Schirmer, S. Grimme and G. Erker, *Angew. Chem., Int. Ed.*, 2011, **50**, 7183–7186; (*d*) R. Liedtke, R. Fröhlich, G. Kehr and G. Erker, *Organometallics*, 2011, **30**, 5222–5232; (*e*) C. Chen, R. Fröhlich, G. Kehr and G. Erker, *Chem. Commun.*, 2010, **46**, 3580–3582.

2 (*a*) O. Ekkert, R. Fröhlich, G. Kehr and G. Erker, *J. Am. Chem. Soc.*, 2011, **133**, 4610–4616; (*b*) O. Ekkert, G. Kehr, R. Fröhlich and G. Erker, *Chem. Commun.*, 2011, **47**, 10482–10484.

3 (*a*) B.-H. Xu, G. Kehr, R. Fröhlich, S. Grimme and G. Erker, *J. Am. Chem. Soc.*, 2011, **113**, 3480–3491; (*b*) C. Chen, G. Kehr, R. Fröhlich and G. Erker, *J. Am. Chem. Soc.*, 2010, **132**, 13594–13595.

4 For a recent review on 1,1-carboboration reactions see: G. Kehr and G. Erker, *Chem. Commun.*, 2012, **48**, 1839–1850.

5 R. L. Melen, L. C. Wilkins, B. M. Kariuki, H. Wadepohl, L. H. Gade, A. S. K. Hashmi, D. W. Stephan and M. M. Hansmann, *Organometallics*, 2015, **34**, 4127–4137.

6 Upon hydrogenation of tetraphenylallene with a frustrated Lewis pair consisting of $PhNMe_2$ and $B(C_6F_5)_3$ Alcarazo and co-workers observed cyclization of the allene as side reaction. However, no

carboboration was reported: B. Inés, D. Palomas, S. Holle, S. Steinberg, J. A. Nicasio and M. Alcarazo, *Angew. Chem., Int. Ed.*, 2012, **51**, 12367–12369.

7 The formation of 2-borylindenes upon the reaction of arylallenes with $ClB(C_6F_5)_2$ and $BrB(C_6F_5)_2$ was reported: X. Tao, C. G. Daniliuc, K. Soloviova, C. A. Strassert, G. Kehra and G. Erker, *Chem. Commun.*, 2019, **55**, 10166–10169.

8 (*a*) X. Tao, C. G. Daniliuc, D. Dittrich, G. Kehr and G. Erker, *Angew. Chem., Int. Ed.*, 2018, **57**, 13922–13926; (*b*) M. Hasenbeck, S. Ahles, A. Averdunk and U. Gellrich, *Angew. Chem., Int. Ed.*, 2020, **59**, 23885–23891.

9 (*a*) D. J. Parks, R. E. von, H. Spence and W. E. Piers, *Angew. Chem., Int. Ed. Engl.*, 1995, **34**, 809–811; (*b*) E. A. Patrick and W. E. Piers, *Chem. Commun.*, 2020, **56**, 841–853.

10 L. P. Hammett, *J. Am. Chem. Soc.*, 1937, **59**, 96–103.

11 (*a*) G. Santra, N. Sylvetsky and J. M. L. Martin, *J. Phys. Chem. A*, 2019, **123**, 5129–5143; (*b*) E. Caldeweyher, C. Bannwarth and S. Grimme, *J. Chem. Phys.*, 2017, **147**, 034112; (*c*) E. Caldeweyher, S. Ehlert, A. Hansen, H. Neugebauer, S. Spicher, C. Bannwarth and S. Grimme, *J. Chem. Phys.*, 2019, **150**, 154122; (*d*) F. Weigend and R. Ahlrichs, *Phys. Chem. Chem. Phys.*, 2005, **7**, 3297–3305; (*e*) A. Hellweg, C. Hattig, S. Hofener and W. Klopper, *Theor. Chem. Acc.*, 2007, **117**, 587–597; (*f*) F. Weigend, *J. Comput. Chem.*, 2008, **29**, 167–175.

12 (*a*) S. Grimme, J. G. Brandenburg, C. Bannwarth and A. Hansen, *J. Chem. Phys.*, 2015, **143**, 054107; (*b*) H. Kruse and S. Grimme, *J. Chem. Phys.*, 2012, **136**, 154101; (*c*) S. Grimme, S. Ehrlich and L. Goerigk, *J. Comput. Chem.*, 2011, **32**, 1456–1465; (*d*) S. Grimme, J. Antony, S. Ehrlich and H. Krieg, *J. Chem. Phys.*, 2010, **132**, 154104; (*e*) F. Weigend, *Phys. Chem. Chem. Phys.*, 2006, **8**, 1057–1065.

13 All computations were performed with the ORCA program package, Version 4.2.1: (*a*) F. Neese, *Wiley Interdiscip. Rev.: Comput. Mol. Sci.*, 2012, **2**, 73–78; (*b*) F. Neese, *Wiley Interdiscip. Rev.: Comput. Mol. Sci.*, 2018, **8**, e1327.

14 A. V. Marenich, C. J. Cramer and D. G. Truhlar, *J. Phys. Chem. B*, 2009, **113**, 6378–6396.

15 A. Music, A. N. Baumann, P. Spieß, A. Plantefol, T. C. Jagau and D. Didier, *J. Am. Chem. Soc.*, 2020, **142**, 4341–4348.

5.8 Piers′ Borane-Induced Tetramerization of Arylacetylenes

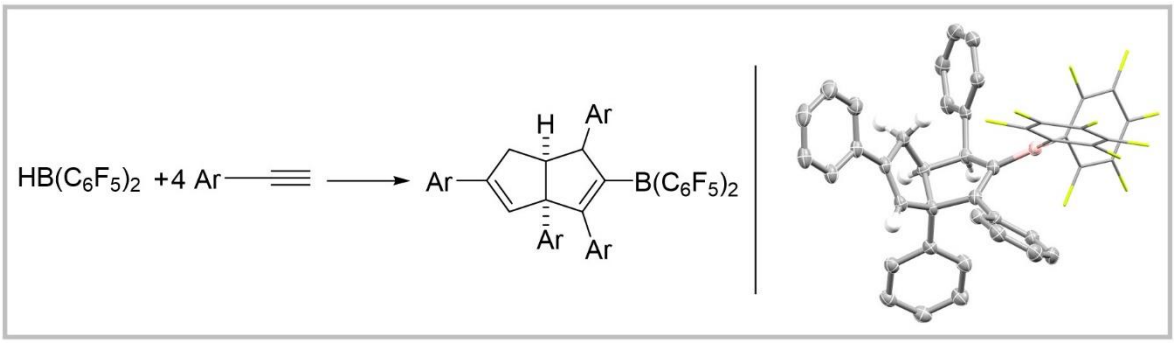

The formation of tetra-aryl-tetrahydropentalenes upon the reaction of arylacetylenes with Piers' borane ($HB(C_6F_5)_2$) is reported. Isotope labeling experiments and DFT computations indicate that the mechanism of this complex transformation commences with a series of unprecedented 1,2-carboborations, followed by an electrocyclization and two skeletal rearrangements.

Max Hasenbeck, Tizian Müller, Arthur Averdunk, Dr. Jonathan Becker, Dr. Urs Gellrich

Chem. Eur. J. **2022**, *28*, e202104254

DOI (englische Version): 10.1002/chem.202104254

Akzeptiertes Manuskript online: 09.12.2021

Final veröffentlichte Version online: 28.12.2021

Chemistry–A European Journal
Research Article
doi.org/10.1002/chem.202104254
Chemistry Europe
European Chemical Societies Publishing
www.chemeurj.org

Piers' Borane-Induced Tetramerization of Arylacetylenes

Max Hasenbeck,[a] Tizian Müller,[a] Arthur Averdunk,[a] Jonathan Becker,[b] and Urs Gellrich*[a]

Abstract: We herein report that the reaction of Piers' borane, *i.e.* $HB(C_6F_5)_2$, with an excess of arylacetylenes at room temperature leads to tetramerization of the acetylene and the diastereoselective formation of boryl-substituted tetra-aryl-tetrahydropentalenes. The reaction mechanism was investigated by isotope labeling experiments and DFT computations. These investigations indicate that a series of 1,2-carboboration reactions form an octatetraene that undergoes an electrocyclization. Two skeletal rearrangements then presumably lead to the formation of the tetrahydropentalene core. Overall, this intricate and unprecedented transformation comprises five carbon-carbon bond formations in a single reaction.

Building molecular complexity from simple starting materials is paramount for synthetic chemistry. Boranes are in this context usually considered as reagents for transition metal-catalyzed C–C and C-Het couplings.[1,2] However, transformations of organic molecules, including skeletal rearrangements and C–C bond formations induced by highly Lewis acidic boranes have been reported recently. Prime examples are the 1,1-carboborations of alkynes and aryl allenes by tris(perfluoro)phenylborane (BCF).[3,4] Furthermore, the Piers' borane-induced catalytic trimerization of alkyl allenes and the dimerization of aryl allenes were reported by Erker and co-workers.[5] These reactions are initiated by the hydroboration of the allene. When introducing $HB(C_6F_5)_2$ as a highly electrophilic borane reagent in 1995, Piers and co-workers described the stoichiometric hydroboration of phenylacetylene by this reagent that leads to the corresponding alkenylborane.[6] We herein report the unexpected finding that the reaction of Piers' borane with an excess of phenylacetylene yields *cis*-2-boryl-1,3,3a,5-tetraphenyl-tetrahydropentalene **1a** (Scheme 1).

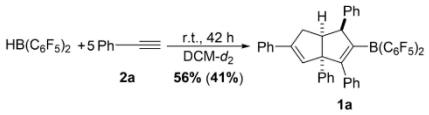

Scheme 1. Formation of *cis*-2-boryl-1,3,3a,5-tetraphenyl-tetrahydropentalene **1a** upon reaction of Piers' borane with five equivalents phenylacetylene. The yield was determined by NMR with trimethoxybenzene as internal standard. The yield of the isolated product is given in parenthesis.

Tetrahydropentalenes are frequently used as ligands in transition-metal catalyzed reactions. Examples are the rhodium-catalyzed 1,2- and 1,4-addition of boronic acids to imines and enones.[7] Recently, a chiral bisborane, synthesized via double hydroboration of a tetrahydropentalene with Piers' borane was used as the catalyst in the enantioselective metal-free hydrogenation of imines.[8] The synthesis of these tetrahydropentalenes requires a multistep procedure starting from octahydropentalenediol or 1,5-cyclooctadiene.[7] Furthermore, the rhodium-mediated formation of hydropentalenyl complexes from terminal alkynes and the palladium-induced cyclotetramerization of acetylenes have been reported.[9] However, the transition-metal free tetramerization of alkynes is to the best of our knowledge unprecedented. Upon reaction of Piers' borane with five equivalents of phenylacetylene at r.t. in DCM, **1a** is obtained after two days in an in situ yield of 56% as determined by NMR. We were not able to detect a diastereomer of **1a**. Subsequently, **1a** was isolated in 41% yield upon crystallization from *n*-hexane and fully characterized. Furthermore, crystals suitable for single-crystal X-ray diffraction (SCXRD) were grown from a saturated *n*-hexane solution. The molecular structure derived from SCXRD supports the structural assignment and confirms the *cis*-relationship of the substituents at the bridgehead positions (Figure 1).

Notably, the reaction also takes place if Piers' borane is reacted with two equivalents phenylacetylene. In this case, hydroboration of the phenylacetylene is observed, followed by the slow formation of **1a** while unreacted alkenylborane remains.[10] The reaction is not limited to phenylacetylene as the substrate: Treatment of alkynes **2b–i** with Piers' borane furnishes the cis-2-boryl-1,3,3a,5-tetra-aryl-tetrahydropentalenes **1b–i** in NMR yields ranging from 32%–55% (Scheme 2).

Erker and co-workers demonstrated that boranes with perfluorophenyl substituents can be engaged in transition-

[a] *M. Hasenbeck, T. Müller, A. Averdunk, Dr. U. Gellrich*
Institut für Organische Chemie
Justus-Liebig-Universität Gießen
Heinrich-Buff-Ring 17, 35392 Gießen (Germany)
E-mail: urs.gellrich@org.chemie.uni-giessen.de
[b] *Dr. J. Becker*
Institut für Anorganische und Analytische Chemie
Justus-Liebig-Universität Gießen
Heinrich-Buff-Ring 17, 35392
Gießen (Germany)

Supporting information for this article is available on the WWW under https://doi.org/10.1002/chem.202104254

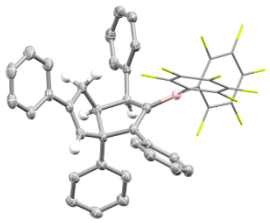

Figure 1. Molecular structure of cis-2-boryl-1,3,3a,5-tetraphenyl-tetrahydropentalene **1 a** derived from SCXRD (50% probability ellipsoids, all hydrogens attached to phenyl rings are omitted and C_6F_5 rings are shown in stick representation for clarity). Selected bond lengths and angles: C1–C2: 1.533(2) Å, C2–C3 1.357(2), C3–C3a 1.542(2) Å, C3a–C4 1.513(2) Å, C4–C5: 1.338(3) Å, C5–C6: 1.509(3) Å, C2–C6a: 1.535(3) Å, C6a–C1: 1.540(2) Å.

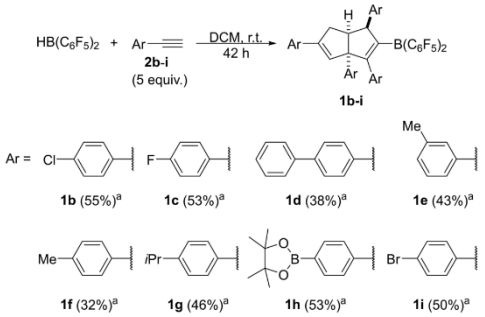

Scheme 2. Tetramerization of aryl allenes by Piers' borane (a) yields determined by ^{1}H NMR with trimethoxybenzene as internal standard. The yields have an estimated error of +/−5% (see Supporting Information for details).

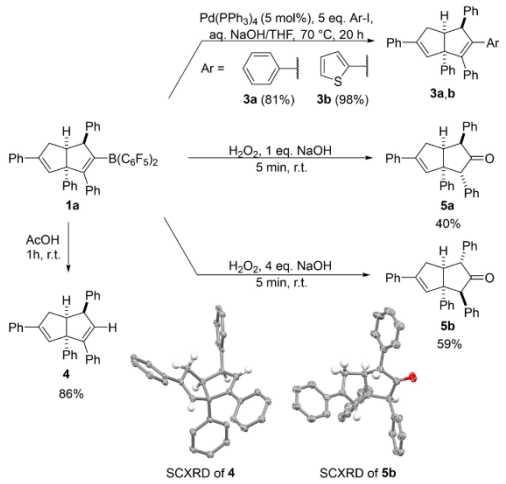

Scheme 3. Follow-up reactivity of **1 a** in a Suzuki-Miyaura coupling, oxidations, and protodeborylation (yields of isolated products given). The insets show the molecular structure for **4** and **5 b** derived from SCXRD analysis (all hydrogens attached to phenyl rings are omitted for clarity).

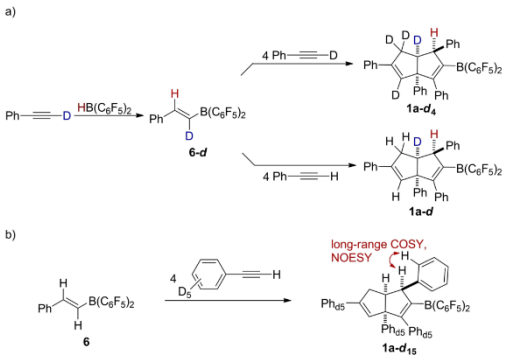

Scheme 4. a) Isotope labeling experiments that reveal the position of hydrogen from Piers' borane and that of the initially hydroborated phenylacetylene in the final product. b) NMR experiment that disclosed the position of the non-deuterated phenyl moiety of **6** in the final product **1 a**-d_{15}. Deuterium incorporation in the indicated position in each case was at least 88%, as determined by ^{1}H NMR.

metal catalyzed coupling reactions.[3c,e,5c] To prove that **1 a** is a suitable substrate for a Suzuki-Miyaura coupling, we reacted **1 a** with phenyl iodide and 2-iodothiophene in the presence of catalytic amounts tetrakis(triphenylphosphine) palladium. This allowed us to isolate the penta-aryl-tetrahydropentalenes **3 a** and **3 b** in very good yields (Scheme 3). Furthermore, **1 a** can be protodeborylated by the addition of acetic acid at room temperature yielding the tetrahydropentalene **4** in very good yield (Scheme 3). The oxidation of **1 a** with H_2O_2 and NaOH leads to the corresponding ketones **5 a** and **5 b**. The diastereoselectivity of this reaction can be controlled by the amount of NaOH added. Both products were isolated as single diastereomers in moderate to good yields and fully characterized including NOESY NMR (Scheme 3).[5c] The structural assignments of **4** and **5 b** are further supported by SCXRD analysis (Scheme 3).

To elucidate the mechanism of the transformation that leads to the formation of **1 a**, we performed a series of isotope labeling experiments. Hydroboration of deuterated phenylacetylene with Piers' borane yielded, as expected, the monodeuterated alkenylborane **6**-***d*** (Scheme 4a). The reaction of **6**-***d*** with four additional equivalents of deuterated phenylacetylene lead to the formation of **1 a**-d_4 with protium exclusively in the 1-position of the pentalene core. On the other hand, the reaction of **6**-***d*** with four equivalents non-deuterated phenylacetylene led to **1 a**-***d*** with deuterium incorporation in the 6a-position. These experiments, therefore, show that the hydrogen of the initial Piers' borane ends up in the 1-position while the hydrogen of the first equivalent of phenylacetylene is incorporated in the 6a-position of **1 a**. Furthermore, the labeling

experiments suggest that the carbon atoms in the 1- and 6a-positions of **1a** originate from phenylacetylene that was hydroborated in the first step of the reaction. To substantiate this hypothesis, we reacted alkenylborane **6** with four equivalents of phenylacetylene bearing fully deuterated phenyl rings (Scheme 4b). As a result, all aromatic ^{1}H NMR signals except those originating from **6** could be suppressed. This enabled us to determine the position of the phenyl moiety of **6** in the product **1a**-d_{15} by long-range COSY and NOESY NMR. This experiment revealed that the phenyl moiety of the alkenylborane which is formed upon initial hydroboration eventually ends up in the 1-position of the final product **1a**.

The position of the first equivalent of phenylacetylene in the final product suggests a reaction that consists of an initial hydroboration and four 1,2-carboborations followed by electrocyclic ring closure of the formed octatetraene.[11,12] Therefore, we investigated the initial steps computationally at the PCM(DCM)-revDSD-PBEP86-D4/def2-QZVPP//PCM(DCM)-PBEh-3c level of theory (Figure 2).[13–16] Furthermore, we considered the barrier for a 1,1-carboboration. According to the computations, the exergonic hydroboration of phenylacetylene by Piers' borane via TS_6 requires a Gibbs free energy of activation of 9.0 kcal mol^{-1}. The 1,2-carboboration of phenylacetylene by alkenylborane **6** is asynchronous: The formation of the C–B bond is further advanced in the transition state structure (see inset in Figure 2). This is certainly a result of the high Lewis acidity of **6** and explains the preference of transition state $TS_{6/7}$ over **TS'**. In the latter, the positive charge arising as a result of asynchronous bond formation is not stabilized by a phenyl substituent. Consequently, the 1,2-carboboration should lead to the diene **7** in which the phenyl substituents are in a 1,3-distance. The barrier for the 1,1-carboboration is computed to be 4.8 kcal mol^{-1} higher than the one for the 1,2-carboboration

We note that the computed transition state structure for the 1,1-carboboration is structurally similar to the one reported by Grimme and Erker for the 1,1-carboboration of alkynes by BCF.[3b] While the barrier for the 1,2-carboboration via $TS_{6/7}$ is surmountable at r.t., the computed barriers for the carboborations via **TS'** (28.8 kcal mol^{-1}) and $TS_{1,1\text{-carboboration}}$ (27.4 kcal mol^{-1}) are conflicting with the experimental observation that the tetramerization occurs at ambient conditions. The findings that the formation of **1a** is also observed when Piers' borane is

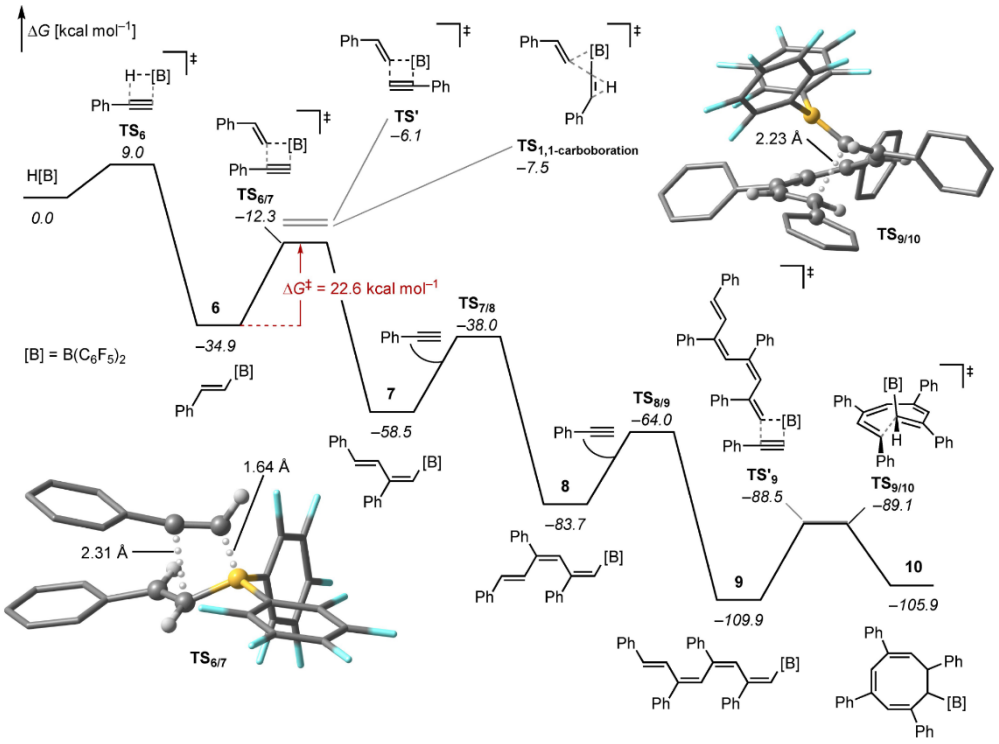

Figure 2. Schematic PES of the formation of the cyclooctatriene **10** and barriers for the 1,2- and 1,1-carboboration of phenylacetylene by **6** computed at PCM(DCM)-revDSD-PBEP86-D4/def2-QZVPP//PCM(DCM)-PBh-3c. The insets show the computed transition state structures of the 1,2-carboboration leading to **7** and the 8π-electrocyclization leading to cycloocatriene **10**.

reacted with only two equivalents phenylacetylene and that no intermediate except alkenylborane **6** can be detected by ^{1}H NMR reaction monitoring further indicate that this initial 1,2-carboboration is rate-determining.[10] Indeed, the computed barriers for the subsequent 1,2-carboborations ($\mathbf{TS}_{7/8}$ and $\mathbf{TS}_{8/9}$) are lower than the one for the initial carboboration. An 8π-electrocyclization of the tetraene **9** via $\mathbf{TS}_{9/10}$ yields then the cyclooctatriene **10**. The computed barrier of 20.8 kcal mol^{-1} for the 8π-electrocyclization of **9** does not differ substantially from the barrier obtained experimentally for the electrocylization of unsubstituted octatetraene (17.0 kcal mol^{-1}) and permits this step to occur readily at r.t.[17] Although a fourth 1,2-carboboration via $\mathbf{TS'}_9$ is slightly disfavored compared to the electrocyclization via $\mathbf{TS}_{9/10}$, both transition states are close in energy so that further oligomerizations could be a possible side reaction. The sequence of 1,2-carboborations and electrocyclization would locate the first equivalent of phenylacetylene in the relative position to the boryl substituent that was deduced from the isotope labeling experiments. The thermal and photochemical rearrangements of cycloocatrienes to semibullvalenes were reported.[18,19] An analogous $_\pi4_a+_\pi2_a$ rearrangement of **10** would lead to tricycle **11** (Scheme 5).

A vinylcyclopropane-cyclopentene rearrangement of **11** would form **12**. These rearrangements usually require high activation energies.[18,20] However, it was shown that Lewis acids can lower the barrier for vinylcyclopropane-cyclopentene rearrangements significantly.[21] Thus, we assume that this transformation is catalyzed by Lewis acidic boranes present in the reaction. Additionally, the electrophilic perfluorophenyl substituted boranes could serve as one-electron acceptors and promote the rearrangement from **10** to **11** via a (di)radical pathway.[22] Finally, a simple proton shift can convert **12** into the experimentally observed product **1a**. According to our computations at PCM(DCM)-revDSD-PBEP86-D4/def2-QZVPP//PCM(DCM)-PBEh-3c, formation of **1a** from **10** is exergonic by 28.2 kcal mol^{-1}. We note that the relative position of the phenyl substituents in **1a** that would result from the proposed $_\pi4_a+_\pi2_a$ rearrangement and the vinylcyclopropane-cyclopentene rearrangement agrees with the experimentally determined one. However, it must be stressed that other reaction pathways cannot be excluded at present and further computational and experimental investigations to clarify the mechanistic details of the formation of **1a** are ongoing.

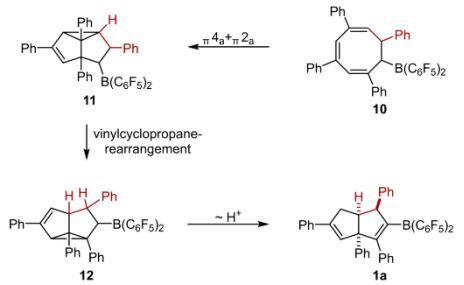

Scheme 5. Proposed mechanism for the formation of **1a**. The first equivalent alkenylborane, whose position was determined by isotope labeling experiments, is highlighted in red.

In summary, we have documented the unprecedented tetramerization of simple arylacetylenes by Piers' borane. We expect this finding to stimulate the development of new methods for organic synthesis that rely on the oligomerization of alkynes by Lewis acidic boranes.

Experimental Section

See the Supporting Information for details.

Deposition Numbers 2107142, 2121641 and 2124445 contain the supplementary crystallographic data for this paper. These data are provided free of charge by the joint Cambridge Crystallographic Data Centre and Fachinformationszentrum Karlsruhe Access Structures service.

Acknowledgements

This work was supported by the DFG (Emmy-Noether program, GE 3117/1-1). The authors thank Dr. H. Hausmann for assistance with NMR experiments, and Dr. D. Gerbig for fruitful discussions. Continuous support by Prof. Dr. P. R. Schreiner, Prof. Dr. R. Göttlich, and Prof. Dr. H. A. Wegner is acknowledged. Open Access funding enabled and organized by Projekt DEAL.

Conflict of Interest

The authors declare no conflict of interest.

Data Availability Statement

The data that support the findings of this study are available in the supplementary material of this article.

Keywords: 1,2-carboboration · alkynes · boranes · density functional theory · Lewis acids

[1] a) N. Miyaura, K. Yamada, A. Suzuki, *Tetrahedron Lett.* **1979**, *20*, 3437–3440; b) N. Miyaura, A. Suzuki, *Chem. Commun.* **1979**, *19*, 866–867; c) N. Miyaura, A. Suzuki, *Chem. Rev.* **1995**, *95*, 2457–2483.
[2] a) D. Chan, K. Monaco, R. Wang, M. Winters, *Tetrahedron Lett.* **1998**, *39*, 2933–2936; b) P. Lam, C. Clark, S. Saubern, J. Adams, M. Winters, D. Chan, A. Combs, *Tetrahedron Lett.* **1998**, *39*, 2941–2944; c) M. J. West, J. W. B. Fyfe, J. C. Vantourout, A. J. B. Watson, *Chem. Rev.* **2019**, *119*, 12491–12523; d) T. Furuya, H. M. Kaiser, T. Ritter, *Angew. Chem. Int. Ed.* **2008**, *47*, 5993–5996; *Angew. Chem.* **2008**, *120*, 6082–6085; e) A. Bonet, M. Odachowski, D. Leonori, S. Essafi, V. K. Aggarwal, *Nat. Chem.* **2014**, *6*, 584–586.
[3] a) C. Jiang, O. Blacque, H. Berke, *Organometallics* **2010**, *29*, 125–133; b) C. Chen, F. Eweiner, B. Wibbeling, R. Fröhlich, S. Senda, Y. Ohki, K. Tatsumi, S. Grimme, G. Kehr, G. Erker, *Chem. Asian J.* **2010**, *5*, 2199–2208; c) C. Chen, G. Kehr, R. Fröhlich, G. Erker, *J. Am. Chem. Soc.* **2010**, *132*, 13594–13595; d) B.-H. Xu, G. Kehr, R. Fröhlich, S. Grimme, G. Erker, *J. Am. Chem. Soc.* **2011**, *133*, 3480–3491; e) C. Chen, T. Voss, R. Fröhlich,

G. Kehr, G. Erker, *Org. Lett.* **2011**, *13*, 62–65; f) B.-H. Xu, G. Kehr, R. Fröhlich, B. Wibbeling, B. Schirmer, S. Grimme, G. Erker, *Angew. Chem. Int. Ed.* **2011**, *50*, 7183–7186; *Angew. Chem.* **2011**, *123*, 7321–7324; g) R. Liedtke, R. Fröhlich, G. Kehr, G. Erker, *Organometallics* **2011**, *30*, 5222–5232; h) C. Chen, R. Fröhlich, G. Kehr, G. Erker, *Chem. Commun.* **2010**, *46*, 3580–3582; i) G. Kehr, G. Erker, *Chem. Commun.* **2012**, *48*, 1839–1850; j) Y.-L. Liu, G. Kehr, C. G. Daniliuc, G. Erker, *Chem. Sci.* **2017**, *8*, 1097–1104; k) M. M. Hansmann, R. L. Melen, F. Rominger, A. S. K. Hashmi, D. W. Stephan, *J. Am. Chem. Soc.* **2014**, *136*, 777–782; l) M. M. Hansmann, R. L. Melen, M. Rudolph, F. Rominger, H. Wadepohl, D. W. Stephan, A. S. K. Hashmi, *J. Am. Chem. Soc.* **2015**, *137*, 15469–15477; m) R. L. Melen, M. M. Hansmann, A. J. Lough, A. S. K. Hashmi, D. W. Stephan, *Chem. Eur. J.* **2013**, *19*, 11928–11938; n) L. C. Wilkins, Y. Soltani, J. R. Lawson, B. Slater, R. L. Melen, *Chem. Eur. J.* **2018**, *24*, 7364–7368.

[4] M. Hasenbeck, F. Wech, A. Averdunk, J. Becker, U. Gellrich, *Chem. Commun.* **2021**, *57*, 5518–5521.

[5] a) X. Tao, G. Kehr, C. G. Daniliuc, G. Erker, *Angew. Chem. Int. Ed.* **2017**, *56*, 1376–1380; *Angew. Chem.* **2017**, *129*, 1396–1400; b) X. Tao, K. Škoch, C. G. Daniliuc, G. Kehr, G. Erker, *Chem. Sci.* **2020**, *11*, 1542–1548; c) X. Tao, C. G. Daniliuc, D. Dittrich, G. Kehr, G. Erker *Angew. Chem. Int. Ed.* **2018**, *57,13922–13926; Angew. Chem.* **2018**, 130, 14118–14122; *Angew. Chem.* **2018**, *130*, 14118–14122.

[6] a) D. J. Parks, R. E. von H. Spence, W. E. Piers, *Angew. Chem. Int. Ed.* **1995**, *34*, 809–811; *Angew. Chem.* **1995**, *107*, 895–897; b) E. A. Patrick, W. E. Piers, *Chem. Commun.* **2020**, *56*, 841–853.

[7] a) C.-G. Feng, Z.-Q. Wang, P. Tian, M.-H. Xu, G.-Q. Lin, *Chem. Asian J.* **2008**, 3, 1511–1516; b) Z.-Q. Wang, C.-G. Feng, M.-H. Xu, G.-Q. Lin, *J. Am. Chem. Soc.* **2007**, *129*, 5336–5337; c) S. Helbig, S. Sauer, N. Cramer, S. Laschat, A. Baro, W. Frey, *Adv. Synth. Catal.* **2007**, *349*, 2331–2337.

[8] X.-S. Tu, N.-N. Zeng, R.-Y. Li, Y.-Q. Zhao, D.-Z. Xie, Q. Peng, X.-C. Wang, *Angew. Chem. Int. Ed.* **2018**, *57*, 15096–15100; *Angew. Chem.* **2018**, *130*, 15316–15320.

[9] a) H. Komatsu, Y. Suzuki, H. Yamazaki, *Chem. Lett.* **2001**, *30*, 998–999; b) A. V. Kolos, Y. V. Nelyubina, B. Sundararaju, D. S. Perekalin, *Organometallics* **2021**, *40*, 3712–3719; c) P. M. Bailey, B. E. Mann, D. I. Brown, P. M. Maitlis, *J. Chem. Soc. Chem. Commun.* **1976**, 238–239.

[10] For details, see the Supporting Information.

[11] a) Y. Shoji, N. Tanaka, S. Muranaka, N. Shigeno, H. Sugiyama, K. Takenouchi, F. Hajjaj, T. Fukushima, *Nat. Commun.* **2016**, *7*, 12704; b) Y. Shoji, N. Shigeno, K. Takenouchi, M. Sugimoto, T. Fukushima, *Chem. Eur. J.* **2018**, *24*, 13223–13230; c) M. Nogami, K. Hirano, M. Kanai, C. Wang, T. Saito, K. Miyamoto, A. Muranaka, M. Uchiyama, *J. Am. Chem. Soc.* **2017**, *139*, 12358–12361; d) M. Hasenbeck, T. Müller, U. Gellrich, *Catal. Sci. Technol.* **2019**, *9*, 2438–2444.

[12] B. E. Thomas IV, J. D. Evanseck, K. N. Houk, *J. Am. Chem. Soc.* **1993**, *115*, 4165–4169.

[13] a) G. Santra, N. Sylvetsky, J. M. L. Martin, *J. Phys. Chem. A* **2019**, *123*, 5129–5143; b) E. Caldeweyher, C. Bannwarth, S. Grimme, *J. Chem. Phys.* **2017**, *147*, 034112; c) E. Caldeweyher, S. Ehlert, A. Hansen, H. Neugebauer, S. Spicher, C. Bannwarth, S. Grimme, *J. Chem. Phys.* **2019**, *150*, 154122; d) F. Weigend, R. Ahlrichs, *Phys. Chem. Chem. Phys.* **2005**, *7*, 3297–3305; e) A. Hellweg, C. Hattig, S. Hofener, W. Klopper, *Theor. Chem. Acc.* **2007**, *117*, 587–597; f) F. Weigend, *J. Comput. Chem.* **2008**, *29*, 167–175.

[14] a) S. Grimme, J. G. Brandenburg, C. Bannwarth, A. Hansen *J. Chem. Phys.* **2015**, *143*, 054107; b) H. Kruse, S. Grimme, *J. Chem. Phys.* **2012**, *136*, 154101; c) S. Grimme, S. Ehrlich, L. Goerigk, *J. Comput. Chem.* **2011**, *32*, 1456–1465; d) S. Grimme, J. Antony, S. Ehrlich, H. Krieg, *J. Chem. Phys.* **2010**, *132*, 154104; e) F. Weigend, *Phys. Chem. Chem. Phys.* **2006**, *8*, 1057–1065.

[15] V. Barone, M. Cossi, *J. Phys. Chem. A* **1998**, *102*, 1995–2001.

[16] All computations were performed with the ORCA program package, Version 4.2.1: a) F. Neese, *WIREs Comput. Mol. Sci.* **2012**, *2*, 73–78; b) F. Neese, *WIREs Comput. Mol. Sci.* **2018**, *8*, e1327.

[17] T. D. Goldfarb, L. J. Landquist, *J. Am. Chem. Soc.* **1967**, *89*, 4588–4592.

[18] a) H. Straub, J. Hambrecht, *Chem. Ber.* **1977**, *110*, 3221–3223; b) W. P. Lay, K. Mackenzie, A. S. Miller, D. L. Williams-Smith, *Tetrahedron* **1980**, *36*, 3021–3031; c) C. Chen, C. Xi, Y. Liu, X. Hong *J. Org. Chem.* **2006**, *71*, 5373–5376.

[19] K. Ohkura, H. Akizawa, M. Kudo, T. Ishihara, N. Oshima, K. Seki, *Heterocycles* **2012**, *84*, 1057–1065.

[20] Z. Goldschmidt, B. Crammer, *Chem. Soc. Rev.* **1988**, *17*, 229–267.

[21] a) T. Hudlicky, F. F. Koszyk, T. M. Kutchan, J. P. Sheth, *J. Org. Chem.* **1980**, *45*, 5020–5027; b) V. Aris, J. M. Brown, J. A. Conneely, B. T. Golding, D. H. Williamson, *J. Chem. Soc. Perkin Trans. 2* **1975**, *2*, 4–10.

[22] a) L. Liu, L. L. Cao, D. Zhu, J. Zhou, D. W. Stephan, *Chem. Commun.* **2018**, *54*, 7431–7434; b) L. Liu, L. L. Cao, Y. Shao, G. Ménard, D. W. Stephan, *Chem* **2017**, *3*, 259–26; c) F. Holtrop, A. R. Jupp, B. J. Kooij, N. P. van Leest, B. de Bruin, J. C. Slootweg, *Angew. Chem. Int. Ed.* **2020**, *59*, 22210–22216; *Angew. Chem.* **2020**, *132*, 22394–22400; d) F. Holtrop, A. R. Jupp, N. P. Van Leest, M. Paradiz Dominguez, R. M. Williams, A. M. Brouwer, B. De Bruin, A. W. Ehlers, J. C. Slootweg, *Chem. Eur. J.* **2020**, *26*, 9005–9011.

Manuscript received: November 29, 2021
Accepted manuscript online: December 9, 2021
Version of record online: December 28, 2021

5.9 1,2-Carboboration of Arylallenes by In Situ Generated Alkenylboranes for the Synthesis of 1,4-Dienes

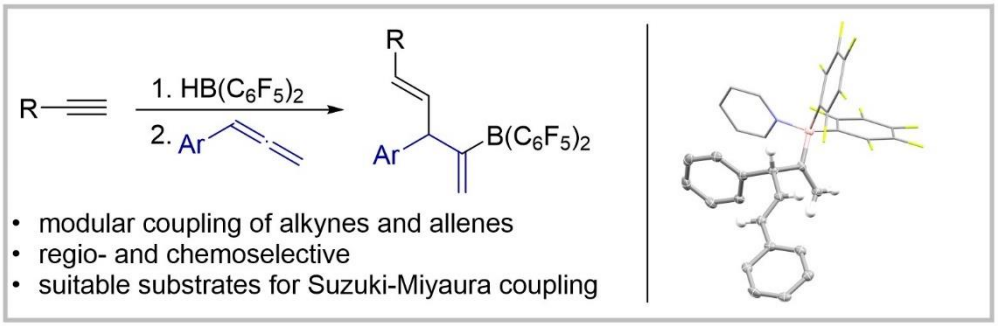

1,2-carboboration of arylallenes by alkenylboranes, formed in situ by hydroboration of alkynes with Piers' borane ($HB(C_6F_5)_2$) is reported. This novel 1,2-carboboration and a subsequent Suzuki-Miyaura coupling were used for the synthesis of twenty new aryl substituted 1,4-dienes.

Arthur Averdunk, Max Hasenbeck, Tizian Müller, Dr. Jonathan Becker, Dr. Urs Gellrich

Chem. Eur. J. **2022**, *28*, e202200470

DOI (englische Version): 10.1002/chem.202200470

Akzeptiertes Manuskript online: 29.03.2022

Final veröffentlichte Version online: 21.04.2022

Chemistry–A European Journal
Research Article
doi.org/10.1002/chem.202200470
Chemistry Europe
European Chemical Societies Publishing
www.chemeurj.org

1,2-Carboboration of Arylallenes by In Situ Generated Alkenylboranes for the Synthesis of 1,4-Dienes

Arthur Averdunk[+],[a] Max Hasenbeck[+],[a] Tizian Müller,[a] Jonathan Becker,[b] and Urs Gellrich*[a]

Abstract: We herein report a novel method for the coupling of unactivated alkynes and arylallenes, which relies on an unprecedented and regioselective 1,2-carboboration of the allene by an alkenylborane. The alkenylborane is conveniently prepared *in situ* by hydroboration of an alkyne with Piers' borane, *i.e.*, $HB(C_6F_5)_2$. The boryl-substituted 1,4-dienes that are formed by this carboboration are well-suited for a subsequent Suzuki-Miyaura coupling with aryl iodides. This allowed us to develop a three-step, one-pot protocol for the synthesis of aryl-substituted 1,4-dienes. The generality of the reaction was demonstrated by the synthesis of twenty dienes with modular variations of all three reaction partners. The mechanism of the new 1,2-carboboration was investigated using dispersion corrected double-hybrid DFT computations that allowed us to rationalize the chemo- and regioselectivity of this key step.

Introduction

Carboborations are a powerful and atom economic synthetic method because they simultaneously form a C–C bond and install a valuable boryl unit into a molecular framework by adding an organoborane to a double or triple bond. In recent years, uncatalyzed direct carboborations by Lewis acidic boranes have received increasing attention.[1] A seminal contribution to this field is the 1,1-carboboration of alkynes by the Lewis acidic tris(perfluorophenyl)borane (BCF) that was independently discovered by Erker and Berke.[2,3] The groups of Hashmi and Stephan reported the cyclopropanation and the formation of allyl boranes by 1,1-carboboration of enynes and propargylic esters, respectively.[2e,j] We recently reported that the reaction of phenylallene with BCF leads to the formation of a C_6F_5-substituted indene via a cyclisation, 1,1-carboboration, retro-hydroboration sequence.[2k] In contrast, there are still only a few reports on uncatalyzed 1,2-carboborations.[4] Melen and co-workers described the 1,2-addition of $B(C_6F_5)_3$ to the terminal double bond of allenylketones (Scheme 1).[4g] In 2021, Studer *et al.* reported the 1,2-carboboration of alkyne-substituted sulphonamides with dichloroarylboranes. The dichloroborane moieties were subsequently transformed *in situ* to their respective pinacol derivatives (Scheme 1).[4b]

We became now interested in devising a protocol that allows the selective group transfer of an easily interchangeable substituent at the boron to a non-activated substrate via a

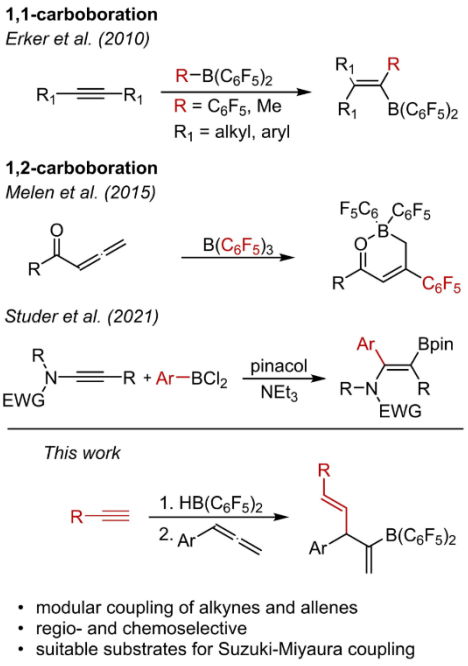

Scheme 1. The context of this work: Recent examples of carboborations and the consecutive hydroboration-1,2-carboboration sequence reported herein.

[a] *A. Averdunk,[+] M. Hasenbeck,[+] T. Müller, Dr. U. Gellrich*
Institut für Organische Chemie
Justus-Liebig-Universität Gießen
Heinrich-Buff-Ring 17, 35392 Gießen (Germany)
E-mail: urs.gellrich@org.chemie.uni-giessen.de
[b] *Dr. J. Becker*
Institut für Anorganische und Analytische Chemie
Justus-Liebig-Universität Gießen
Heinrich-Buff-Ring 17, 35392 Gießen (Germany)
[+] *These authors contributed equally to this work.*
Supporting information for this article is available on the WWW under https://doi.org/10.1002/chem.202200470

carboboration. A fast and convenient way to synthesize electron-poor boranes is the hydroboration of alkynes by the very active hydroboration reagent $HB(C_6F_5)_2$, also known as Piers' borane.[5] Since allenes are reactive towards strong boron-based Lewis acids, we aimed to elucidate whether the reaction of electron-poor alkenylboranes, synthesized by hydroboration of alkynes, could lead to a selective transfer of the vinyl group to an allene in a carboboration reaction.[4g,6,7]

Results and Discussion

We commenced our attempts by preparing alkenylborane **2** by hydroboration of phenylacetylene with Piers' borane **1** in deuterated dichloromethane (Scheme 2).[5] The corresponding ^{1}H NMR shows complete conversion to alkenylborane **2** after 10 min at r.t. Next, phenylallene was added to the reaction mixture.

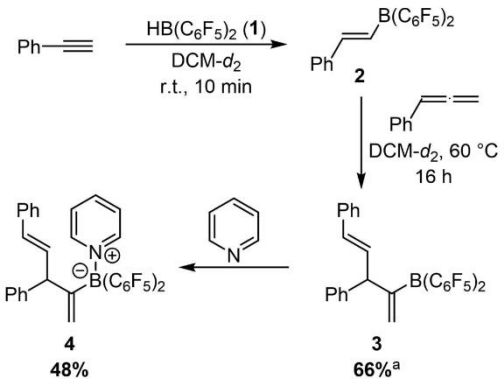

Scheme 2. Formation of the 1,4-diene **3** upon 1,2-carboboration of phenylallene by the alkenylborane **2** and isolation of the respective pyridine adduct **4**. a) Yield determined by ^{1}H NMR with trimethoxybenzene as internal standard.

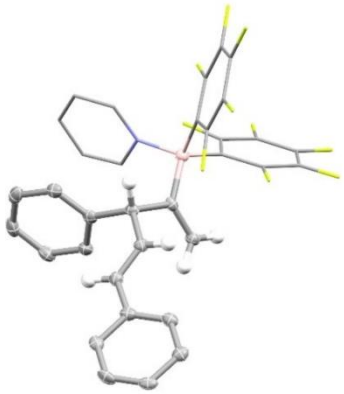

Figure 1. Molecular structure of 4 derived from SCXRD (50% probability ellipsoids, all hydrogens attached to phenyl rings are omitted and pyridine and C6F5 rings are shown in stick representation for clarity).

Upon heating to 60 °C in a sealed NMR tube, the formation of the 1,4-diene **3**, which is the product of a formal 1,2-carboboration to the internal double bond of the allene, was observed. While we have recently proposed that the Piers' borane mediated tetramerization of alkynes commences with a carboboration of an alkyne by an alkenylborane, the carboboration of an allene by an alkenylborane is, to the best of our knowledge, unprecedented.[4f] After 16 h, the yield of **3** was determined by ^{1}H NMR to be 66%. The reaction was repeated on a preparative scale in 1,2-dichloroethane at 80 °C and the diene **3** was isolated as pyridine adduct **4** in 48% yield by crystallization (Scheme 2). The structural assignment of **4** is further supported by single-crystal X-ray diffraction (SCXRD, Figure 1). With these promising initial experimental results in hand, we addressed the mechanism and the observed regioselectivity of the 1,2-carboboration by DFT computations at the PCM(DCM)-revDSD-PBEP86-D4/def2-QZVPP//PCM(DCM)-PBEh-3c level of theory (Figure 2).[8] The dispersion corrected, spin-component scaled double hybrid functional revDSD-PBEP86-D4 was recently shown to be one of the most accurate DFT functionals by benchmark computations against the GMTKN55 database.[8b] Since zwitterionic structures are likely to be part of the mechanism, the structures were optimized with an implicit solvent model for dichloromethane. According to the computations, the exergonic hydroboration of phenylacetylene by Piers' borane **1** via $\mathbf{TS_{1/2}}$ requires a Gibbs free activation energy of 9.0 kcal mol^{-1}. The coordination of phenylallene to the alkenylborane $\mathbf{TS_{2/5}}$ is computed to be rate determining.

Furthermore, this step dictates the regioselectivity of the carboboration. The central carbon of the allene binds to the borane so that in the zwitterion **5** the positive charge is resonance stabilized and in a benzylic and allylic position.[2k,6b] The computed barrier of 20.8 kcal mol^{-1} for the formation of the zwitterion **5** is in favourable agreement with the mild reaction conditions. Attempts to locate minima on the potential energy surface for the two other zwitterionic regioisomers of the coordination of the allene to the borane lead to the direct dissociation of the respective structures. A virtually barrierless migration of the alkenyl substituent yields than the 1,4-diene **3** in an exergonic reaction. In contrast, the transfer of a pentafluorophenyl ring via **TS'** has an activation barrier of 12.5 kcal mol^{-1} (see inset Figure 2). Thus, the computations agree with the experimentally observed chemoselectivity. We further considered the formation of an indene ring system by an intramolecular Friedel-Crafts type reaction.[2k,6b] Again, the respective transition state $\mathbf{TS_{indene}}$ is kinetically disfavoured by 7.1 kcal mol^{-1} (see inset Figure 2).

Erker and co-workers showed that $B(C_6F_5)_2$ groups are suitable coupling partners in Suzuki-Miyaura[9,10] cross-coupling reactions.[2a,c,6a,11] Therefore, we probed if it is possible to develop a one-pot procedure for a 1,2-carboboration of allenes by alkenylboranes and a consecutive Suzuki-Miyaura coupling.

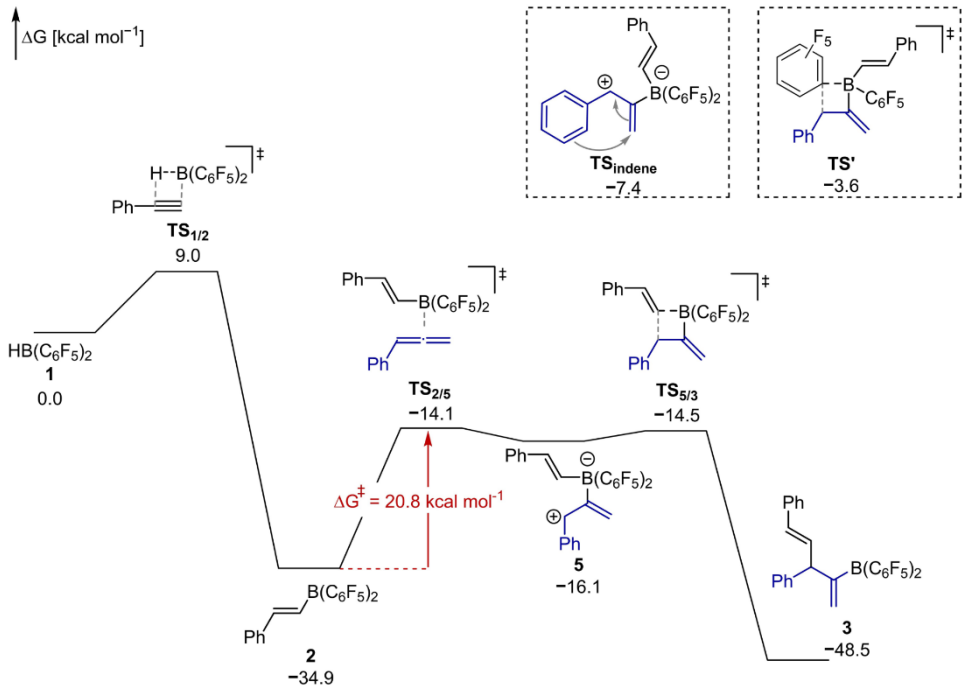

Figure 2. Gibbs free energies for the 1,2-carboboration of phenylallene by the alkenylborane **2** computed at PCM(DCM)-revDSD-PBEP86-D4/def2-QZVPP//PCM(DCM)-PBEh-3c.

Indeed, the reaction of **3**, formed *in situ*, with phenyliodide under basic conditions lead to the formation of the diene **6a** in 52% yield (Scheme 3). Notably, the reaction sequence did not require the isolation of **3**, only the solvent was removed before the Suzuki-Miyaura coupling. This three-step one-pot method with the 1,2-carboboration as key step offers a potentially broad scope. As aforementioned, a variety of alkenylboranes is accessible by hydroboration of different alkynes with Piers' borane **1**.[5] Furthermore, by adding different allenes the substitution pattern of the boryl substituted 1,4-dienes can be easily altered. Finally, these key intermediates can be cross-coupled with different organoiodides to access various 1,4-dienes. 1,4- or skipped dienes are of synthetic interest due to their prevalence in several natural products.[12,13] Therefore, we explored the scope of this reaction sequence (Scheme 3). First, we screened different allenes. Besides phenylallene, the corresponding *para*-substituted methyl, *iso*-propyl, and *tert*-butyl phenylallenes (**6b**–**6d**) are suitable reaction partners. With 64 to 74%, the yields for these substrates are better than for the unsubstituted phenylallene. Additionally, the 1,2-carboboration of *para*-*t*Bu-phenylallene proceeds at r.t. while the reaction with phenylallene requires elevated temperatures. These results support the proposed mechanism: Electron donating groups stabilize the (partial) positive charge which is present in the zwitterionic intermediate and the respective transition state.[14] While alcohols themselves are problematic substrates because of the strong Lewis acidic character of the boron moiety, protected alcohols like methyl aryl ethers are tolerated, as it was demonstrated by the synthesis of **6e** in 39% yield.[15] The carboboration and coupling of *para*-fluorophenylallene gives the respective diene **6f** in 73% yield. We then tested different alkynes. The reaction with alkyl- and phenyl-substituted phenylacetylenes gives the dienes **7a**–**7c** in moderate yields. Furthermore, alkynes with electron withdrawing groups like fluorine, chlorine, and bromine can also be used as coupling partners with yields between 51–60% (**7d**–**7g**). To elucidate whether aliphatic alkynes are suitable substrates for the carboboration, we reacted ethynyl-cyclohexene and adamantylacetylene with Piers' borane and *p*-*t*Bu-phenylallene and *p*-*i*Pr-phenylallene, respectively. Subsequent coupling with phenyliodide gave **7h** and **7i** in 39% and 36% yield. The synthesis of **7h** demonstrates that double bonds are tolerated during the carboboration. Additionally, several organoiodides were tested. The reaction with 3-iodopyridine as an example for a heterocycle gave diene **8a** in 54% yield. The reaction with 4-iodobenzonitrile and biphenyliodide gave the respective products **8b** and **8c** in 39% and 48% yield, respectively.

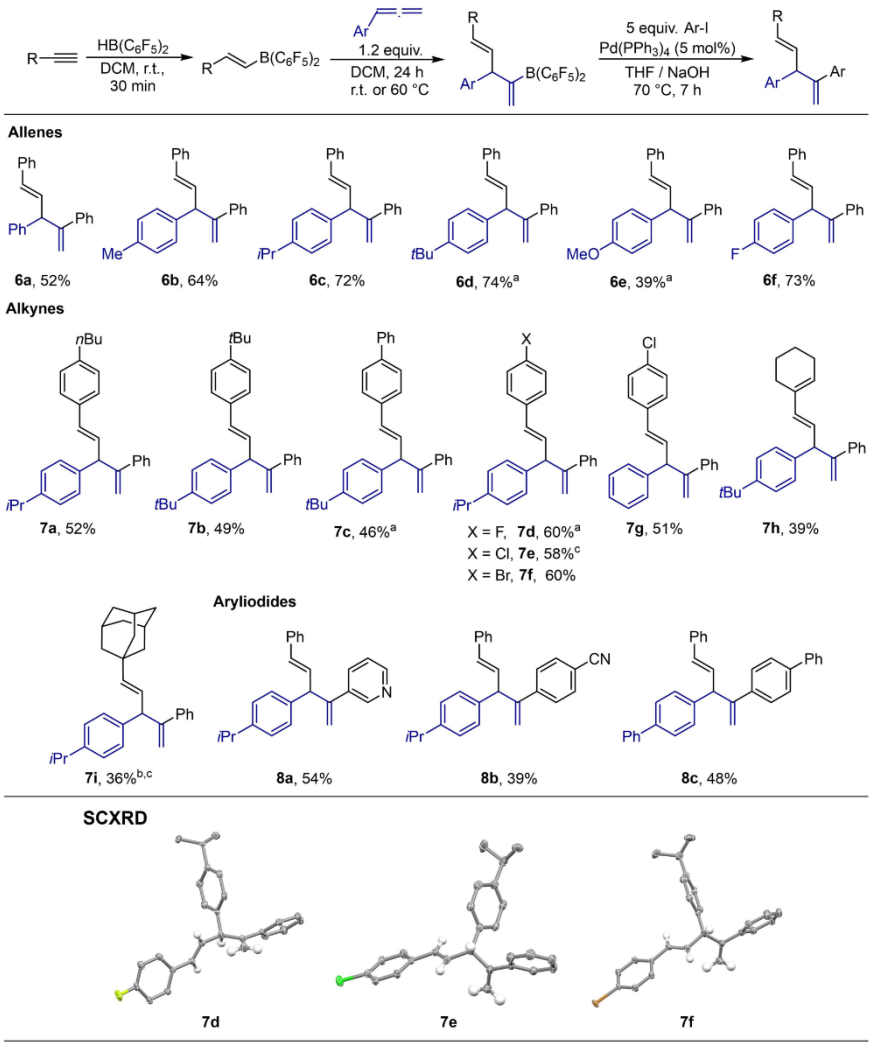

Scheme 3. Scope of the consecutive hydroboration, carboboration, and Suzuki-Miyaura coupling and molecular structures derived from SCXRD (50% probability ellipsoids, for clarity only the hydrogens of the 1,4-diene core are shown) a) The carboboration step was done at r.t. b) The reaction time for the carboboration was 3 days c) Products contained ca. 5% impurities after column chromatography and two distillations.

The reaction of commercially available *para*-Bpin substituted phenylacetylene with *p*-*i*Pr-phenylallene under the standard conditions led to the replacement of both boron groups upon coupling with phenyliodide. The respective product **9** with four aromatic rings was isolated in 41% yield (Scheme 4). The hydroboration of two equivalents of *para*-F-phenylacetylene, the addition of one equivalent of diallene **10**, and a subsequent Suzuki-Miyaura coupling yielded the phenyl bridged bis-1,4-diene **11** in 39% (Scheme 4). Products **9** and **11** demonstrate that complex molecular frameworks can be synthesized from non- or low-functionalised starting materials using the protocol presented herein. The structure of the dienes **7d**, **7e**, **7f**, and **9** was additionally supported by SCXRD (Schemes 3 and 4). Regarding the limitations of this method, we observed that the internal alkynes 3-hexyne and diphenylacetylene are readily hydroborated by **1** but the resulting alkenylbor-

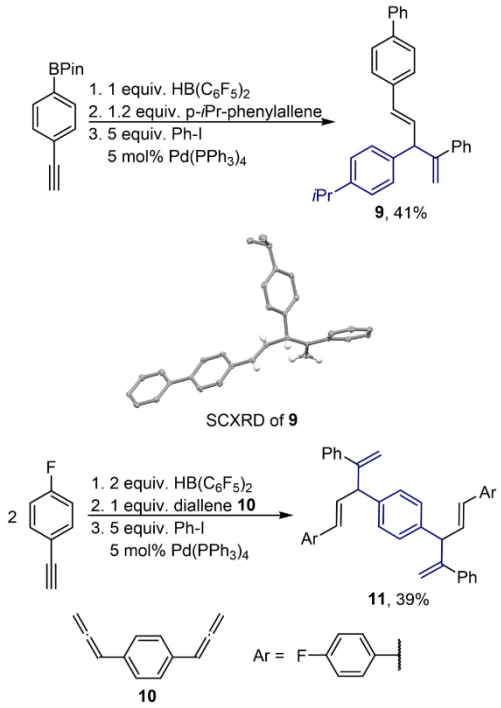

Scheme 4. Special substrates of the hydroboration, carboboration, and Suzuki-Miyaura coupling sequence and the molecular structure of diene **9** derived from SCXRD (50% probability ellipsoids, for clarity only the hydrogens of the 1,4-diene core are shown).

anes did not react with phenylallene. We further found that alkynes with Lewis basic sides such as ethynyl phenylmethyl ether and 2-ethynylthiophene are not suitable for this reaction sequence. Furthermore, the carboboration of cyclohexylallene with **2** was not successful. This is probably because of the lacking stabilization of the positive charge in the rate-determining transition state and the zwitterionic intermediate.

Conclusion

In summary, we report a novel and regioselective 1,2-carboboration as the key step of a three-step one-pot protocol for the synthesis of aryl-substituted 1,4-dienes from alkynes, allenes, and organoiodides. This unprecedented 1,2-carboboration transfers a vinyl group of an *in situ* generated alkenylborane to the benzylic position of the aryl allene. All three components of the reaction sequence that forms two C–C bonds can be modified. Therefore, a variety of aryl-substituted 1,4-dienes is accessible by this modular approach. The usefulness of this protocol was demonstrated by the synthesis of twenty different dienes. We expect this finding to stimulate the development of new applications of carboboration reactions for organic synthesis.

Crystal structures

Deposition Number(s) 2150152 (for 4 at 100 K), 2150153 (for 7e at 100 K), 2150154 (for 7d at 100 K), 2150155 (for 9 at 100 K), and 2150156 (for 7f at 100 K) contain(s) the supplementary crystallographic data for this paper. These data are provided free of charge by the joint Cambridge Crystallographic Data Centre and Fachinformationszentrum Karlsruhe Access Structures service.

Acknowledgements

This work was supported by the DFG (Emmy-Noether program, GE 3117/1-1). The authors thank Dr. H. Hausmann for her assistance with NMR experiments. Continuous support by Prof. Dr. P. R. Schreiner, Prof. Dr. R. Göttlich, and Prof. Dr. H. A. Wegner is acknowledged. Open Access funding enabled and organized by Projekt DEAL.

Conflict of Interest

The authors declare no conflict of interest.

Data Availability Statement

The data that support the findings of this study are available in the supplementary material of this article.

Keywords: 1,2-carboboration · 1,4-dienes · boranes · density functional theory · Lewis acids

[1] For selective review articles on transition-metal catalyzed carboboration reactions see: a) M. Suginome, *Chem. Rec.* **2010**, *10*, 348–358; b) Z. Liu, Y. Gao, T. Zeng, K. M. Engle, *Isr. J. Chem.* **2020**, *60*, 219–229; c) S. K. Dorn, M. K. Brown, *ACS Catal.* **2022**, 2058–2063.

[2] For selected examples of uncatalyzed 1,1-carboborations see: a) C. Chen, G. Kehr, R. Fröhlich, G. Erker, *J. Am. Chem. Soc.* **2010**, *132*, 13594–13595; b) C. Jiang, O. Blacque, H. Berke, *Organometallics* **2010**, *29*, 125–133; c) C. Chen, T. Voss, R. Fröhlich, G. Kehra, G. Erker, *Org. Lett.* **2011**, *13*, 62–65; d) G. Menz, B. Wrackmeyer, *Z. Naturforsch.* **1977**, *32*, 1400–1407; e) M. M. Hansmann, R. L. Melen, M. Rudolph, F. Rominger, H. Wadepohl, D. W. Stephan, A. S. K. Hashmi, *J. Am. Chem. Soc.* **2015**, *137*, 15469–15477; f) R. L. Melen, M. M. Hansmann, A. J. Lough, A. S. K. Hashmi, D. W. Stephan, *Chem. Eur. J.* **2013**, *19*, 11928–11938; g) C. Chen, F. Eweiner, B. Wibbeling, R. Fröhlich, S. Senda, Y. Ohki, K. Tatsumi, S. Grimme, G. Kehr, G. Erker, *Chem. Asian J.* **2010**, *5*, 2199–2208; h) R. Liedtke, R. Fröhlich, G. Kehr, G. Erker, *Organometallics* **2011**, *30*, 5222–5232; i) C. Chen, C. G. Daniliuc, C. Mück-Lichtenfeld, G. Kehr, G. Erker, *Chem. Commun.* **2020**, *56*, 8806–8809; j) M. M. Hansmann, R. L. Melen, F. Rominger, A. S. K. Hashmi, D. W. Stephan, *J. Am. Chem. Soc.* **2014**, *136*, 777–782; k) M. Hasenbeck, F. Wech, A. Averdunk, J. Becker, U. Gellrich, *Chem. Commun.* **2021**, *57*, 5518–5521.

[3] For selected review articles on 1,1-carboborations see: a) B. Wrackmeyer, *Coord. Chem. Rev.* **1995**, *145*, 125–156; b) G. Kehr, G. Erker, *Chem. Commun.* **2012**, *48*, 1839–1850; c) G. Kehr, G. Erker, *Chem. Sci.* **2016**, *7*, 56–65.
[4] a) M. Hasenbeck, T. Müller, U. Gellrich, *Catal. Sci. Technol.* **2019**, *9*, 2438–2444; b) C. You, M. Sakai, C. G. Daniliuc, K. Bergander, S. Yamaguchi, A. Studer, *Angew. Chem. Int. Ed.* **2021**, *60*, 21697–21701; *Angew. Chem.* **2021**, *133*, 21865–21869; c) I. A. Cade, M. J. Ingleson, *Chem. Eur. J.* **2014**, *20*, 12874–12880; d) Y. Shoji, N. Tanaka, S. Muranaka, N. Shigeno, H. Sugiyama, K. Takenouchi, F. Hajjaj, T. Fukushima, *Nat. Commun.* **2016**, *7*, 12704; e) J. R. Sanzone, C. T. Hu, K. A. Woerpel, *J. Am. Chem. Soc.* **2017**, *139*, 8404–8407; f) M. Hasenbeck, T. Müller, A. Averdunk, J. Becker, U. Gellrich, *Chem. Eur. J.* **2022**, e202104254; g) R. L. Melen, L. C. Wilkins, B. M. Kariuki, H. Wadepohl, L. H. Gade, A. S. K. Hashmi, D. W. Stephan, M. M. Hansmann, *Organometallics* **2015**, *34*, 4127–4137; h) M. Devillard, R. Brousses, K. Miqueu, G. Bouhadir, D. Bourissou, *Angew. Chem. Int. Ed.* **2015**, *54*, 5722–5726; *Angew. Chem.* **2015**, *127*, 5814–5818.
[5] a) D. J. Parks, W. E. Piers, G. P. A. Yap, *Organometallics* **1998**, *17*, 5492–5503; b) D. J. Parks, R. E. von H. Spence, W. E. Piers, *Angew. Chem. Int. Ed.* **1995**, *34*, 809–811.
[6] a) X. Tao, C. G. Daniliuc, D. Dittrich, G. Kehr, G. Erker, *Angew. Chem. Int. Ed.* **2018**, *57*, 13922–13926; *Angew. Chem.* **2018**, *130*, 14118–14122; b) X. Tao, C. G. Daniliuc, K. Soloviova, C. A. Strassert, G. Kehr, G. Erker, *Chem. Commun.* **2019**, *55*, 10166–10169; c) X. Tao, K. Škoch, C. G. Daniliuc, G. Kehr, G. Erker, *Chem. Sci.* **2020**, *11*, 1542–1548; d) X. Tao, G. Kehr, C. G. Daniliuc, G. Erker, *Angew. Chem. Int. Ed.* **2017**, *56*, 1376–1380; *Angew. Chem.* **2017**, *129*, 1396–1400.
[7] For a review article on the reactions of allenes with strong boron-based Lewis acids see: U. Gellrich, *Eur. J. Org. Chem.* **2021**, *2021*, 4707–4714.
[8] a) S. Grimme, J. G. Brandenburg, C. Bannwarth, A. Hansen, *J. Chem. Phys.* **2015**, *143*, 054107; b) G. Santra, N. Sylvetsky, J. M. L. Martin, *J. Phys. Chem. A* **2019**, *123*, 5129–5143; c) E. Caldeweyher, S. Ehlert, A. Hansen, H. Neugebauer, S. Spicher, C. Bannwarth, S. Grimme, *J. Chem. Phys.* **2019**, *150*, 154122; d) F. Weigend, R. Ahlrichs, *Phys. Chem. Chem. Phys.* **2005**, *7*, 3297–3305; e) L. Goerigk, A. Hansen, C. Bauer, S. Ehrlich, A. Najibi, S. Grimme, *Phys. Chem. Chem. Phys.* **2017**, *19*, 32184–32215; f) F. Neese, *Wiley Interdiscip. Rev.: Comput. Mol. Sci.* **2012**, *2*, 73–78; g) F. Neese, F. Wennmohs, U. Becker, C. Riplinger, *J. Chem. Phys.* **2020**, 152, 224108; h) V. Barone, M. Cossi, *J. Phys. Chem. A* **1998**, *102*, 1995–2001.
[9] a) N. Miyaura, A. Suzuki, *J. Chem. Soc. Chem. Commun.* **1979**, 866–867; b) N. Miyaura, K. Yamada, A. Suzuki, *Tetrahedron Lett.* **1979**, *20*, 3437–3440.
[10] For selected review articles on the Suzuki-Miyaura coupling see: a) A. Taheri Kal Koshvandi, M. M. Heravi, T. Momeni, *Appl. Organomet. Chem.* **2018**, *32*, e4210; b) I. Maluenda, O. Navarro, *Molecules* **2015**, *20*, 7528–7557; c) C. C. C. Johansson Seechurn, M. O. Kitching, T. J. Colacot, V. Snieckus, *Angew. Chem. Int. Ed.* **2012**, *51*, 5062–5085; *Angew. Chem.* **2012**, *124*, 5150–5174; d) M. M. Heravi, E. Hashemi, *Tetrahedron* **2012**, *68*, 9145–9178.
[11] For a review article on frequently used boron groups in the Suzuki-Miyaura coupling see: A. J. J. Lennox, G. C. Lloyd-Jones, *Chem. Soc. Rev.* **2014**, *43*, 412–443.
[12] For selected examples of the total synthesis and review articles on natural products containing 1,4-diene motives see: a) T. Sato, T. Suto, Y. Nagashima, S. Mukai, N. Chida, *Asian J. Org. Chem.* **2021**, *10*, 2486–2502; b) G. Petruncio, Z. Shellnutt, S. Elahi-Mohassel, S. Alishetty, M. Paige, *Nat. Prod. Rep.* **2021**, *38*, 2187–2213; c) P. Liu, E. N. Jacobsen, *J. Am. Chem. Soc.* **2001**, *123*, 10772–10773; d) B. M. Trost, P. E. Harrington, J. D. Chisholm, S. T. Wrobleski, *J. Am. Chem. Soc.* **2005**, *127*, 13598–13610.
[13] Other selected methods for the synthesis of 1,4-diene motives include olefinations a) F. Lindner, S. Friedrich, F. Hahn, *J. Org. Chem.* **2018**, *83*, 14091–14101; b) S. Peng, C. M. McGinley, W. A. van der Donk, *Org. Lett.* **2004**, *6*, 349–352; c) D. Menche, J. Hassfeld, J. Li, S. Rudolph, *J. Am. Chem. Soc.* **2007**, *129*, 6100–6101; allylic nucleophilic substitutions d) Y. Huang, M. Fañanás-Mastral, A. J. Minnaard, B. L. Feringa, *Chem. Commun.* **2013**, *49*, 3309–3311; divinylcyclopropane rearrangements: e) H. Ito, S. Takeguchi, T. Kawagishi, K. Iguchi, *Org. Lett.* **2006**, *8*, 4883–4885; catalysed olefin rearrangements: f) F. Weber, A. Schmidt, P. Röse, M. Fischer, O. Burghaus, G. Hilt, *Org. Lett.* **2015**, *17*, 2952–2955; catalysed dimerization and hydroboration of allenes: g) Y. Zhao, S. Ge, *Angew. Chem. Int. Ed.* **2021**, *60*, 2149–2154; *Angew. Chem.* **2021**, *133*, 2177–2182.
[14] C. Hansch, A. Leo, R. W. Taft, *Chem. Rev.* **1991**, *91*, 165–195.
[15] a) J. A. Lawson, J. I. DeGraw, *J. Med. Chem.* **1977**, *20*, 165–166; b) S. Zeisel, *Monatsh. Chem.* **1885**, *6*, 989–997; c) J. McOmie, D. West, *Org. Synth.* **2003**, *49*, 50–50.

Manuscript received: February 13, 2022
Accepted manuscript online: March 29, 2022
Version of record online: April 21, 2022

6 Zusammenfassung und Schlussfolgerung

Die Anwendung der *Bor-Liganden-Kooperation* in der Katalyse zeigt, wie dieses Konzept die Reaktivität von klassischen frustrierten Lewis-Paaren, durch die *in situ* Erzeugung von Boranen statt Boraten ergänzt.

Die Entstehung von Piers Boran **46** bei der H_2-Aktivierung durch Boroxypyridin **1** ermöglicht die Hydroborierung von Alkinen und Allenen zu den entsprechenden Alkenyl- und Allylboranen. Erstere Reaktion ermöglicht die katalytische *Z*-selektive Semihydrierung von internen Alkinen und die erste metallfreie katalytische Semihydrierung von terminalen Alkinen. Letztere Reaktion ermöglicht die Allylborierung von Acetonitril zu Allyliminen mit BCF **12** als zusätzliche Lewis-Säure. Dies ist die erste Allylborierung, die nur katalytische Mengen eines *in situ* erzeugten Allylierungsreagenz benötigt und die konzeptionell eine neue Methode für die Nutzung von H_2 in der organischen Synthese zeigt. Die C–H-Aktivierung von terminalen Alkinen und das Entstehen der entsprechenden Alkinylborane durch Dissoziation ermöglichte die katalytische *gem*-selektive Homodimerisierung von terminalen Alkinen zu den entsprechenden Eninen. Schlüsselschritt in dieser Katalyse ist eine neuartige 1,2-Carboborierung von Alkinen durch Alkinylborane. In allen drei Fällen wird der Katalysezyklus durch eine Protodeborylierung geschlossen, wodurch sich das intramolekulare FLP **1** regeneriert.

Darüber hinaus ermöglichte das Konzept der BLK die erste organokatalytische Dehydrierung von Amminboran durch Thiopyridon **92** bzw. dessen Tautomer Mercaptopyridin **93**. Dieses reagiert mit der aciden S–H-Bindung in einer dehydrogenativen Kupplung mit der hydridischen B–H-Bindung von Amminboran. Durch eine intramolekulare Deprotonierung der N–H-Bindung durch die Pyridinfunktionalität des Katalysators bildet sich Thiopyridon, das durch Tautomerisierung zum Mercaptopyridin den Katalysezyklus schließen kann.

Zusätzlich wurden neue Carboborierungen von Boranen mit C–C-π-Systemen entwickelt. So führt die Reaktion von Arylallenen mit BCF **12** über einen intramolekularen Ringschluss mit Übertragung eines C_6F_5-Rings in einer 1,1-Carboborierung zur Bildung eines Indens. Als Nebenprodukt entsteht über eine Retrohydroborierung Piers Boran. Die Reaktion von Alkenylboranen, die durch die Hydroborierung von Alkinen durch Piers Boran *in situ* erzeugt wurden, mit einem Überschuss Alkin führt zu $B(C_6F_5)_2$-substituierten Tetrahydropentalenen. Experimentelle und computerchemische Untersuchungen deuten darauf hin, dass diese Reaktionskaskade durch eine Serie von 1,2-Carboborierungen von Alkenylboranen an Alkinen initiiert wird. In dieser Reaktion werden insgesamt fünf neue C–C-σ-Bindungen gebildet.

Während die synthetische Vielseitigkeit der Tetramerisierung von Alkinen und der Indenbildung aus Arylallenen begrenzt ist, konnte gezeigt werden, dass elektronenarme Alkenylborane mit Allenen chemo- und regioselektiv den Alkenylrest in einer 1,2-Carboborierung übertragen. Entsprechende Alkenylborane lassen sich leicht und variabel durch die Hydroborierung von terminalen Alkinen mit Piers Boran **46** synthetisieren. Die nach der 1,2-Carboborierung erhaltenen borylsubstituierten 1,4-Diene konnten in einer Eintopfreaktion in einer Suzuki-Miyaura-Kupplung mit verschiedenen Organoiodiden gekuppelt werden. Alle drei Reaktionskomponenten (Alkin, Allen und Organoiodid) konnten unabhängig voneinander variiert werde und die synthetische Anwendungsbreite dieser Methode konnte durch die Synthese von 20 verschiedenen 1,4-Dienen gezeigt werden.

7 Danksagung

Natürlich wäre diese Arbeit nicht ohne die Hilfe von vielen anderen möglich gewesen. Dafür möchte ich meinen herzlichen Dank aussprechen:

Dieser gilt Dr. Urs Gellrich für die produktive Zusammenarbeit, die Förderung meiner Fähigkeit, die vielen lehrreichen und auch amüsanten Unterhaltungen und seine stets offene Tür für Probleme aller Art.

Prof. Dr. Schreiner für die Übernahme des Zweitgutachtens und die freundliche Aufnahme in das OC-Institut und die Arbeitsgruppenseminare.

Der ganzen (doch gut gewachsenen) Arbeitsgruppe Gellrich: Meinen „ersten“ Kollegen Tizian Müller und Jama Ariai: Ich habe sehr gerne mit Euch zusammengearbeitet, das neue Labor eingerichtet und den alltäglichen Laborwahnsinn mit Euch geteilt.

John Liebig ohne den (meine Zeit in) Gießen nicht mal halb so schön wäre.

Felix Wech, Arthur „*Ich schmeiß mal BCF drauf*“ Averdunk und Niklas Koch, die trotz meiner Betreuung während Ihres Studiums dabei geblieben sind ;-).

Den „weißbärtigen“ Postdoktoranden Dr. Sebastian Ahles und Dr. Ravindra Phatake für die Beantwortung etlicher Fragen.

Jil und Tim Kramer, Jean-Marie Pohl, Dr. Alex Francke, Lena Lipovsek und Fabian Stöhr und für die Aufnahme in Gießen und der Arbeitsgruppe Göttlich.

Prof. Dr. Richard Göttlich und Prof. Dr. Wegner für die Möglichkeit in der Anfangszeit Chemie ohne eigenes Labor und Ausrüstung machen zu können.

Dr. Heike Hausmann, Dr. Jonathan Becker und Dr. Dennis Gerbig und dem Team der OC-Analytik mit deren Hilfe aus farblosen oder farbigen Flüssigkeiten und Kristallen Strukturen auf dem Blatt Papier werden.

Der Chemikalien- und Geräteausgabe, der Glasbläserei, den Feinmechanikern, Edgar Reitz und den Hausmeistern ohne die wahrscheinlich nichts mehr funktionieren würde.

Michaela Richter und Anika Jäger ohne die hier noch weniger laufen würde.

Meiner Familie Bettina, Michael, Felix Hasenbeck, Midori de la Rosa, Matthias Oelmann und meinen Freunden für die jetzt schon 29 Jahre andauernde Unterstützung.

Cathi ohne die die ganze Arbeit mindestens doppelt so schwer gewesen wäre ☺.